Role of reactive oxygen species in Ras-mediated leukaemogenesis

Paul Spencer Hole

ProQuest LLC
789 East Eisenhower Parkway
P.O. Box 1346
Ann Arbor, MI 48106-1346

Declaration and statements

DECLARATION

This work has not previously been accepted in substance for any degree and is not concurrently submitted in candidature for any degree.

Signed ..... (candidate) Date .....

STATEMENT 1

This thesis is being submitted in partial fulfillment of the requirements for the degree of Doctor of Philosophy (Ph.D).

Signed ..... (candidate) Date .....

STATEMENT 2

This thesis is the result of my own independent work/investigation, except where otherwise stated. Other sources are acknowledged by explicit references.

Signed ..... (candidate) Date .....

STATEMENT 3

I hereby give consent for my thesis, if accepted, to be available for photocopying and for inter-library loan, and for the title and summary to be made available to outside organisations.

Signed ..... (candidate) Date .....

Acknowledgements

I would like to acknowledge the invaluable contributions of several individuals:

Prof. Alan Burnett for contributing the necessary funds to allowing this research to be performed and making it possible for this work to continue in the future.

My supervisors Dr. Alex Tonks and Dr. Richard Darley for their supervision and immense patience.

Lorna Pearn and Dr. Amanda Tonks for lending their laboratory experience.

Dr. Philip James for contributing his time and expertise during the EPR experiments.

Prof. Ajay Shah and Dr. Colin Murdoch (King's College, London) for donating mice and their time.

Prof. Mary Dinauer for donation of PLB-985 cell lines.

Rhys Morgan, Steve Coles, Nader Omidvar, Paul Baines and others in the Department of Haematology who emphasized the fun in fundamental haematology research.

Finally, I gratefully acknowledge the Medical Research Council for funding this work.

Foreword

An electronic version of this document is provided on the accompanying CD (see back sleeve). In the electronic version of the document, all cross-references act as hyperlinks.

The accompanying CD also contains supplementary material.

Dedicated to my children, Joseph and Meghan;
and to my wife, Afton.

Publications and presentations

Publications

Hole, P. S., Pearn, L., Tonks, A. J., James, P. E., Burnett, A. K., Darley, R. L., & Tonks, A. Ras-induced reactive oxygen species promote growth factor-independent proliferation in human $CD34^+$ haematopoietic progenitor cells. *Blood.* 2009; doi:10.1182/blood-2009-06-222869. (see pg 247)

Abstracts

Hole, P. S., Pearn, L., James, P. E., Burnett, A. K., Darley, R. L., & Tonks, A. Ras promotes production of reactive oxygen species in normal human $CD34^+$ cells. *ASH Annual Meeting Abstracts. 2008.* 112 (11), p 3797. (poster presentation).

Hole, P. S., Pearn, L., James, P. E., Burnett, A. K., Darley, R. L., & Tonks, A. The role of reactive oxygen species in Ras-mediated leukaemogenesis. *Abstracts of the British Society of Haematology 48th Annual Scientific Meeting. 2008.* 141 (S1), p 46. (poster presentation).

Oral presentations

"Mutant Ras promotes production of Reactive Oxygen Species in human blood cell progenitors" *23nd Annual School of Medicine Postgraduate Research Day.* Nov 2008
2nd prize awarded for oral presentation.

"Reactive Oxygen Species and Ras-mediated Leukaemias: Is there a link?" *1st Wales Cancer Conference,* Apr 2008 (accompanied by poster) and *Joint Haematology/Pathology seminars,* Sept 2008.

"Ras and ROS: The story so far..." *Department of Haematology seminar series.* Mar 2008.

"The Role of Reactive Oxygen Species in Ras-mediated Leukaemogenesis". *22nd Annual School of Medicine Postgraduate Research Day.* Nov 2007.
1st prize awarded for poster presentation.

"From Retrovirus to Ras to ROS: Review, Results and Reflection". *Department of Haematology seminar series* and *Joint Haematology/Pathology seminars* Mar-Apr 2007.

Abstract

Mutations of Ras and activation of the Ras pathway are amongst the most common abnormalities detected in human cancer (~20%), and in myeloid neoplasia. In addition, excessive production of reactive oxygen species (ROS) is a common feature of human malignancy and is often triggered by activation of Ras oncogenes. ROS act as second messengers and can influence a variety of cellular process including growth factor responses and cell survival. This study examined the contribution of ROS production to the phenotype of mutationally-activated Ras in normal human $CD34^+$ haematopoietic progenitor cells. For the first time, this study demonstrated that Ras strongly upregulated the production of both superoxide and hydrogen peroxide (H_2O_2) in these cells, through the stimulation of NOX oxidase activity, without affecting the expression of endogenous antioxidants or the production of mitochondrial ROS. Ras also promoted both the survival and the growth factor independent proliferation of $CD34^+$ cells. Using oxidase inhibitors and antioxidants, it was found that excessive ROS production by these cells did not contribute to their enhanced survival; rather, this study presents the first data demonstrating that ROS promoted their growth factor-independent proliferation. While Ras-induced ROS production specifically activated the $p38^{MAPK}$ oxidative stress response, this failed to induce expression of the cell cycle inhibitor $p16^{INK4A}$; instead, ROS promoted the expression of cyclin D1 and D3. Expression of activated Ras in human haematopoietic progenitors drives hyperphosphorylation of PKC family members, which mediates several phenotypes of mutant Ras in haematopoietic cells including dysregulated development. This study demonstrated that endogenous H_2O_2 production contributes to hyperphosphorylation of PKC in this model, and that exogenous H_2O_2 can drive phosphorylation of PKC in a similar manner. Finally, this study presents preliminary data obtained by kinomic PepChip analysis suggesting that endogenous ROS production driven by mutant Ras can influence the kinase activity of these cells, consistent with the hypothesis that ROS may promote protein phosphorylation via phosphatase inhibition.

In summary, this study presents novel data showing endogenous ROS production makes a significant contribution to the phenotype of human haematopoietic progenitor cells expressing mutant Ras and suggests that targeting ROS may be a valid approach in acute myeloid leukaemia therapy.

List of Abbreviations

2-ME	2-methoxyestradiol
4EBP	eIF4E-binding protein
4HPR	N-(4-hydroxyphenyl) retinamide
7-AAD	7-aminoactinomycin D
ADP	adenosine diphosphate
AGC	protein A, protein G and protein C kinase family
AIR	autoinhibitory region
Akt	v-Akt murine thymoma viral oncogene homologue (aka PKB)
ALL	acute lymphocytic leukaemia
ALS	amyotrophic lateral sclerosis
AML	acute myeloid leukaemia
Ang II	angiotensin II
Ang-1	angiopoietin-1
ANOVA	analysis of variance
ANT	adenine nucleotide translocase
AP-1	activating protein-1
APC	allophycocyanin
APL	acute promyelocytic leukaemia
Arg	arginine
ASK1	apoptosis signal-regulating kinase-1
ATCC	American Type Culture Collection
ATM	mutated in ataxia telangiectasia
ATP	adenosine triphosphate
ATR	ataxia telangiectasia and Rad3 related protein
ATRA	all-trans retinoic acid
BAALC	brain and acute leukaemia cytoplasmic
BCL-2	B-cell CLL/lymphoma-2
Bis-Tris	bis (2-hydroxyethyl) imino-tris (hydroxymethyl) methane-HCl
BMEC	bone marrow microvascular endothelial cells
bp	base pair
BSA	bovine serum albumin
CAK	CDK-activating kinase
CBF	core binding factor
CBP	CREB-binding protein
CD	cluster of differentiation
CDK	cyclin-dependent kinase
CDKI	cyclin-dependent kinase inhibitor
CEBP	CCAAT/enhancer binding protein
CFC	colony-forming cells
CFU	colony-forming unit
Ci	Curie
CLL	chronic lymphocytic leukaemia
CLSM	confocal laser scanning microscopy

CML	chronic myeloid leukaemia
CMML	chronic myelomonocytic leukaemia
CMP	common myeloid progenitor
CoQ	coenzyme Q (aka ubiquinone)
CSF	colony stimulating factor
Cys	cysteine
Cyt c	cytochrome c
DCFDA	2',7'-dichlorodihydrofluoroscein diacetate
ddNTP	dideoxynucleotide triphosphate
DEPMPO	N-(diethoxyphosphoryl)-5-methyl-1-pyrroline-N-oxide
dH_2O	distilled H_2O
DMEM	Dulbecco's Modified Eagle's Medium
DMPO	5,5-dimethyl-pyrroline-1-oxide
DMSO	dimethylsulphoxide
DNA	deoxyribonucleic acid
DNAse	deoxyribonuclease
dNTP	deoxynucleotide triphosphate
DPI	diphenyleneiodonium
DPX	distyrene-plasticiser-xylene
DTPA	diethylenetriamine penta-acetic acid
DTT	dithiothreitol
DUOX	dual oxidase
DUOXA1	dual oxidase maturation factor
E2F	E2 promoter-binding factor
EBV	Epstein-Barr virus
EGF	epidermal growth factor
eIF4E	eukaryotic translation initiation factor-4E
EM	electromagnetic
env	viral envelope and structural protein genes
EPO	erythropoietin
EPR	electron paramagnetic resonance
ERK	extracellular signal-regulated kinase
ETC	electron transport chain
FAB	French-American-British
FACS	fluorescence-activated cell sorting
FAD	flavin adenine dinucleotide
Fc	fragment crystallisable
FcR	Fc receptor
FCS	fetal calf serum
FDCP	factor-dependent cell Patersen
FeTCPP	iron (III) porphyrin
FITC	fluorescein isothiocyanate
FLT3	fms-like tyrosine kinase-3
FLT3L	FLT3 ligand
FMN	flavin mononucleotide
FOXO	forkhead box-O
FT	farnesyl transferase

g	acceleration due to gravity; 9.8 ms^{-2}
Gab	GRB2 associated binder
gag	group-specific antigen
GAP	GTPase-activating protein
GAPDH	glyceraldehyde 3-phosphate dehydrogenase
GATA-1	GATA binding protein-1
G-CSF	granulocyte-colony stimulating factor
GDP	guanosine diphosphate
GEF	Ras guanine nucleotide exchange factor
GFI	growth factor independent-1
GFP	green fluorescent protein
GM-CSF	granulocyte monocyte-colony stimulating factor
GMP	granulocyte-monocyte progenitors
GOX	glucose oxidase
GRB2	growth factor receptor-bound protein-2
GSH	glutathione
GSSG	oxidised dimerised GSH
GTP	guanosine triphosphate
h	hours
H_2O_2	hydrogen peroxide
HBSS	Hank's balanced salt solution
HDM2	human homologue of murine Mdm2
HEPES	4-(2-hydroxyethyl)-1-piperazine-ethanesulfonic acid
HIF-1α	hypoxia-inducible factor-1α
HOCl	hypochlorous acid
HRP	horseradish peroxidase
HSC	haematopoietic stem cell
HX	hypoxanthine
i.v.	intravenous
IAP	inhibitor of apoptosis protein
ICSBP	interferon consensus sequence-binding protein
IL	interleukin
IMDM	Iscove's Modified Dulbecco's Medium
INK	inhibitor of kinase
IRF	interferon regulatory factor
ITD	internal tandem duplication
IU	international unit
JAK	Janus kinase
JMML	juvenile myelomonocytic leukaemia
JNK	Jun N-terminal kinase
Kbp	kilobase-pair
KDa	kiloDalton
LB	Luria-Bertani
LDS	lithium dodecyl sulphate
LED	light-emitting diode
L-NAME	L-nitro-arginine methyl ester
L-NMMA	NG-monomethyl-L-arginine acetate

LPS	lipopolysaccharide (aka endotoxin)
LSC	leukaemic stem cell
LT-HSC	long term HSC
M	molarity (moles per L)
MACS	magnetic-activated cell sorting
MAPK	mitogen-activated protein kinase
MCS	multiple cloning site
M-CSF	macrophage colony-stimulating factor
MDS	myelodysplastic syndrome
MEK	mitogen-activated protein kinase kinase
MEP	megakaryocyte-erythroid progenitor
min	minutes
MKP-3	mitogen-activated protein kinase phosphatase-3
MLL	mixed lineage leukaemia
MMLV	Moloney murine leukaemia virus
MOPS	3-(N-morpholino) propane sulphonic acid
MPD	myeloproliferative disorder (aka MPN)
MPN	myeloproliferative neoplasm (aka MPD)
MPO	myeloperoxidase
MRD	minimum residual disease
Mrp8	myeloid-related protein-8
MSV	murine sarcoma virus
mTOR	mammalian target of rapamycin
Myc	myelocytomatosis oncogene
NAC	N-acteyl cysteine
NADH	nicotinamide adenine dinucleotide
NAPDH	nicotinamide adenine dinucleotide phosphate
NBT	nitroblue tetrazolium
NCF	neutrophil cytosolic factor
NF1	neurofibromin
NF-κB	nuclear factor-κB
NMR	nuclear magnetic resonance
NOD/SCID	non-obese diabetic/severe combined immunodeficient
NOS	nitric oxide synthase
NOX	NADPH oxidase
NOXA1	NADPH oxidase activator-1
NOXO1	NADPH oxidase organiser-1
NPM1	nucleophosmin
ORC	origin of replication complex
PB1	Phox and Bem1 domain
PBS	phosphate-buffered saline
PCR	polymerase chain reaction
PDGF	platelet-derived growth factor
PDK1	phosphoinositide-dependent kinase-1
PE	R-phycoerythrin
PEITC	phenethyl isothiocyanate

PGK-1	3-phosphoglycerate kinase-1
PHD	proline hydroxlase
Phox	phagocyte oxidase (aka NADPH oxidase complex)
PI	propidium iodide
PI(3,5)P_2	phosphatidylinositol 3,5-bisphosphate
PI3K	phosphoinositide 3-kinase
PIP_2	phosphatidylinositol 4,5-bisphosphate
PIP_3	phosphatidylinositol 3,4,5-triphosphate
PKB	protein kinase B (aka Akt)
PKC	protein kinase C
PLC	phospholipase C
PMA	phorbol 12-myristate 13-acetate (aka TPA)
pol	viral reverse transcriptase gene
PP1	protein phosphatase-1
PP2A	protein phosphatase-2A
PR or PRR	proline rich region
Pro	proline
Prx	peroxiredoxin
PS	phosphatidylserine
PTD	partial tandem duplication
PTEN	phosphatase and tensin homologue
PTP	protein tyrosine phosphatase
PU.1	human homologue of murine Spi-1
pUC	'plasmid University of California'; plasmid maintenance sequence
PX	Phox homology domain
Ras	rat sarcoma
RasGRP	Ras guanine-nucleotide release proteins
Rb	retinoblastoma protein
RCM	retrovirus-containing medium
RLU	relative light units
RNA	ribonucleic acid
RNAse	ribonuclease
RNS	reactive nitrogen species
ROS	reactive oxygen species
rpm	revolutions per minute
RPMI	Roswell Park Memorial Institute
RT-PCR	reverse-transcriptase PCR
S.D.	standard deviation
Sca-1	stem cell antigen-1
SCF	stem cell factor (aka Steel factor)
SCF (p 41)	Skp1/Cullin/F-box
SCT	stem cell transplant
SDS	sodium dodecyl sulphate
sec	seconds
Ser	serine
SH2	Src-homology-2 domain
SH3	Src-homology-3 domain

Shc	Src homologous and collagen protein
SHIP	Src homology-2 domain-containing inositol polyphosphate 5'-phosphatase
SHP2	SH2 domain-containing protein-tyrosine phosphatase
SOC	super-optimal broth (catabolite-repressing)
SOD	superoxide dismutase
SOS	son of sevenless
Spi-1	spleen focus-forming virus proviral integration oncogene-1 (see also PU.1)
Src	cellular homologue of sarcoma inducing gene of Rous sarcoma virus
Srx	sulphiredoxin
STAT	signal transducer and activator of transcription
ST-HSC	short term HSC
Thr	threonine
TIAM1	T-cell lymphoma invasion and metastasis-1
TPA	12-O-tetradecanoylphorbol-13-acetate (aka PMA)
TPO	thrombopoietin
TPR	tricodecapeptide repeat
TRAIL	TNF-related apoptosis-inducing ligand
Trx	thioredoxin
TSC2	tuberous sclerosis-2
VEGF	vascular endothelial growth factor
vHLF	von Hippel-Landau factor
VLA	very late antigen
WHO	World Health Organisation
WT-1	Wilms tumor-1
XO	xanthine oxidase
ZONAB	ZO-1–associated nucleic acid binding protein

Summary of Figures

Table of Contents

1 Introduction

1.1 NORMAL HAEMATOPOIESIS

1.1.1 OVERVIEW OF HAEMATOPOIESIS

Haematopoiesis is the ordered process of production and maintenance of all mature blood cell types. An estimated 10^{12} mature blood cells are generated by the haematopoietic system per day; and these are responsible for critical processes in host maintenance including oxygen transport, innate and adaptive immunity, blood coagulation and tissue repair after injury. The mature blood cells that perform these functions in the host bear morphological and biochemical features which specialise them for their respective tasks. For example, red blood cells (erythrocytes) express high levels of haemoglobin, the protein responsible for oxygen and carbon dioxide transport around the body and their unique biconcave morphology enables them traverse the fine capillaries which perfuse hose tissues. Granulocytes (neutrophils, eosinophils and basophils) and peripheral blood monocytes (and their mature tissue-localised descendents, macrophages) express high levels of anti-microbial proteins (e.g. major basic protein expressed by eosinophils) and inflammatory mediators. Furthermore, phagocytic cells (neutrophils, monocytes and macrophages) express oxidases capable of generating reactive oxygen species (ROS), which in turn contribute to the killing of phagocytosed pathogens. Cytokines and chemokines secreted by innate immune cells prime a secondary, highly specific adaptive immune response, led by B and T lymphocytes. B lymphocytes are capable of generating high levels of antigen-specific immunoglobulin, while T lymphocytes play diverse roles, both orchestrating the adaptive response (helper T cells, regulatory T cells) and mediating direct cytotoxicity ($CD8^+$ T cells). Finally, thrombocytes (platelets) are critical for initiation of blood coagulation cascades which limit blood loss after injury and lay the foundation for tissue regeneration and repair. Importantly, the output of the haematopoietic system is dynamic can respond to changes in the environment; for example reduced oxygen at high altitude stimulates the production of erythrocytes; whilst pathogenic bacteria or parasites can stimulate mobilisation and production of neutrophils or eosinophils respectively. *In vitro* studies of primary haematopoietic cells and haematopoietic cell lines, together with *in vivo* murine studies have contributed to the current model of the haematopoietic system in mammals (discussed

in section 1.1.2). The majority of evidence suggests that the generation of mature cells by the haematopoietic system is hierarchical, with all mature haematopoietic cells originating from a single cell, the pluripotent haematopoietic stem cell (HSC;Figure 1.1). HSCs generate mature blood cells through an ordered process of lineage commitment, during which HSC progeny become increasingly restricted in their developmental potential, and ultimately become committed to the generation of a single mature cell type. The output of the haematopoietic system (i.e. how many cells of each mature cell type are produced) are governed by two main mechanisms: lineage decisions are primarily dictated by the repertoire of haematopoietic transcription factors, while the proliferation, survival and terminal maturation of committed progenitors is governed by the presence or absence of haematopoietic growth factors. Thus, mainly through these two mechanisms, the haematopoietic system adjusts the number of mature cells generated as required by the host.

1.1.2 MODELS FOR STUDYING NORMAL HAEMATOPOIESIS

1.1.2.1 In vitro models: ex vivo primary haematopoietic cell culture and haematopoietic cell lines

Following the groundbreaking work by Till *et al.* (section 1.1.2.2), important experiments were performed using *ex* vivo bone-marrow cultures in order to discover the factors that governed the differentiation of the proposed HSC (Dao, C. *et al.* 1977b; Dao, C. *et al.* 1977a). Primary human bone marrow cells immobilised in semisolid medium (soft agar or methylcellulose) were cultured in the presence of recently discovered 'colony stimulating factors' (CSFs), which were derived from cultured normal leukocytes. Since the cells were immobilised, the progeny of single cells could be scored. It was observed that CSFs could induce the formation of discrete mature colonies of cells e.g. neutrophils or macrophages or in some cases a mixture of both, depending on which CSF was used. These studies laid the ground work for our current understanding the role of CSFs and other growth factors in, leading eventually to the characterisation of the immunophenotypes of the committed progenitors and HSC compartments of mice and humans (section 1.1.2.2).

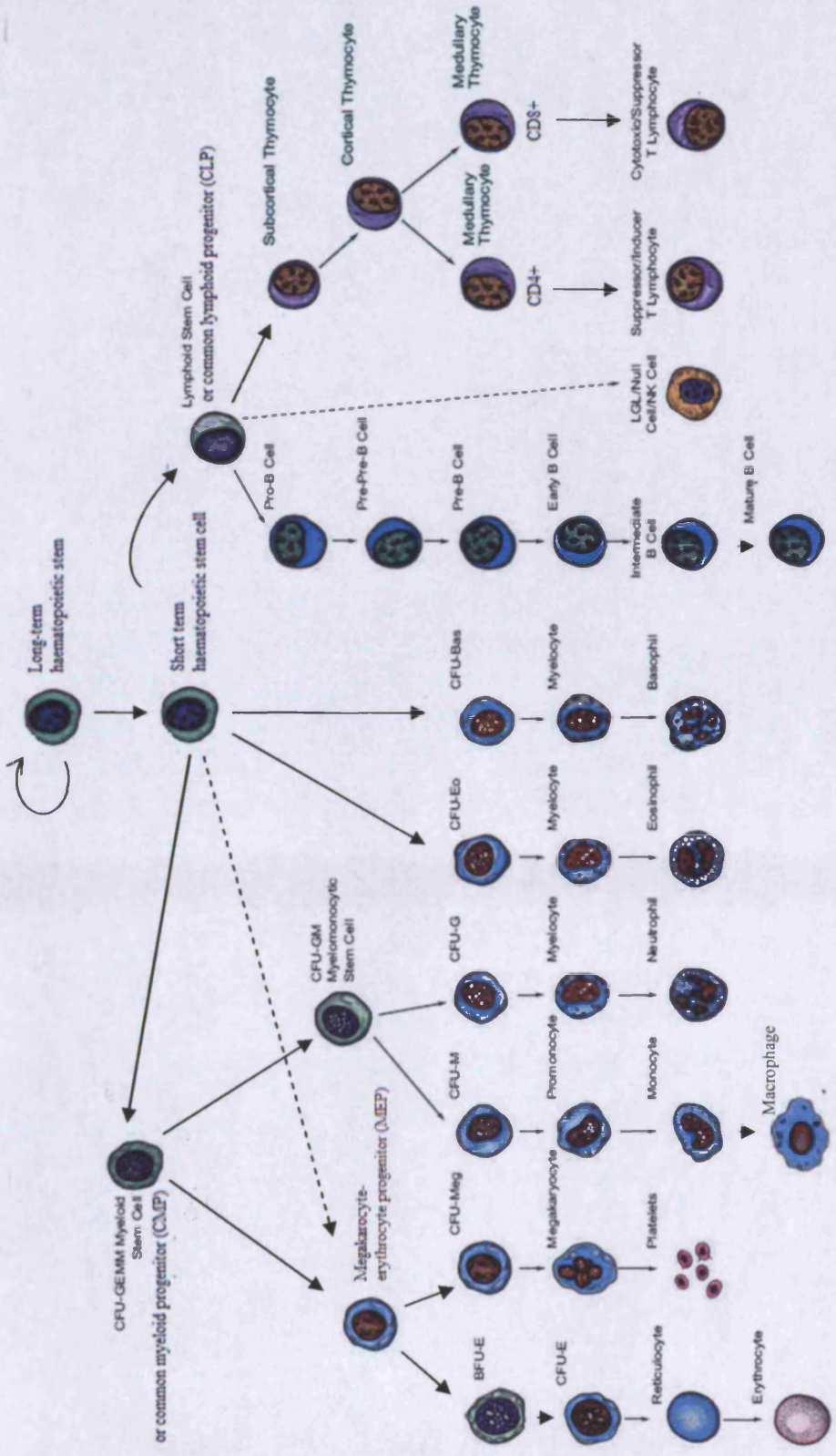

Figure 1.1 Pathways in haematopoietic lineage commitment

Straight arrows represent steps in lineage commitment, curved arrows represent self-renewal potential and dashed arrows represent putative lineage commitment pathways. Adapted from www.abdserotec.com. CFU = colony-forming unit, NK cell = natural killer cell

While primary cell studies are the most relevant model for study of haematopoiesis, studies are often hampered by small sample sizes and difficulty in maintaining undifferentiated primary cells in long term culture.

Cell lines are immortalised clonal cultures of cells that are able to replicate indefinitely without becoming senescent (Dao, M.A. and Nolta, J.A. 1999). In contrast to primary cells, cell lines provide a near unlimited amount of cell material for investigation. In addition, some cell lines exhibit limited differentiation potential presenting a convenient means of studying haematopoietic development. Examples of human haematopoietic cell lines with myeloid differentiating potential include U937, a monocytic leukaemia cell derived from a patient with histiocytic lymphoma (Sundstrom, C. and Nilsson, K. 1976) which can be induced to undergo monocytic differentiation; and HL60 or NB4 cells which were both derived from patients with acute promyelocytic leukaemia (Collins, S.J. *et al.* 1977; Lanotte, M. *et al.* 1991) which undergo granulocytic differentiation in response to DMSO or the vitamin A analogue all-trans retinoic acid (ATRA) (Collins, S.J. *et al.* 1978; Lanotte, M. *et al.* 1991). These observations ultimately led to the successful use of ATRA in treatment of APL patients (Flynn, P.J. *et al.* 1983). However, it should be noted that in addition to immortalisation, cell lines invariably harbour additional abnormalities such as chromosome translocations, which preclude the use of cell lines to draw any definitive conclusions regarding normal haematopoiesis (Furukawa, Y. 2002). Murine haematopoietic cells lines have also proved useful for example, FDCP-mix, an IL-3-dependent multipotent cell line derived from murine bone marrow after infection with Src-MMLV (Spooncer, E. *et al.* 1986). These cells are useful in that they have a normal karyotype and no known molecular abnormalities and have been induced to differentiate into several mature cell types. Indeed, FDCP-mix cells can generate mature neutrophils (Heyworth, C.M. *et al.* 1991) and dendritic cells (Schroeder, T. *et al.* 2000). However, erythroid differentiation is incomplete (Heyworth, C.M. *et al.* 1995), suggesting there are limitations to the use of these cells for modelling normal haematopoiesis.

1.1.2.2 In vivo models of haematopoiesis

Haematopoietic transplantation of primary haematopoietic cells into murine recipients bypasses the difficulties associated with working with cell lines and also some of the artefacts of *ex vivo* culture; as a result these studies have proved invaluable understanding the haematopoietic system.

Early *in vivo* experiments which suggested that single progenitor cells had the potential to generate more than one mature cell type were performed by Till *et al.* This

group noticed that allotransplants of murine bone marrow cells appeared to form colonies in the spleens of the recipients. Furthermore, there appeared to be evidence of multi-lineage differentiation in the colonies (Till, J.E. and McCulloch, E.A. 1961). To establish whether these colonies arose from single cells, murine bone marrow cells were irradiated prior to transplantation, which induced chromosomal aberrations that (if not fatal for the cell) would theoretically be detected in all members of a colony (if that colony was derived from a single cell). The finding that the majority of cells in each colony harboured the same chromosomal aberrations provided the first evidence that a single progenitor cell existed that may give rise to all mature blood cell types (Becker, A.J. *et al.* 1963).

Since then, assays for functional HSCs have been developed, the most stringent of these being the long-term repopulation assays. These assays originally involved allotransplantation of candidate HSC populations into lethally irradiated mice, which would die without complete rescue of the haematopoietic system. Putative HSC populations are those capable of rescuing haematopoiesis in primary, secondary and even tertiary irradiated recipients (Dick, J.E. 1996); a strong indication of maximal self-renewal capacity – the hallmark of an HSC. Through the work of John Dick's group, murine HSCs were functionally purified, and this group demonstrated that a single functional HSC could mediate the long term haematopoietic reconstitution of a transplant recipient (Dick, J.E. *et al.* 1985). However, xenotransplantation of human haematopoietic cells was hindered by immunological rejection of human cells even in irradiated recipients. An important step forward for xenotransplantation of human haematopoietic cells was the development of the beige/nude/xid (bnx) mouse (Andriole, G.L. *et al.* 1985). These mice have combined defects in T and B cell function, and the lack of adequate adaptive immune response in these animals allowed the first examples of successful xenotransplantation of human haematopoietic cells (Kamel-Reid, S. and Dick, J.E. 1988).

Since the late 80's, xenotransplantation has improved due to the development of mouse strains with further suppressed immune function, such as the non-obese diabetic/ severe combined immunodeficient (NOD/SCID) mouse, increased longevity such as the NOD/SCID/nude (Dick, J.E. 1996), and also 'humanised' mouse models which express human growth factors such as IL-3 by co-transplantation of IL-3 expressing stromal cells (Brouard, N. *et al.* 1998). With the development of flow cytometric methods including fluorescence activated cell-sorting (FACS), the Weissman group succeeded in characterising the immunophenotype of the major developmental stages of the murine and human haematopoietic hierarchy, culminating in the report of the immunophenotype of functional murine HSCs (Spangrude, G.J. *et al.* 1988) and human HSCs shortly afterwards

(Baum, C.M. *et al.* 1992). These findings are the basis for the current consensus on the haematopoietic hierarchy.

1.1.3 NORMAL MYELOID HAEMATOPOIESIS

1.1.3.1 Properties of HSCs

As mentioned above, Weissman *et al.* were the first to propose the immunophenotype of the murine and human HSC. A recent review stated the phenotype for [a]murine LT-HSCs is Lineage^{neg}, Sca-1^{+}, c-Kit^{+}, Flk2^{neg}, CD34^{neg}, CD150^{+}, while [b]human LT-HSCs are contained within the Lineage^{neg}, CD34^{+}, FLT3^{+}, CD90^{+}, CD45RA$^{lo/neg}$ compartment (Weissman, I.L. and Shizuru, J.A. 2008). Furthermore, human bone-marrow that is enriched for CD34^{+} cells shows improved engraftment after transplantation to myeloablated patients (Siena, S. *et al.* 2000). Additional immunophenotypic markers have been proposed for human LT-HSCs, most notably CD123^{+} (IL-3α chain) (Taussig, D.C. *et al.* 2005). As stated previously, the hallmark of LT-HSCs is their capacity for self renewal. The factors governing the self-renewing properties of LT-HSCs are poorly understood, however, recent evidence suggests that HOX genes play an important role in maintaining self-renewal capacity (Argiropoulos, B. and Humphries, R.K. 2007). HOX genes are class I homeobox genes distributed within the human genome in 4 discrete clusters. Each of the human gene clusters show homology to the Drosophila Antennepedia and Bithorax cluster of homeotic genes; mutations in which have been shown to have spectacular effects on *D. melanogaster* development (Kaufman, T.C. 1978). Evidence that HOX genes may play a role in HSC function initially came from gene expression profiling of murine HSCs showing that Hoxb4 and Hoxa9 are highly expressed in early progenitors but are downregulated during lineage commitment. Indeed over expression of Hoxb4 in haematopoietic progenitors promoted marked expansion of murine, human cell and primate models (Antonchuk, J. *et al.* 2001; Buske, C. *et al.* 2002; Zhang, X.B. *et al.* 2006), without leading to leukaemia. Hoxa9 overexpression also promoted of murine HSC expansion, but with the tendency to initiate leukaemic disease (Thorsteinsdottir, U. *et al.* 2002). Interestingly, the mixed lineage leukaemia (MLL) protein, which is a master regulator of HOX gene expression (Schuettengruber, B. *et al.* 2007), is also implicated in self-renewal (McMahon, K.A. *et al.* 2007), presumably through its influence on HOX gene expression, and is frequently targeted in chromosome

[a] c-Kit is the receptor for SCF, Flk2 is the murine homologue of human Flt3, CD150 is also known as signalling lymphocytic activation molecule family member 1 (SLAMf1).

[b] CD90 is also known as Thy1.

translocations detected in acute myeloid leukaemia (AML) (De Braekeleer, M. *et al.* 2005). However, the extrinsic and intrinsic cues that govern MLL and HOX gene expression are not understood, neither are the mechanisms by which HOX genes promote self renewal.

In summary, LT-HSC are cells with the potential to reconstitute the entire haematopoietic system, their immunophenotype has been reasonably well-defined, and they exhibit the exclusive stem-cell ability of long-term self renewal, which may be in part mediated by expression of HOX genes.

1.1.3.2 The HSC niche

HSCs are primarily quiescent, with an estimated 3.8% in S+G_2M phases of the cell cycle at a given time (Kiel, M.J. and Morrison, S.J. 2008). The quiescence of HSCs; together with their ability to home to the bone marrow (Kopp, H.G. *et al.* 2005) has been exploited to locate the normal resting place of the HSCs *in vivo*, using label retaining cell (LRC) assays. As with many of the studies described this far, studies such as LRC assays cannot be performed in humans for ethical reasons; therefore much of what is known about the stem cell niche is based on observations from murine models. LRC assays employ sorted murine HSCs populations which are labelled with BrdU. This label is incorporated into the DNA of replicating cells in during culture. These labelled HSCs are then transplanted into a lethally irradiated recipient. In quiescent cells (such as HSCs) the BrdU label can be retained for months, allowing tracking and localisation of the LRCs. Using this approach, it has been found that the majority of LRCs are associated with particular regions of the endosteum (the cellular lining separating bone from bone marrow) located within the cords (narrow filament-like passages) of the trabecular bone (Zhang, J. *et al.* 2003). It is likely that these LRC populations are enriched for HSCs; however formal confirmation of this is not possible since BrdU assays require that LRCs are fixed for analysis, which precludes assessment of their function. LRCs are also known to associate with specialised endothelial cells (BMEC) of the sinusoids, and this region has been proposed to act as a secondary 'vascular' HSC niche (Kiel, M.J. *et al.* 2005).

Approaches using conditional expression of proteins which stimulate osteoblast growth under the control of the type 1 collagen α promoter (expressed by early osteoblasts) show that HSC numbers increase in accordance with osteoblast numbers (Calvi, L.M. *et al.* 2003); and conditional ablation of osteoblasts by targeted expression of thymidine kinase and treatment with gancyclovir resulted in a depletion of HSC numbers (Corral, D.A. *et al.* 1998). These data strongly suggest that osteoblasts are an important part of the endosteal niche, and govern the size of the HSC pool, possibly through physical interaction. The

interactions of niche osteoblasts and HSCs are complex, but can be grouped into two main categories (Wilson, A. and Trumpp, A. 2006). The first are primarily adhesion interactions via N-cadherin and integrins such as VLA-4 and VLA-5. These interactions, together with binding to ECM-bound factors such as osteopontin and hyaluronic acid via CD44, promote the close contact of HSC with osteoblasts encouraging a second category of interactions to occur. Several of these secondary interactions appear to mediate quiescence and survival signals, e.g. Ang-1 secreted by niche osteoblasts activates the Tie-2 receptor on HSCs; resulting in upregulation of $p21^{Cip1}$ and quiescence, while SCF bound to the osteoblast membrane activates the c-Kit receptor on HSCs promoting survival and cell-cell adhesion. Furthermore, some of these signalling interactions serve several purposes, e.g. osteopontin promotes HSC adhesion but also has been shown to be a negative regulator of the HSC pool and c-Kit signalling not only promotes survival, but can also increase the avidity of integrin adhesion, strengthening the osteoblast-HSC interaction. Overexpression of Jagged (the Notch ligand) led to expansion to HSCs *in vivo*, suggesting the Notch signalling may be involved in self-renewal signals in HSCs. However, the observation that Notch signalling and also classical Wnt signalling are dispensable for normal haematopoiesis (Cobas, M. *et al.* 2004) suggests that (in murine haematopoiesis at least) there are other undiscovered factors that govern self renewal.

Whereas the above interactions appear to govern mainly adhesion and quiescence, the essential question of how HSC are driven to leave the niche and undergo asymmetric division remains unanswered. Murine osteoblasts can respond to extrinsic signalling molecules such as parathyroid hormone (PTH) which induces prostaglandin E_2 (PGE_2) production (Kawaguchi, H. *et al.* 1994; Tetradis, S. *et al.* 1997), and this has very recently been shown to augment HSC self-renewal (Frisch, B.J. *et al.* 2009). Although no definitive evidence exists at the present time, these reports support the notion that extrinsic or intrinsic cues could lead to alterations in the composition of osteoblast surface molecules. Such a shift could represent a change from niche-derived quiescence signals to self-renewal or differentiation signals.

1.1.3.3 Factors governing the development of committed haematopoietic progenitors

Regardless of the mechanisms which govern initiation of HSC lineage commitment, it is known that differentiation of an uncommitted HSC to a mature cell is characterised by a rapid loss of self-renewal capacity, associated with downregulation of transcription factors that promote self-renewal, such as Hox genes (section 1.1.3.1) and upregulation of transcription factors associated with lineage commitment. Subsequently,

the proliferation, survival and terminal maturation of committed progenitors are largely governed by the presence of haematopoietic growth factors (Figure 1.2). Studies of haematopoietic differentiation in the presence of cytokines led to the proposal that growth factors play an instructive role in lineage decisions (section 1.1.3.4); modulating haematopoietic transcription factor expression and thus deciding the fate of developing progenitors and these findings form the basis of the 'instructive' model of haematopoietic development. Alternatively, the stochastic model proposes that growth factor signalling merely provides survival and proliferation signals to committed progenitors whose lineage decisions are driven solely by the intrinsic cues of transcription factor expression. The evidence supporting both these models is discussed below; however most of the evidence supports the stochastic model.

1.1.3.4 The role of growth factor signalling in haematopoietic development

Haematopoietic growth factors (or cytokines) are secreted or membrane-anchored glycoproteins which bind to and activate cognate receptors (Robb, L. 2007). During myeloid development, the most influential growth factors are FLT3L, SCF, IL-3, IL-6, G-CSF, M-CSF and GM-CSF. The majority of haematopoietic cytokine receptors fall into the class-I cytokine receptor family, defined by the presence of a palindromic WSXSW motif and fibronectin type III domain in the extracellular portion, and conserved Box1/2 domains in the cytoplasmic portion which interact with Janus kinases (JAKs). Several important haematopoietic growth factor receptors are members of the receptor tyrosine kinase superfamily e.g. FLT3, c-KIT (SCF receptor) and M-CSFR; these receptors contain their own tyrosine kinase domain and therefore do not require association with JAKs. Finally, a few cytokines with influence in the haematopoietic system signal through type II cytokine receptors (e.g. IL-10 and interferons). These receptors are similar to type I in structure, with the exception that they lack the WSXSW motif.

Type I haematopoietic cytokine receptors are categorised by their formation of either homodimers (G-CSFR, EPOR and c-Mpl which is the TPO receptor) or heterodimers/trimers. Heterodimeric/trimeric class I cytokine receptors are further classified based on their association with a common receptor subunit; either the common the common β-chain (β_c) (e.g. IL-3R, GM-CSFR, IL-5R); the gp130 chain (e.g. IL-11R) or the common γ-chain (γ_c) (e.g. IL-2R, IL-4R, IL-7R). Since many of these receptors share a common chain, ligand specificity is conferred by association of the common chain with a specific α subunit.

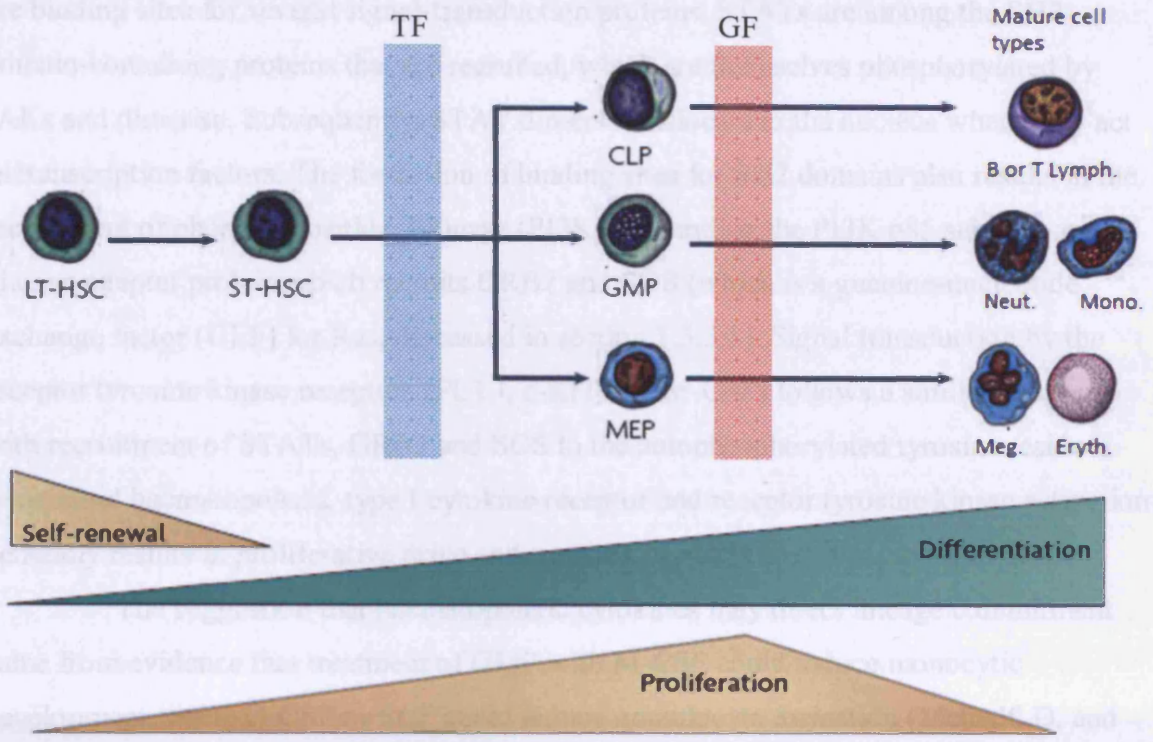

Figure 1.2 The roles of transcription factors and growth factors in haematopoietic lineage commitment

A simplified pathway is shown from long-term (LT) and short-term (ST) HSCs, leading to multipotent/bipotent progenitors; common lymphoid progenitors (CLP), granulocyte/macrophage progenitors (GMP) and megakaryocyte/erythrocyte progenitors (MEP) and finally mature cell types. Progress in lineage commitment is accompanied by a loss in self renewal and the acquisition of morphological and biochemical features associated with mature cells. The lineage selection decisions are dictated by transcription factors (TF), and subsequently growth factors (GF) promote the proliferation of committed progenitors.

Upon binding their cognate ligand, hetero- or homo-dimerisation of these receptor subunits (or conformational change in the preformed homodimeric EPO-R) leads to activation of JAKs bound to the Box1/2 domains. Phosphorylation of tyrosine residues on the cytoplasmic tail of the receptor by JAKs creates SH2 domain binding sites which are binding sites for several signal-transduction proteins. STATs are among the SH2-domain-containing proteins that are recruited, which are themselves phosphorylated by JAKs and dimerise. Subsequently, STAT dimers translocate to the nucleus where they act as transcription factors. The formation of binding sites for SH2 domains also results in the recruitment of phosphoinositide 3-kinase (PI3K) via binding the PI3K p85 subunit, and Shc, an adapter protein which recruits GRB2 and SOS (which is a guanine-nucleotide exchange factor (GEF) for Ras, discussed in section 1.3.3.1). Signal transduction by the receptor tyrosine kinase receptors (FLT3, c-KIT and M-CSF) follows a similar course, with recruitment of STATs, GRB2 and SOS to the autophosphorylated tyrosine residues. In myeloid haematopoiesis, type I cytokine receptor and receptor tyrosine kinase activation generally results in proliferative drive and survival.

The suggestion that haematopoietic cytokines may direct lineage commitment came from evidence that treatment of GMP with M-CSF could induce monocytic development, while G-CSF or SCF could induce granulocyte formation (Metcalf, D. and Burgess, A.W. 1982). Other groups demonstrated that IL-7α–deficient lymphoid progenitors show a block in lymphoid development, but could be stimulated to become myeloid cells by ectopic expression of GM-CSFRα and treatment with GM-CSF (Iwasaki-Arai, J. *et al.* 2003). Furthermore, IL-3 dependent FDCP-mix cells expressing a chimaeric IL-3 receptor fused to the cytoplasmic domain of GM-CSFR underwent granulocytic/monocytic differentiation in the presence of IL-3 (Evans, C.A. *et al.* 1999). These examples appear to demonstrate a role for growth factor signalling in haematopoietic lineage commitment, however, transgenic studies of murine growth factor genes and their receptors in murine models have revealed that the phenotype is surprisingly mild in most cases, and critically, lineage decisions can be made in the absence of one or more of these genes. For example, inactivating mutations of G-CSF or the β_c chain had no appreciable effect on myeloid cell development (Stanley, E. *et al.* 1994; Robb, L. *et al.* 1995). EpoR deficiency has a somewhat stronger phenotype; EpoR-null mice are embryonic lethal due to inadequate erythropoiesis. However, early erythroid progenitors are detected in these aborted embryos (Wu, H. *et al.* 1995). Similarly, although mice deficient for IL-7α are incapable for terminal lymphoid differentiation, early lymphoid progenitors are still detectable in these mice (Peschon, J.J. *et al.* 1994). Further evidence

that growth factors do not specifically influence lineage decisions (but rather promote survival and proliferation) came from transgenic experiments in which the cytoplasmic tail of the murine wild-type G-CSFR was replaced with that of the murine EpoR, resulting in a chimaeric receptor that transduced EpoR signals in response to G-CSF. Surprisingly, treatment with G-CSF did not alter myeloid or erythroid progenitor frequency in these cells (although neutrophil function was impaired) (Semerad, C.L. *et al.* 1999). Finally, expression of human GM-CSFR in murine EpoR null fetal liver cells was capable of rescuing erythropoiesis after GM-CSF treatment (Hisakawa, H. *et al.* 2001).

The lack of a strong phenotype in some single cytokine knockout models (e.g. G-CSF, G-CSFR knockouts) may be due to functional redundancy of some cytokine pathways, which may mask any deleterious effects of the knockout. However, the majority of evidence lends strong support for the stochastic model, and suggest that for the most part, cytokines promote the survival, proliferation and terminal maturation of committed progenitors, but have a limited influence on lineage selection. Nevertheless, the selective expansion of particular lineages by cytokine signalling represents a major control mechanism for the output of the haematopoietic system. In addition to positive regulation in the presence of cytokines, the haematopoietic system is subject to negative regulation by apoptosis in the absence of the required cytokines. Indeed, it has long been known that Epo is not required for early erythroid development prior to the MEP stage. However, beyond this point, EPO (or TPO) is required to prevent MEP death by apoptosis (Testa, U. 2004).

1.1.3.5 Role of transcription factors in haematopoietic development

Much experimental evidence suggests that it is transcription factor expression that determines HSC fate (Rosenbauer, F. and Tenen, D.G. 2007). Indeed some of the most important transcription factors necessary for myeloid lineage selection have now been identified. These include PU.1, GATA binding protein-1 (GATA-1), interferon regulatory factor-8 (IRF8) and CCAAT/enhancer binding protein (CEBP)α/ϵ. The earliest step in differentiation of HSCs is the decision to become a common myeloid or common lymphoid progenitor. The level of expression of PU.1 (Spi-1 in mice) plays a critical role in this decision. High levels of PU.1 expression favours generation of CMPs. Subsequently, commitment to the erythroid lineage is directed by preferential expression of GATA-1 in CMPs (which antagonises PU.1). Alternatively, upregulation of CEBPα (instead of GATA-1) indicates commitment to become a granulocyte/monocyte progenitor (GMP). Final specification of monocytes is dictated by expression of IRF8 in combination with PU.1, whereas granulocyte formation requires downregulation of PU.1 and

upregulation of CEBPϵ and growth factor independent-1 (GFI1) (Yamanaka, R. *et al.* 1997; Hock, H. *et al.* 2003). Interestingly, it is not just the presence or absence of a transcription factor that is important, but its level of expression also. Again, expression of PU.1 provides a good example of this principle. Whereas high levels of PU.1 favour CMP formation (described above), low (but appreciable) levels favour B-lymphoid development (DeKoter, R.P. and Singh, H. 2000). Critically, Spi-1 null mice show the expected block in monocyte development but are unable to generate competent granulocytes, whereas haploinsufficiency of Spi-1 retains monocytic failure, but restores normal granulocyte development (Rosenbauer, F. *et al.* 2004). The role of these transcription factors in the lineage decisions discussed has been (in the main) determined by targeted disruption of each factor in a murine model. In contrast to the milder phenotypes associated with growth factor deficiency, inactivation of these transcription factors results in complete loss of the associated lineage. Furthermore, the effects of transcription factor deletion are not restricted to lineage failure. For example CEBPα inactivation causes failure of granulopoiesis but also promotes expansion of HSC populations, suggesting that CEBPα normally acts to negatively regulate HSC pools (Zhang, P. *et al.* 2004). In general ,the lack of a given transcription factor results in failure to upregulate target genes required for the next stage of differentiation, combined with failure to downregulate antagonistic transcription factors which are associated with other lineages. Alternatively, failure to down regulate transcription factors associated with self-renewal (e.g. HOX genes) can confer self-renewal capacity on committed progenitors. The importance of correctly regulated transcription factor activity is highlighted by the fact that abnormal transcription factor activity is closely associated with leukaemia. For example IFR8-null mice are deficient for macrophage development, but also show a large increase in myeloid progenitor proliferation and develop disease closely resembling chronic myeloid leukaemia (CML). Reduced CEBPα expression, due to increased expression of a dominant negative splice variant or loss of the carboxy-terminal DNA binding domain, is detected in 7-9% of AML cases (Rosenbauer, F. and Tenen, D.G. 2007). Finally, the most common abnormality associated with AML, the t(8;21) translocation leading to the expression of the RUNX1-ETO fusion transcript (aka AML1-ETO), is detected in 12-15% of AML cases and is believed to result in repression of RUNX1, PU.1 and CEBPα-dependent gene transcription (Speck, N.A. and Gilliland, D.G. 2002). The cues that govern co-ordinated transcription factor expression in haematopoietic cells are unknown, and have even been proposed to be governed by chance (Abkowitz, J.L. *et al.* 1996). Nevertheless, the bulk of

evidence suggests that haematopoietic transcriptions factors are the most important factor in deciding the lineage fate of HSCs.

1.2 MYELOID LEUKAEMIAS

Leukaemias are clonal disorders of haematopoiesis that develop as a result of several genetic defects in the malignant clone. Commonly, three major cell properties are affected by these defects, cell survival, proliferation and differentiation. Initiating events may not immediately lead to leukaemia, but successive genetic defects in the same cell are cumulative, generating a malignant clone that is unable to terminally differentiate and has acquired growth and survival advantages.

Myeloid neoplasias are classified at diagnosis using the current guidelines for classification of myeloid neoplasms and acute leukaemia described in the 4th edition of WHO Classification of Tumors of the Hematopoietic and Lymphoid Tissues (Swerdlow, S.H. *et al.* 2008). This is an update on the 3rd edition (Jaffe, E.S. *et al.* 2001), which proposed an alternative to the French-American-British (FAB) disease classification system originally proposed in 1976 (Bennett, J.M. *et al.* 1976). Whereas the FAB system was based on morphological analysis and clinical features at diagnosis; the WHO classification also considers all available data including cytogenetic, immunophenotypic and molecular genetic data to assign a diagnosis. For the purposes of diagnosis, myeloid cells are defined as those from the granulocytic (neutrophils, basophil, eosinophils); monocyte/macrophage, erythroid, megakaryocytic or mast cell lineages. Where possible, the myeloid lineage from which the neoplasm is most likely to have arisen is determined through a combination of morphological analysis and immunophenotyping. The presence of known cytogenetic and molecular abnormalities which are relevant to treatment and prognosis, combined with the number of blasts detected in the peripheral blood and bone marrow at presentation, help to further specify the diagnosis. Broadly speaking, myeloid neoplasms are grouped into four main categories; myeloproliferative neoplasms (MPN, previously called MPD), myelodysplastic syndromes (MDS), disorders with features that overlap MPN and MDS (MPN/MDS), and AML. AML is diagnosed if the bone marrow or peripheral blood blasts exceed 20%. Cases where blasts are less than 20% may also be designated AML if a known cytogenetic/genetic abnormality associated with AML is detected (for example, the t(8;21) translocation which creates the RUNX1-ETO fusion gene).

Amongst the non-AML myeloid neoplasms, MDS is characterised by refractory anaemia with a hyper- or normo-cellular none marrow and uni- or multi-lineage dysplasia. The specific form of MDS (of which there are currently 7 described) depends on the morphological features on the malignant cells (e.g. the presence or absence of ring sideroblasts or the presence of Auer rods) combined with the specific blast percentage (Nimer, S.D. 2008).

MPNs are characterised by an often hypercellular bone marrow or peripheral blood with evidence of increased proliferation of one lineage. Most common among these disorders is BCR-ABL$^+$ CML.

MDS/MPNs are a group of disorders which present difficulties for classification as either MDS of MPN due to the presence of both lineage hyperplasia and hypoplasia. Amongst these disorders are chronic myelomonocytic leukaemia (CMML) and juvenile myelomonocytic leukaemia (JMML). CMML and JMML are closely associated with activating mutations in the Ras pathway (Tefferi, A. and Gilliland, D.G. 2007).

1.2.1 ACUTE MYELOID LEUKAEMIA

1.2.1.1 Epidemiology, pathophysiology and pathogenesis of AML

AML is characterised by a rapid accumulation of immature myeloid lineage cells ('blasts') in the bone marrow and peripheral blood of the host, which have lost the ability to spontaneously differentiate and have also acquired a proliferation and/or survival advantage. In the UK, the incidence of AML is 3.4 cases per 100,000 people, with a significant increase in incidence in persons over 60; indeed, the median age of AML patients is 65 years (Milligan, D.W. *et al.* 2006). Development of AML in under 18s is rare; instead, childhood acute lymphoblastic leukaemia (ALL; median age 3) and JMML (median age 1.4) are prevalent in this age group (Mitchell, C. *et al.* 2009; Locatelli, F. *et al.* 2005).

AML patients will often present with signs of anaemia (lethargy, shortness of breath), and/or difficulty clearing infection, with excessive bleeding and predisposition to bruising. Patients may also suffer from abdominal discomfort due to enlarged liver and/or spleen (hepato- or splenomegaly). Each of these symptoms either represents a consequence of one or more haematopoietic lineage failures or signs of organ invasion. The rapid onset of fatal symptoms in AML, such as bleeding, infection or organ infiltration usually occurs within 1 year of diagnosis if not treated. This contrasts with the slow development of CMLs, which is characterised by the protracted expansion of more mature myeloid cells

over the course of months or years, which can progress to an acute phase with more rapid expansion the abnormal cell population leading to similar symptoms to that of terminal AML.

Aside from old-age, there are several known risk factors for developing AML; including exposure to environmental mutagens such as radiation and benzene, previous myeloid neoplasia (e.g. MDS), and prior cytotoxic chemotherapy (often for an unrelated cancer). AMLs resulting from previous MDS or therapy-related AMLs tend to be more aggressive than de novo AML (Estey, E. *et al.* 1997). Each of these risk factors accelerates the DNA mutation rate, which presumably accelerates disease development. In some cases, the predisposition of some individuals to succumb to AML development when exposed to environmental risk factors has been explained by the prevalence of polymorphisms in foreign-toxic-substance (xenobiotic) detoxifying enzymes. Briefly, detoxification of xenobiotics occurs in two phases mediated by two classes of detoxifying enzymes. First, metabolic phase 1 enzymes (e.g. P450 cytochrome enzymes) transfer electrons onto the xenobiotic molecule generating a highly reactive intermediate, which is then primed for detoxification by metabolic phase 2 enzymes, e.g. glutathione-S-transferases or NADPH quinone oxidoreductase (NQO1) (Farquhar, M.J. and Bowen, D.T. 2003). Polymorphisms which confer increased phase 1 activity or decreased phase 2 activity, if not compensated for, can result in elevated levels of highly reactive intermediates, which will likely react with and damage most biomolecules including DNA. For example in the case of benzene detoxification, a C609T polymorphism in the gene encoding NQO1 (a metabolic phase 2 enzyme) confers decreased benzene detoxification activity and is associated with an increased tendency to develop AML in two separate studies (Larson, R.A. *et al.* 1999; Smith, M.T. *et al.* 2001). Similarly, an allele (CYP1A1*2B) which confers increased activity of CYP1A1 (a metabolic phase 1 cytochrome P450 enzyme) was not associated with increased tendency to develop AML overall, but was over-represented in a subset of AMLs with a poor risk karyotype and activating mutations in N-Ras (Bowen, D.T. *et al.* 2003).

1.2.1.2 Current understanding of AML aetiology

It has been estimated that a human cell must (correctly) repair approximately 10,000 DNA lesions per day to maintain the integrity of DNA helix under normal conditions (Lindahl, T. 1993). Exposure to environmental mutagens and other AML risk factors accelerate the DNA damage rate, and as a consequence, misrepaired (or unrepaired) DNA damage can lead to permanent changes (mutations) in the genetic code. Such

mutations can accumulate in long-lived cells (such as HSCs) over time leading to an increased risk of cancer development with age (DePinho, R.A. 2000).

Leukaemia development has been proposed to occur via a 'two-hit' process (Kelly, L.M. and Gilliland, D.G. 2002). This model suggests that the combination of mutations of two classes of genes (termed class I and class II genes) can lead to AML. Class I genes are those which transduce proliferation and survival signals while class II genes promote differentiation (i.e. haematopoietic transcription factors). The two-hit model proposes that activating mutations in class I genes (inactivation of negative regulators e.g. NF1 or activation of signal transducers such as Ras, FLT3 or c-KIT), combined with mutations which inactivate class II gene pathways (e.g. inactivating point mutations in CEBPα, or translocations involving RUNX1) may provide the necessary conditions for leukaemia to develop.

Although there is evidence that this model does not explain the behaviour of some leukaemias (Coulon, S. *et al.* 2007), there is strong evidence of co-operation of so-called class I and class II gene mutations in core-binding factor leukaemia; especially in cases involving mutations of Ras, FLT3 and c-KIT (Schneider, F. *et al.* 2007; Pinheiro, R.F. *et al.* 2007; Boissel, N. *et al.* 2006; Schnittger, S. *et al.* 2006) and the t(8;21) translocation (generating the RUNX1-ETO fusion gene). In these examples, the RUNX1 fusion of the haematopoietic transactivator RUNX1 is fused to the co-repressor domain of ETO, resulting in suppression of RUNX1 target gene transcription (Gardini, A. *et al.* 2008). The fact that loss of RUNX1 does cause a block in differentiation is observed in conditional RUNX1 knockouts in mice, which show a block in lymphoid development and reduced platelet formation (Ichikawa, M. *et al.* 2004). Constitutive signalling via Ras, FLT3 or c-KIT then provides the cooperating proliferation and survival signals, and in the case of c-KIT, leads to a poorer prognosis (Schnittger, S. *et al.* 2006). Further support for the two-hit hypothesis comes from studies showing that there is a significant negative association between mutations of class I genes, e.g. activating mutations of Ras and FLT3 (both class I genes) are rarely found together in the same patient, suggesting that co-existent class I genes mutations do not efficiently co-operate during disease development (Stirewalt, D.L. *et al.* 2001; Bowen, D.T. *et al.* 2005).

Chromosomal translocations are a common feature of myeloid leukaemias (Rabbitts, T.H. 1994) and provided the first prognostic indicators for AML patients (section 1.2.1.3). Translocations can have several consequences defined mainly by the features of the genes involved in the translocation and the domains that are preserved in the fusion product. For example, the t(9;22) fusion generates the BCR-ABL fusion gene

(characteristic of CML). In this way, the kinase activity of c-ABL is dysregulated by being placed under the control of the BCR promoter, resulting in a fusion protein with aberrant kinase activity. A similar example is found in some B-cell lymphomas, where BCL family members (which promote survival) are placed under control of the highly expressed immunoglobulin heavy-chain (IgH) genes. A final type of chromosome translocation results in the inactivation of one (or both) of the genes involved, and this type is common in myeloid leukaemia, commonly involving CBPβ (e.g. CBPβ-MYH11), p300 (e.g MOZ-p300) and RUNX1 (e.g. RUNX1-ETO), resulting in suppression of their target genes. Abnormalities of 11q23 (involving the MLL1 gene, encoding a histone-methyltransferase (Rabbitts, T.H. 1994)) results in increased MLL1 activity permitting aberrant transcription of target genes including HOX genes (Jude, C.D. *et al.* 2007). In short, these abnormalities of 'class I' genes are overwhelmingly associated with defective gene transcription, with the common result that haematopoietic cells are unable to correctly initiate development programmes.

As mentioned above, activating mutations in class I genes such as FLT3 include internal tandem duplications (ITDs), tyrosine kinase domain duplications (TKDs) and point mutations (D835Y). c-KIT is commonly mutated in exon 8 resulting in constitutive activation. Ras proteins may be constitutively activated due mutations most commonly in exons 12, 13 or 61. All of these events lead to activation of pro-proliferative pathways such as the Raf, mitogen-activated protein kinase kinase, extracellular signal-regulated kinase (Raf-MEK-ERK) pathway; the JAK-STAT pathway, and survival pathways such as the PI3K-Akt and nuclear factor-κB (NF-κB) pathways.

The requirement for both lesions to occur in the appropriate genes within the same cell suggests that such a process may take time to occur; implying that the only cells likely to be able accumulate the necessary mutations would be long-lived cells, such as HSCs. Furthermore, there is evidence that some abnormalities associated with leukaemia can be detected in both lymphoid and myeloid lineages, indicating that the abnormality arose in a common precursor e.g. AML1-ETO (Miyamoto, T. *et al.* 2000), strongly supporting the notion that AML arises from genetic damage sustained by HSCs. These observations have led to the proposal that leukaemic 'hits' occur at the level of the HSC. Moreover, it has been proposed that myeloid leukaemia may exist in an aberrant hierarchy analogous to that seen in normal haematopoiesis. This notion is supported by experiments which show that only rare cells with an immature immunophenotype ('leukaemic stem cells' or LSCs) are capable of reconstituting disease in an irradiated mouse (Dick, J.E. 2005). The existence of an LSC may explain the phenomenon of relapse after remission is

achieved; since it may be these LSCs are resistant to standard chemotherapy (if like normal HSCs they are relatively quiescent and receive survival signals from the bone marrow stroma). The impact of these genetic defects on prognosis and treatment are discussed in the next two sections.

1.2.1.3 Prognosis

The prognosis of a given patient diagnosed with AML is dependent on two main factors. First, the likelihood that the patient will survive primary induction and consolidation therapy, and secondly, the probability that the disease will respond to treatment. The former of these factors is adversely affected by age, but more specific indicators of fitness to undergo treatment can be obtained by examining serum albumin, creatinine, bilirubin and excluding the presence of ongoing infection. Patient performance scoring systems (such as the Zubrod scoring system (Oken, M.M. *et al.* 1982)) are also used as a measure of the patient's quality of life, where 0 is perfect health and increasing score indicates diminishing quality of life leading to a maximum score of 5 (death). These performance scores aid in the assessment of the urgency of treatment.

It is now appreciated that the latter of the two factors (likelihood of response to treatment) is highly dependent on the cytogenetic and molecular genetic defects which are present at the time of diagnosis. Early studies noted that the response of patients to the standard treatment regimens was highly variable; but that cytogenetic status (the presence or absence of chromosome translocations, deletions or aneuploidy) was a strong prognostic indicator of clinical outcome (Estey, E. and Dohner, H. 2006). Using the cytogenetic status of the patient at diagnosis, patients are stratified into three prognostic groups (favourable, intermediate or poor) based on their likely clinical outcome. Cases in the favourable cytogenetic group are predominantly the core-binding factor AMLs positive for t(8;21), inv(16) or t(16;16) (CBFB-MYH11) or t(15;17) (PML-RARα). The reason for the favourable response of these patient to standard therapy is generally unclear, with the exception of acute promyelocytic leukaemia (APL) patients (harbouring a t(15;17) translocation), whose improved outcome is due to specific targeting of the molecular abnormality (the PML-RARα fusion protein) with ATRA (Flynn, P.J. *et al.* 1983). Patients in the intermediate prognostic group are predominantly those with normal cytogenetics (which represents 45% of all patients). Also included in this group are patients with trisomies (e.g. +11, +21). Patients with complex cytogenetics (3 or more abnormalities) or inv(3)/t(3;3) are consistently assigned to the poor prognostic group. There are several other AML associated cytogenetic abnormalities with disputed prognostic importance, with

disagreement mainly on whether these abnormalities confer intermediate or poor prognosis (Estey, E. and Dohner, H. 2006).

The prognostic value of cytogenetic status has been verified by several large studies (Grimwade, D. *et al.* 1998; Grimwade, D. *et al.* 2001; Slovak, M.L. *et al.* 2000). However, there is still considerable heterogeneity in clinical outcome within each prognostic group. Most puzzling to early investigators was the large variation of outcome in patients with no visible cytogenetic abnormalities. This observation suggested that in patients with normal cytogenetics, molecular genetic defects were the most likely determinants of clinical outcome. Subsequently, it has been shown that molecular genetic defects affecting NPM1, CEBPα, MLL, EVI1, BAALC and FLT3 do have significant prognostic value in AML patients with normal cytogenetics. Favourable prognostic markers include inactivating mutations of NPM1 and CEBPα, which are associated with better relapse-free and better overall survival, whilst MLL-PTD, overexpression of EVI1, overexpression of BAALC and presence of FLT3-ITD confer a poorer prognosis (Estey, E. and Dohner, H. 2006). In particular, FLT3-ITD is one of the most consistent indicators of poor outcome in patients with normal cytogenetics (Kottaridis, P.D. *et al.* 2001; Frohling, S. *et al.* 2002; Valk, P.J. *et al.* 2004). Although N-Ras and K-Ras mutations are shown to be overrepresented in certain AML subtypes, e.g. those with t(3;5)(q21-25;q31-q35) or inv(16)(p13q22) respectively (Bowen, D.T. *et al.* 2005), there is little evidence that Ras mutations have prognostic significance (section 1.3.5.2).

Studies of co-expression of several prognostic indicators suggest that it is difficult to predict which prognostic factor will be dominant, but evidence from AML patients with normal cytogenetics suggest that in general, poor prognostic markers are dominant over favourable ones. For example, the favourable effect of NPM1 mutation is nullified by the co-expression of FLT3-ITD (Schnittger, S. *et al.* 2005). In addition, co-expression of poor prognostic markers such as FLT3-ITD and BAALC appears to have an additive effect (Baldus, C.D. *et al.* 2006). In contrast to studies of patients with normal cytogenetics, the prognostic influence of molecular abnormalities in AML patients with abnormal cytogenetics is less clear; however in general the cytogenetic abnormality appears to be dominant. However, activating mutations of c-KIT have been shown to negatively affect prognosis of patients with favourable cytogenetics i.e. t(8;21) and inv(16) (Care, R.S. *et al.* 2003; Cairoli, R. *et al.* 2006; Schnittger, S. *et al.* 2006), demonstrating that molecular defects can have some influence on prognosis, even in core-binding factor AML. Table 1.1 summarises the prognostic effects of the most common molecular

abnormalities found in some types of AML with normal (diploid) and abnormal cytogenetics.

Molecular abnormality	AML subtype	Disease-free survival	Overall survival
MLL PTD	Diploid, trisomy 11	Shortened	None
FLT-3 mutations	Diploid	Shortened	Shortened
FLT-3 mutations	APL	None	None
↑ BAALC mRNA	Diploid	Shortened	Shortened
CEBPα mutation	Diploid	Prolonged	Prolonged
NPM mutation	Diploid	Prolonged	Prolonged
WT-1	All subtypes	Not reported	Shortened
NRAS mutation	All subtypes	None	None
c-KIT mutation	inv(16), t(8;21)	Shortened	Shortened
↑ ERG mRNA	Diploid	Shortened	Shortened
↑ EVI1 mRNA	3q26, unfavourable	Shortened	Shortened

Table 1.1 Prognostic influence of some common molecular abnormalities detected in AML

MLL PTD = mixed lineage leukaemia partial tandem duplication; FLT-3 ITD = FMS-like tyrosine kinase-3 internal tandem duplication; BAALC = brain and acute leukaemia cytoplasmic; CEBPα = CCAAT/enhancer binding protein-α; NPM = nucleophosmin; WT-1 = Wilms tumor-1; ERG = ETS-related gene; APL = acute promyelocytic leukaemia. Adapted from Ravandi *et al.* (Ravandi, F. *et al.* 2007).

1.2.1.4 Therapy

Broadly speaking, the aim of any AML therapy is to induce a complete remission of the disease (less than 5% blasts in peripheral blood and marrow), followed by consolidation therapy to maintain the remission. How this is achieved for each patient is decided after consideration of the patient's fitness, likelihood of imminent disease progression, and their genetic prognostic indications (as described in section 1.2.1.3).

Amongst younger patients (<60 years old), standard '3+7' induction regimens (intravenous (iv) administration of daunorubicin (which is known to generate ROS production and also intercalates into DNA stalling replication) for 3 days followed by i.v. cytarabine (a nucleoside analogue aka ara-C) over 7 days)) results in complete remission of 65-75% of patients (Estey, E. and Dohner, H. 2006). Subsequently, younger patients with favourable risk are currently treated with high-dose cytarabine as a consolidation therapy, which leads to sustained remission in 60-75% of cases. Although the same approach leads to lower overall survival in the intermediate prognostic groups, it is still the approach of choice in the light of evidence that autologous and allogeneic stem-cell transplants (SCTs) offer no significant benefit. Less than 10% of patients in the poor risk group maintain remission with standard high-dose cytarabine consolidation after induction therapy. Under these conditions, there is evidence that allogeneic SCT may improve this dismal outcome. Alternatively, patients in the poor prognostic group (or those with better genetic prognoses but are considered unlikely to survive standard induction therapy) can opt to enrol in clinical trials and receive investigational therapy or choose palliative care. Perhaps unsurprisingly, in elderly patients (>60 years) the situation is correspondingly worse in each risk group, with 20% of patients surviving 2 years after diagnosis partly due to a higher chance of death during standard induction regimens. As a result, the majority of elderly patients are offered investigational therapy or palliative care.

In some cases where complete remission is achieved by induction therapy, the disease later relapses, suggesting that drug resistant clones (LSCs) remain after induction therapy that are capable of re-establishing the disease (section 1.2.1.2). Indeed, it is often possible to detect markers of minimum residual disease (MRD) in patients which have achieved remission, either through PCR-based methods (used mostly to detect fusion transcripts e.g. PML-RARα (Lo, C.F. *et al.* 1999)) and flow cytometric methods to monitor the presence of abnormal blasts by virtue of their often aberrant surface marker expression (Vidriales, M.B. *et al.* 2003).

Several studies have examined whether clinical outcome could be improved using less-toxic analogues of the mainstay drugs cytarabine (e.g. clofarabine) and

daunorubicin (e.g. doxorubicin, idarubicin, epirubucin), as well as combination therapy with topoisomerase inhibitors (etoposide and mitoxantrone). However, in general these studies have failed to demonstrate any significant improvement in outcome (Estey, E. and Dohner, H. 2006). New agents are currently undergoing clinical trials; many of them targeting recently discovered molecular abnormalities, for example lestaurinib (CEP-701) and PKC412 are small-molecule inhibitors of FLT3-ITD. Both these agents have demonstrated a clinical effect, but this effect is not sustained (Knapper, S. 2007). In summary, treatment of AML remains a difficult task, especially for those younger patients assigned to intermediate and poor prognostic groups; and elderly patients in general.

1.3 RAS PROTEINS

1.3.1 AN OVERVIEW OF THE RAS SUPERFAMILY

The Ras (rat sarcoma) protein superfamily of small GTPases currently consists of ~170 described isoforms encoded by ~160 genes (in humans), grouped into 5 main subfamilies: Ras, Rho, Rab, Ran and Arf (Wennerberg, K. *et al.* 2005). Members of this large protein family participate in diverse cellular functions, with members within each subfamily grouped together mainly on the basis of structural similarity. For example, members of the Ras subfamily are primarily involved in proliferation and survival signalling; Rab and Arf subfamilies govern vesicular transport; Ran participates in nuclear/cytoplasmic shuttling of RNA and protein, and Rho subfamily members are primarily involved in cytoskeletal remodelling. There is also evidence that Ras subfamily members (e.g. H-Ras and K-Ras) also play an important role in development, since hereditary activating mutations in Ras signalling pathways have been detected in congenital developmental disorders (Schubbert, S. *et al.* 2007). There are also several Ras superfamily proteins which do not appear to fall into the five main subfamilies, and may represent novel subfamilies, e.g. the Miro proteins which play important roles in mitochondrial biogenesis and homeostasis (Wennerberg, K. *et al.* 2005).

All Ras superfamily proteins contain a conserved G domain which is homologous to the GTP-binding domain found in the α subunit of heterotrimeric G-proteins (Karnoub, A.E. and Weinberg, R.A. 2008). The G domain contains several conserved 'G motifs', which form the guanine nucleotide binding pocket (phosphate-binding or P-loop) and also confer a weak intrinsic GTPase activity. Ras superfamily proteins are activated when bound to GTP, and generally inactive when bound to GDP; although in the case of Rab, Ran and Arf proteins, the GDP-bound form may also

participate in signalling processes distinct from those of the GTP-bound form (Wennerberg, K. *et al.* 2005). Thus Ras superfamily members all act as binary molecular switches, in general providing an 'on' or 'off' signal depending on whether GTP or GDP is bound respectively.

X-ray crystallographic studies of Ras proteins bound to either GDP or GTP show that large conformational changes are induced in the Ras protein when GDP is exchanged for GTP and vice-versa (Milburn, M.V. *et al.* 1990; Schlichting, I. *et al.* 1990). Moreover, these conformational changes are localised to two flexible loop regions which are termed Switch I and Switch II. Switch regions I and II are critical for Ras superfamily protein signalling and regulation because it is via these regions that Ras proteins make physical contact with their downstream effectors and also upstream regulators (Karnoub, A.E. and Weinberg, R.A. 2008). Accordingly, the switch regions are present in all of the Ras superfamily proteins.

By virtue of their weak intrinsic GTPase activity, Ras proteins can hydrolyse bound GTP to form GDP and inorganic phosphate; thus activated Ras molecules are intrinsically capable of self-limiting their activation. However, efficient GTP hydrolysis requires the presence GTPase activating proteins (GAPs) which greatly augment the intrinsic GTPase activity of Ras proteins and thus act as negative regulators. X-ray crystallographic studies of Ras proteins complexed with GAPs e.g. neurofibromin (NF1), revealed that a conserved arginine finger domain within the GAP protein inserts into the nucleotide binding pocket on the Ras protein. This arginine residue stabilises a transition state during the catalytic hydrolysis of GTP; and the lowered activation energy for this step of the reaction results in (approximately) a 1000 fold increase in GTPase activity. Thus, GAPs promote the rapid accumulation of GDP-bound Ras (Ahmadian, M.R. *et al.* 1997).

Whereas GAPs are negative regulators, the guanine nucleotide exchange factors (GEFs) are positive regulators of Ras proteins. GEFs associate with inactive GDP-bound Ras proteins and induce a conformational change which promotes the release of GDP. Since GTP is approximately 10-fold more abundant inside the cell than GDP (Karnoub, A.E. and Weinberg, R.A. 2008), GTP preferentially binds, and the Ras protein is activated.

In addition to GAPs and GEFs, Rho-guanine nucleotide dissociation inhibitors (Rho-GDIs) are a unique group of proteins which specifically regulate Rho subfamily members (Sahai, E. and Marshall, C.J. 2002), including Rac. Rho-GDIs bind to and mask lipid groups of Rho proteins added by post-translational modification (these modifications are discussed below) and thus sequester them in the cytosol. Rho proteins bound by Rho-GDI remain in the GDP-bound state and are therefore inactive.

Most of the Ras superfamily proteins require post-translational attachment of lipid molecules before they are able to function. For the majority of Ras and Rho subfamily proteins (which are the best studied), this modification occurs in four stages. First, the newly-translated Ras molecule is prenylated in the cytosol by farnesyl transferase (FT) or geranylgeranyl transferase I, which attach either farnesyl or geranylgeranyl groups respectively to the Cys residue within a C-terminal 'CAAX' motif of the Ras protein (where A is an aliphatic amino acid and X is any amino acid). Second, prenylated Ras proteins then associate with the ER, where the C-terminal -AAX tripeptide is cleaved by Ras converting enzyme-1. Thirdly, the C-terminal cysteine is carboxymethylated by isoprenylcysteine carboxymethyltransferase-1 (Bivona, T.G. and Philips, M.R. 2003). There is evidence that these first three steps are necessary and sufficient to activate Ras subfamily proteins; prenylated H-Ras and K-Ras4A oncoproteins are capable of transforming murine fibroblasts without further post-translational modification (Hancock, J.F. *et al.* 1990). However, most Ras superfamily proteins undergo additional post-translational modifications to strengthen their association with the plasma membrane, sometimes referred to as the 'second signal'. This fourth step is required for efficient activation of ERK by H-Ras in *Xenopus* oocytes (Dudler, T. and Gelb, M.H. 1996) and may also be required for the full spectrum of Ras2 signalling in *S. cerevisiae* (Bhattacharya, S. *et al.* 1995) . For H-Ras, N-Ras and K-Ras4A, this palmitoylation step occurs during transit through the Golgi apparatus, and involves attachment of myristic acid or palmitic acid by myristoyltransferase or palmitoyltransferase (myristoylation or palmitoylation) of selected cysteine residues located N-terminal to the prenylated cysteine.

Some Ras superfamily members are exceptions to the process of post-translation modification described above. For example, whereas K-Ras4A undergoes the process described above, the closely related isoform K-Ras4B lacks the cysteine residues that are normally palmitoylated, and instead bears a basic poly-lysine sequence which appears to serve a similar role to palmitoylation in that it strengthens membrane association. Rab subfamily proteins do not possess a CAAX motif and are not prenylated by FT or geranylgeranyl transferase I, but instead encode one of several C-terminal sequences (CC, CXC, CCX, CCXX, or CCXXX), which are recognised and prenylated by geranylgeranyl transferase II. Finally, several Ras superfamily proteins do not undergo post-translational modification by lipids at all, for example Rit1, Rit2 and Miro proteins can associate with membranes despite a lack of prenylation, whilst Ran and Rerg lack any C-terminal motif containing cysteine, and do not require modification by lipids or association with membranes in order to function.

1.3.2 H-RAS, K-RAS AND N-RAS: FOUNDING MEMBERS OF THE RAS PROTEIN SUPERFAMILY

H-Ras (Harvey-Ras or Ha-Ras), K-Ras (Kirsten-Ras or Ki-Ras) and N-Ras (neuroblastoma-Ras) proteins were discovered during the late 1970s and early 1980s, and are the founding members of the Ras superfamily. They are the best-understood members of the Ras superfamily, and are the principal members of the subfamily of the same name, which (in humans) currently comprises 39 protein isoforms with molecular weights ranging from 20-29 KDa encoded by 36 genes (Wennerberg, K. *et al.* 2005). The endogenous wild-type genes encoding H-Ras and K-Ras proteins were identified in rats, mice and humans due to their homology with transforming retroviral oncogenes expressed by Harvey and Kirsten strains of MSV (murine sarcoma virus) (DeFeo, D. *et al.* 1981; Ellis, R.W. *et al.* 1982; Chang, E.H. *et al.* 1982). A short time later, an activated form of a third Ras gene, N-Ras, was isolated from neuroblastoma cells (Shimizu, K. *et al.* 1983); two different sarcoma cell lines (Hall, A. *et al.* 1983) and also in the HL60 leukaemia cell line (Murray, M.J. *et al.* 1983).

H-Ras (located on human chromosome 11p15.5), N-Ras (human chromosome 1p13.2), and the two known isoforms of K-Ras (K-Ras4A and K-Ras4B, generated by alternative splicing of the K-Ras gene on human chromosome 12p12.1) show a high degree of homology within the N-terminus, which contains the GTP binding G domain. In contrast, the C-terminal region shows considerable diversity when comparing isoforms, and is referred to as the hypervariable region (Figure 1.3). It is likely that differences in this region contributes to the differing subcellular localisation of each different isoform (Bivona, T.G. and Philips, M.R. 2003). In the case of H-Ras, N-Ras and K-Ras, the CAAX motif is farnesylated on the conserved cysteine by FT, although N-Ras and K-Ras can be geranylgeranylated in the presence of FT inhibitors (Whyte, D.B. *et al.* 1997).

H-Ras, N-Ras and K-Ras4A all undergo subsequent palmitoylation on one or two cysteine residues near the farnesylation site (Figure 1.3). In addition, these proteins bind a single Mg^{2+} ion, which plays a role in the guanine nucleotide-binding interaction in the mature folded form.

The tertiary structure of these proteins is globular, with a hydrophobic core composed of five α-helices and six β-sheets, linked together by 10 polypeptide loops. Five of these loops are of particular importance for Ras protein function; loops 1, 2, and 4 form the guanine nucleotide binding pocket, with loop 1 (the phosphate loop or P-loop spanning amino acids 10-17) forming a close association with the guanine nucleotide phosphate groups. The two remaining loops (3 and 5) form switch regions I and II, spanning amino

acids 30-38 and 59-67 respectively. The conformational changes induced by GTP-binding in switch I and II form a distinct 3-dimensional surface on the Ras protein which are recognised and bound by downstream effectors of Ras. These same switch regions are also the binding sites for the upstream regulators of Ras, the RasGAPs and RasGEFs, which recognise the conformation of the switch regions when bound to either GTP or GDP respectively (section 1.3.3).

Early investigations into the biochemical basis of oncogenic transformation by Ras mutants noted that activating mutations of the Ras protein were clustered in codons 12 and 13 (within the P-loop) and 61 (within switch II) (Krengel, U. *et al.* 1990); and also that the intrinsic GTPase activity of these mutant proteins was greatly reduced when compared to the normal alleles, even in the presence of GAPs (Gibbs, J.B. *et al.* 1984; McGrath, J.P. *et al.* 1984; Sweet, R.W. *et al.* 1984). Subsequent studies have revealed that amino acids at these positions (12, 13 and 61) play critical roles in the mechanism of intrinsic GTP hydrolysis by Ras. In each Ras isoform, the 12^{th} and 13^{th} codons encode glycine, which is the only amino acid without a side chain. Therefore, any mis-sense mutation at these positions leads to inclusion of an amino acid with a side chain. The most common substitutions in human cancers replace glycine with valine or aspartate at these positions. The bulky side chains of these residues case a steric clash with the side chains of catalytic residues during GTP hydrolysis, resulting in a drastic decrease in GTPase activity (Schubbert, S. *et al.* 2007). Thus, substitutions at codons 12 or 13 lead to an accumulation of GTP-bound (and therefore activated) Ras. Codon 61 encodes a conserved glutamine residue which forms an important hydrogen bond with the catalytic arginine of GAPs during GAP-assisted GTP-hydrolysis (Karnoub, A.E. and Weinberg, R.A. 2008) and loss of this interaction (by substitution of the conserved glutamine) severely impairs GTP hydrolysis, again resulting in the accumulation of GTP-bound Ras.

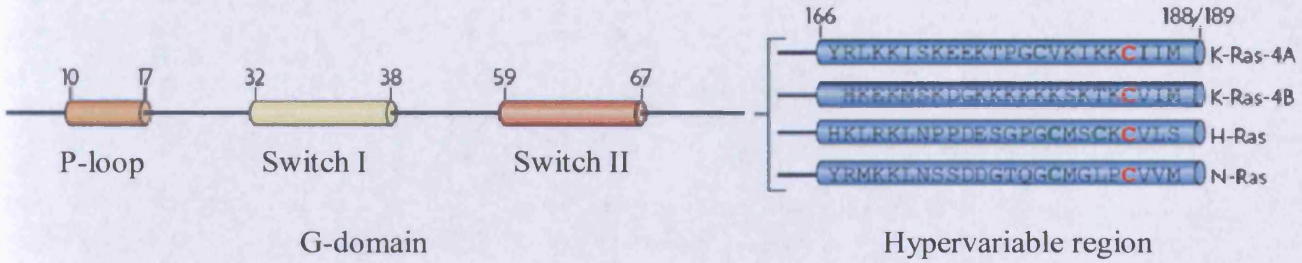

Figure 1.3 The primary structure of classical Ras proteins

H-Ras, N-Ras and K-Ras4A and K-Ras4B are 188-189 amino acids in length. Each of these isoforms has an almost identical sequence for the first 165 amino acids (spanning the conserved GTP-binding G-domain). Within the G-domain are the phosphate-binding P-loop and switch regions I and II. The switch regions are the location of dynamic conformational changes when GDP is exchanged for GTP, and it is the conformation of these switch regions that are recognised and bound by Ras upstream regulators and downstream effectors. The last ~20 amino acids show considerable heterogeneity and are referred to as the hypervariable region. Within this region, there is a conserved CAAX motif which is the site of Ras prenylation by prenyltransferases such as FT. The prenylated cysteine within this motif is highlighted in red. With the exception of K-Ras4B, Ras proteins also contain some additional cysteine residues which are the site(s) of palmitoylation (highlighted in green). K-Ras4B (the most abundant of the two K-Ras isoforms) has no additional cysteine residues, but instead contains a polybasic string of lysine residues. The net positive charges of these residues interacts with the negatively charged phospholipid heads in the plasma membrane thus serving a similar role to palmitoylation. Adapted from Karnoub, 2008 (Karnoub, A.E. and Weinberg, R.A. 2008).

1.3.3 RAS SIGNALLING IN HAEMATOPOIETIC CELLS

1.3.3.1 Upstream regulation of Ras activity

The principal known function of Ras proteins is to transduce signals from the cytoplasmic domains of activated growth factor receptors to downstream effectors, resulting in cell cycle progression, survival and increased cell motility. H-Ras, N-Ras and K-Ras4B are all expressed in mammalian haematopoietic cells, although N-Ras and K-Ras4B are most abundant (Shen, W.P. *et al.* 1987), and function as common downstream effectors of the majority of haematopoietic growth factor-receptors, including FLT3-L, SCF, IL-3, G/GM-CSF and EPO. The sequence of events that connect growth factor binding to Ras protein activation are very similar for each receptor, and ultimately result in the recruitment and activation of RasGEFs (primarily son of sevenless (SOS) proteins) which promote the accumulation of activated GTP-bound Ras. This process is summarised in Figure 1.4.

In general, binding of growth factors to their cognate receptors induces conformational changes in the cytoplasmic regions of the receptors which drive phosphorylation of tyrosine residues within the cytoplasmic tail of the receptor (section 1.1.3.4). In the case of RTKs this is an autophosphorylation event, while type I and type II cytokine receptors become phosphorylated after activation of associated JAK kinases. Phosphorylated tyrosine residues in the cytoplasmic tail of activated growth factor receptors form docking sites for proteins containing an SH2 domain. One such protein is the adaptor molecule GRB2, which links the activated receptor to SOS family proteins, which are RasGEFs. Together with additional adaptor proteins (SHC and Gab family proteins), this complex co-localises SOS proteins with membrane-bound Ras-GDP, which is then converted by SOS to the active GTP-bound form. Recruitment of the tyrosine phosphatase SHP2 to the activated receptor complex (via binding to Gab) is also required for efficient Ras signalling. SHP2 is somewhat unusual in that, unlike most phosphatases, it is a positive regulator of signalling, although the exact manner in which it promotes Ras activation is not understood. For example, mice with homozygous deletion of a large portion of the *Ptpn11* gene (encoding Shp2) die during embryogenesis due to improper gastrulation, and fibroblasts from these mice show decreased responsiveness to FGF and EGF (Matozaki, T. *et al.* 2009).

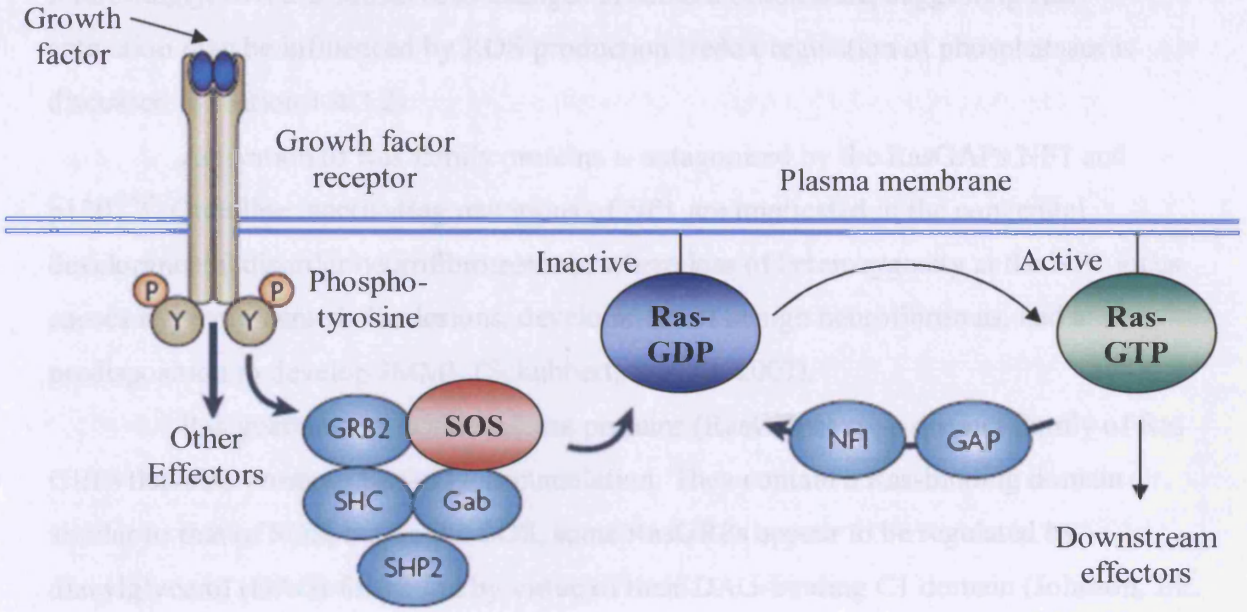

Figure 1.4 Activation of Ras by growth factor receptors

The diagram depicts a typical scheme whereby Ras proteins are activated following binding of a growth factor (e.g. FLT3L) to its receptor. Growth factor-induced dimerisation of growth factor receptors results in phosphorylation of tyrosine residues in the cytoplasmic tail of the receptor. Phosphotyrosine forms binding sites for proteins containing SH2 domains, such as GRB2, SHC, Gab and the tyrosine phosphatase SHP2. GRB2 is an adaptor protein which is tethered to SOS, a RasGEF, thus, recruitment of GRB2 and SOS to the activated receptor co-localises SOS with membrane bound Ras-GDP. SOS promotes binding of GTP to Ras and Ras then binds and activates its downstream effectors. SOS is antagonised by the RasGAPs NF1 and $p120^{GAP}$ (labelled GAP) which accelerate the intrinsic GTPase activity of Ras proteins and thus inactivate them. H-Ras, N-Ras and K-Ras all follow a similar route to activation, but the distinct subcellular localisation may restrict access of each isoform to a specific subset of effectors, which may result in a degree of non-redundant signalling for each isoform. Indeed, it is important to note that this diagram depicts activation of Ras at the plasma membrane, however, activation of Ras by extracellular growth factors has been reported on endomembranes, though the mechanism by which this occurs is poorly understood. Adapted from Schubbert *et al.* (Schubbert, S. *et al.* 2007).

Conversely, mutations in SHP2 that result in constitutive activation of the Ras pathway are closely associated with developmental disorders such as Noonan's and cardio-facio-cutaneous (CFC) syndromes, and are also frequently detected in JMML. Interestingly, SHP2 is sensitive to changes in cellular redox state, suggesting Ras activation may be influenced by ROS production (redox regulation of phosphatases is discussed in section 1.4.3.2).

Activation of Ras family proteins is antagonised by the RasGAPs NF1 and $p120^{GAP}$. Germline inactivating mutations of NF1 are implicated in the congenital developmental disorder neurofibromatosis, where loss of heterozygosity at the NF1 locus causes hyperpigmented skin lesions, development of benign neurofibromas, and a predisposition to develop JMML (Schubbert, S. *et al.* 2007).

Ras guanine-nucleotide release proteins (RasGRPs) are a distinct family of Ras GEFs that also promote Ras-GTP accumulation. They contain a Ras-binding domain similar to that of SOS, but unlike SOS, some RasGRPs appear to be regulated by diacylglycerol (DAG) formation by virtue of their DAG-binding C1 domain (Johnson, J.E. *et al.* 2007), and may therefore be regulated by phospholipases in an analogous manner to protein kinase C (PKC) (section 1.3.3.2).

In addition to the actions of RasGAPs and GEFs, subcellular localisation of the Ras protein may also play a role in regulating Ras signalling. As discussed in section 1.3.2, H-Ras, N-Ras and K-Ras4B undergo a primary farnesylation step, followed by palmitoylation ('the second signal') to generate mature Ras proteins. However, while the site of farnesylation is conserved in each isoform, the site(s) of palmitoylation differ due to unique sequences in the hypervariable region upstream of the CAAX motif. Indeed, it is believed that this unique 'second signal' contributes to the different subcellular localisation of each isoform. For example, mature H-Ras and N-Ras can be detected in both the plasma membrane and the Golgi under normal conditions, whereas K-Ras4B (which is not palmitoylated) is located solely in the plasma membrane. Furthermore, within the plasma membrane there is a preference of some isoforms for particular membrane microdomains; for example H-Ras is primarily associated with lipid-rafts, while K-Ras4B is located in the bulk plasma membrane. Indeed, it has been demonstrated (at least in yeast) that forced localisation of *S. pombe* Ras1 to either the ER ($Ras1^{C215S}$ mutant) or plasma membrane (recombinant Ras1 fused to RitC plasma membrane-targeting sequence) selectively blocked sexual maturation or adoption of a normal morphology respectively (Onken, B. *et al.* 2006), suggesting that Ras signalling may have different consequences depending the subcellular origin of the signal (presumably some Ras1 effectors are themselves restricted

to the ER or plasma membrane which would allow such endomembrane-specific signalling to occur). This subcellular localisation may offer an explanation as to how mammalian Ras isoforms with similar sequences can have such diverse (and in some cases) non-redundant functions, for example, K-Ras-null mice are not viable (Koera, K. *et al.* 1997), whereas N-Ras and/or H-Ras-null mice are viable and fertile (Esteban, L.M. *et al.* 2001). There is also evidence for cyclical depalmitoylation of mature N-Ras and H-Ras which results in retraction of these proteins from the plasma membrane and re-entry into the Golgi, where they may be re-palmitoylated and returned to the plasma membrane. This cycle may be important for regulation of Ras activity and access to its effectors; indeed it has been demonstrated in mammalian cells that endogenous Ras proteins resident in the ER and Golgi can respond to stimulation by EGF within minutes, and that ER-restricted H-Ras is capable of activating ERK, after EGF treatment, suggesting that Ras signalling on endomembranes may be an important addition to signalling originating from the plasma membrane (Chiu, V.K. *et al.* 2002). However, the significance of these mechanisms for Ras signalling in haematopoietic cells has not been explored.

1.3.3.2 Ras effectors and downstream signalling

After Ras has bound to GTP, switch regions I and II adopt conformations which form binding sites for a variety of downstream effectors. The first of these to be discovered was Raf, a serine/threonine kinase which (like Ras) was known to be the cellular homologue of a known retroviral oncogene. Raf was shown to directly bind Ras-GTP (Warne, P.H. *et al.* 1993; Zhang, X.F. *et al.* 1993) and was also shown to be important in mediating the phenotype of mutant Ras in *C. elegans* (Han, M. *et al.* 1993). Later, Raf itself was shown to be mutated at a surprisingly high frequency in human cancer, particularly the V600E constitutively active mutant (Davies, H. *et al.* 2002). Binding of Raf to Ras-GTP activates Raf, which resides at the start of the first serine/threonine kinase cascade to be characterised, the Raf-MEK-ERK signalling pathway, the architecture of which was subsequently found to be common among several kinase cascades. Activated ERK (a serine/threonine kinase) phosphorylates and activates several protein targets, notably, Elk, c-Myc, c-Jun and c-Fos transcription factors. Phosphorylation of c-Myc by ERK promotes heterodimerisation with Max, a c-Myc co-activator. c-Myc-Max dimers act as transcription factors activating several genes including the cyclin D genes (Grandori, C. *et al.* 2000). c-Myc also forms heterodimers with Miz and c-Myc-Miz dimers are transcriptional repressors which downregulate the transcription of several cell cycle inhibitor genes (Seoane, J. *et al.* 2002), which are discussed further in section 1.3.4.3.

c-Jun and c-Fos heterodimerise forming the activating protein-1 (AP-1) family of transcription factors, which promote cell cycle entry via direct transactivation of the cyclin D1 gene (*CCND1*) and downregulation of p53, $p21^{Cip1}$ and $p16^{INK4A}$, which are negative regulators of the cell cycle (Shaulian, E. and Karin, M. 2002). Thus, activation of the Raf-MEK-ERK pathway by Ras results in a strong drive towards proliferation.

A short time after the discovery of Raf as an effector of Ras, Julian Downward and co-workers demonstrated that Ras-GTP also bound the catalytic subunit (p110) of PI3K (Rodriguez-Viciana, P. *et al.* 1994), which confirmed a previous report by Sjolander *et al.* (Sjolander, A. *et al.* 1991). PI3K activation by growth factor-receptors was already appreciated at that time, but the placement of Ras-GTP upstream of PI3K activation was a significant step forward in the understanding of Ras biology. PI3K kinases are heterodimeric lipid kinases consisting of the catalytic subunit and a regulatory subunit (p85), which catalyse the addition of inorganic phosphate groups to the 3' position of the inositol ring of phosphatidylinositol-(4,5)-diphosphate (PIP_2) on the inner leaflet of the plasma membrane, forming $PI(3,4,5)P_3$ (PIP_3). PIP_3 forms a binding site at the membrane for proteins containing a Pleckstrin homology (PH) domain, and in general, binding of PH domain-containing proteins to PIP_3 co-localises them with upstream regulators and downstream effectors which may also be localised to the plasma membrane. One of the key downstream effectors of PI3K is Akt (aka PKB), a serine/threonine kinase which is recruited to the plasma membrane by binding of its PH domain to PIP_3 and is subsequently phosphorylated by phosphoinositide-dependent kinase-1 (PDK1) on Ser 308, and by mammalian target of rapamycin (mTOR) on Ser 473. Akt thus phosphorylated is active, and is an important mediator of anti-apoptotic signalling (Osaki, M. *et al.* 2004). The substrates of Akt are many, and include phosphorylation and inactivation of forkhead box-O (FOXO) transcription factors, the pro-apoptotic protein Bad; and also activation of IKKα (a positive regulator of NF-κB signalling). Akt also contributes to cell cycle progression by direct phosphorylation of $p21^{Cip1}$ and $p27^{Kip1}$, which results in sequestration of these proteins in the cytosol (Zhou, B.P. *et al.* 2001). Akt also phosphorylates and deactivates TSC2, an inhibitor of mTOR. mTOR plays an important role in regulating protein synthesis (and therefore growth), primarily by activating p70S6K, which in turn phosphorylates ribosomal protein S6, which accelerates ribosomal protein translation. mTOR also releases eIF4E from inhibition by 4-EBP allowing eIF4E to bind to the 7-methyl-guanosine cap of mRNAs and guide them to the ribosome for translation.

Opposing the activation of Akt (and other PH domain-containing proteins) by PI3K are the lipid phosphatases phosphatase and tensin homologue (PTEN) and SHIP.

These phosphatases catalyse the removal of either the 3' or 5' phosphate group from PIP_3 respectively, rendering these lipids unattractive for PH domain-binding. Loss of PTEN is a common occurrence in a variety of cancers, most notoriously in colon carcinomas (Goel, A. *et al.* 2004), resulting in hyperactive PI3K signalling and aberrant Akt activation.

Just a few months after Julian Downward identified PI3K as a Ras effector, a third Ras effector was identified, RalGDS (Hofer, F. *et al.* 1994), a member of a family of proteins which are now known to be GEFs for RalA and RalB. Ral proteins are small GTPases belonging to the Ras superfamily and follow some of the conventions of the other family members. Activated Ral (bound to GTP) plays an important role in vesicular trafficking mainly through its role in organising the Exocyst complex by acting directly on the Sec5 and Exo84 subunits of this hetero-octameric complex. Exocyst then orchestrates sorting of proteins into exocytic vesicles and their tethering to the appropriate plasma membrane domains prior to excretion. In addition, Ral proteins also positively regulate ZONAB, a Y-box transcription factor which can promote cell cycle progression through transactivation of the genes encoding cyclin D1 and PCNA (Bodemann, B.O. and White, M.A. 2008). In a haematopoietic context, Ral proteins have been shown to mediate the block in granulocytic differentiation of murine haematopoietic cells by mutant Ras (Omidvar, N. *et al.* 2006).

Raf, PI3K and RalGDS represent the principal molecules of the three best characterised Ras effector pathways, activation of which results in a consensus drive towards increased proliferation and cell survival. Additional effectors of Ras have been identified, such as TIAM1 and phospholipase C-ϵ (PLCϵ), which intersect with pathways and signalling proteins of interest. TIAM1 is activated by Ras-GTP and is a GEF for the Rac subfamily of small GTPases. Rac proteins play important roles in cytoskeletal remodelling, and are therefore important components in the mechanisms that govern cell motility, phagocytosis and other cellular functions where movement of the cell is required. Rac proteins also form a key component of several NOX family oxidase complexes which are responsible for generating superoxide in phagocytic and non-phagocytic cells (Rygiel, T.P. *et al.* 2008) (section 1.4.2.1 and Figure 1.5; also see Figure 1.11).

PLCϵ is a relatively recent addition to the phospholipase C family, and represents a fourth class of phospholipase enzymes (in addition to PLCβ, PLCγ and PLCδ). In addition to the PLC domains (which bind the Gα subunit of activated G-proteins), PLCϵ contains two C-terminal Ras-binding domains (RA1 and RA2) similar to that found in Raf

proteins. Indeed, Ras-GTP has been demonstrated to bind to and activate PLCϵ in an RA domain-dependent manner (Kelley, G.G. *et al.* 2001).

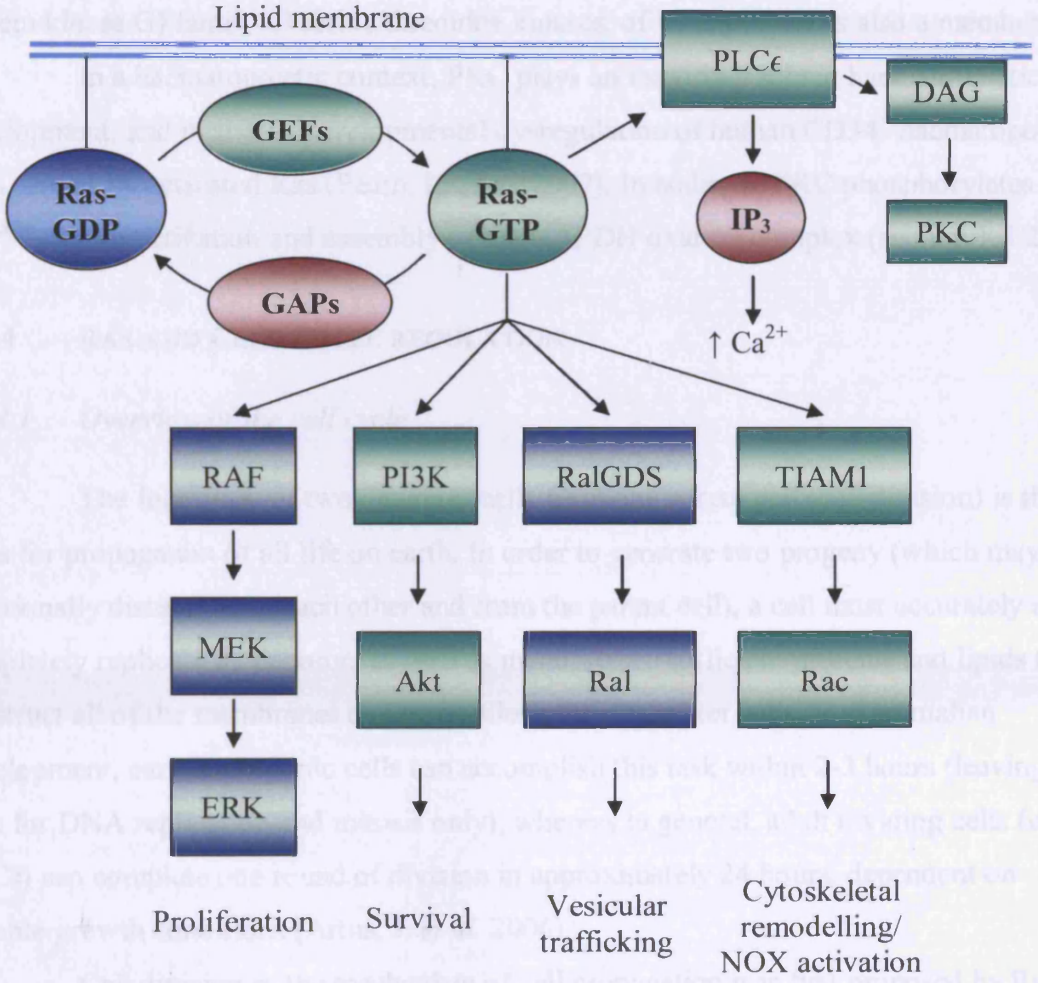

Figure 1.5 Important Ras effector pathways

Activation of Ras initiates several signalling pathways, including the Raf-MEK-ERK serine/threonine kinase cascade, the PI3K-Akt pathway, the Ral pathway and the Rac pathways via activation of the Rho-family GEF TIAM1. In addition, Ras activates PKC by activating PLCϵ. PLCϵ generates IP_3, which in turn increases cytosolic Ca^{2+}, and also generates DAG which binds to and activates PKC. Details of these pathways are discussed in the text.

Upon activation, PLCϵ (like other PLC family members) cleaves PIP_3 forming membrane-bound DAG and releasing IP_3 into the cytosol. IP_3 binds to and opens IP_3-gated Ca^{2+} channels in the ER, releasing Ca^{2+} into the cytoplasm. Meanwhile, DAG forms a membrane binding site for classical and novel members of the PKC family of serine threonine kinases. PKCs are a subfamily of the AGC (protein kinase A, protein kinase G, protein kinase G) family of serine/threonine kinases, of which PDK1 is also a member.

In a haematopoietic context, PKC plays an important role in haematopoietic development, and mediates developmental dysregulation of human $CD34^+$ haematopoietic cells caused by activated Ras (Pearn, L. *et al.* 2007). In addition, PKC phosphorylates $p47^{phox}$ during activation and assembly of the NAPDH oxidase complex (section 1.4.2.1).

1.3.4 Ras and Cell Cycle regulation

1.3.4.1 Overview of the cell cycle

The formation of two daughter cells from one parent cell (cell division) is the basis for propagation of all life on earth. In order to generate two progeny (which may be functionally distinct from each other and from the parent cell), a cell must accurately and completely replicate its genome, as well as manufacture sufficient proteins and lipids to construct all of the membranes and organelles of the daughter cells. In mammalian development, early embryonic cells can accomplish this task within 2-3 hours (leaving time for DNA replication and mitosis only), whereas in general, adult dividing cells (e.g. HSCs) can complete one round of division in approximately 24 hours, dependent on suitable growth conditions (Artus, J. *et al.* 2006).

Cell division as the mechanism of cell propagation was first proposed by Rudolf Virchow and colleagues during the 19^{th} century, as an alternative to the prevailing theories of the day (Mazzarello, P. 1999). However, the mechanisms by which this process was orchestrated remained a mystery, until Tim Hunt and colleagues identified a family of proteins in sea urchin cells that were cyclically synthesized and degraded during cell division in an oscillating manner (Evans, T. *et al.* 1983). These proteins were named cyclins, and subsequent work has shown that cyclins play a critical role in directing the ordered sequence of events that constitute cell division, referred to as the cell cycle. The cell cycle is divided into four consecutive phases; Gap 1 (G_1), Synthesis (S), Gap 2 (G_2) and Mitosis (M) (Figure 1.6). During the G_1 and G_2 phases, the dividing cells pause while proteins and organelles are synthesised for the subsequent phase; this pause also provides time for the cell to respond to intracellular or extracellular signals which can regulate cell

cycle progression. During S phase, the entire genome of the cell is replicated. Finally, during M phase, the genome is packaged into condensed mitotic chromosomes and the chromosomes are segregated equally to the far corners of the parent cell. Subsequently, the parent cell physically cleaves in two, yielding two daughter cells in a process called cytokinesis. Some embryonic cells are an exception to this scheme in that they have shortened or absent G_1 and G_2 phases, and this lack of G_1 and G_2 phases means that the cells have little or no time to grow (acquire mass) between divisions and hence become smaller with each round of the cycle (a requirement during early embryogenesis). Cells may also occupy a fifth state, G_0, which is a quiescent state occupied by cells that are not currently participating in the cell cycle. Cells in G_0 include those that have temporarily ceased dividing, as well as those which have terminally differentiated and permanently lost the ability to enter the cell cycle.

1.3.4.2 Cyclin-dependent kinases drive the cell cycle

During the cell cycle, the transition from one phase to the next is driven by the activities of a family of serine/threonine kinases called cyclin dependent kinases (CDKs). Native CDKs are inactive due to an autoinhibitory domain which occludes the active site of the catalytic domain (Alberts, B. *et al.* 2002). However, binding of the CDK to its partner cyclin induces a conformational change in the CDK subunit which partially reveals the kinase domain. Thus the cyclical synthesis and degradation of cyclin proteins observed by Tim Hunt and colleagues causes a corresponding cyclical oscillation in CDK kinase activity. As shown in Figure 1.6, several different CDK-cyclin complexes exist, and each phase of the cell cycle is overseen by a single (or group of closely related) CDK-cyclin complex(es); CDK4/6-cyclin D activity is required to progress through the restriction point in late G_1 (section 1.3.4.4), CDK2-cyclin E/A are required for initiation of and transit through S phase respectively, and finally CDK1-cyclin B is required for initiation of mitosis in M phase.

The kinase activity of each of these CDK-cyclin complexes waxes and wanes in a regular fashion; each driving the transcription of genes required to progress to the next phase. For example, CDK2-cyclin E initiates replication complex firing at the start of S phase by phosphorylating and inactivating cell division cycle-6 protein, which restrains DNA replication by restraining the assembled origin of replication complexes (Borlado, L.R. and Mendez, J. 2008).

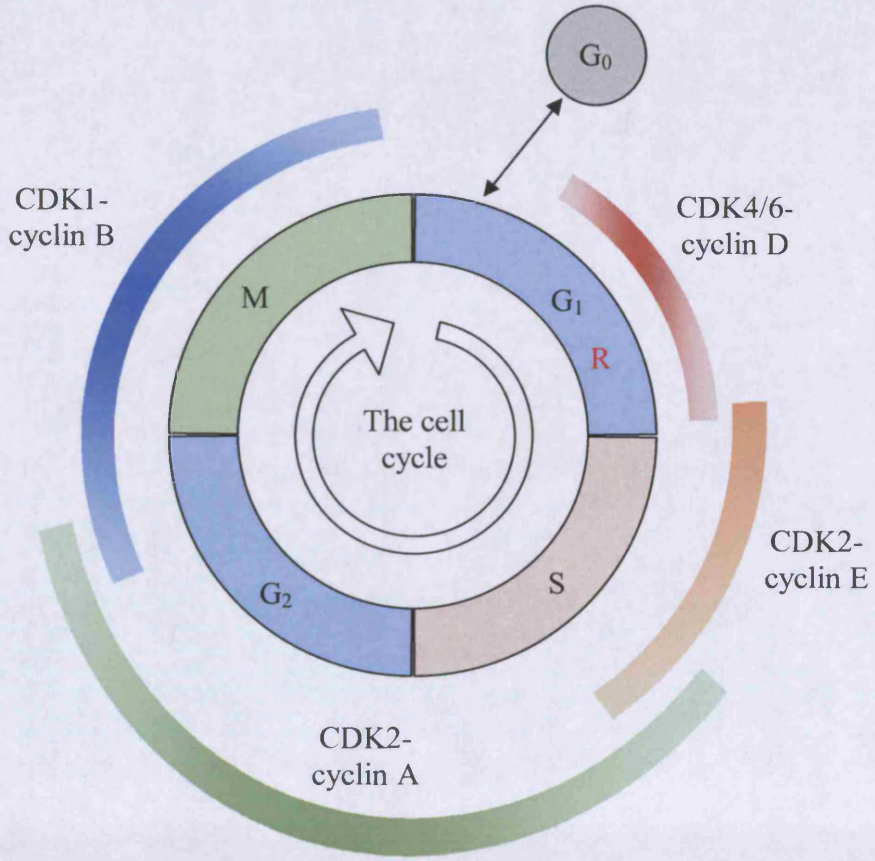

Figure 1.6 Phases of the mammalian cell cycle and timepoints over which each CDK-cyclin complex operates

The cell cycle consists of four phases which occur in the following sequence: G_1, S, G_2, M. Cells may exit the cell cycle temporarily or permanently and occupy a non-cycling state called G_0. Proliferative signals originating from Ras signal transduction pathways result in the upregulation of cyclin D, which promotes the activity of CDK4 and CDK6. CDK4 and CDK6 phosphorylate and inactivate the restriction point (R) enforcers, the retinoblastoma (Rb) proteins, allowing progression through the restriction point. Initiation of S phase is driven by CDK2 combined with cyclin E, exit from S phase and progression through G_2 is driven by CDK2-cyclin A. Finally, initiation of mitosis is driven by CDK1-cyclin B. The targeted destruction of cyclins is orchestrated by ubiquitin ligases which ensure that the activity of CDKs is controlled appropriately throughout the cycle.

During G_2, CDK2-cyclin A and CDK1-cyclin B phosphorylate nuclear lamins other constituents of the nuclear cytoskeleton in preparation for disintegration of the nuclear envelope prior to mitosis in M phase (Kill, I.R. and Hutchison, C.J. 1995).

Cyclins serve not only to activate CDKs but also direct their partner CDK to particular substrates. Additional substrate specificity may be imposed on CDKs due to phase-specific expression of some substrates; therefore, the substrates which can be phosphorylated by a given CDK depends on which stage of the cell cycle has been reached. Despite a degree of CDK substrate specificity, there is evidence of some functional redundancy among certain CDK-cyclin complexes, for example, mice lacking all three cyclin D1 genes die during gestation due to severe anaemia, suggesting that D-type cyclins are critical for HSCs to complete the cell cycle. However organogenesis in these embryos is generally normal, suggesting other CDKs (particularly CDK2-cyclin E) can perform the functions of CDK4 and CDK6 (Kozar, K. *et al.* 2004).

1.3.4.3 Positive and negative regulation of CDKs

The activity of CDKs is subject to several levels of regulation (Figure 1.7; black detail). CDK-cyclin complexes are regulated by both activating and inhibitory phosphorylation events. Although CDKs are partially activated by binding a partner cyclin, CDKs require phosphorylation on a conserved threonine residue by CDK-activating kinase (CAK) to fully expose the kinase domain and reach full activity (Drapkin, R. *et al.* 1996).

Wee1 kinase acts as a negative regulator of CDKs by phosphorylating two conserved residues near the catalytic domain which blocks kinase activity (Alberts, B. *et al.* 2002). These inhibitory phosphate groups can be removed by phosphatases of the cdc25 family (cdc25A and cdc25B). Thus CAK, Wee1 and cdc25 phosphatase form a CDK regulatory network which can be influenced by intracellular and extracellular stimuli.

In addition to regulation by phosphorylation, the availability and assembly of CDKs and cyclins is controlled by the expression of several cyclin-dependent kinase inhibitor (CDKI) proteins; the best understood of these are the inhibitor of kinase-4 (INK4) and $p21^{Cip1}$ families. The INK4 protein family ($p16^{INK4A}$, $p15^{INK4B}$, $p18^{INK4C}$ and $p19^{INK4D}$) share varying copy numbers of a conserved protein-binding domain called an ankyrin repeat, via which members of the INK4 family bind to CDK4 and CDK6 specifically. When bound to members of the INK4 family, CDK4 and CDK6 are unable to bind to their partner D-type cyclins and therefore remain inactive. The $p21^{Cip1}$ (aka $p21^{Waf1}$) family includes $p21^{Cip1}$, $p27^{Kip1}$ and $p57^{Kip2}$. This protein family is structurally distinct from the INK4 family, and contain N-terminal binding sites for both CDKs and cyclins.

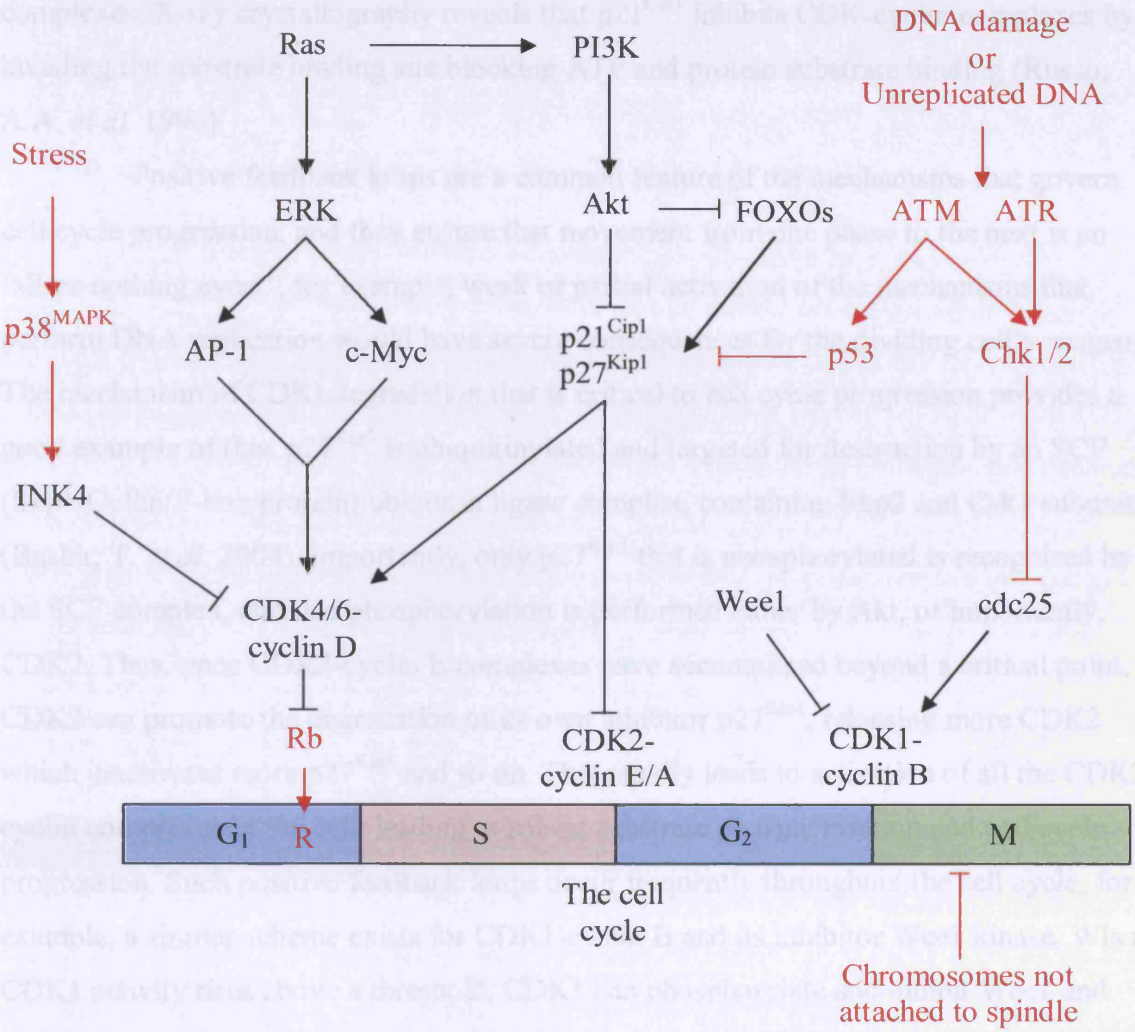

Figure 1.7 Cell cycle regulation networks and cell cycle checkpoints

The activities of CDKs are governed by a host of positive and negative regulators which transmit information about the environment and conditions to the cell cycle machinery. Not shown on the diagram is CAK, which phosphorylates and promotes activation of all CDKs. Several mechanisms exist to halt the cell cycle in the event of cell stress or damaged/unreplicated DNA. These mechanisms enforce a halt on the cell cycle at several defined points, known as cell cycle checkpoints. Unfavourable conditions or stress stimuli activate stress kinases such as $p38^{MAPK}$, which engage INK4 proteins and reinforce the Restriction point. Later on in the cell cycle, DNA damage or unreplicated DNA can lead to activation of p53 and $p21^{Cip1}$ and inhibition of cdc25. Finally, improperly aligned chromosomes during mitosis send negative signals which halt M phase until the chromosomes are mounted on the spindle.

Unlike INK4 proteins (which bind to CDK monomers), the $p21^{Cip1}$ family proteins main mode of action is to bind to and inhibit assembled CDK2-cyclin E/A complexes. X-ray crystallography reveals that $p21^{Cip1}$ inhibits CDK-cyclin complexes by invading the substrate binding site blocking ATP and protein substrate binding (Russo, A.A. *et al.* 1996).

Positive feedback loops are a common feature of the mechanisms that govern cell cycle progression, and they ensure that movement from one phase to the next is an 'all-or-nothing event'; for example, weak or partial activation of the mechanisms that perform DNA replication would have severe consequences for the dividing cell's progeny. The mechanism of CDKI degradation that is critical to cell cycle progression provides a good example of this. $p27^{Kip1}$ is ubiquitinylated and targeted for destruction by an SCF (Skp1/Cullin/F-box protein) ubiquitin ligase complex, containing Skp2 and Csk1 subunits (Bashir, T. *et al.* 2004). Importantly, only $p27^{Kip1}$ that is phosphorylated is recognised by the SCF complex, and this phosphorylation is performed either by Akt, or importantly, CDK2. Thus, once CDK2-cyclin E complexes have accumulated beyond a critical point, CDK2 can promote the degradation of its own inhibitor $p27^{Kip1}$, releasing more CDK2 which inactivates more $p27^{Kip1}$ and so on. This rapidly leads to activation of all the CDK2-cyclin complexes in the cell, leading to robust substrate phosphorylation and cell cycle progression. Such positive feedback loops occur frequently throughout the cell cycle, for example, a similar scheme exists for CDK1-cyclin B and its inhibitor Wee1 kinase. When CDK1 activity rises above a threshold, CDK1 can phosphorylate and inhibit Wee1 and rapidly accumulate to promote entry into M phase.

It is of interest to note that, in addition to binding to and inhibiting CDK2-cyclin E/A complexes, $p21^{Cip1}$ is also capable of binding to CDK4/6-cyclin D complexes, though (paradoxically) this does not inhibit CDK4/6 kinase activity (Sherr, C.J. and Roberts, J.M. 1999; Ortega, S. *et al.* 2002). Rather, $p21^{Cip1}$ family proteins actually promote assembly of CDK4/6-cyclin D complexes by virtue of their ability to bind both of the subunits and bring them into close proximity without inhibiting them, indeed active CDK4/6-cyclin D complexes precipitated from several mammalian cell types have been shown to also contain $p21^{Cip1}$ or $p27^{Kip1}$ (McConnell, B.B. *et al.* 1999; Parry, D. *et al.* 1999). $p21^{Cip1}$-assisted assembly of CDK4/6-cyclin D complexes has been demonstrated *in vitro* and *in vivo* (LaBaer, J. *et al.* 1997). In addition, mice deficient for $p21^{Cip1}$ or $p27^{Kip1}$ (or both) showed decreased CDK4-cyclin D1 complex formation (Cheng, M. *et al.* 1999). This feature of $p21^{Cip1}$ family proteins has the consequence that when cyclin D expression increases (e.g. upon Ras activation and downstream transcription of the cyclin D1 gene),

active CDK4/6-cyclin D complexes assemble, and sequester $p21^{Cip1}$ family proteins, which relieves CDK2-cyclin E inhibition and allows CDK2 to function. In the absence of cyclin D, $p21^{Cip1}$ proteins bind CDK2-cyclin E/A complexes, preventing CDK2 substrate phosphorylation and therefore the cell cycle is halted.

1.3.4.4 Cell cycle checkpoints

It is of critical importance that the cell cycle proceeds only under the correct conditions and at the correct time, indeed, failure to properly control cell cycle entry and progression is a major feature of malignant cells. As discussed in section 1.3.4.3, there are several regulatory mechanisms operating in mammalian cells to control the activity of CDKs and it is the active engagement of negative regulators of the cell cycle (in response to stress stimuli, DNA damage, incomplete or improper DNA replication, incomplete alignment of chromosomes during mitosis or a simple lack of proliferative signals) that constitutes these cell cycle checkpoints (Figure 1.7; red detail). When the proteins that enforce these checkpoints are activated, cell cycle progression halts. In the case of DNA damage, this pause provides time for DNA damage to be repaired, and if the damage is irreparable, the apoptotic machinery can be activated. Alternatively, the G_1 checkpoint (also known as the restriction point, R) restricts cell cycle progression in the absence of growth factor stimuli. The restriction point is particularly important because it represents the point of no return, beyond which the cell becomes completely committed to completing a round of cell division (provided that one of the other checkpoints is not triggered).

The restriction point was named by Arthur Pardee in 1974, who noted that there was a time point during late G_1 beyond which mammalian cells in culture would proceed to undergo cell division even if growth factors were removed. In contrast, withdrawal of factors before this time point (i.e. within 3-4 hours of completing mitosis) would result in growth arrest. Importantly, Pardee observed that this restriction point was defective in cancer cell lines (Pardee, A.B. 1974). It is now known that the restriction point checkpoint is enforced by the actions of retinoblastoma (Rb) family proteins, which, in their active state, bind to and inhibit E2 promoter-binding factor (E2F) family transcription factors, preventing E2F target gene transcription by sequestering E2F and also acting as an active repressor of E2F gene targets. Phosphorylation of Rb proteins by CDK4/6-cyclin D complexes releases E2F from Rb and allows E2F to transactivate a large number of genes including the gene encoding cyclin E, which arbitrates the G1 to S transition. In the absence of cyclin D expression, CDK4/6 are inactive, and the Rb checkpoint remains in force. Similarly, stress stimuli (such as UV exposure or exposure to excessive ROS) can

activate $p38^{MAPK}$ and FOXOs, which upregulate $p16^{INK4A}$ and $p21^{Cip1}$ family proteins respectively. These in turn inhibit CDK4/6 and CDK2-cyclin E/A complexes respectively, and again the Rb checkpoint is enforced.

So how is the restriction point overcome, e.g. upon receipt of extracellular growth signals? The answer to this is partly through the activation of Ras proteins. As mentioned in section 1.3.3.2, Ras proteins transduce signals from a variety of growth-factor receptors and initiate several signalling cascades, many of which converge on regulators of the cell cycle. Importantly, Ras activates AP-1 and c-Myc transcription factors which directly bind to the cyclin D1 promoter and initiate cyclin D1 gene transcription (Massague, J. 2004). Myc also directly represses CDKIs such as $p21^{Cip1}$ and $p15^{INK4B}$ (Wanzel, M. *et al.* 2003). Additionally, via the PI3K pathway, Ras further suppresses CDKI expression by Akt-mediated suppression of FOXOs. When combined, these signals (driven by Ras) strongly promote activity of CDK4/6 leading to inactivation of Rb and progression through the restriction point. DNA damage also leads to the enforcement of a distinct checkpoint, which can activate at any point during cell cycle progression (Zhou, B.B. and Elledge, S.J. 2000). In general, the DNA damage-responsive kinases ATM and ATR are responsible for transmitting an alarm signal from damaged DNA to several downstream substrates. These include Chk1, which phosphorylates and inhibits cdc25 phosphatase, halting CDK1 activity. In addition ATM phosphorylates and inhibits HDM2 (in humans) which is a ubiquitin ligase for the tumour suppressor p53 (aka TP53). Concurrent phosphorylation of p53 itself by ATM leads to stabilisation and homodimerisation of p53, which acts as a transcription factor to promote $p21^{Cip1}$ resulting in inhibition of CDK2-cyclin E/A complexes, and can also co-ordinate apoptosis if DNA damage cannot be repaired (a process that is also orchestrated by ATM kinase). ATR kinase appears to arbitrate a similar but distinct checkpoint to ATM, specifically; ATR enforces the DNA-replication checkpoint that prevents exit from S phase in the presence of unreplicated DNA or stalled replication forks. Finally, the G2 checkpoint prevents entry into M phase in the presence of unresolved DNA damage, while the spindle checkpoints delays the start of anaphase (chromosome segregation) until all of the chromosomes are correctly aligned (Kastan, M.B. and Bartek, J. 2004). The importance of these checkpoints for controlling unwanted cell growth is underscored by the fact that many of the key proteins that enforce these checkpoints are dysregulated in cancer. Loss of heterozygosity in persons with a hereditary Rb mutation can lead to retinal carcinoma (Benedict, W.F. *et al.* 1983), whilst inactivating mutations of p53 are amongst the most common mutations detected in human cancers (Levesque, A.A. and Eastman, A. 2007).

1.3.5 RAS ONCOGENES IN CANCER AND AML

1.3.5.1 Ras oncogenes in human cancer

The close association of aberrantly activated Ras proteins and cancer dates back to their discovery as the viral gene product responsible for transformation of rat cells by murine sarcoma viruses (section 1.3.2). During these early years of Ras research, activated Ras proteins were increasingly implicated in non-viral tumour formation. For example activated forms of H-Ras, K-Ras and N-Ras were detected in murine tumours induced by topically applied carcinogens (Balmain, A. and Pragnell, I.B. 1983; Guerrero, I. *et al.* 1984a) or by γ-radiation (Guerrero, I. *et al.* 1984b); and activated H-Ras was detected in human bladder cancers and lung cancers (Der, C.J. *et al.* 1982; Parada, L.F. *et al.* 1982; Santos, E. *et al.* 1982). Indeed, according to recent estimates, activated Ras proteins are detectable in ~30% of all human cancers (Schubbert, S. *et al.* 2007). In addition, mutations in particular Ras isoforms appear to be associated with particular cancers. K-Ras is the most commonly activated Ras isoform detected in a wide variety of human cancers including ovarian, lung and liver cancer, but shows a particularly high incidence in pancreatic cancers (60% of cases examined) and cancers of the intestinal tract (33%). Activated N-Ras is prevalent in melanoma (18%) and myeloid malignancies (14%), while activated H-Ras is detected in cancers of the thyroid and cervix, and 11% of bladder cancers. The majority of mutations involving activated Ras in these cancers target codons 12, 13 and 61, the so-called 'hot-spots', named due to the ability of mutations in these codons to promote accumulation of Ras-GTP (section 1.3.2).

1.3.5.2 Ras oncogenes in AML

Ras oncogenes are detected in 20-40% of AML cases (Gougopoulou, D.M. *et al.* 1996) and at similar frequency in cases of MDS, a pre-leukaemic condition (Bartram, C.R. 1992). Numerous *in vitro*, *in vivo* and clinical studies have been performed with the aim to understand the role of Ras mutations in the pathogenesis of AML.

The two-hit hypothesis of leukaemogenesis proposes that when mutations which promote proliferation (e.g. activating mutations of class I genes) co-localise with mutations in genes required for differentiation (class II genes), the result is generation of a clone with leukaemic potential (section 1.2.1.2). Ras oncogenes primarily act as pro-proliferative class I genes, since they activate a variety of pathways that lead to proliferation of haematopoietic cells (section 1.3.3.2). However, *in vitro* studies indicate that Ras activation can also impact on haematopoietic differentiation and development, since

activated Ras can bias human $CD34^+$ cell development towards the myelomonocytic lineage at the expense of erythroid and granulocytic cells in a PKC dependent manner (Darley, R.L. *et al.* 1997; Pearn, L. *et al.* 2007). This may be in part due to the fact that PKC can phosphorylate the critical haematopoietic transcription factor CEBPα (a class II gene), leading to an alteration in CEBPα function (Behre, G. *et al.* 2002). Increased proliferation and a bias towards myeloid differentiation has also been demonstrated in murine haematopoietic cells expressing activated N-Ras (Shen, S.W. *et al.* 2004), and these same cells also show increased engraftment and a similar differentiation bias *in vivo* when transplanted in NOD-SCID recipient mice, however, these NOD-SCID mice did not develop any overt disease (although the mice were only observed for six weeks post-transplant). Similar results were obtained from longer duration *in vivo* studies performed by Rassool and colleagues (Rassool, F.V. *et al.* 2007; Omidvar, N. *et al.* 2007). These studies showed that activated N-Ras expressed under the control of the Myeloid-related protein-8 (*Mrp8*) promoter (i.e. restricted to the haematopoietic system) induced a mild-myeloproliferative effect, but did not induce overt disease during a six month observation period. Strikingly, when mice bearing activated N-Ras mutations were crossed with mice overexpressing BCL-2 (generating an N-Ras/BCL-2 double transgenic), a reproducible disease developed with features similar to MDS or pre-AML. These data provide strong evidence for a two-hit model of leukaemogenesis in the mouse. Using a retroviral vector to overexpress activated Ras in murine haematopoietic progenitors, Parikh *et al.* have shown that overexpression of oncogenic Ras alone is capable of inducing a fatal myeloproliferative disease in mice, though H-Ras, N-Ras and K-Ras showed a progressively longer disease latency and features that ranged from closely resembling acute leukaemia (H-Ras) to those more closely resembling CMML (K-Ras) (Parikh, C. *et al.* 2007). In addition, it has been shown that knock-in of oncogenic $K\text{-}Ras^{G12D}$ into the normal murine K-Ras locus leads to a fatal myeloproliferative disease with 100% penetrance (Braun, B.S. *et al.* 2004).

Extensive efforts have also been made to establish whether *in vitro* and *in vivo* findings are consistent with clinical observations. These clinical studies aim to understand how Ras mutations contribute to leukaemogenesis in human patients, whether Ras mutations have any prognostic significance in AML, and whether there is evidence to support case for therapeutic targeting of Ras.

Although 20-40% of AML patients show mutations in one (or more) of their Ras genes, N-Ras mutations are the most common, followed by K-Ras. In contrast, although H-Ras mutations in AML patients have been reported (Imamura, N. *et al.* 1993), they are

generally rare in AML. There is some evidence that Ras mutations are over-represented in monocytic M4 and M5 AML FAB subtypes (consistent with *in vitro* studies showing that activated Ras drives monocytic differentiation) and also that Ras mutations are associated with particular cytogenetic subgroups, however, a consistent conclusion of the majority of clinical studies is that Ras mutations in AML do not significantly influence prognosis (Bowen, D.T. *et al.* 2005; Bacher, U. *et al.* 2006; Stirewalt, D.L. *et al.* 2001; Kiyoi, H. *et al.* 1999). Some studies have concluded that Ras mutations confer an improvement in prognosis, but this is either limited to younger patients (less than 60 years old) (Illmer, T. *et al.* 2005) or the effect was mild (Neubauer, A. *et al.* 1994).

So what role does Ras play in AML development and AML maintenance? This is a difficult question to answer, but there is evidence that Ras does contribute to the conversion of MDS (considered to be a pre-AML state) to full blown AML; in a study of paired samples from 70 patients with MDS who later progressed to AML, 11 acquired mutations in N-Ras when progressing to AML while only one patient lost an N-Ras mutation (Shih, L.Y. *et al.* 2004). In addition, when considering only MDS patients, another study showed that although Ras mutations were relatively rare (9% of MDS patients examined), these mutations were associated with a significantly decreased survival and increased potential to progress to AML (Paquette, R.L. *et al.* 1993). The strong correlation between acquisition of Ras mutations and progression from MDS to AML is consistent with the notion that Ras mutations may compliment existing mutations in MDS patients leading to completion of the multi-hit model. Indeed, in AML it has been shown that activating mutations in Ras (or mutations that activate the Ras pathway) preferentially co-exist in cells with mutations in core binding factor (CBF) proteins (Goemans, B.F. *et al.* 2005), while there is a significant negative correlation of mutations in two or more isoforms of Ras or mutations that affect similar pathways (Bowen, D.T. *et al.* 2005). However, whereas in MDS there is evidence for a net gain of Ras mutations upon progression to AML, once AML has been established there appears to be less need to maintain N-Ras mutations. In particular, one study examined N-Ras mutation status in paired samples from patients at diagnosis and also at first relapse. Amongst those patients whose N-Ras mutation status changed between these two time points, three patients lost an N-Ras mutation upon relapse compared to two patients that gained an N-Ras mutation upon relapse (Nakano, Y. *et al.* 1999). Indeed, it has been shown that there is significant heterogeneity in the distribution of Ras mutations within a typical AML cell population; with only a minority of AML blasts from Ras mutation-positive patients harbouring detectable Ras mutations (Bowen, D.T. *et al.* 2005). Taken together it appears that

activated Ras does indeed appear to act primarily as a class I gene mutation in human MDS and AML development (similar to *in vivo* findings) and may also serve this same role in established AML, however it appears that in overt AML the role of Ras as a class I gene is interchangeable with other mutations which have a similar effect. One possible role for Ras proteins is to contribute to early disease progression by inducing DNA damage. Indeed, *in vivo* models have shown a strong correlation with mutant N-Ras and ROS stress in the murine haematopoietic system (Rassool, F.V. *et al.* 2007), and Ras is also over-represented in a subgroup patients with deficient metabolism of toxic intermediates (Bowen, D.T. *et al.* 2003). In summary, the role of activated Ras in AML pathogenesis remains ambiguous, though its high frequency in AML continues to suggest that it does confer a clonal advantage.

1.4 REACTIVE OXYGEN SPECIES

1.4.1 INTRODUCTION TO REACTIVE OXYGEN SPECIES

ROS are a heterogeneous group of inorganic molecules and free radicals derived from diatomic oxygen, with a wide spectrum of lifespan and reactivity. In physiological systems, ROS formation begins with the univalent reduction of oxygen to produce superoxide radicals, which lie at the hub of a variety of potential chemical reactions (Figure 1.8). (To avoid confusion, note that unpaired electrons themselves are often erroneously referred to as radicals. However, the term radical (or free radical) refers to the molecule or atom that bears an unpaired electron). For example, superoxide can dismutate (either spontaneously or by catalysis) to form hydrogen peroxide (H_2O_2), a membrane permeable mildly pro-oxidant molecule. Further processing of H_2O_2 either through Fenton chemistry (section 1.4.1.1) or by enzymatic catalysis can lead to formation of several highly oxidising derivatives including hydroxyl radicals and hypochlorous acid (HOCl). These molecules' high reactivity results in short half lives and broader target specificity than superoxide or H_2O_2. For example hydroxyl radicals can abstract protons from the DNA backbone causing double strand breaks or can react with guanine residues forming 8-oxo-guanine (an important mechanism in GC to AT transversion in the genetic code). Hydroxyl radicals can also initiate lipid peroxidation chain reactions leading to disruption of lipid bilayers (Valko, M. *et al.* 2007). The toxic properties of ROS derived from H_2O_2 are harnessed by phagocytes of the immune system, which bombard pathogens with ROS during phagocytosis. However, since ROS are equally toxic to host tissues, ROS production must be tightly regulated to avoid unwanted oxidative damage. Finally,

although reactive nitrogen species (RNS) are not a focus of this study, they can be formed via reaction of nitric oxide and superoxide. The proximal RNS generated in peroxynitrite, which can participate in several subsequent reactions to generate various oxides of nitrogen (N_xO_y) (Valko, M. *et al.* 2007). Indeed, S-nitrosylation of protein cysteine residues has been reported to alter protein function (Leslie, N.R. 2006), although the full physiological significance of these modifications are unknown.

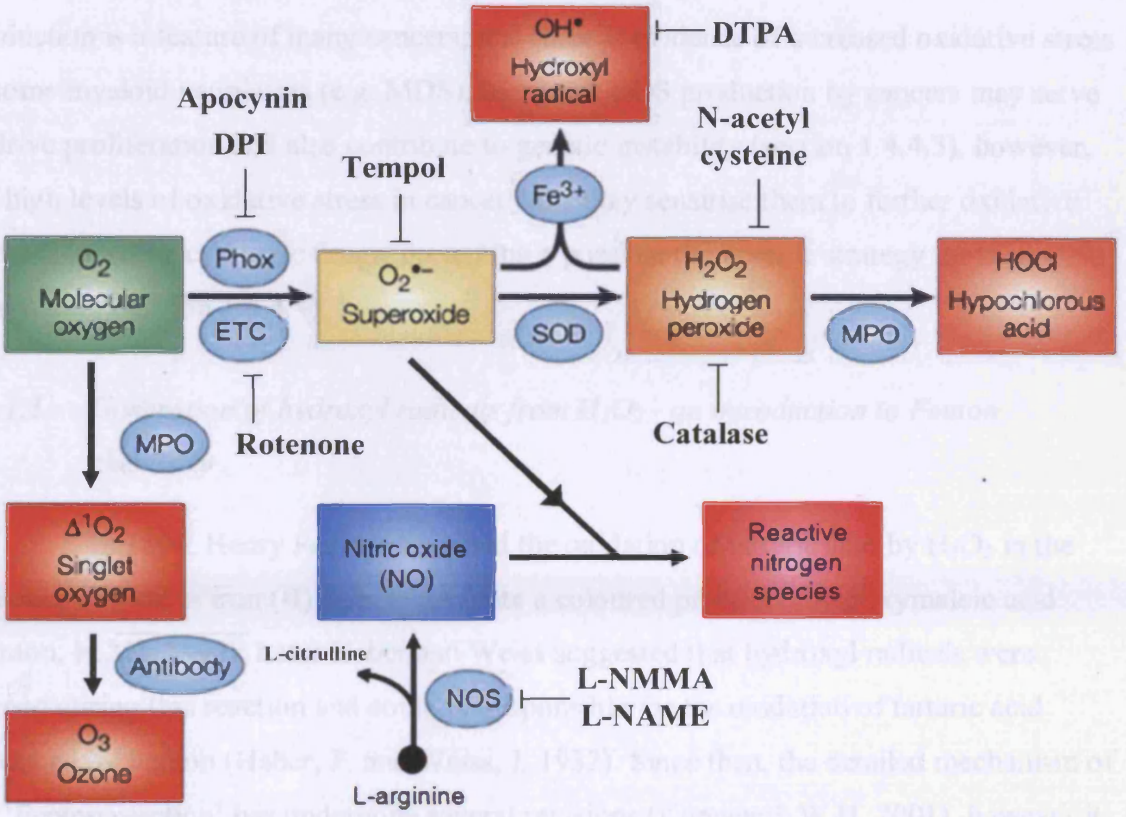

Figure 1.8 Physiological ROS and RNS generation

Superoxide radicals are the proximal ROS from which several other ROS are derived. Superoxide radicals are generated mainly by the mitochondrial electron transport chain (ETC) and professional oxidases e.g. NOX family oxidases such as Phox (containing NOX2). The archetypal professional oxidase is Phox, which is expressed at high levels in phagocytic cells. Under normal conditions, superoxide dismutase (SOD) promotes conversion of superoxide to H_2O_2. In an inflammatory environment, myeloperoxidase (MPO) activity can result in HOCl production and also generation of singlet oxygen, which may be further processed into ozone in the presence of immunoglobulins. Hydroxyl radicals may be formed in the presence of Fe^{3+} ions by Fenton chemical reactions. In addition, superoxide may react with nitric oxide (NO) generated by nitric oxide synthase (NOS) to form reactive nitrogen species such as peroxynitrite. Adapted from J.D Lambeth, 2004 (Lambeth, J.D. 2004).

Studies demonstrating that ROS may play an important role in proliferative signalling (Sundaresan, M. *et al.* 1995; Irani, K. *et al.* 1997; Sattler, M. *et al.* 1999), together with the discovery of non-phagocytic homologues of the Phox oxidase catalytic subunit (NOX2 aka $gp91^{phox}$) in non-phagocytic cells (Lambeth, J.D. 2004), raised the possibility that the physiological roles of ROS production may not be restricted to immune defence. Since then, the capacity of H_2O_2 in particular to act as a signalling molecule has been well established (section 1.4.3.2). Furthermore, it appears that increased ROS production is a feature of many cancers; and there is evidence of increased oxidative stress in some myeloid neoplasias (e.g. MDS). Increased ROS production by cancers may serve to drive proliferation and also contribute to genetic instability (section 1.4.4.3), however, the high levels of oxidative stress in cancer cells may sensitise them to further oxidative stress induced by cytotoxic drugs, presenting a possible therapeutic strategy for their elimination (section 1.4.4.4).

1.4.1.1 Generation of hydroxyl radicals from H_2O_2 - an introduction to Fenton chemistry

In 1894, Henry Fenton described the oxidation of tartaric acid by H_2O_2 in the presence of ferrous iron (II) salts to generate a coloured product dihydroxymaleic acid (Fenton, H.J.H. 1894). Later Haber and Weiss suggested that hydroxyl radicals were formed during this reaction and could be responsible for the oxidation of tartaric acid described by Fenton (Haber, F. and Weiss, J. 1932). Since then, the detailed mechanism of the 'Fenton reaction' has undergone several revisions (Koppenol, W.H. 2001), however it is agreed that during the reaction, Fe^{2+} ions catalyse the degradation of H_2O_2 forming several products, including hydroxyl radicals.

Due the variety of side reactions that can occur in the Fenton system, it has been argued that it is more appropriate to speak of Fenton chemistry rather than the Fenton reaction. While a detailed discussion of Fenton chemistry is beyond the scope of this study, for the purposes of this thesis it is pertinent to mention that both physiological forms of iron (Fe^{2+} and Fe^{3+}) can initiate Fenton chemical reactions in the presence of endogenously generated H_2O_2 resulting in hydroxyl radical generation (Figure 1.9).

One the one hand, Fe^{2+} ions can react with H_2O_2 yielding a hydroxyl radical, hydroxide ion and Fe^{3+} (Reaction 1). Reaction of Fe^{3+} with superoxide regenerates Fe^{2+} (Reaction 2), thus iron plays a catalytic role in this reaction. Superoxide radicals for Reaction 2 may be generated in physiological systems by the mitochondrial ETC, NOX oxidases or by reaction of hydroxyl radicals with H_2O_2 (Reactions 3 and 4).

Clearly, in the presence of mitochondrial or NOX-derived superoxide generation, Fe^{3+} ions may also initiate this cycle starting with Reaction 2 generating Fe^{2+}, which can participate in Reaction 1. Iron in the body is usually sequestered within storage proteins (such as ferritin) or bound in the haem moiety of haemoglobin in erythrocytes. However, since the action of iron in this reaction is catalytic, even trace amounts of free iron can lead to considerable hydroxyl radical generation. The mechanism of hydroxyl radical generation described here may also serve to partly explain the oxidative stress observed in patients with iron-overload (Lehmann, D.J. *et al.* 2006).

$Fe^{2+} + H_2O_2 \rightarrow Fe^{3+} + {}^{-}OH + {}^{\bullet}OH$ (1)

$Fe^{3+} + O_2^{\bullet -} \rightarrow Fe^{2+} + O_2$ (2)

Superoxide in reaction (2) can be generated by mitochondrial ETC, NOX oxidases, or during reactions (3) and (4) below.

${}^{\bullet}OH + H_2O_2 \rightarrow H_2O + HO_2^{\bullet}$ (3)

$HO_2^{\bullet} \leftrightharpoons O_2^{\bullet -} + H^+$ (4)

Cupric ions may participate in a similar catalytic cycle resulting in hydroxyl radical formation.

$Cu^{2+} + O_2^{\bullet -} \rightarrow Cu^{+} + O_2$ (5)

$Cu^{+} + H_2O_2 \rightarrow Cu^{2+} + {}^{-}OH + {}^{\bullet}OH$ (6)

Figure 1.9 Generation of hydroxyl radicals by Fenton chemistry

Red text indicates the reduced form of the metal ions, green indicates the oxidised form of the metal ions. Blue text highlights the points at which hydroxyl radicals are formed during the reactions.

Cupric ions (Cu^{2+}) participate in similar reactions to those described for iron resulting in hydroxyl radical formation from H_2O_2 as shown in Reactions 5 and 6 (Simpson, J.A. *et al.* 1988). As with iron, free Cu^{2+} ions are rarely detected under physiological conditions; however, Cu^{2+} is often bound in proteins and also to DNA (Lewis, C.D. and Laemmli, U.K. 1982; Sagripanti, J.L. *et al.* 1991), which may localise hydroxyl radical production at these sites in the presence of superoxide and H_2O_2.

1.4.2 ROS HOMEOSTASIS

1.4.2.1 Production of ROS by NOX-family oxidases

The NOX family of NADPH oxidases are a family of membrane-bound proteins with homology to NOX2, the founding member of the family originally identified as the catalytic subunit of Phox, the source of ROS production in activated phagocytes (Bedard, K. and Krause, K.H. 2007). The enzymes of this family (NOX1-5 and DUOX1-2) catalyse the transfer of high energy electrons from NADPH to diatomic oxygen, generating superoxide, which leads to generation of H_2O_2 and several other reactive species as described in section 1.4.1.

NOX2 is a membrane-spanning protein with six transmembrane α-helices. The extracellular domains of the protein are highly glycosylated, and the intracellular portion contains domains for binding NADPH and FAD. NOX2 forms a mutually stabilising heterodimer with $p22^{phox}$; forming a unit known as cytochrome b_{558} (Sumimoto, H. 2008). However, cytochrome b_{558} is not functional (i.e. cannot generate superoxide) until assembled in a complex with at least 4 other regulatory proteins, $p67^{phox}$ (aka NCF4), $p47^{phox}$ (aka NCF1), $p40^{phox}$ and the small GTPase Rac. In a resting phagocyte, $p47^{phox}$ exists in a folded, inactive conformation (by virtue of association of its autoinhibitory domain with its lipid-binding PX domain) and is bound to $p67^{phox}$ and $p40^{phox}$ in a heterotrimeric complex in the cytosol. Likewise, Rac is bound in an inactive state to Rho-GDI which promotes GTP release from Rac preventing its activation (Figure 1.10).

Upon phagocyte stimulation, $p47^{phox}$ is phosphorylated by conventional PKC isoforms (Zhao, X. *et al.* 2005). This causes unfolding of the $p47^{phox}$ protein revealing the PX domain, which binds 3'-phosphosphorylated inositol lipids (such as those generated by activated PI3K). The interaction of the PX domains with membrane lipids localises the entire heterotrimeric complex to the lipid membrane. Subsequently bis-SH3 domains on $p47^{phox}$ bind tandem proline-rich regions on $p22^{phox}$, promoting association of the heterotrimeric complex with cytochrome b_{558}. This $p47^{phox}$-led model of membrane localisation of the heterotrimeric complex is based on evidence that $p67^{phox}$ and $p40^{phox}$ fail to associate with cytochrome b_{558} in the absence of $p47^{phox}$ (Dusi, S. *et al.* 1996; Heyworth, P.G. *et al.* 1991). The close association of $p67^{phox}$ with cytochrome b_{558} allows juxtaposition of the $p67^{phox}$ activation domain with critical residues on NOX2 resulting in formation of the catalytic core necessary for electron transfer.

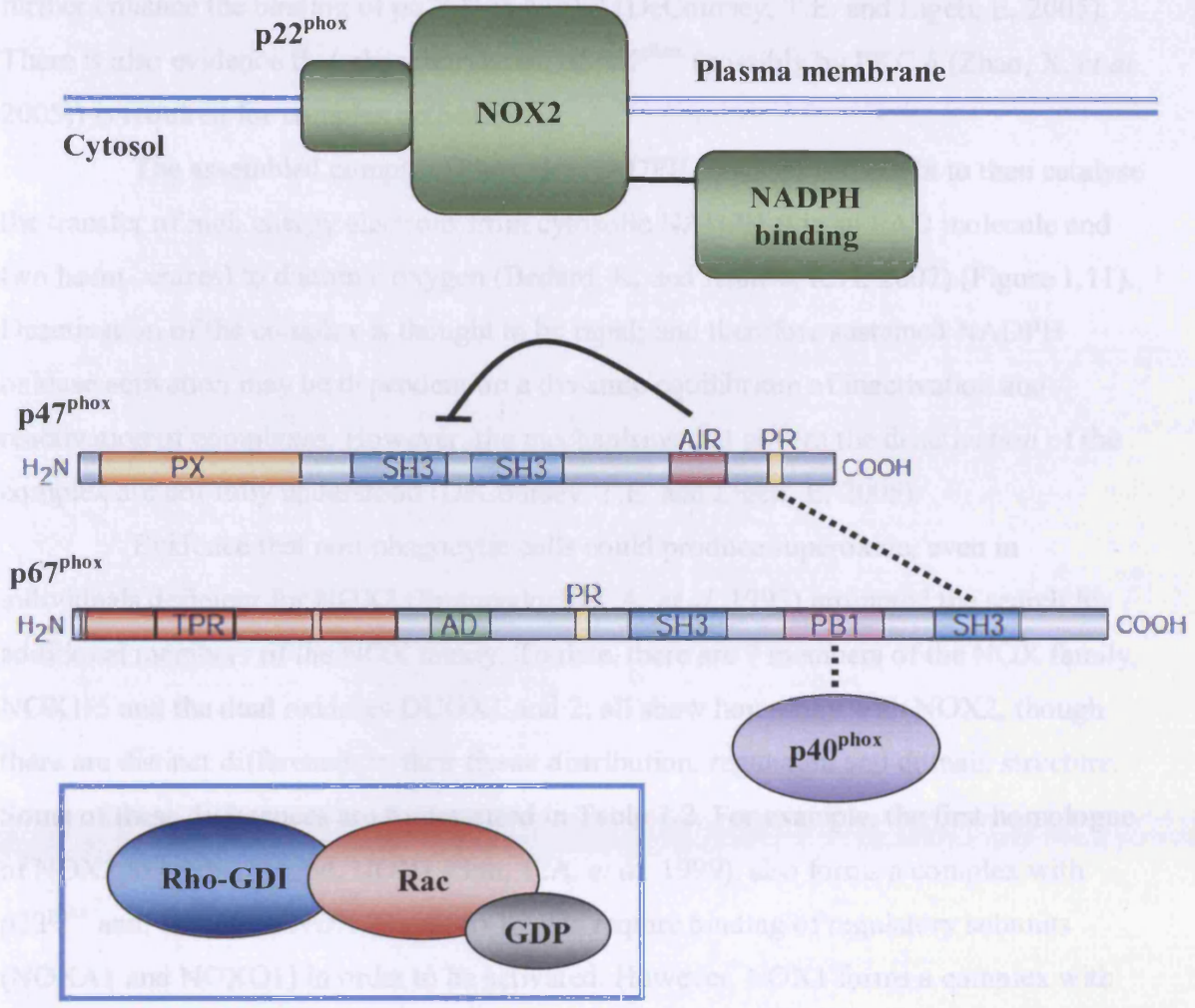

Figure 1.10 Components of Phox oxidase in the inactive state

In resting cells, the heterotrimeric complex consisting of Phox regulatory subunits $p47^{phox}$, $p67^{phox}$ and $p40^{phox}$ resides in the cytosol. Under these conditions, $p47^{phox}$ exists in a folded state, with its bis-SH3 domains bound to the C-terminal AIR domain. $p47^{phox}$ is bound to $p67^{phox}$ via an interaction with the C-terminal PR domain or $p47^{phox}$ and the C-terminal SH3 domain of $p67^{phox}$. $p40^{phox}$ is bound to the PB1 domain of $p67^{phox}$. Similarly, the small GTPase Rac is bound to its inhibitor, Rho-GDI, which promotes dissociation of guanosine triphosphate (GTP) from Rac in favour of guanosine diphosphate (GDP) binding. Dotted lines indicate physical associations between domains. AIR = autoinhibitory region, PX = Phox homology domain, PB1 = Phox and Bem1 domain, SH3 = Src-homology-3 domain, PR = Proline rich region (aka PRR), TPR = tricodecapeptide repeat, AD = Activation domain. Adapted from J. Lambeth, 2004 (Lambeth, J.D. 2004).

Meanwhile, activation of Rac promotes dissociation from its negative regulator (Rho-GDI); and Rac-GTP also binds to the nascent oxidase complex, which is thought to further enhance the binding of $p67^{phox}$ to NOX2 (DeCoursey, T.E. and Ligeti, E. 2005). There is also evidence that phosphorylation of $p67^{phox}$ (possibly by PKC δ (Zhao, X. *et al.* 2005)) is required for complex activation.

The assembled complex (Phox aka NADPH oxidase) is thought to then catalyse the transfer of high energy electrons from cytosolic NADPH (via an FAD molecule and two haem centres) to diatomic oxygen (Bedard, K. and Krause, K.H. 2007) (Figure 1.11). Deactivation of the complex is thought to be rapid; and therefore sustained NADPH oxidase activation may be dependent on a dynamic equilibrium of inactivation and reactivation of complexes. However, the mechanisms that govern the deactivation of the complex are not fully understood (DeCoursey, T.E. and Ligeti, E. 2005).

Evidence that non-phagocytic cells could produce superoxide, even in individuals deficient for NOX2 (Emmendorffer, A. *et al.* 1993) prompted the search for additional members of the NOX family. To date, there are 7 members of the NOX family, NOX1-5 and the dual oxidases DUOX1 and 2; all show homology with NOX2, though there are distinct differences in their tissue distribution, regulation and domain structure. Some of these differences are summarised in Table 1.2. For example, the first homologue of NOX2 to be discovered, NOX1 (Suh, Y.A. *et al.* 1999), also forms a complex with $p22^{phox}$ and, similar to NOX 2, appears to also require binding of regulatory subunits (NOXA1 and NOXO1) in order to be activated. However, NOX1 forms a complex with these regulatory proteins in resting cells, and (unlike NOX2) is constitutively active. NOX1 activity can be augmented by PKC activity, and has also been noted to mediate ROS production driven by mutant Ras in some contexts (Mitsushita, J. *et al.* 2004; Shinohara, M. *et al.* 2007).

The inclusion of an EF-hand (calcium-binding) domain in NOX5, and DUOX1 and 2 suggest that these oxidases may be regulated by Ca^{2+} without the need for interaction with any regulatory subunits, including $p22^{phox}$ (Sumimoto, H. 2008). Indeed it has been shown that calcium ionophores activate NOX5 (Banfi, B. *et al.* 2001). DUOX oxidases have an additional domain not observed in the rest of the NOX family, with homology to the peroxidase domain of myeloperoxidase which suggests their ability to immediately catabolise the H_2O_2 that they generate to form more reactive species such as hydroxyl radicals (Lambeth, J.D. 2004).

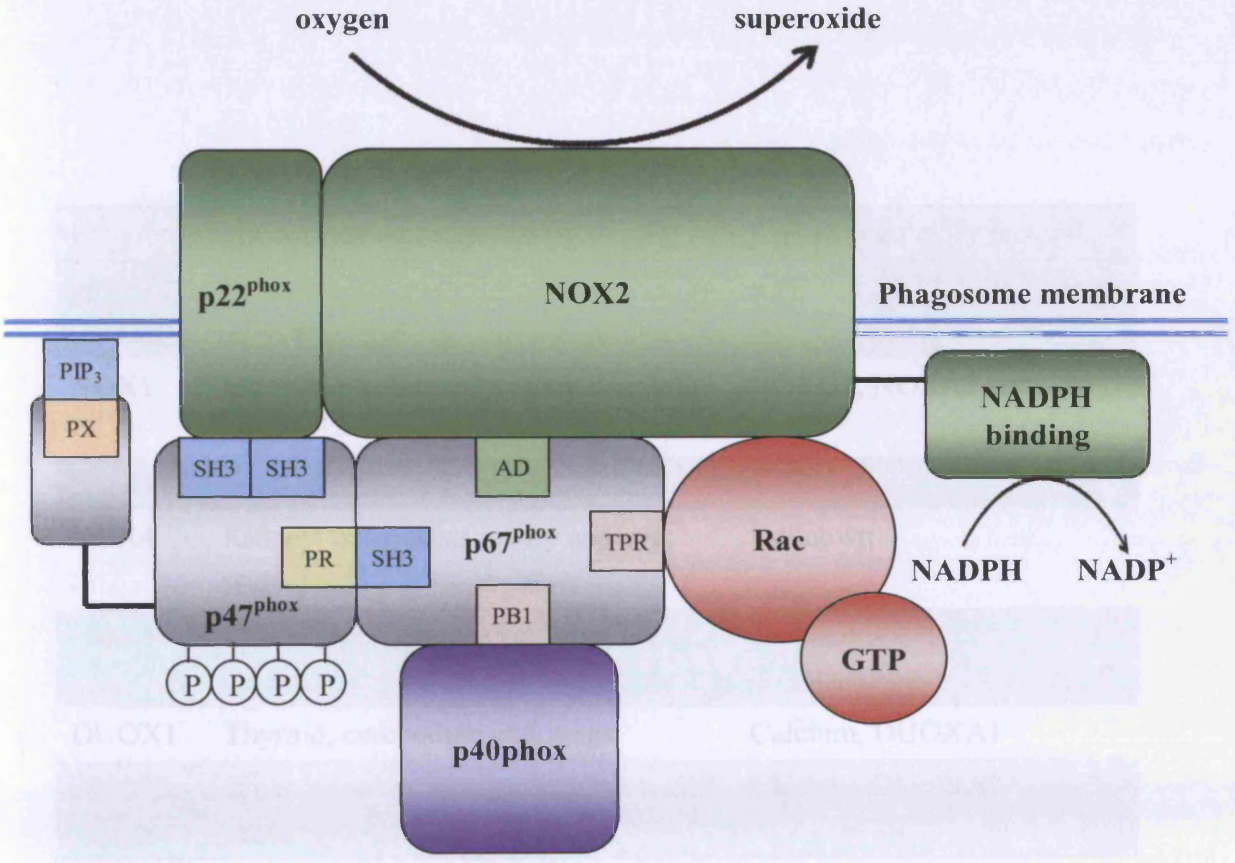

Figure 1.11 The activated Phox complex

As described in the text, activation of the Phox complex in phagocytic cells requires association of the heterotrimeric complex of $p47^{phox}$, $p67^{phox}$ and $p40^{phox}$, with cytochrome b_{558} in the phagosome membrane. This is initiated by phosphorylation of $p47^{phox}$ which promotes unfolding. Unfolding of $p47^{phox}$ allows localisation of the heterotrimeric complex to the lipid membrane by the association of the PX domain of $p47^{phox}$ with PIP_3 (generated by PI3K). Subsequently, $p47^{phox}$ and $p67^{phox}$ associate with $p22^{phox}$ and NOX2 respectively, via the bis-SH3 domain or activation domain (AD). For the complex to be fully functional, Rac must also be bound. In the absence of binding to Rho-GDI, Rac binds GTP, and subsequently binds to $p67^{phox}$ via the TPR domains and also interacts with NOX2. The assembled, activated complex generates superoxide by transferring electrons from cytosolic NAPDH across the lipid membrane to diatomic oxygen. P = phosphate groups.

Enzyme	Highest level of expression	Known regulatory factors
gp91^{phox} (NOX2)	Phagocytes	p47^{phox}, p67^{phox}, p40^{phox} and Rac
NOX1	Inducible: colon and vascular smooth muscle	NOXO1, NOXA1 and p22^{phox}
NOX3	Fetal kidney	Unknown
NOX4	Kidney, osteoclasts, ovary and eye; widespread	Unknown
NOX5	Spleen, sperm, mammary glands and cerebrum	Calcium
DUOX1	Thyroid, cerebellum and lungs	Calcium, DUOXA1
DUOX2	Thyroid, colon, pancreatic islets and prostate	Calcium, DUOXA2

Table 1.2 NOX family oxidases: Tissue distribution and known regulatory factors

DUOX enzymes are highly expressed in the thyroid, and are required for thyroid hormone production; inherited inactivating mutations in DUOX enzymes lead to congenital hypothyroidism (Moreno, J.C. *et al.* 2002). Finally, NOX3 and NOX4 (like NOX1, 2) also require association with $p22^{phox}$, though their requirement for additional subunits for activity is unclear.

The discovery of non-phagocytic NOX family members raises questions about the physiological roles of these proteins. For example, almost all of the NOX family members (together with most of the regulatory proteins) have been shown to be expressed in human haematopoietic progenitor cells ($CD34^+$ cells) (Piccoli, C. *et al.* 2007), but their roles in these cells are not understood. While some roles of these oxidases have been elucidated (e.g. DUOX enzymes), their existence suggests that ROS production may also be important in physiological processes other than fighting infection. Indeed, as discussed in section 1.4.3.2, several roles for ROS in normal cell signalling have been proposed.

1.4.2.2 Production of ROS by the mitochondria

The mitochondrial electron transport chain is a multi-component sequence of redox-coupled proteins expressed in the internal mitochondrial membrane (Figure 1.12, (Genova, M.L. *et al.* 2003). The proximal complex in the mitochondrial electron transport chain is the NADH dehydrogenase complex (aka complex I), which accepts high-energy electrons from NADH, an important electron donor molecule generated from pyruvate and fatty acids during the citric acid cycle which occurs in the mitochondrial matrix. The electrons are passed from NADH to complex I via a flavin mononucleotide (FMN) cofactor, and are circulated within complex I before being transferred to coenzyme Q (CoQ aka ubiquinone). Note that CoQ can also accept electrons from $FADH_2$ or from succinate dehydrogenase (aka complex II). Electrons carried by CoQ are subsequently transferred (in this order) to the cytochrome b-c_1 complex (aka cytochrome c reductase or complex III), cytochrome c, and finally cytochrome oxidase (aka complex IV), where the electron transport chain terminates with the tetravalent reduction of diatomic oxygen to two molecules of water. During electron transport, the high energy of the electrons is harnessed to drive active transport of protons into the intermembrane space forming a pH and voltage gradient across the inner mitochondrial membrane. The resulting proton electrochemical gradient induces a protein motive force which drives the re-entry of protons to the matrix via ATP synthases; these protein complexes harness the energy of protons travelling back into the matrix to generate ATP from ADP and inorganic phosphate. Thus, the electron transport chain is a critical source of ATP generation for the cell. Studies using isolated

mitochondria show that these organelles can generate superoxide and H_2O_2 *in vitro* (Murphy, M.P. 2009). In simple terms, these studies suggest that production of superoxide occurs when electrons 'leak' from the transport chain before reaching the terminus.

In isolated mitochondria, electron leakage is proposed to occur primarily at complex I, by two main mechanisms. Which mechanism operates depends on whether the isolated mitochondria are operating under conditions where NADH/NAD^+ ratio is high and ATP production is low (known as mode 1); or conditions where the $CoQ/CoQH_2$ ratio is low, membrane potential is high and ATP production is low (known as mode 2).

The first scenario (mode 1) results in a build up of completely reduced FMN in complex I, which can univalently reduce oxygen to superoxide. In the second scenario (mode 2) the high membrane potential encourages electrons to travel from $CoQH_2$ back through complex I in a process called reverse electron transport (RET). During RET, electrons travel back to the FMN site in complex I, where oxygen can accept these electrons forming superoxide (Chance, B. and Hollunger, G. 1961). Under conditions of hypoxia, superoxide may also be generated at complex III (discussed in section 1.4.4.2).

Intracellular probes sensitive for mitochondrial superoxide suggest that this process may also occur *in vivo* (Mukhopadhyay, P. *et al.* 2007; Zimmerman, M.C. *et al.* 2007), indeed, mitochondrial ROS are proposed to participate in intracellular signalling (Balaban, R.S. *et al.* 2005). However, mitochondria *in vivo* are thought to primarily operate in mode 3 (high ATP production rate), and critically, the mechanisms by which ROS are produced by mitochondria operating in mode 3 are not understood due to the difficulties of carrying out detailed mechanistic studies on mitochondria within intact cells.

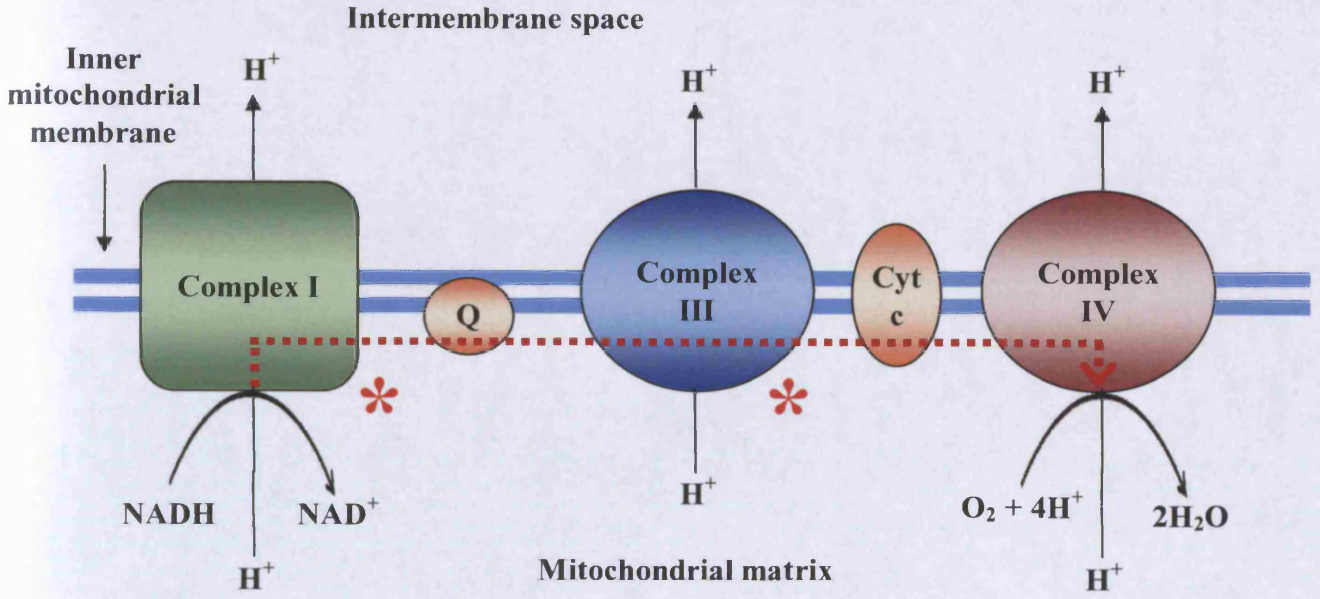

Figure 1.12 Sources of superoxide in the mitochondrial electron transport chain

The mitochondrial electron transport chain transfers high energy electrons from NADH to oxygen, resulting in the reduction of oxygen to water. During electron transport, the energy of the electrons is harnessed to transport protons (H^+) across the inner mitochondrial membrane into the intermembrane space. The resulting pH and electrochemical gradient creates an electromotive force which drives the return of H^+ back in to the matrix via ATP synthases, which generate ATP from ADP and inorganic phosphate. Dotted red arrow indicates path followed by electrons within the electron transport chain. Red stars indicate known locations of superoxide production within the electron transport chain. NADH = nicotinamide adenine dinucleotide, Q = ubiquinone, Cyt c = cytochrome c.

1.4.2.3 Destruction of ROS by endogenous mechanisms

The potential toxicity of ROS (especially hydroxyl radicals) demands that ROS production is controlled and promptly terminated when not required. Accordingly, several ROS catabolising enzymes and molecules are expressed by virtually all human cells for the purpose of eliminating ROS. SOD is the main line of defence against superoxide production, while there are several mechanisms which eliminate H_2O_2, such as catalase, the peroxiredoxins (Prxs) and the glutathione (GSH) system.

There are three forms of SOD expressed in mammals, cytosolic SOD1 (aka Cu/Zn SOD), mitochondrial SOD2 (aka Mn SOD) and extracellular SOD3 (a variant Cu/Zn SOD). SOD catalyses the dismutation of superoxide forming H_2O_2, and the mechanism starts with the univalent reduction of a co-ordinated active site metal ion (either Cu^{2+} or Mn^{3+} in Cu/Zn or Mn SOD enzymes respectively) by a first superoxide radical, liberating diatomic oxygen. A second molecule of superoxide is then itself reduced by the metal ion regenerating the enzyme and releasing a peroxide anion, which abstracts protons from the solvent to form H_2O_2 (Bannister, J.V. *et al.* 1987). Since superoxide can react with NO to form peroxynitrite, SOD plays an important role in suppressing peroxynitrite formation by converting superoxide to H_2O_2. However, H_2O_2 breakdown can subsequently lead to hydroxyl radical formation (section 1.4.1.1), hence there are several endogenous mechanisms in place which subsequently detoxify H_2O_2 generated by SOD, discussed below. Catalase may also serve to scavenge H_2O_2 generated as by products of cyclo-oxygenases and lipoxygenases (Kim, C. *et al.* 2008).

Catalase catalyses the conversion of H_2O_2 to oxygen and water. The mechanism occurs by oxidation of a first H_2O_2 molecule by a haem moiety in the active site of catalase, forming a cationic oxy-haem porphyrin radical and liberating a water molecule. This oxy-haem intermediate then oxidises a second H_2O_2 molecule regenerating the haem and releasing a second water molecule and diatomic oxygen (Kirkman, H.N. and Gaetani, G.F. 2007). Catalase protein in human cells is usually restricted to peroxisomes, which are sub-cytoplasmic organelles harbouring enzymes with a variety of functions including oxidation of long-chain fatty acids which contributes to the production of acetyl-CoA, the priming molecule for the Krebs cycle (Alberts, B. *et al.* 2002). During this oxidation process, H_2O_2 is produced, therefore catalase regulates H_2O_2 accumulation. Catalase may also degrade H_2O_2 that diffuses into the peroxisome from the cytosol, however, H_2O_2 destruction in the cytosol is mainly achieved through the actions of glutathione peroxidase as part of the GSH system.

GSH is a tripeptide containing a central cysteine residue, and is the most abundant thiol in mammalian cells, with reported concentrations approaching 10 mM (Komatsu, H. and Obata, F. 2003). GSH represents the main cellular defence against H_2O_2, oxidising H_2O_2 to form H_2O and O_2 in a reaction catalysed by glutathione peroxidase. During this reaction, oxidised GSH dimers (GSSG) are generated. GSH is regenerated from GSSG dimers by glutathione reductase in a process which uses electrons donated by NADPH or NADH (Ballatori, N. *et al.* 2009).

Finally, Prxs provide an additional line of defence against H_2O_2 (Rhee, S.G. *et al.* 2005). Prxs are homodimeric cytosolic proteins containing a conserved N-terminal cysteine residue (Cys51 in mammalian Prx) which is sensitive to oxidation by H_2O_2. There are three main Prx families (2-cys, atypical 2-cis and 1-cis Prxs); however the functions of the 2-cys Prxs are the best understood. All 4 members of the 2-cys Prx family (Prx I-IV) contain an additional cysteine residue (e.g. Cys172 in Prx I), which (in the homodimeric complex) is located in close proximity to Cys51 of the companion subunit. H_2O_2 reacts with Cys51 forming sulphenic acid (-SOH), which reacts with the sulphydryl group (-SH) of Cys172 forming an intermolecular disulphide bond (S-S). Oxidised 2-cys Prxs are subsequently reduced by thioredoxin and can participate in further reactions with H_2O_2, thus 2-cys Prxs catalytically destroy H_2O_2. The mechanisms which drive the cycles of Prx oxidation and regeneration are key processes which are able to regenerate oxidised cysteine residues in several other protein targets.

Figure 1.13 summarises two of the major antioxidant systems (in addition to catalase) which are capable of destroying H_2O_2, the GSH and the Prx systems.

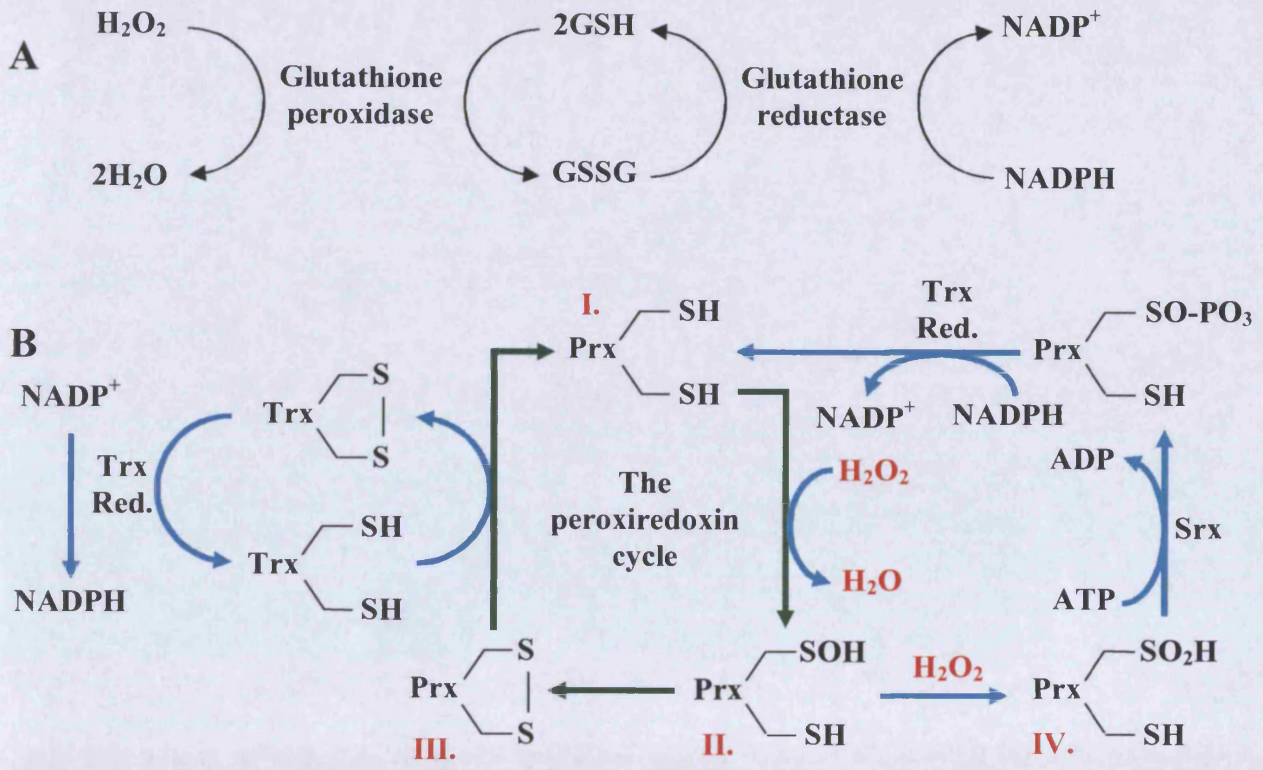

Figure 1.13 Endogenous pathways which degrade H_2O_2

H_2O_2 is destroyed by several endogneous mechanisms, including the actions of glutathione peroxidase, and the peroxiredoxins (Prxs). **(A)** Glutathione peroxidase catalyses the reduction of H_2O_2 to water using GSH as an electron donor. Oxidised GSH (GSSG) is regenerated by glutathione reductase using electrons donated from NADPH. **(B)** Green arrows indicate oxidation and reduction cycle of 2-Cys Prxs. Reduced Prx (I), is oxidised forming a sulphenic acid group at Cys51 (II), and subsequently a disulphide bond forms (III) between Cys51 and Cys172 (in Prx1). The disulphide bond is reduced by thioredoxin (Trx) which is oxidised in the process. Trx is subsequently regenerated by thioredoxin reductase (Trx Red.). Alternatively, Prx sulphenic acid groups (II) can be further oxidised by H_2O_2 forming a sulphinic acid group (IV). Sulphinic acid groups in Prx1 can be resolved by sulphiredoxin (Srx), in a reaction which requires ATP. Native Prx1 is then regenerated by the actions of Trx Red.

1.4.3 PHYSIOLOGICAL ROLES OF ROS

1.4.3.1 Role of ROS production in the innate immune response

Early experiments that involved mixing bacterial preparations with dog leukocytes noted a sharp increase in oxygen consumption, which was attributed to an increase in respiration during phagocytosis (Baldridge, C.W. and Gerard, R.W. 1932). The notion that a 'respiratory burst' occurred during phagocytosis persisted until 1961, when it was noted that the increased oxygen consumption of phagocytes during phagocytosis was accompanied by the increased ability to oxidise formate, suggestive of oxidant production. Importantly, addition of pyruvate (which stimulates respiration) did not augment formate oxidation, suggesting that a cellular process distinct from respiration was responsible for oxidant production (Iyer, G.Y.N. *et al.* 1961). Subsequent studies identified superoxide as the proximal molecule formed during phagocytosis, leading to H_2O_2 production formation via a dismutation reaction (Babior, B.M. *et al.* 1973). Eventually, the gene encoding the catalytic subunit (NOX2 aka $gp91^{phox}$) of the protein complex responsible for superoxide production (Phox aka NADPH oxidase) was cloned (Teahan, C. *et al.* 1987; Royer-Pokora, B. *et al.* 1986).

The importance of NAPDH oxidase activity during immune responses is highlighted in patients with chronic granulomatous disease (CGD) first described by Berendes *et al.* in 1957 (Berendes, H. *et al.* 1957). These patients suffer from several symptoms, including a strong predisposition to pyrogenic bacterial infections. Early studies noted that the phagocytes of CGD patients could phagocytose pathogens as normal, but superoxide production was absent (Quie, P.G. *et al.* 1967). Later, CGD patients were shown to be either deficient for cytochrome b_{558} (the NOX2-$p22^{phox}$ complex) (Segal, A.W. *et al.* 1978) or deficient for some regulatory subunits of NADPH oxidase e.g. $p47^{phox}$ and $p67^{phox}$ (Nunoi, H. *et al.* 1988; Volpp, B.D. *et al.* 1988).

NADPH oxidase is activated in endocytic compartments (phagosomes) formed during phagocytosis; and the subsequent ROS production contributes to the death of pathogens by two main mechanisms. The most predictable of these is by inflicting direct oxidative damage on pathogen biomolecules causing loss of homeostasis, for example, HOCl (derived from H_2O_2 by phagocyte myeloperoxidase) has been shown to initiate lipid peroxidation reactions, which disrupt the microbial membrane (Nauseef, W.M. 2001). More recently, ROS has been implicated in microbial killing by an indirect mechanism. Superoxide production inside the phagosome leads to an increased intra-phagosomal pH (primarily due to consumption of protons during dismutation (Segal, A.W. *et al.* 1981))

and increased intra-phagosomal negative charge (Schrenzel, J. *et al.* 1998) - because superoxide is negatively charged. These effects are compensated for by influx of H^+ and K^+ ions through phagosomal ion channels; and it has been proposed that the increased ionic strength of the phagosome interior leads to elution of cationic proteases from the microbial cell-walls and membranes resulting in accelerated degradation of the pathogen (Reeves, E.P. *et al.* 2002).

1.4.3.2 ROS signalling

As described above (section 1.4), ROS have the potential to react with and disrupt proteins, DNA and lipids, and these properties may be employed in the destruction of pathogens by phagocytes. However, during the late 1980s and early 1990s, it was observed that exogenous superoxide and H_2O_2 appeared able to promote cell proliferation in a variety of contexts. In 1988, Shibanuma *et al.* proposed that superoxide may act as a signalling 'messenger' after observing that superoxide drove increased proliferation of human U397 histocytic leukaemia cells (Shibanuma, M. *et al.* 1988). Superoxide and H_2O_2-driven proliferation was also observed in hamster BHK-21 and rat 208F fibroblast cell lines (Burdon, R.H. and Rice-Evans, C. 1989; Burdon, R.H. *et al.* 1989; Burdon, R.H. *et al.* 1990); and shortly afterwards in human fibroblasts and amnion cells (Murrell, G.A. *et al.* 1990; Ikebuchi, Y. *et al.* 1991). Subsequent studies demonstrated that ROS production may be an important feature of growth factor receptor signalling; PDGF (Sundaresan, M. *et al.* 1995), EGF (Bae, Y.S. *et al.* 1997) and angiotensin II (Ushio-Fukai, M. *et al.* 1999) signals were all shown to be dependent on downstream H_2O_2 production. In addition, several haematopoietic growth factor signals were shown to promote ROS production and cell cycle progression, and blockade of growth factor-induced ROS suppressed proliferation and viability (Sattler, M. *et al.* 1999). However, the mechanisms by which ROS promote proliferation are not well understood. Superoxide is also known to have the potential to act as a signalling molecule, indeed a seminal study by Irani *et al.* concluded that mitogenic signalling driven by mutant Ras was mediated by superoxide production (although H_2O_2 may also have contributed, (Irani, K. *et al.* 1997)). Furthermore, in prokaryotes, the superoxide-sensitive transcription factor SoxR contains iron-sulphur redox centres which react directly with superoxide leading to transcription of antioxidant genes (D'Autreaux, B. and Toledano, M.B. 2007). However, in mammalian cell systems, most studies have focused on H_2O_2 as a potential ROS signalling molecule (Rhee, S.G. 2006). Indeed, in addition to proliferation, H_2O_2 signalling has been implicated in diverse

processes including cell-transformation, senescence, apoptosis and extracellular matrix remodelling (Finkel, T. 2003; Lambeth, J.D. 2004).

H_2O_2 has peculiar properties which set it apart from other ROS and allow its function as a second messenger. First, it is uncharged and membrane permeable, allowing it access to all subcellular compartments. Second, its relatively low reactivity (c.f. hydroxyl radicals, HOCl) result in a narrower range of target molecules than more reactive ROS, and third, a conserved antioxidant network exists that can efficiently eliminate H_2O_2, enabling prompt H_2O_2 signal termination (section 1.4.2.3). The best understood mechanism of H_2O_2 signalling is via the reversible inactivation of phosphatases. Protein tyrosine phosphatases (e.g. PTP1B) are well established targets for inactivation by H_2O_2 (den Hertog, J. *et al.* 2005), but recent evidence suggests that the lipid phosphatase PTEN (Rhee, S.G. *et al.* 2005) and some serine/threonine phosphatases e.g. protein phosphatase-1 and 2A (PP1 and PP2A) may also be susceptible to oxidative inactivation (O'Loghlen, A. *et al.* 2003; Rao, R.K. and Clayton, L.W. 2002).

Protein tyrosine phosphatases (PTPs) such as PTP1B contain a conserved cysteine residue within a characteristic His–Cys–X–X–Gly–X–X–Arg–Ser/Thr motif in the active site. The invariant positively-charged arginine in this motif reduces the pKa of the cysteine sulphydryl group to ~4 (free cysteine sulphydryl pKa ~8.5), and thus stabilises the thiolate form ($Cys\text{-}S^-$) of the sulphydryl group. Therefore, at physiological pH the active site cysteine of such phosphatases exists primarily in the 'activated' thiolate form, which is required for the catalytic mechanism to proceed (Jackson, M.D. and Denu, J.M. 2001). In contrast, most other cellular cysteine residues will preferentially exist in the less reactive sulphydryl form. Critically, H_2O_2 does not efficiently react with non-activated sulphydryl groups, making the thiolate in the active site of tyrosine phosphatases (such as PTP1B) a preferential target of H_2O_2. The reaction of the thiolate with H_2O_2 involves oxidation to form sulphenic acid (Cys-SOH) and water (essentially the same mechanism as described for Prx oxidation; section 1.4.2.3). Since the thiolate group is required for the catalytic mechanism to occur, the phosphatase is rendered inactive. Recent evidence suggests that sulphenic acid rapidly forms a cyclic sulphenamide by reacting with a nearby nitrogen atom in the peptide backbone (den Hertog, J. *et al.* 2005). Unlike the sulphenic acid, this cyclic sulphenamide group is resistant to further oxidation by H_2O_2, and can be restored to the thiolate by S-glutathionylation (essentially forming a disulphide bond with GSH) and reduction by glutaredoxin (Gallogly, M.M. and Mieyal, J.J. 2007). This final step in the cycle regenerates the phosphatase activity, satisfying the condition that the effects of H_2O_2 must be reversible in order to be considered a credible second messenger.

The lipid phosphatase PTEN is also known to be regulated by H_2O_2. PTEN is a lipid phosphatase which catalyses the removal of 3'-phospho groups from $PI(3,4,5)P_3$ and therefore directly antagonises PI3K activity (which catalyses the formation of $PI(3,4,5)P_3$ from $PI(4,5)P_2$ (Fresno Vara, J.A. *et al.* 2004). PTEN is reversibly inhibited by H_2O_2 via a mechanism similar to that observed in PTPs. The catalytic Cys124 residue of PTEN is primarily in the thiolate form (similar the catalytic Cys of PTPs), due to being surrounded by three positively charged amino acids. Therefore Cys124 is susceptible to reaction with H_2O_2 to form sulphenic acid, in a similar manner to PTPs. However, rather than forming a cyclic sulphenamide, sulphenic acid formed at Cys124 reacts with nearby Cys71 to form an intramolecular disulphide bridge. Like the cyclic sulphenamide formed in PTPs, this protects PTEN from further oxidation by H_2O_2. Oxidised PTEN is regenerated by thioredoxin (Lee, S.R. *et al.* 2002).

It is only very recently, that some serine/threonine phosphatases such as PP1 and PP2A have been included in the list of redox-sensitive phosphatases. These phosphatases do not rely on an activated cysteine residue in the active site for their catalytic activity; however, recent studies have demonstrated that oxidation of cysteine residues located outside the active site may have an allosteric effect on phosphatase activity. For example, PP2A has recently been shown to undergo oxidative cross-linking of vicinal cysteine residues in a Cys-X-X-Cys motif located in the catalytic subunit ($PP2A_C$), which led to the ablation of phosphatase function (Foley, T.D. *et al.* 2007). Furthermore, PP2A (and PP5) expressed in rat PC12 cells and human SH-SY5Y neuroblastoma cells were shown to be inhibited by H_2O_2 treatment (Chen, L. *et al.* 2009).

Importantly, temporary inhibition of phosphatases may be necessary for signal transduction. In general terms, phosphatase activities are several orders of magnitude greater than kinase activities (Reth, M. 2002), suggesting that kinase activation alone may be insufficient to overcome the negative influence of phosphatases. Rather, a combination of increased kinase activity and phosphatase inhibition may be required for signal transduction. Indeed, studies using in the RAW264.7 macrophage cell line showed that upon stimulation with TPA and LPS (which activate NOX2), ~10% of PTEN molecules were reversibly inactivated and PTEN inactivation contributed to the activation of Akt in these cells (Leslie, N.R. *et al.* 2003). A similar but less pronounced inhibition of PTEN was observed in PDGF-stimulated NIH 3T3 cells overexpressing NOX1 (Kwon, J. *et al.* 2004). Importantly, oxidative inhibition of PTEN is suppressed by antioxidants with an associated decreased in Akt activation (Rhee, S.G. *et al.* 2005). The putative role of H_2O_2 in transient inhibition of phosphatases for successful signal transduction could therefore

explain why EGF, PDGF and (angiotensin II) Ang II signals are blocked by H_2O_2 scavengers (Bae, Y.S. *et al.* 1997; Sundaresan, M. *et al.* 1995; Ushio-Fukai, M. *et al.* 1999).

While kinases tend to receive the majority of credit for signal transduction, it is clear that phosphatases are obviously vital for correct signalling and mutations in several phosphatases are associated with human disease. For example, activating mutations in SHP2 are common in JMML (Tefferi, A. and Gilliland, D.G. 2007), while constitutive activation of PTP1B contributes to breast cancer progression (Tonks, N.K. and Muthuswamy, S.K. 2007). In contrast, inactivation of PP2A is implicated in myeloid leukaemia (Neviani, P. *et al.* 2005; Fukukawa, C. *et al.* 2005). The fact that phosphatase dysregulation contributes to human cancers suggest that oxidative regulation of phosphatases by H_2O_2 could potentially play a role in human disease. However, the downstream effects of oxidative phosphatase inhibition are likely to be highly complex and difficult to predict, due to the broad target specificity of some phosphatases (e.g. PP2A), together with evidence that some phosphatases themselves may also be regulated by phosphorylation (den Hertog, J. *et al.* 2008).

Oxidative modification of cysteine residues is not restricted to phosphatases. Of relevance to the present study, it has been shown that Ras proteins contain a conserved cysteine residue (Cys118) which is located near the GTP-binding region. Cell-free studies have shown that oxidative modification of this residue (either by NO or H_2O_2) in H-Ras causes increased GTP-loading (Lander, H.M. *et al.* 1995). Moreover, oxidative modification of Ras Cys118 has been reported in a cardiac cell model, and interestingly, ablation of oxidative modification by targeted mutation of Cys118 blocks Ras activation and prevents downstream activation of ERK (Pimentel, D.R. *et al.* 2006). This cysteine residue is conserved in Ras subfamily proteins (Barbacid, M. 1987), and it is possible that this mode of redox regulation applies to several Ras proteins in a similar fashion. Ras signalling promotes NOX oxidase activation (section 1.3.3.2), therefore a positive feedback loop may exist which sustains Ras activity via ROS production.

Finally, it is important to note that H_2O_2 is membrane permeable, meaning it has the potential to leave the vicinity of the generating cell and influence the biochemistry of nearby neighbours in a paracrine fashion, which has implications for ROS signalling in densely cellular regions such as the bone marrow.

In summary, ROS (in particular H_2O_2) appears to influence a variety of cell processes, mainly through its ability to reversibly oxidise cysteine residues within proteins.

1.4.3.3 Role of ROS in self-renewal of HSCs

Several studies have concluded that ROS negatively regulate self renewal in HSCs. Therefore, to maintain HSC function, physiological ROS generation in HSCs (either by mitochondria or oxidases) must be controlled. One particular study showed that FoxO transcription factors are a functionally redundant family of proteins which form one mechanism for controlling physiological ROS production in murine HSCs (Tothova, Z. *et al.* 2007). Under normal conditions FoxO proteins are phosphorylated by Akt which promotes nuclear export and subsequent degradation. However, in the absence of Akt signalling or in the presence of a cellular stress, FoxOs accumulate in the nucleus where they promote the transcription of genes which promote senescence (e.g. $p27^{Kip1}$, $p21^{Cip1}$, cyclin G and cyclin B), apoptosis (Bim, Fas ligand and TRAIL) and also genes encoding catalase and SOD which catabolise endogenous ROS. Conditional deletion of a single FoxO gene in adult mice showed no overt phenotype; however, simultaneous deletion of FoxO1, FoxO3, and FoxO4 resulted in increased intracellular ROS, increased HSC proliferation and a reduction in long-term repopulating capacity (indicating a decreased capacity for self-renewal). Importantly, the effects of FoxO deletion were rescued by introduction of NAC into the diet of FoxO deficient mice, strongly suggesting that tight regulation of physiological ROS is a major function of FoxOs in maintaining quiescence and self-renewal of normal HSCs. Similarly, ATM-deficient mice also show excessive ROS production in HSCs, and show similar increase in HSC proliferation and decrease in self-renewal capacity to FoxO deficient mice. Again, antioxidant treatment can restore HSC function in ATM-deficient mice (Ito, K. *et al.* 2004). Furthermore excessive ROS production by HSCs promotes HSC migration away from the bone marrow niche (Hosokawa, K. *et al.* 2007).

To summarise, it appears that in normal HSCs, ROS rapidly accumulates in the absence of antioxidant mechanisms, and this ROS accumulation forces HSCs into cell cycle and lineage commitment, at the expense of self-renewal capacity. As a result, increased ROS production in the HSC population eventually leads to bone marrow failure. However, the exact mechanisms whereby ROS induce these effects are currently unknown.

1.4.4 ROS IN PATHOLOGY

In addition to playing important roles in normal physiology (section 1.4.3.3), ROS have long been known to play a role in some pathological conditions. Prolonged and excessive ROS production establishes a state known as oxidative stress manifested by

increased DNA oxidation, lipid peroxidation, and an increase in intracellular pH (Finkel, T. 2003). Chronic oxidative stress plays a key role in the development and maintenance of conditions such as atherosclerosis, rheumatoid arthritis and amyotrophic lateral sclerosis (a form of motor neurone disease) (Droge, W. 2002). ROS are also thought to contribute to carcinogenesis.

1.4.4.1 ROS contributes to a variety of chronic disorders

Atherosclerosis is a chronic inflammatory condition, characterised by the formation of thickened, hardened regions in the vascular wall (atherosclerotic lesions). Migration of T-cells and monocytes into the vascular wall is an early step in the development of these lesions. Subsequently these lesions are exacerbated by activation of resident monocytes by binding to oxidised low-density lipoprotein (LDL). Monocyte activation leads to increased ROS and inflammatory mediator production (Alexander, R.W. 1995). Underscoring the role of ROS in this process, atherosclerosis-prone mice deficient for vitamin E (an endogenous antioxidant molecule) showed worsened atherosclerotic lesion formation. Moreover, vascular function was improved by treating atherosclerosis patients with L-2-oxo-4-thiazolidine carboxylate, a precursor of GSH (Vita, J.A. *et al.* 1998).

Similarly, establishment of an inappropriate inflammatory response is a major feature of rheumatoid arthritis. In this case, auto-reactive T-cells and activated monocytes invade the synovium resulting in its gradual destruction. T cells extracted from the joints of rheumatoid arthritis show evidence of increased oxidative stress (Maurice, M.M. *et al.* 1997), and it has been proposed this leads to aberrant oxidative modification of proteins which may maintain the auto-immune reaction (Mapp, P.I. *et al.* 1995).

Amyotrophic lateral sclerosis (ALS) a terminal degenerative disease characterised by loss of motor neurones primarily from the spinal cord and brain stem resulting in a progressive loss of motor function. Inactivating mutations of SOD1 (Cu/Zn SOD) are detected in 20% of familial ALS cases (Zimmerman, M.C. *et al.* 2007). It has been proposed that in these patients, inadequate superoxide catabolism leads to oxidative stress and toxicity, resulting in increased apoptosis of motor neurones, via activation of caspase-1 and caspase-3 (Pasinelli, P. *et al.* 2000). Furthermore, mice deficient for SOD1 have a shortened lifespan and develop symptoms similar to those seen in ALS patients (Tu, P.H. *et al.* 1996; Tu, P.H. *et al.* 1997).

1.4.4.2 Cancer cells frequently overproduce ROS via the mitochondria or NOX oxidases

Elevated ROS production is a common feature of a wide variety of cancers (Pelicano, H. *et al.* 2004; Benhar, M. *et al.* 2002), including cancers of the pancreas (Vaquero, E.C. *et al.* 2004), prostate (Khandrika, L. *et al.* 2009; Kumar, B. *et al.* 2008), skin (especially melanoma) (Fruehauf, J.P. and Trapp, V. 2008), lung (Tsao, S.M. *et al.* 2007) and haematopoietic system e.g. CML (Sattler, M. *et al.* 2000; Kim, J.H. *et al.* 2005) and hairy cell leukaemia (Kamiguti, A.S. *et al.* 2005). Evidence of oxidative stress has also been observed in chronic lymphocytic leukaemia (CLL) (Zhou, Y. *et al.* 2003) and MDS (Farquhar, M.J. and Bowen, D.T. 2003).

Investigations into the source of excess ROS in tumour cells have implicated both the mitochondrial ETC and NOX oxidases. The mitochondria of cancer cells over produce ROS by several mechanisms in addition to those discussed in section 1.4.2.2. For example, increased mitochondrial ROS may be simply be a consequence of increased metabolic activity in cancer cells; resulting in a greater than normal level of ROS production by the mitochondrial ETC. Indeed, studies in BCR-ABL$^+$ CML cells indicate that elevated ROS generation was connected to accelerated glucose metabolism (Kim, J.H. *et al.* 2005). The mitochondria can also generate increased ROS under conditions of hypoxia, a common consequence of tumour growth. This apparent paradox is explained by the fact that in hypoxic mitochondria, the delayed acceptance of electrons by oxygen at the ETC terminus prolongs the lifetime of ubisemiquinone radicals (usually formed transiently at complex III of the mitochondrial ETC), which can participate in univalent reduction of oxygen to superoxide (Fruehauf, J.P. and Meyskens, F.L., Jr. 2007). Finally, mutations in mitochondrial DNA are also implicated in increased ROS production. The proximity to the mitochondrial ETC together with the lack of chromatin proteins mean that mitochondrial DNA is at an increased risk of oxidative damage and mutation. Mutations in mitochondrial DNA are frequently detected in cancers (Brandon, M. *et al.* 2006), and mutations in genes encoding components of the mitochondrial ETC can cause increased ROS (Indo, H.P. *et al.* 2007). Interestingly, mitochondrial DNA mutations which induce ROS have been shown to confer increased metastatic potential e.g. in murine A11 lung carcinoma cells, and this increased metastatic potential can be transferred to poorly metastatic (P29) cell lines simply by introducing the mutant mitochondria DNA (Ishikawa, K. *et al.* 2008).

In some cancers, elevated ROS production is attributable to hyperactivation of NOX oxidases. For example, NOX1 is upregulated in gastric cancers (Tominaga, K. *et al.* 2007) and in 80% of prostate tumours (Lim, S.D. *et al.* 2005). NOX4 is overexpressed and active in pancreatic cancer (Vaquero, E.C. *et al.* 2004) and melanoma cells (Sander, C.S. *et*

al. 2003), whilst hairy cells from hairy cell leukaemia show increased expression and activation of NOX5 (Kamiguti, A.S. *et al.* 2005). Furthermore there is evidence that oncogene activation may be upstream of NOX activation in some cancers. Specifically, Ras oncogenes are have been associated with NOX activation in human fibroblasts (Lee, A.C. *et al.* 1999), neuroblastoma cells (Seru, R. *et al.* 2004) and embryonic lung cells (Liu, R. *et al.* 2001), and in a murine model of AML (Rassool, F.V. *et al.* 2007). The mechanisms by which Ras oncogenes activate NOX are not fully understood, but it appears Ras oncogenes can activate NOX by activating Rac and PKC (section 1.3.3.2). Ras may also regulate NOX1 activity at the transcriptional level; Ras^{G12V} induced NOX1 expression in colon carcinoma Caco-1 cells by promoting GATA-6 dependent transcription of the NOX1 gene (Adachi, Y. *et al.* 2008). It is important to note that while mitochondria and NOX oxidases are implicated in ROS production in tumour cells, these sources of ROS are not mutually exclusive and may indeed operate simultaneously within the same cell.

1.4.4.3 ROS generated by cancer cells may influence the malignant phenotype

Several studies indicate that ROS generated by cancer cells (from either the mitochondria or NOX oxidases) play an important role in key phenotypes of tumour cells, including proliferation, angiogenesis, migration/metastasis, and survival.

ROS production is required for effective growth factor signalling and cell-cycle progression in normal cells (section 1.4.3.2), and it appears that some cancer cells exhibit a dependence on ROS production for proliferation. For example, knockdown of NOX4 in melanoma cells causes rapid sequestration of cdc25 phosphatase (which normally dephosphorylates and activates CDKs) by 14-3-3 proteins and subsequent cell cycle arrest (Yamaura, M. *et al.* 2009). Through both overexpression and targeted knockdown, NOX1 has been shown to play a role in promoting proliferation of colon cancer cells (de Carvalho, D.D. *et al.* 2008) and prostate cancer cells (Arnold, R.S. *et al.* 2007; Arbiser, J.L. *et al.* 2002). In addition, the proliferation of Her-2/neu-transformed rat fibroblasts growth is suppressed by catalase (Preston, T.J. *et al.* 2001), suggesting that H_2O_2 in particular may be an efficient driver of proliferation in cancer cells. DNA damage driven by ROS (section 1.4.1) can also contribute to genomic instability, which may promote disease progression.

However, there is also evidence that ROS generation can mediate cell cycle arrest and senescence, especially in the context of mutant Ras expression. For example, expression of mutant Ras in primary human fibroblasts (Lee, A.C. *et al.* 1999; Wang, W. *et al.* 2002) or epithelial cells (Nicke, B. *et al.* 2005) led to a stress response and cell cycle

arrest, which was attributed to ROS production. Reports such as these appear to conflict with those already discussed which propose that ROS promote proliferation, and not cell cycle arrest. This paradox was investigated by Dolado *et al.*, who showed that mutant H-Ras expression in normal primary human fibroblasts induces a stress response resulting in activation of $p38^{MAPK}$ and subsequent cell cycle arrest/apoptosis (Dolado, I. *et al.* 2007). However $p38^{MAPK}$ activation and cell cycle arrest driven by mutant Ras could be bypassed by co-expression of Gstm2, an enzyme involved in GSH synthesis. Importantly, this group demonstrated that several ROS producing cancer cell lines have specifically silenced $p38^{MAPK}$ activation by ROS, while $p38^{MAPK}$ activation by UV or osmotic shock was normal. This important study suggests that while ROS induced by oncogenic Ras can promote cell cycle arrest in normal primary cells via $p38^{MAPK}$, cancer cells may evolve to evade this response, and hence benefit from increased ROS production in terms of increased proliferation.

Both mitochondrial and NOX derived ROS production are known to play a role in angiogenesis (the remodelling of existing vasculature to establish blood supply to hypoxic/damaged tissues) and this may be due to the ability of ROS to stabilise hypoxia-inducible factor -1α (HIF-1α). Under normoxic conditions, HIF-1α has an extremely short half-life (<5 min), due the actions of proline hydroxlases (PHDs) which remove the hydroxyl groups from Pro564 and Pro402 of HIF-1α, and dehydroxylated HIF-1α is then bound by von Hippel-Landau factor (vHLF). Since vHLF is a recognition component for an E3-ubiquitin ligase, association of HIF-1α with vHLF leads to rapid proteasomal degradation of HIF-1α. H_2O_2 generated by the mitochondria during hypoxia (1.4.2.2) inhibits PHDs (Fruehauf, J.P. and Meyskens, F.L., Jr. 2007), which allows accumulation of HIF-1α. HIF-1α then heterodimerises with HIF-1β, and initiates the transcription of genes that promote angiogenesis e.g. through VEGF production (Vaupel, P. 2004). Additionally, it appears that NOX derived H_2O_2 can augment VEGF signalling. VEGF promotes angiogenesis by inducing the proliferation and migration of vascular endothelial cells via VEGF receptor type 2 signalling (VEGFR2 aka Flk1; a receptor tyrosine kinase). NOX-derived H_2O_2 'amplifies' VEGFR2 signals by prolonging receptor phosphorylation, probably by inhibiting tyrosine phosphatases such as Shp-1, Shp-2 and PTP1B (Ushio-Fukai, M. and Nakamura, Y. 2008).

NOX-derived ROS have also been implicated in vasculogenesis; a process which co-operates with angiogenesis, but (unlike angiogenesis) involves the generation of new vasculature from endothelial progenitor cells (EPCs) derived from the bone marrow. Effective vasculogenesis requires that EPCs efficiently home to the ischaemic site. In a

mouse model of vasculogenesis, hindlimb ischaemia resulted in upregulation of NOX2 in bone marrow mononuclear cells, increased ROS and increased EPC mobilisation. Interestingly, Nox2-deficient mice showed markedly decreased vascular recovery after ischaemia, reduced EPC mobilisation, and ineffective EPC homing to the ischaemic site. Transplantation of Nox2-deficient bone marrow recapitulated the defect in wild type mice, while wild-type bone marrow could rescue the defect when transplanted in Nox2-deficient mice (Urao, N. *et al.* 2008). These studies strongly support the positive influence of ROS production on angiogenesis and vasculogenesis.

There is also evidence that ROS production can contribute to metastasis in solid tumours (Wu, W.S. 2006; Nishikawa, M. *et al.* 2005). Nishikawa *et al.* examined the effects of ROS production on metastasis using colon28 cells and B16-BL6/Luc melanoma cells injected intravenously into recipient mice. In both of these studies respectively, catalase treatment suppressed metastatic colony formation in the liver or lungs of recipient mice. Targeting the catalase enzyme to specific organs by chemical modification of the catalase molecule further suppressed metastasis in those organs, suggesting that H_2O_2 augments the metastatic potential of these cells. Similarly, Wu *et al.* showed that TPA-induced migration of human HepG2 hepatocarcinoma cells was suppressed by a variety of antioxidant molecules including catalase, mannitol and NAC. In this case, it appeared that ROS-dependent migration of HepG2 cells was dependent on ROS-mediated activation of ERK and transcription of several integrin genes which promote migration.

The long held belief that ROS are exclusively pro-apoptotic has been challenged by recent evidence suggesting that ROS may participate in pro-survival signals (Groeger, G. *et al.* 2009), and this may be exploited by some cancer cells. For example, targeted knockdown or inhibition of NOX4 in pancreatic cancer cells induces apoptosis, suggesting NOX4-derived ROS promoted the survival of these cells (Mochizuki, T. *et al.* 2006), which may be in part due to the ability of NOX4-derived ROS to activate JAK2, an anti-apoptotic kinase (Lee, J.K. *et al.* 2007). Similarly, NOX4-derived ROS appeared to promote survival of $BCR\text{-}ABL^+$ CML cells, via oxidative inhibition of PTEN and PP2A, resulting in augmented PI3K-Akt signalling (Naughton, R. *et al.* 2009).

While the evidence presented above demonstrated that ROS can promote cancer cell survival, it is clear that excessive ROS can be pro-apoptotic. As discussed in section 1.4.1, excessive ROS causes widespread damage to DNA, lipids and proteins, and this can lead to necrotic cell death. However, it is also possible that subtle levels of ROS generated by the mitochondria may directly promote apoptosis by the intrinsic pathway. Studies in isolated rat mitochondria showed that mitochondrial ROS can oxidise cysteine residues of

the adenine nucleotide translocase (ANT) component of the mitochondrial permeability transition pore complex. Oxidation of ANT promotes opening of the pore (Costantini, P. *et al.* 2000), leading loss of mitochondrial homeostasis followed by mitochondrial rupture, releasing pro-apoptotic factors such as cytochrome C into the cytosol (Fruehauf, J.P. and Meyskens, F.L., Jr. 2007). However, it is not currently known whether this mechanism operates in intact cells or indeed *in vivo*.

It is important to note that the outcome of ROS generation within a cell is highly dependent on several factors including the levels of ROS produced, the duration of production and the subcellular location. The high concentration of intracellular antioxidants in normal cells means that ROS production and signalling can potentially be very tightly controlled (Leslie, N.R. 2006), but in conditions where ROS production is augmented (or antioxidant systems are compromised), there is scope for dysregulation of ROS signalling. In short, the body of evidence strongly suggests that ROS must be maintained within a defined range to exert its physiological effects, and drastic increases or decreases in ROS are likely to lead to non-physiological or pathophysiological conditions. It is also clear that ROS production is not an absolute prerequisite feature of all tumour cells, indeed, there is evidence breast cancer 'stem' cells show consistently lower levels of ROS than their normal counterparts (Diehn, M. *et al.* 2009). Nevertheless it is clear that ROS production can influence the behaviour of a wide variety of tumour cells that overproduce them.

1.4.4.4 Targeting ROS in cancer therapy

It has been proposed that the increased ROS production observed in some cancer cells may be exploited for therapeutic gain (Benhar, M. *et al.* 2002; Trachootham, D. *et al.* 2009). Targeting ROS in cancer therapy can take two approaches – the first involves further promotion of ROS production in cancer cells by treating them with pro-oxidants (compounds which introduce exogenous ROS or promote its production), or by inhibiting intracellular antioxidants. Certainly, there is evidence that intracellular antioxidant pools (such as GSH) are augmented in cancer cells (possibly in response to increased oxidative stress) and that this increased antioxidant capacity may play a role in drug resistance (Townsend, D.M. and Tew, K.D. 2003; Townsend, D.M. *et al.* 2005). Indeed, it appears that a pro-oxidant therapeutic approach is effective in several cancer types; for example arsenic trioxide (As_2O_3) is a pro-oxidant molecule which is currently approved for treatment of relapsed APL. As_2O_3 may act through inhibition of thioredoxin function (Lu, J. *et al.* 2007) and also by augmentation of ROS produced by the mitochondrial ETC

(Pelicano, H. *et al.* 2003). Phenethyl isothiocyanate (PEITC) is another pro-oxidant molecule which acts by depleting GSH pools, leading to elevated oxidative stress. This compound has shown promise in treating drug-resistant leukaemias; it was shown to be effective in killing fludarabine-resistant CLL cells (Trachootham, D. *et al.* 2008) and also-Gleevec resistant CML cells (Zhang, H. *et al.* 2008). However, in using such pro-oxidant approaches, it is important to note that that oxidative stress would increase in normal cells, which may cause increased toxicity and may also induce de novo mutations.

An alternative approach to targeting ROS is to use antioxidants to suppress the high levels in cancer cells; with the rationale that ROS-generating cancers may develop a degree of dependence on high levels of ROS (apoptosis in pancreatic cancer cells after knockdown of NOX4 supports this notion). In addition, antioxidant treatment as an adjunct to standard therapies may reduce toxicity. On the other hand, several mainstay chemotherapeutic agents (examples) are known to depend on ROS generation for their cytotoxic effects; moreover, ROS depletion may suppress tumour cell proliferation, which potentially conflicts with the actions of agents which specifically target proliferating cells (e.g. nucleoside analogues such as cytarabine). However, a recent review of clinical trials which employed antioxidants in addition to standard chemotherapy in a variety of cancers concluded that antioxidants were not antagonistic to cancer therapy, in fact several studies reported decreased treatment-associated toxicity, allowing an increased proportion of patients to complete their therapy (Block, K.I. *et al.* 2008).

In summary, targeting ROS in cancer therapy is an exciting approach that is attracting significant interest; indeed, as discussed above, many agents that target ROS are now in clinical trials or have been approved for use in the clinic.

1.4.5 DETECTION OF ROS

ROS are a chemically heterogeneous group of molecules which are (in the main) moderate to strong oxidants, meaning they favour acquisition of electrons from donor molecules. However, their high reactivity makes them relatively short lived and therefore difficult to detect. Early studies exploited the oxidative capacity of ROS to detect these species *in vitro*. For example, superoxide has been measured historically oxidation of cytochrome c and nitroblue tetrazolium (NBT) could be measured by optical spectroscopic methods (Tarpey, M.M. and Fridovich, I. 2001). However optical spectroscopic approaches suffer from a relatively low sensitivity and a narrow dynamic range, which limits their usefulness. In contrast, fluorescent and chemiluminescent assays offer superior sensitivity, and extremely large dynamic range (Wardman, P. 2007). Therefore, the present

study employed chemiluminescence and several fluorescence-based assays for detection of ROS. An additional technique for studying oxygen centred radicals is electron paramagnetic resonance (EPR) spectroscopy. This technique (while technically demanding) offers the benefit of unequivocal identification of oxygen-centred radicals, and is therefore a useful tool to verify the results of fluorescence and chemiluminescence-based assays.

1.4.5.1 Principles of fluorescence and chemiluminescence

Fluorescence occurs when an electron within a fluorochrome (a molecule that exhibits fluorescence) absorbs the energy of an incident photon (becomes excited), and subsequently releases some of that energy as an emitted photon. The excitable electrons within a fluorochrome molecule are located within a particular moiety or functional group of the molecule; this region is called the fluorophore. During the first step in fluorescence, the excited electron is promoted from a relatively stable low-energy state (ground state) to an unstable (and therefore transient) excited state, for example the electron can be promoted to a higher energy molecular orbital (E1 or E2 in Figure 1.14). Within that higher energy orbital, the electron may occupy one of several vibrational or rotational energy states (Figure 1.14). Due to the principle of energy quantisation, an electron may only possess discrete energies, therefore, absorption of an incident photon will only occur when the energy of that photon exactly matches the energy required to complete one of the possible transitions (green arrows in Figure 1.14). Since the energy of a photon is directly related to its frequency by Planck's equation ($E=h\nu$, where E is the energy of the photon, h is Planck's constant, and ν is the frequency of the incident photon), only photons with a given frequency (and therefore wavelength) are efficiently absorbed.

Since there are many possible electronic transitions in a given fluorochrome molecule, there is an accordingly broad range of wavelengths that can potentially be absorbed resulting in a unique spectrum of absorption for every different fluorochrome molecule (the absorption spectrum). However, some electronic transitions are more probable than others and this is reflected in the shape of the absorption spectrum, with maximal absorption (absorption maxima) occurring at the wavelengths corresponding to the energy of the most probable electronic transition (Figure 1.15).

Since the electron in the excited state is unstable, conversion back to the stable ground state is favourable. To achieve this, the electron must release all of the energy (relaxation) which was acquired from the incident photon, which can occur by several different processes. Some energy is lost by descending through various rotational and

vibrational energy states (released as heat, or kinetic energy) or by internal conversion (transition between two high energy orbitals), until the lowest vibrational energy state within the E_1 excited molecular orbital is reached (yellow wavy arrows in Figure 1.14). From this point, a transition between electronic energy levels can occur; during this transition energy is released by the electron in the form of a photon (fluorescence; shown as red arrows in Figure 1.14). Critically, since some of the original photons energy was lost by non-radiative means, the energy of the emitted photon is less than that of the original photon and therefore has a longer wavelength. Again, since there are several routes that the relaxing electron can take in order to release its energy (and some are more probable than others) there is an accordingly broad range of emitted wavelengths (the emission spectrum), with the most commonly emitted wavelength (the emission maxima) corresponding to the energy of the most probable electronic relaxation (Figure 1.15). The difference in wavelength of the excitation and emission maxima for a particular fluorochrome is often referred to as the Stoke's shift, and this effect is a key factor in the high sensitivity of fluorescence-based approaches. Using a combination of controlled excitation wavelengths (generated by lasers or LEDs) and optical filters, the photon emission by a fluorochrome can be isolated from the excitation photons, allowing background to be substantially reduced. Furthermore, the development of high-voltage photomultiplier tubes enabled the amplification of even weak fluorescent signals. Finally, a fluorescent molecule can undergo many cycles of absorption and emission which further improves the sensitivity. Modern flow cytometers and laser-scanning confocal microscopes combine all of these technologies enabling the sensitive assay of both intra- and extracellular targets at the sub-cellular level.

However, fluorescence-based approaches are not without their limitations. For example, although fluorochromes may indeed undergo several emission cycles, most molecules cannot do this indefinitely. The high energy associated with the excited state of the molecule can often promote inter- or intramolecular reactions which may destroy the fluorophore (photobleaching). Thus over time the fluorescence falls below that expected over time. Also, the Stoke's shift for some fluorochromes is small, making it more difficult to separate the excitation light source from the emitted light. Similarly, care must taken when choosing multiple fluorochromes for use within a single assay, since the excitation and emission spectra of some fluorochrome are so similar as to render them incompatible for simultaneous use. On the other hand, the development of optimised fluorescent dyes with well-separated excitation and emission spectra, and a resistance to photobleaching (e.g. Alexa Fluors®), go some way to address these limitations.

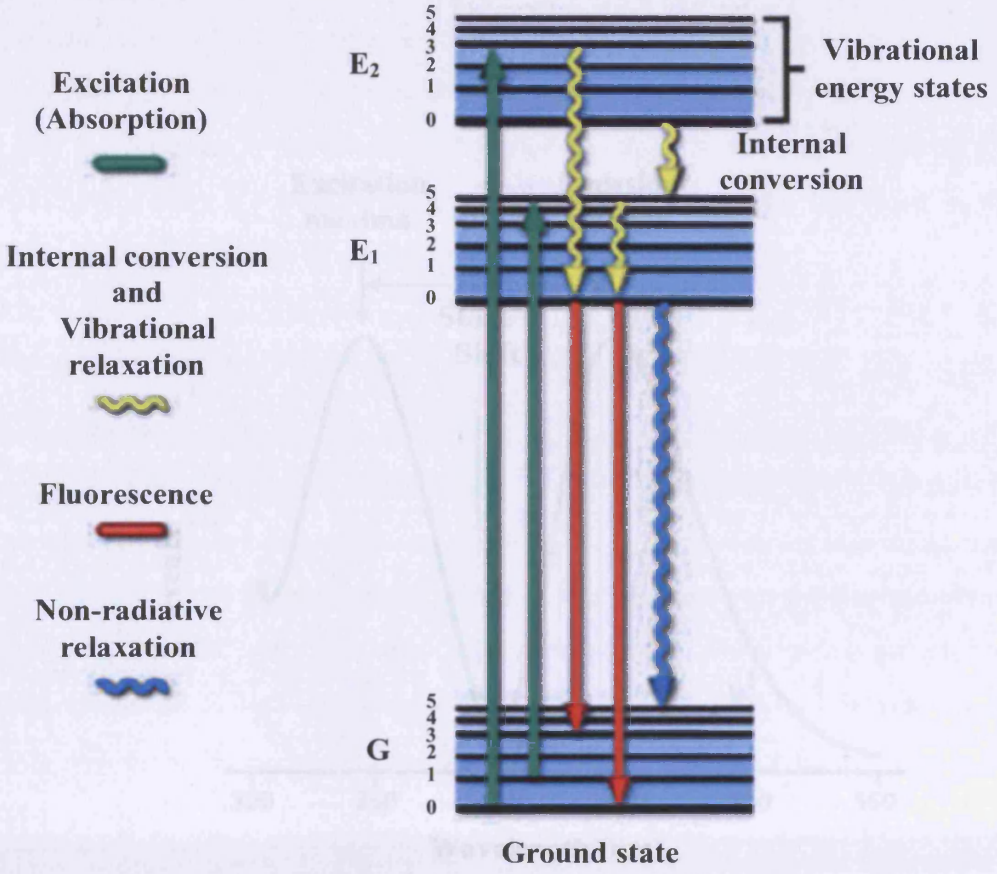

Figure 1.14 A simple electron energy level diagram highlighting the basic principles of fluorescence

Electrons in the stable ground state (G) may absorb the energy of incident photons if the photon's energy matches the energy gap between one of the allowed electronic transitions (green arrows) to a higher energy orbital (E_1 or E_2). Within each higher energy orbital, the electrons may also occupy one of several rotational or vibrational energy states (labelled 0-5). The excited state is transient and the electrons gradually return to the ground state via descent to the $E_1 = 0$ energy level (yellow curvy arrows). Electronic transitions from here to within the G energy level are accompanied by a release of energy as an emitted photon. Since energy is lost prior to photon emission, the emitted photon has less energy (longer wavelength) than the incident photon. Some transitions from $E_1 = 0$ to G are non-radiative (blue curvy arrows), meaning the energy is not released as a photon. Adapted from http://www.olympusconfocal.com.

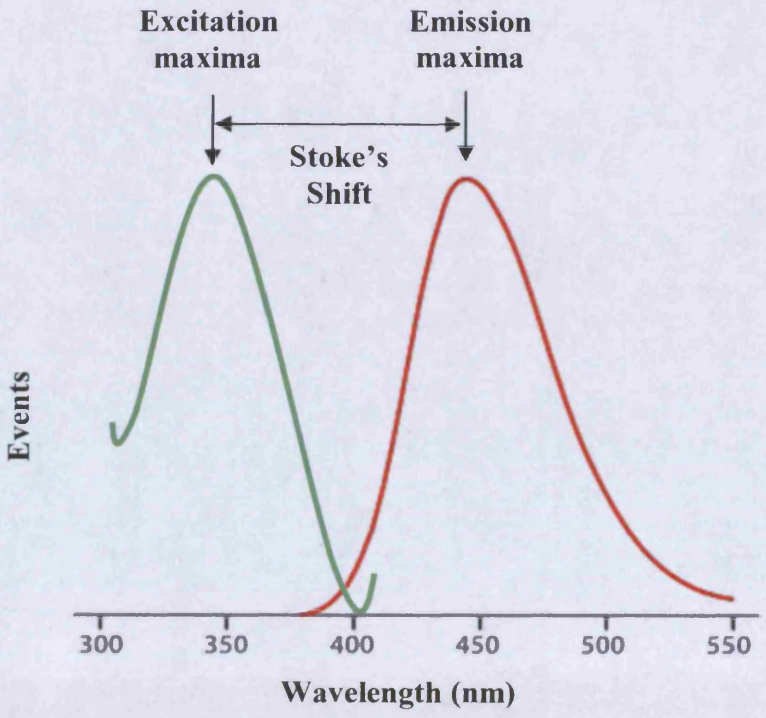

Figure 1.15 Examples of excitation and emission spectra

The above traces demonstrate the principles of absorption (or excitation spectra) and emission spectra. The green line depicts how the number of incident photons absorbed varies with the wavelength of those photons, and marks out a range of wavelengths over which absorption occurs. Similarly, the red line depicts how the number of photons emitted varies with wavelength, again marking out a range of wavelengths over which emission is detected. Note that the curves both exhibit a peak (maxima). The wavelengths at which these maxima occur correspond to the energies of the most probable transitions that occur during absorption and emission within the fluorochrome. The difference between the excitation and emission maxima is referred to as the Stokes's shift (see text for an explanation of this phenomenon).

Chemiluminescence is similar to fluorescence in that it describes the emission of photons by an electronically excited molecule or species; however it differs from fluorescence in that the excitation energy is supplied by a chemical reaction, rather than by incident photons. Detection of chemiluminescence is achieved using similar technology to that used for detection of fluorescence, with the simplification that optical filters are not essential, since there is no excitation light source. Since there is no significant background, chemiluminescent techniques exhibit an extremely high sensitivity.

1.4.5.2 Fluorescent and chemiluminescent probes for ROS detection

Fluorescent probes are an iteration of fluorochrome chemistry. Whereas fluorochromes will always fluoresce when exposed to electromagnetic radiation of the correct wavelength, fluorescent probes are designed to fluoresce in a controlled manner only under specific conditions i.e. in the presence of the probe target. Since ROS are predominantly oxidising agents, most of the commonly used fluorescent probes for ROS detection are reduced forms of fluorochrome molecules. The reduced form of the probe is either non-fluorescent, or has a significantly different emission maxima to that of the oxidised probe.

A useful example of this principle is the commonly used probe for ROS detection dihydrodicholorofluoroscein diacetate (H_2DCFDA), which is a reduced form of the green fluorescent probe dichlorofluoroscein (DCF). The reduced form (H_2DCFDA) is non-fluorescent, since the additional hydrogen atoms in the structure disrupt the delocalised π-electron system which forms the fluorophore in DCF. The acetyl groups improve membrane permeability of the probe, and are quickly cleaved by intracellular esterases. The deacetylated probe is less membrane permeable than the acetylated form, which confers a degree of increased intracellular loading of the probe. In the presence of oxidising agents, the electrons binding the two critical H atoms to the H_2DCF molecule are lost, resulting in the formation of the fluorescent oxidised form of the probe (DCF).

A similar principle applies to the mechanism of action of the fluorescent probes used to detect ROS in the present study; Amplex Red and MitoSOX were used to detect H_2O_2 and mitochondrial superoxide respectively, sections 3.2.4 and 3.2.3 respectively.

In the case of chemiluminescent probes for ROS, oxidation of the probe invariably initiates a chemical reaction which results in the formation of the electronically excited molecule. This study employed Diogenes, a chemiluminescent probe based on luminol (section 3.2.1).

It has been noted that some commonly used probes used for ROS detection (for example H_2DCFDA) are rather non-specific in that they can become fluorescent in the presence of several different oxidant molecules (Wardman, P. 2007). Therefore the present study has avoided the use of DCF in favour of more recently developed (and potentially more specific) probes. However, to verify the specificity of the chosen probes, this study has employed a variety of ROS scavengers and inhibitors of ROS production, and has used several different assays to verify the presence of a particular species (such as superoxide). Several of the ROS inhibitors used are exquisitely specific (for example, the enzymes catalase and SOD), which goes some way to compensate for any lack of specificity of the probes.

1.4.5.3 Detection of oxygen-centred radicals using EPR spectroscopy

Electron paramagnetic resonance (EPR) spectroscopy is a technique which can detect unpaired electrons (radicals) within a molecule and gain information about the local molecular structure by virtue of radicals' ability to absorb electromagnetic radiation, in an analogous manner to the way nuclear magnetic resonance (NMR) spectroscopy can detect specific nuclei. It is based on the principle that radicals can absorb X-band (9.25 GHz) microwave energy when placed in a strong magnetic field (~3000 Gauss).

A detailed discourse on quantum mechanics is beyond the scope of this thesis; however, it is useful to consider some properties of electrons which will allow (in basic terms) an understanding of the principles of EPR spectroscopy. Electrons are negatively charged particles with a quantum mechanical property called spin (m_s), which describes the intrinsic angular momentum of the electron (m_s is one of four quantum numbers that define each particle in quantum mechanics). While there is no precise classical analogy for this property, for the purposes of this thesis it is best to consider that an electron spins about an internal axis; and the value given for m_s relates to the number of different spin states the electron can occupy. In the case of electrons, $m_s = ½$; and this has the consequence that an electron can occupy two distinct spin energy states (spin-up or spin-down).

Since the electron has an intrinsic angular momentum and is charged, the electron has an associated magnetic moment (i.e. it has its own magnetic field and acts like a tiny magnet). When a strong magnetic field is applied, the electron's own magnetic field interacts with the applied field; as a result the electron can adopt one of two energy states (remember that m_s is ½). The electron can either align its own magnetic field with the applied field (which is the lower energy state) or it can anti-align with the applied field, which is a higher energy state. The energy difference between these two states is

dependent on the strength of the applied magnetic field. Importantly, electrons in the low energy state can be encouraged to jump to the higher energy state by irradiating them with microwaves. Similar to absorption of light energy leading to fluorescence, absorption of microwaves by the electrons only occurs when the energy of the incident microwaves exactly matches the energy gap between the two possible states. Hence, in a constant magnetic field, a sample can be irradiated with microwaves of varying energy resulting in an absorption spectrum (an EPR spectrum). The particular frequency of microwave energy that the unpaired electrons will absorb is highly dependent on the properties of the electron and its molecular environment. Alternatively the microwave energy can be kept constant and the magnetic field can be varied giving the same EPR spectrum result. Again, the properties of the electron and its molecular environment define the magnetic field strength at which absorption will occur. It turns out that the latter method is more precise and it is the method used in all modern EPR instruments.

It might be expected that the EPR spectrum obtained from a single unpaired electron within a molecule would consist of one absorption peak, however, EPR spectra are often more complex, consisting of several separate peaks which form the EPR spectrum. This phenomenon occurs due to interactions between the magnetic moment of the unpaired electron and the magnetic moments of nearby spin-active nuclei. These interactions result in additional allowed spin-energy states causing splitting of the electron absorption signal into several absorption peaks. This phenomenon is known as hyperfine splitting or hyperfine coupling and is analogous to J-coupling observed in NMR spectroscopy. The spacings between the additional peaks are dependent on the properties of the coupling nuclei and their distance from the unpaired electron, and are referred to as hyperfine coupling constants, denoted a_X, where X is the element symbol of the nucleus that is causing the hyperfine splitting to occur. Hyperfine coupling constants observed in unidentified EPR spectra can be measured and can indicate which nuclei are proximal to the unpaired electron and hence provide data on the likely molecular structure of the molecule.

DEPMPO is a beta-phosphorylated nitrone which stabilises short-lived radical molecules such as superoxide and hydroxyl radicals by reacting with them to form a relatively long-lived radical molecule known as a spin adduct. Each spin adduct has a unique EPR spectrum which enables free radical identification. Until recently, trapping and identifying oxygen-centred radicals (such as superoxide radicals) was often performed using the spin trap probe DMPO, a molecule closely related to DEMPO. However, the spin adduct formed by the reaction of DMPO with superoxide (DMPO-OOH) is relatively short

lived (half life 60 sec) due to an intramolecular elimination reaction which forms a molecule identical to the adduct formed when DMPO reacts with hydroxyl radicals (DMPO-OH). Therefore, when trapping superoxide radicals with DMPO, this phenomenon results in an EPR spectrum which is a superimposition of both the DMPO-OOH and DMPO-OH spectra, which evolves over time to that of a 'pure' DMPO-OH EPR spectrum.

DEPMPO offers an advantage over DMPO because rate of the intramolecular elimination reaction is much slower in DEPMPO, resulting in a 15 fold greater persistence of the DEPMPO-OOH adduct than the DMPO-OOH adduct (Frejaville, C. *et al.* 1995), enabling easier detection and identification of superoxide radicals. Importantly, DEPMPO itself does not contain any radicals and so does not have an EPR spectrum - EPR spectra are only observed from molecules derived from DEPMPO which contain a radical i.e. the spin adducts of DEPMPO, DEPMPO-OOH and DEPMPO-OH. The EPR spectra of the spin adducts formed when superoxide or hydroxyl radicals react with DEPMPO (DEPMPO-OOH and DEPMPO-OH respectively) have been characterised previously (Mojovic, M. *et al.* 2005; Dikalov, S. *et al.* 2005), therefore EPR spectroscopy using DEPMPO is a useful technique to verify superoxide and hydroxyl production indicated using other detection methods. Figure 1.16 illustrates the absorption of microwave energy by unpaired electrons.

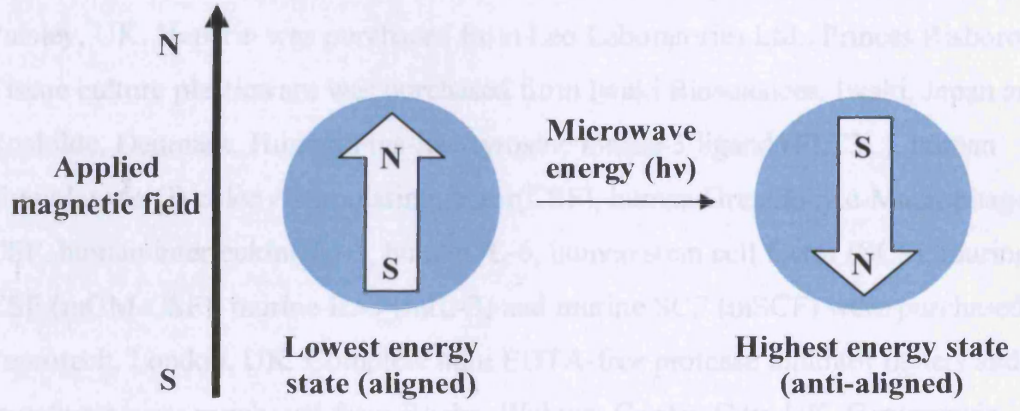

Figure 1.16 Absorption of microwave energy by electrons in an applied magnetic field

Electrons (blue circles) have an associated magnetic field (represented by North and South poles, N and S). In an applied magnetic field, electrons will preferentially adopt an energy state which aligns their intrinsic magnetic field with the applied field. However, electrons may also occupy a higher energy state, where the intrinsic magnetic field is anti-aligned with the applied field. Microwave radiation can supply the energy required for the electron to move to the higher energy state, in which case the microwave energy is absorbed. An absorption spectrum (EPR spectrum) can therefore be obtained by keeping the microwave energy (wavelength) constant while cycling through an increasing magnetic field.

2 General Materials and Methods

2.1 MATERIALS AND BUFFER FORMULATIONS

2.1.1 MATERIALS

Materials in general use are listed below, grouped by manufacturer/supplier and listed in alphabetical order followed by synonyms in parentheses. All reagents were of Analar grade and/or tissue-culture tested unless otherwise stated. Bacto-tryptone®, Bacto-yeast® and Ficoll-Paque® were purchased from BD Biosciences, Oxford, UK. Fetal calf serum (FCS) was purchased from BioSera, Ringmer, UK. Ultra-purified H_2O was obtained using a PureLab® Ultra water purification unit manufactured by Elga LabWater, High Wycombe, UK. Liquid nitrogen (N_2) was purchased from BOC, Guildford, UK. Tissue culture grade H_2O was purchased from Hameln Pharmaceuticals, Gloucester, UK. Agarose, dithiothreitol (DTT), Hank's Balanced Salt Solution (HBSS), penicillin, Phosphate Buffered Saline (D-PBS; PBS), streptomycin, Super-Optimal medium (Catabolite-repressing) (SOC medium) and trypsin were purchased from Invitrogen, Paisley, UK. Heparin was purchased from Leo Laboratories Ltd., Princes Risborough, UK. Tissue culture plasticware was purchased from Iwaki Biosciences, Iwaki, Japan and Nunc, Roskilde, Denmark. Human Fms-like tyrosine kinase-3 ligand (FLT3L), human Granulocyte(G) colony-stimulating factor(CSF), human Granulocyte-Macrophage(GM)–CSF, human interleukin(IL)-3, human IL-6, human stem cell factor (SCF), murine GM-CSF (mGM-CSF), murine IL-3 (mIL-3) and murine SCF (mSCF) were purchased from Peprotech, London, UK. Complete mini EDTA-free protease inhibitor tablets and human transferrin were purchased from Roche, Welwyn Garden City, UK. Gentamycin (Cidomycin®) was purchased from Sanofi-Aventis, Guildford, UK. Phosphatase Inhibitor Cocktail for Western blotting was purchased from Santa Cruz Biotechnology, CA, USA. Ampicillin, apocynin (4'-Hydroxy-3'-methoxyacetophenone; acetovanillone), Bradford's Reagent, bovine serum albumin fraction V (BSA), calcium chloride ($CaCl_2$), catalase, chloroquine (N'-(7-chloroquinolin-4-yl)-N,N-diethyl-pentane-1,4-diamine), diphenyleneiodonium (DPI), Dulbecco's Modified Eagle's Medium (DMEM), deoxyribonuclease I (DNAse I), ethylenediamine-tetraacetic acid (EDTA), ethylene glycol-bis(2-aminoethylether)-N,N,N',N'-tetraacetic acid (EGTA), ethanoic acid, ethanol, α-D-

glucose, glucose oxidase (GOX), glycerol, hydrochloric acid (HCl), hypoxanthine (6-hydroxypurine), Iscove's Modified Dulbecco's Medium (IMDM), L-glutamine, magnesium chloride ($MgCl_2$), magnesium sulphate ($MgSO_4$), mercaptoethanol (β-mercaptoethanol), methanol, N-acetyl cysteine (NAC), polybrene, Ponceau S Reagent, potassium chloride (KCl), potassium dihydrogen phosphate (KH_2PO_4), rotenone, Roswell Park Memorial Institute 1640 culture medium (RPMI 1640), sodium chloride (NaCl), sodium hydroxide (NaOH), sodium orthovanadate (Na_3VO_4), sodium phosphate (Na_2HPO_4), SOD1 (bovine Cu/Zn SOD), tempol (4-Hydroxy-2,2,6,6-tetramethylpiperidine 1-oxyl), TPA (12-O-tetradecanoylphorbol-13-acetate; aka phorbol 12-myristate 13-acetate (PMA)), Tris (tris(hydroxymethyl)aminomethane), Triton X-100 (4-(1,1,3,3-tetramethylbutyl)phenyl-polyethylene glycol), Tween-20 (polyethylene glycol sorbitan monolaurate) and xanthine oxidase were purchased from Sigma-Aldrich, Poole, UK. Retronectin was purchased from Takara, Shiga, Japan.

2.1.2 FORMULATION OF BUFFERS AND SOLUTIONS

Formulations of buffers that are not defined in the text are given below in alphabetical order. Where appropriate, solutions were autoclaved for 20 min at 15 lb/sq.in after preparation, but before addition of labile substances, such as antibiotics. Where autoclaving was inappropriate, solutions were passed through a 0.45 µm sterile filter. All solutions are aqueous unless otherwise stated.

Diogenes buffer (section 3.2.1.1): 4.6 mM KH_2PO_4, 8.0 mM Na_2HPO_4, 130.0 mM NaCl, 4.4 mM KCl, 5.5 mM glucose, 0.5 mM $MgCl_2$, 0.5 mM $CaCl_2$, 0.1% BSA, dissolved in dH_2O, pH 7.4. **Krebs-Ringer phosphate-glucose buffer (KRPG)** (section 3.2.4.2): 145 mM NaCl, 5.7 mM NaH_2PO_4, 4.9 mM KCl, 0.5 mM $CaCl_2$, 1.2 mM $MgSO_4$, 5.5 mM glucose, dissolved in dH_2O, pH 7.4. **Lysis buffer** (section 2.5.1): 10 mM HEPES-KOH, 10 mM betamercaptoethanol, 1mM magnesium acetate, 0.5 mM EDTA, 0.5 mM EGTA, 0.25 M sucrose, 1 mM Na_3VO_4, 1 complete protease inhibitor tablet per 10 ml, dissolved in dH_2O, pH 7.2. **Magnetic activated cell sorting (MACS) buffer** (section 2.3.2): PBS containing 0.5% BSA, 5 mM $MgCl_2$, dissolved in dH_2O, 0.45µm filtered, degassed under negative pressure for 30 min. **PepChip activation mix** (section 5.2.2.2): 2 mCi/ml γ-^{33}P-ATP, 50% glycerol, 5 mM DTT, 50 mM $MgCl_2$, 50 mM $MnCl_2$, 250 µg/ml polyethylene glycol 8000, 250 µg/ml BSA. **PepChip lysate dilution buffer** (section 5.2.2.2): 50 mM HEPES-KOH (pH 7.5), 10 mM $MgCl_2$, 10 mM $MnCl_2$, one complete protease inhibitor cocktail tablet per 10 ml. **Ponceau S** (section 2.5.3): 1.3 mM Ponceau S, dissolved in 0.83 M ethanoic acid. **Selective Luria-Bertani (LB) broth** (section 2.4.2):

10g Bacto-Tryptone, 5g Bacto-yeast extract, 10g NaCl dissolved in 1 L dH_2O, pH 7. 50 µg/ml ampicillin added just before use. **Selective LB agar** (section 2.4.2): As selective LB broth with addition of 15 g/L agarose. 50 µg/ml ampicillin added just before use. **Staining buffer for flow cytometry** (section 2.6): PBS containing 1% BSA, 3.1 mM NaN_3, dissolved in dH_2O. **Tris-buffered saline (TBS)** (section 2.5.1): 1 M Tris-HCl, 130.0 mM NaCl, dissolved in dH_2O, pH 7.6. **TBS-Tween-20 (TBS-T)** (section 2.5.3): TBS containing 0.1% Tween-20. **Tris-EDTA (TE) buffer** (section 2.4.5): 10 mM Tris-HCl, 1 mM EDTA, pH 7.5.

2.2 CELL CULTURE AND CRYOPRESERVATION

2.2.1 CRYOPRESERVATION AND THAWING OF CELL SAMPLES

Cell suspension (500 µl in appropriate growth medium) was mixed with 500µl of IMDM containing 30% FCS and 20% DMSO. Samples were transferred to 1.8 ml vials and immediately placed in a controlled refrigeration container (using 100% isopropanol as the thermal interface) which had been equilibrated to room temperature before use. Controlled refrigeration containers were then immediately placed in a -80°C freezer until samples had equilibrated. For long term storage, frozen samples were transferred to liquid N_2 storage.

Cryopreserved primary cells were recovered by rapid defrosting in a 37°C water bath in the presence of 900 µl 0.45µm-filtered FCS and 200 µg sterile DNAse I. Cryoprotectant was slowly diluted by dropwise addition of an equal volume of MACS buffer over 3 min. This addition of an equal volume over 3 min was performed twice more, and primary cells were then recovered by centrifugation at 180 g for 10 min and resuspended in growth medium (section 2.2.3) and allowed to recover for 16-24 h in a 5% CO_2 humidified atmosphere at 37°C.

Cryopreserved cell lines were recovered by rapid defrosting in a 37°C waterbath followed by dropwise addition of 5 ml growth medium (section 2.2.3). Cell lines were then recovered by centrifugation at 180 g for 5 min and resuspended in growth medium and allowed to recover for 16-24 h at 37°C in a 5% CO_2 humidified atmosphere at 37°C.

2.2.2 DETERMINATION OF CELL COUNT

Cellularity of cultures was determined using a glass haemocytometer with counting chambers delineated with improved Neubauer ruling (Hawksley, Brighton, UK). Briefly, 8 µl was removed from cell suspension with a known total volume and placed into

a counting chamber. The haemocytometer is etched with ruled lines marking a counting space which has a known volume (0.9 µl). This volume is subdivided by ruled lines into 9 cuboids equivalent to 100 nl each. The cellularity of the sample in cells/ml is given by the average number of cells per cuboid multiplied by $1x10^4$.

2.2.3 CULTURE OF PRIMARY AND TRANSFORMED CELL LINES

All cell lines listed below were obtained from ATCC (Teddington, UK) unless otherwise stated, and cultured at 37°C in a humidified 5% CO_2 atmosphere in RPMI 1640 containing 10% FCS and 20µg/ml gentamycin, unless otherwise stated. Cell lines were certified mycoplasma free by the supplier. Cells beyond passage 15 from receipt were discarded. For primary cell cultures, the age of the culture is quoted in days since isolation. Normal human primary $CD34^+$ haematopoietic cells were isolated as described in section 2.3.2.; primary murine Sca-1^+ haematopoietic cells were isolated as described in section 3.2.5.

2.2.3.1 Culture of primary human $CD34^+$ haematopoietic progenitor cells

Transduced human $CD34^+$ cells were cultured at 37°C in a humidified 5% CO_2 atmosphere 37°C and were maintained at 2-$4x10^5$ cells/ml in supplemented IMDM (section 2.3.2) containing 5 ng/ml human(hu)IL-3, huG-CSF and huGM-CSF and 20 ng/ml huSCF, unless otherwise stated. In all cases, media were renewed as necessary or once a week.

2.2.3.2 Culture of primary murine Sca-1^+ haematopoietic progenitor cells

Transduced murine Sca-1^+ cells were cultured under the same conditions as human $CD34^+$ cells (section 2.2.3.1); in supplemented IMDM (section 2.3.2) containing 5 ng/ml murine(mu)IL-3, huG-CSF and muGM-CSF and 20 ng/ml muSCF, unless otherwise stated. In all cases, media were renewed as necessary or once a week.

2.2.3.3 Mono-Mac 6 cells

Mono-Mac 6 (MM6) cells are a human acute monocytic leukaemia cell line established from the peripheral blood of a 64-year-old man with relapsed acute monocytic leukaemia (AML FAB M5) in 1985 following myeloid metaplasia (Ziegler-Heitbrock, H.W. *et al.* 1988). They have previously been used as a model of human monocytes capable of producing superoxide upon stimulation with lipopolysaccharide (LPS aka

endotoxin) or TPA (Tonks, A.J. *et al.* 2003). MM6 cells were maintained at 0.3-1.0x10^6 cells/ml, and were subcultured 1:2 with fresh medium as necessary or every 60 h.

2.2.3.4 HL60 cells

HL60 cells are a promyelocytic cell line derived in 1977 by leukapheresis from a 36-year-old patient with acute promyelocytic leukaemia (Collins, S.J. *et al.* 1978). HL60 cells were maintained at 2-5x10^5 cells/ml to minimise spontaneous differentiation and were subcultured 1:2 with fresh medium as necessary or every 24-36 h.

2.2.3.5 PLB-985 cells

PLB-985 cells are a subclone of HL60 cells (section 2.2.3.4) and can be induced to differentiate in a similar way to HL60 cells when treated with certain agents (Neildez-Nguyen, T.M. *et al.* 1998). PLB-985 cells and a PLB-985 subline deficient for NOX2 expression (PLB-985 NOX2$^{-/-}$)were obtained from Mary Dinuaer, Department of Medical and Molecular Genetics, Indiana University, USA. PLB-985 cells express the Phox complex and can produce superoxide when treated with TPA (section 3.3.2.2), while PLB-985 NOX2$^{-/-}$ cells cannot produce superoxide via Phox (Zhen, L. *et al.* 1993). PLB-985 cells were maintained at 2-5x10^5 cells/ml and were subcultured 1:2 with fresh medium as necessary or every 36 h.

2.2.3.6 HeLa cells

HeLa cells are an adherent cell line derived from cervical cancer cells cultured from a 31 year old patient in 1951 (Masters, J.R. 2002). HeLa cells were cultured in DMEM containing 10% FCS and 20µg/ml gentamycin. Confluent cultures were detached from cell culture plasticware by incubation with 1 ml 500µg/ml trypsin solution containing 0.53mM EDTA (per 25 cm^2 vessel surface area) for 3 min. Trypsin was neutralised with 5 ml warm growth medium and cells were disaggregated by pipetting. Cells were centrifuged for 180 g for 5 min and resuspended in fresh growth medium. Cells were subcultured 1:4 as necessary or every 72 h.

2.2.3.7 Phoenix virus-packaging cells

Phoenix retroviral-packaging cells, which are derived from HEK 293T cells (Kinsella, T.M. and Nolan, G.P. 1996), were obtained from Garry Nolan (Dept. of Microbiology and Immunology, Stanford University, MA) and cultured in DMEM

containing 10% FCS and 20μg/ml gentamycin. Confluent cultures were detached from cell culture plasticware as for HeLa cells (section 2.2.3.6). Cells were subcultured 1:3 as necessary or every 36 h.

2.3 ISOLATION OF NORMAL HUMAN CD34$^+$ HAEMATOPOIETIC PROGENITOR CELLS FROM HUMAN CORD BLOOD

2.3.1 ISOLATION OF HUMAN MONONUCLEAR CELLS FROM WHOLE CORD BLOOD

Human cord blood was obtained from healthy full-term pregnancies at the Maternity Unit, University Hospital Wales, Cardiff, UK. These were obtained with informed consent and with approval from the South East Wales Research Ethics Committee performed in accordance with the 1964 Declaration of Helsinki. Cord blood samples were aseptically collected into tubes containing 500 μl heparin (1000 U[a]/ml) and mononuclear cells were immediately isolated by density centrifugation over Ficoll-Paque®. Briefly, cord blood was diluted with an equal volume of Hank's balanced salt solution (HBSS) containing 25 mM HEPES, 100 μg/ml gentamycin and 1 U/ml heparin. Diluted blood (7 ml) was layered onto Ficoll-Paque® (5 ml) and centrifuged at 400 g for 40 min (brake disengaged). A distinct layer of mononuclear cells formed at the plasma-Ficoll interface; this layer was recovered and initially washed with RPMI 1640 containing 5% FCS and 1 U/ml heparin. The washed mononuclear cells were recovered by centrifugation at 200 g for 10 min (brake disengaged) and were further washed in RPMI 1640 containing 10% FCS until platelet contamination had been removed, verified by microscopic inspection in a haemocytometer chamber. Mononuclear cells were counted using a haemocytometer (section 2.2.2) and stored under liquid N_2 (section 2.2.1).

2.3.2 ISOLATION OF HUMAN CD34$^+$ HAEMATOPOIETIC CELLS FROM TOTAL MONONUCLEAR CELLS

Human CD34$^+$ haematopoietic progenitor cells were isolated from total mononuclear cells by positive selection using the miniMACS® CD34$^+$ Progenitor Cell Isolation Kit (Miltenyi Biotec, Bisley, UK) according to the manufacturer's instructions. Briefly, cryopreserved mononuclear cells prepared as above were thawed (section 2.2.1) and resuspended in MACS buffer (section 2.1.2) at 6.5×10^8 cells/ml. The cells were then

[a] U equates to one international unit (IU) of heparin, currently equivalent to the activity contained in 0.0077 mg of the Second International Standard for heparin (Bangham, D.R. and Mussett, M.V. 1959).

incubated for 15 min at 4°C with 50 µl anti-CD34 antibody (clone QBEND/10) per 10^8 cells in the presence of an FcR blocking agent and were subsequently washed with 5 ml MACS buffer by centrifugation at 180 g for 5 min. Washed mononuclear cells were then incubated at 4°C with magnetic anti-Fc microbeads followed by washing as above. Magnetically-labelled $CD34^+$ cells were isolated from total mononuclear cells by passing the labelled cells through an MS^+ separation column. $CD34^+$ cells were then eluted from the column in the absence of a magnetic field by rinsing the column with 1 ml MACS buffer. A small sample of isolated $CD34^+$ cells (~$1x10^4$) was stained with anti-human CD34 antibody conjugated to R-phycoerythrin (PE) (BD Biosciences), and analysed by flow cytometry (section 2.6) to check for purity. Freshly isolated $CD34^+$ cells were cultured in supplemented IMDM (IMDM containing 1% BSA fraction V, 20% FCS, 45 µM beta-mercaptoethanol, 360 µg/ml 30% iron-saturated human transferrin, 100 U[a]/ml penicillin, 100µg/ml streptomycin) containing 50 ng/ml huIL-3, huSCF, huFLT3L and 25 ng/ml huIL-6, huG-CSF and huGM-CSF.

2.4 GENERATION OF HUMAN $CD34^+$ HAEMATOPOIETIC PROGENITOR CELLS EXPRESSING H-RAS^{G12V} OR N-RAS^{G12D}

Retroviral transduction presents an extremely effective method of gene transfer to haematopoietic cells. The retroviral infection process involves reverse transcription of the RNA viral genome to DNA and integration of the viral DNA into the host genome (Buchschacher, G.L., Jr. 2001). This method offers the major advantage of stable gene expression, which is maintained in the progeny of transduced cells as opposed to transient gene transfer methods based on DNA transfection, such as calcium phosphate transfection, electroporation and liposomal gene transfer. The PINCO amphotrophic retroviral vector has previously been shown to effectively deliver genetic material to a variety of cell types including enriched haematopoietic progenitor cells (Grignani, F. *et al.* 1998) and has been engineered to produce extremely high titres when produced in Phoenix virus-packaging cells (Pear, W.S. *et al.* 1993). Finally, the use of a GFP reporter gene instead of a drug resistance gene eliminates drug-selection regimes and drug-associated artifacts, and enables simple measurement of transduction efficiency by flow cytometry.

Amphotrophic retroviral particles harvested from transfected Phoenix cells have a similar structure to MMLV virions, since both are constructed from proteins encoded by

[a] U equates to one international unit (IU) of crystalline penicillin G, equivalent to the activity of 0.5988 µg of the current International Standard for penicillin.

the MMLV *gag*, *pol* and modified *env* genes, driven by the MMLV LTR promoter sequences. The similarity in virion structure means that recombinant PINCO retroviruses infect cells and integrate as proviral DNA into the host genome in an analogous manner to MMLV. An important difference is that PINCO derived retroviruses are replication deficient, because they do not carry RNA encoding *gag*, *pol* or *env*. Instead, they carry recombinant RNA, engineered to contain the MMLV RNA packaging signal sequence (Ψ). This sequence is recognised by viral proteins which package that RNA molecule into a virion.

2.4.1 GENERATION OF RECOMBINANT PINCO PLASMID DNA ENCODING H-RAS^{G12V}, N-RAS^{G12D} OR CONTROL

Ectopic expression of H-Ras^{G12V} or N-Ras^{G12D} in normal human CD34^{+} haematopoietic cells was achieved using the PINCO retroviral expression vector (Grignani, F. *et al.* 1998) (Figure 2.1). This vector expresses green fluorescent protein (GFP) as a reporter gene. In addition, a modified PINCO vector was produced which expressed the reporter gene DsRed. The use of these plasmids allowed the identification of transduced cells by flow cytometry.

Full length cDNA encoding H-Ras^{G12V} was provided by Julian Downward, CRUK London Research Institute, UK and cDNA encoding N-Ras^{G12D} was provided by Alan Hall, University College of London, UK. Control vectors received a non-translated DNA stuffer fragment (1.2Kb). The presence of the stuffer fragment prevented excessive expression of the reporter gene in control cells. This resulted in a similar level of reporter gene expression in all transduced cells. cDNA sequence information is found in Appendix 1. Directional subcloning of full length cDNAs into the original and modified PINCO plasmid was performed previously (Pearn, L. *et al.* 2007; Pearn, L. 2008). The presence of the expected inserts in the recombinant PINCO plasmid was verified by agarose gel electrophoresis and by direct sequencing (section 2.4.5).

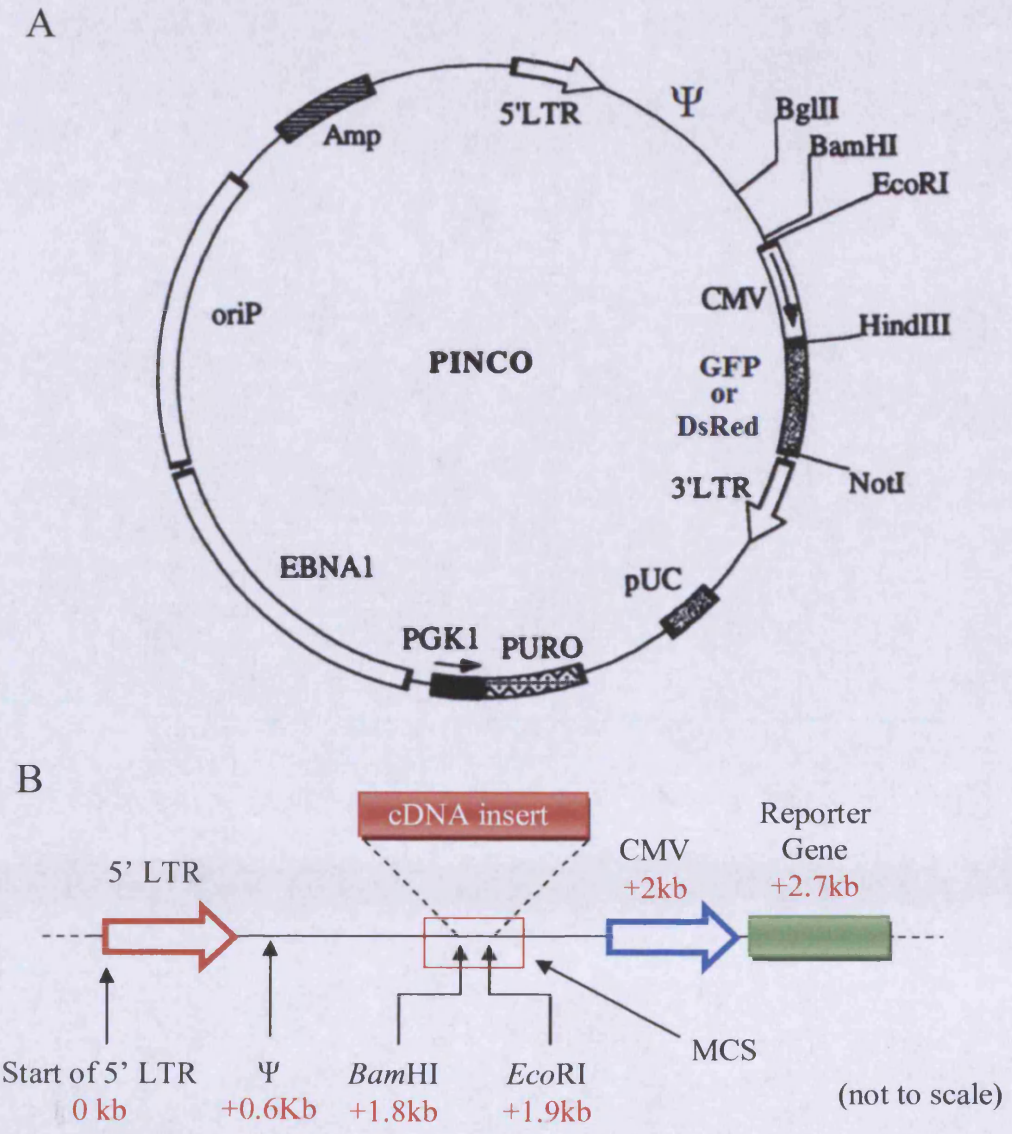

Figure 2.1 A limited restriction enzyme map of the PINCO retroviral vector plasmid

(A) The retroviral vector PINCO was used to generate retrovirus encoding H-Ras^{G12V} and N-Ras^{G12D}. The map shows locations of restriction enzyme recognition sequences and the location of major sequences of interest. Adapted from Grignani, 1998 (Grignani, F. *et al.* 1998). **(B)** Diagram represents short section of PINCO plasmid containing multiple cloning site (MCS) and flanking sequences of interest. Distances in kilobases (kb) represent distance from start of the 5' LTR sequence to the start of sequences indicated in the original PINCO plasmid. Restriction enzyme digestion at the MCS enabled insertion of H-Ras^{G12V}, N-Ras^{G12D} or control cDNAs as described in section 2.4.1. oriP = EBV origin of replication, EBNA1 = EBV EBNA1 gene involved in episomal maintenance, PURO = Puromycin resistance gene under control of PGK-1 promoter, pUC = pUC prokaryotic control sequence, Amp = Ampicillin resistance gene, LTR = MMLV Long Terminal Repeats, Ψ = retroviral RNA packaging signal sequence, CMV = cytomegalovirus promoter, GFP = Enhanced green fluorescent protein gene, DsRed = red fluorescent protein gene

2.4.2 TRANSFORMATION OF COMPETENT *ESCHERICHIA COLI* WITH RECOMBINANT PINCO PLASMID DNA

In order to generate sufficient plasmid DNA for subsequent transfection of virus-packaging cells, plasmid DNA was amplified in *Escherichia coli* (*E.coli*). Recombinant PINCO plasmid DNA (2.5 µg) was added to one freshly thawed vial of competent *E.coli* (One Shot TOP10®, Invitrogen) followed by gentle tapping to mix.

Following incubation on ice for 30 min, the cells were subjected to heat shock (42°C for 30 sec), then returned to ice and allowed to recover on a rotary shaker (225 rpm) for 1 h at 37°C in the presence of SOC medium. During the recovery period, selective Luria-Bertani (LB) agar plates were prepared by melting LB agar which was allowed to cool to 42°C before adding 50 µg/ml ampicillin. Selective LB agar (30 ml) was poured into 90 mm petri dishes and allowed to cool in a sterile environment. After the recovery period, 100 µl of transformed *E. coli* suspension was spread on selective LB agar plates using a sterile loop and incubated for 16 h at 37°C. Single colonies were harvested and used to inoculate 5 ml selective LB broth cultures containing 50 µg/ml ampicillin (added just before use) which were incubated for 8 h at 37°C on a rotary shaker as above. These 'starter' cultures were diluted in selective LB broth (300 µl starter culture in 150 ml broth) and incubated for 16 h at 37°C on a rotary shaker as above. DNA was purified from these bacterial cultures as described in section 2.4.3. Purified DNA was used for transfection of Phoenix cells (for transfection method section 2.4.6, for cell line information see section 2.2.3.7). Additional starter cultures were used to prepare bacterial glycerols (section 2.4.4), and to verify successful transformation (section 2.4.5).

2.4.3 ISOLATION AND QUANTITATION OF AMPLIFIED RECOMBINANT PINCO PLASMID DNA

Transformed *E.coli* which had been incubated in 150 ml selective LB broth for 16 h at 37°C with on a rotary shaker were collected by centrifugation at 6,000 g for 15 min, and high-purity plasmid DNA was obtained using the HiSpeed Midi-Prep DNA isolation kit (Qiagen, Crawley, UK) according to the manufacturer's instructions. This kit is based on the principle of preferential renaturation of plasmid DNA after alkaline lysis. Purified DNA was quantitated using a NanoDrop spectrophotometer (Thermo Fisher Scientific, Loughborough, UK) according to the manufacturer's instructions. The purity of DNA was confirmed by A_{260}/A_{280} which was 1.8±0.1. Insert integrity was also checked by restriction enzyme digestion (section 2.4.5).

2.4.4 CRYOPRESERVATION AND THAWING OF TRANSFORMED *E.COLI*

For long term storage of transformed *E. coli*, 850 µl of LB broth cell suspension was mixed with 150 µl glycerol and stored at -80°C. Cryopreserved *E.coli* were recovered from storage by streaking selective LB agar plates with a sterile loop dipped into partially thawed storage mixture. Selective plates were then incubated for 16 h at 37°C in a dry incubator. Single colonies were harvested and expanded in selective LB broth as above (section 2.4.2).

2.4.5 RECOMBINANT PINCO PLASMID DNA VERIFICATION

To verify the insertion of H-Ras^{G12V} or N-Ras^{G12D} or control cDNAs into the PINCO plasmid and to verify successful transformation of *E. coli*, 5µg PINCO plasmid DNA isolated as above was incubated with 50 U *Eco*RI and *Bam*HI in 1X *Eco*RI buffer (all from NEB, Hitchin, UK) for 1 h at 37°C in a water bath. Restriction enzymes and other contaminants were removed by passing DNA sample through a QIAquick Spin Column (Qiagen) according to the manufacturer's instructions and eluted DNA was resuspended in TE buffer at 50 µg/ml. An agarose gel was prepared by creating a 1% agarose solution in TE buffer containing 500 µg/ml ethidium bromide and allowing gel to solidify in a flat-bed electrophoresis tank. DNA samples for loading contained 500 ng DNA, 0.34 M glycerol, 200 µM bromophenol blue and 120 µM xylene cyanol and 20 µl of sample was loaded per lane. Samples were electrophoresed in TE buffer at 80V for 20 min and DNA was visualised by UV transillumination using a LAS-3000 digital imaging device (Fujifilm UK Ltd., Bedford, UK). The size of DNA fragments or plasmids was estimated using a 1 Kb DNA Ladder (NEB), which was run in parallel with samples. Digital images were processed and analysed using AIDA Image Analyzer v4.19 (Fujifilm UK). The degradation of DNA restriction enzyme digestion was compared to expected restriction mapping (Figure 2.2A).

The insertion of the cDNAs into the plasmids was also verified by direct sequencing. Sequencing was performed using the BigDye® Terminator v3.1 Cycle Sequencing Kit (Applied Biosystems, Warrington, UK) according to the manufacturer's instructions. This kit provides sequence data based on the principle of dye-labelled dideoxynucleotide terminators first described by Fred Sanger (Sanger, F. and Coulson, A.R. 1975). Briefly, a sequencing reaction mixture was prepared containing 8 µl of Ready Reaction Mix (containing DNA polymerase, dNTPs and dye-labelled ddNTPs), 10 ng of DNA template (PINCO plasmid) and 3.2 pmol primer in a final volume of 20 µl of 1X

BigDye® sequencing buffer. The primers were designed to anneal at PINCO-specific sequences 5' and 3' of the MCS respectively (Figure 2.2B). Forward primer sequence was 5'-TAG AAC CTC GCT GGA AAG GA-3', reverse primer sequence was 5'-TTA TGT AAC GCG GAA CTC CA-3'.

Primers were obtained from Eurofins MWG Operon, London, UK. Sequencing reactions containing either forward or reverse primers were carried out in a GeneAmp® 9700 thermal cycler with initial denaturation stage of 96°C for 1min followed by 25 cycles of: denaturation at 96°C for 10 sec then annealing at 50°C for 5 sec then extension at 60°C for 4 min. Reaction was cooled to 4°C after 25 cycles and held. Sequencing reactions (20 µl) were passed through a DyeEx 2.0 spin column (Qiagen) and centrifuged at 750 g for 3 min in order to remove contaminating polymerase and unincorporated dNTPs and ddNTPs. Samples were then sequenced using an ABI Prism® 3130xl Genetic Analyser (Applied Biosystems) performed by staff at Core Biotechnology Services (CBS), School of Medicine, Cardiff University, and analysed using SeqMan® II v5.07 (DNAStar Inc., Madison, WI).

2.4.6 TRANSFECTION OF PHOENIX VIRUS-PACKAGING CELL LINE

PINCO plasmid DNA harvested from transformed *E.coli* was used to transfect Phoenix virus-packaging cells in order to produce recombinant retrovirus. An aqueous plasmid DNA solution (450 µl) containing 10-45 µg plasmid DNA and 250 mM $CaCl_2$ was added dropwise to 450 µl of 2X HEPES-buffered saline (HBS). During the dropwise addition, the HBS was bubbled using an automatic pipette, which encouraged a DNA-$CaCl_2$ precipitate to form. The DNA precipitate was allowed to sit undisturbed for 20 min. Phoenix virus-packaging cells (see 2.2.3.7) in logarithmic growth phase at either 60-70% confluence (H-Ras^{G12V} and N-Ras^{G12D}) or 30-40% confluence (control) were incubated with 25 µM chloroquine for 5 min at 37°C prior to addition of the DNA-$CaCl_2$ precipitate. Retrovirus-containing medium (RCM) was harvested 48 and 72 h post-transfection with a medium change (8 ml) being made 16 h prior to harvesting. RCM was centrifuged in sealed centrifuge buckets at 180 g for 10 min and aliquoted in 1 ml freezing vials before snap freezing in liquid nitrogen. RCM was stored at -80°C.

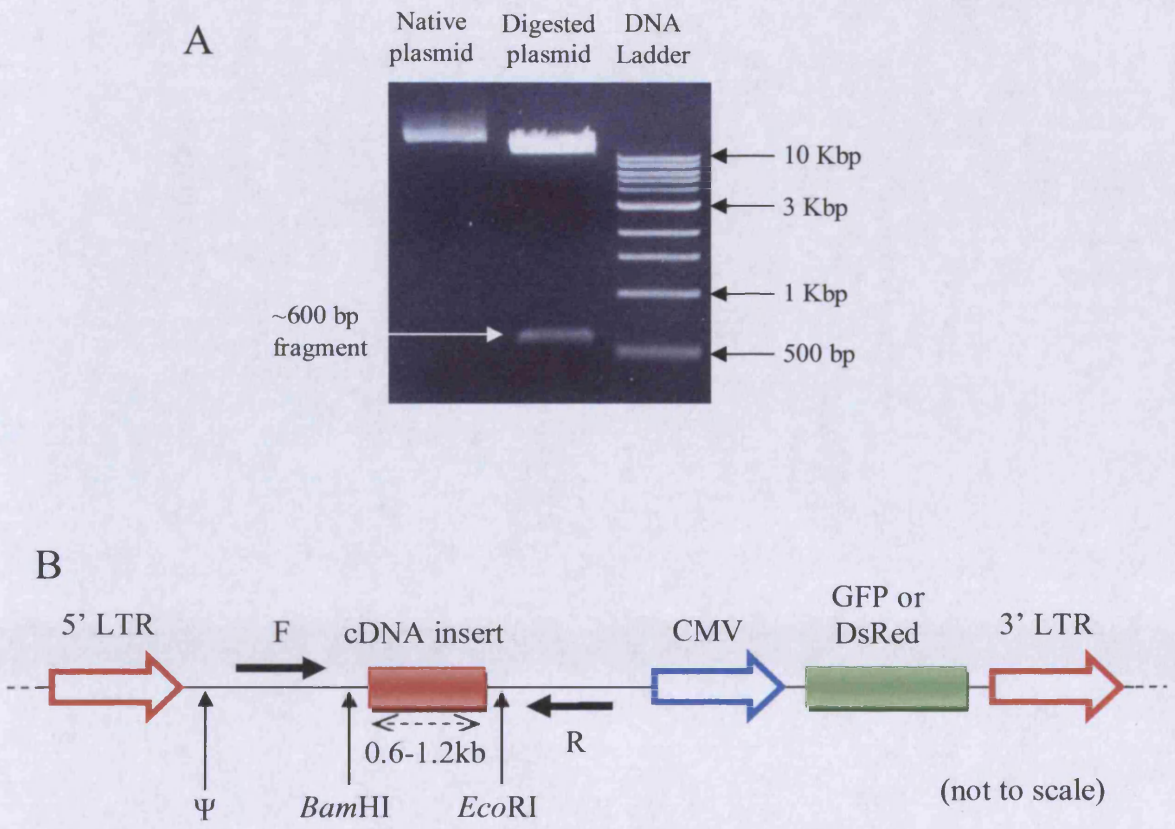

Figure 2.2 Recombinant PINCO plasmid DNA verification by direct sequencing and restriction enzyme digestion

(A) Recombinant PINCO plasmid DNA obtained from ligation reactions was digested with restriction enzymes *Eco*RI and *Bam*HI, electrophoresed, and visualised by UV transillumination of ethidium bromide-stained DNA. The figure shows results of digestion of PINCO plasmid with H-Ras^{G12V} cDNA insert. As expected, a 600bp fragment was detected, as well as a ~12Kb bands corresponding to the digested and native plasmids. Ψ = retroviral RNA packaging signal. **(B)** Limited sequence map depicting region of PINCO plasmid flanked by 5' and 3' LTR sequences (red arrows). Location of *Eco*RI and *Bam*HI recognition sites are labelled, and the annealing sites of forward and reverse primers used to confirm cDNA insertion by sequencing are also labelled (heavy black arrows).

2.4.7 RETROVIRAL TRANSDUCTION OF NORMAL HUMAN $CD34^+$ PROGENITOR CELLS

Normal human haematopoietic $CD34^+$ progenitor cells obtained from neonatal cord blood (section 2.2) were cultured overnight in supplemented IMDM containing growth factors as described in section 2.3.2, which promoted cell-cycle entry, a necessary condition for successful retroviral transduction. $CD34^+$ progenitor cells were transduced with retrovirus encoding $H\text{-}Ras^{G12V}$, $N\text{-}Ras^{G12D}$ or control (section 2.4.6) using an optimised force pre-loading method (Tonks, A. *et al.* 2005b) with minor modifications. For mock gene transductions, RCM was supplanted with conditioned growth medium from untransfected Phoenix cells. Non-treated tissue culture plates were coated with 100 µl/cm^2 of 100 µg/ml reconstituted Retronectin® for two hours at room temperature. Retronectin solution was removed and immediately replaced with PBS containing 1% BSA and incubated at room temperature for 30 min. During this incubation, 1 ml of RCM was treated with 320 µg/ml polybrene and incubated at 37°C for 20 min. PBS containing 1% BSA was then removed from the tissue culture wells and immediately replaced with polybrene-treated RCM. These tissue culture plates were centrifuged at 2000 g for 120 min after which, the supernatant was removed and immediately replaced by 1 ml of RPMI 1640 containing 10% FCS (pre-warmed to 37°C) and plates were incubated for 5 min at room temperature. This RPMI 1640 wash was then removed and immediately replaced with 500 µl of supplemented IMDM medium (section 2.3.2) containing $1x10^5$ $CD34^+$ cells. Cell cultures were then incubated for 16 h at 37°C in a humidified 5% CO_2 atmosphere. The following day, the infection process was repeated by aspirating the $CD34^+$ cells, re-coating the well with virus as above and returning the cells to the virus coated well followed by a further 16 h at 37°C in a humidified 5% CO_2 atmosphere. On day 3 post-isolation, cell transduction frequency was assessed by flow cytometry to detect GFP or DsRed expression (section 2.6) and either cryopreserved (section 2.2.1) or continued in culture (section 2.2.3.1) for determination of experimental endpoints.

2.5 WESTERN BLOTTING

2.5.1 CELL LYSIS AND PROTEIN PREPARATION

Cells were harvested and counted and centrifuged at 180 g for 5 min. The supernatant was removed and the cell pellet was washed twice in ice-cold 10 ml TBS followed by centrifugation and removal of supernatant as above. To ensure full cell

fragmentation, the washed cell pellet was then flash frozen in liquid N_2 and stored at -80°C until ready for processing unless otherwise stated. Volumes of protein extracts were recorded during extraction to enable total protein quantitation.

2.5.1.1 Preparation of whole-cell protein extracts

Flash frozen cell pellets were thawed on ice with gentle tapping in the presence of 10 µg DNAse I per $1x10^6$ cells (minimum 10 µg). Thawed cells were resuspended in a minimum of 50 µl ice-cold lysis buffer containing 1% Triton X-100 per $1x10^6$ cells (section 2.1.2) and incubated on ice for 30 min with occasional vortexing to promote protein solubilisation. Detergent-insoluble material was sedimented by centrifugation at 16,000 g for 5 min at 4°C and supernatants were recovered to fresh tubes and protein concentration was determined (section 2.5.2). Protein extracts were stored at -80°C.

2.5.1.2 Preparation of cytosol-membrane fractionated protein extracts

Flash frozen cell pellets were thawed on ice with gentle tapping in the presence of 4 µg DNAse I per $1x10^5$ cells (minimum 10 µg). Thawed cells were resuspended in 20 µl ice-cold lysis buffer (no detergent) per $1x10^5$ cells (minimum volume 50µl). A maximum of 100 µl of this cell suspension was transferred to a fresh tube and was flash frozen in liquid N_2 followed by rapid thawing in a 37°C water bath, taking care to maintain the sample at 0°C or below. This freeze-thaw cycle was repeated followed by centrifugation of the sample at 16,000 g for 1 h at 4°C. The supernatant (containing cytosolic proteins) was carefully removed and stored in a fresh tube on ice and the pellet (membrane fragments) was resuspended in 25 µl ice-cold lysis buffer containing 1% Triton X-100. The resuspended pellet was incubated on ice for 30 min with occasional vortexing followed by centrifugation at 16,000 g for 15 min at 4°C. The supernatant (containing soluble membrane associated proteins) was transferred to a fresh tube and both fractions were stored at -80°C.

2.5.1.3 Preparation of cytosol/membrane-nucleus fractionated protein extracts

Cells were washed in TBS as in section 2.5.1 and transferred into fresh tubes. Separate protein extracts containing enriched cytosol, membrane and nuclear proteins were obtained using a Cellular Fractionation Kit (Perkin Elmer, Waltham, MA) according to the manufacturer's instructions. Briefly, cells were washed in 2 ml Wash Buffer by centrifugation at 300 g for 10 min. Washed cells were resuspended in 500 µl ice-cold

Cytosol Protein Buffer containing 2.5 µl Protease Inhibitor solution per $3x10^6$ cells and incubated on ice for 10 min on a rotary shaker. Detergent-insoluble material was sedimented by centrifugation at 1000 g for 10 min at 4°C, and the supernatant (containing cytosol proteins) was stored in a fresh tube at 4°C. The detergent-insoluble pellet was resuspended in 500 µl ice-cold Membrane/Organelle Protein buffer containing 2.5 µl Protease Inhibitor solution per $3x10^6$ cells and incubated on ice for 30 min on a rotary shaker. Detergent-insoluble material was sedimented by centrifugation at 5500 g for 10 min at 4°C and the supernatant (containing membrane and organelle proteins) was added to the tube containing the cytosol proteins and the mixed protein extract containing cytosol, membrane and organelle proteins was stored at -80°C. The detergent-insoluble pellet was resuspended in 500 µl ice-cold Nuclear Protein buffer containing 5 µl Protease Inhibitor and 1.5 µl Nuclease solution per $3x10^6$ cells and incubated on ice for 10 min on a rotary shaker. Detergent-insoluble material was sedimented by centrifugation at 6800 g for 10 min at 4°C and the supernatant (containing nuclear proteins) was transferred to a fresh tube and stored at -80°C. Nuclear protein extracts were concentrated into a 100 µl volume using a Microcon YM-3 Ultracentrifuge filter (Millipore, Watford, UK). Nuclear extract (500 µl) was added to a YM-3 filter unit assembly and the unit was centrifuged at 12,000 g for 50 min. Protein concentrate was recovered by inverting the filter unit and placing into a clean tube and centrifuging at 180 g for 5 min.

2.5.2 PROTEIN QUANTITATION

Protein concentration in the protein extracts obtained above were determined using Bradford's reagent (Sigma-Aldrich; based on Coomassie Blue G-250 dye (Bradford, M.M. 1976)). Bradford's reagent was diluted with an equal volume of water to create sufficient diluted reagent (190 µl per test well). Protein extracts were diluted a minimum of 10 fold and 10 µl of diluted extract was mixed in a 96-well plate with 190 µl diluted Bradford's reagent in duplicate and absorbance at 590 nm was measured using a spectrophotometer. BSA standard solutions were assayed in duplicate alongside protein extract samples to create a standard curve, which enabled calculation of protein extract concentration.

In the case of fractionated protein extracts obtained from the Cellular Fractionation Kit, where the formulation of the buffers are proprietary, the DC Protein Assay (BioRad, Hemel Hempstead, UK) was used to quantitate protein concentration according to the manufacturer's instructions. The DC Protein Assay is based on a modified Lowry method (Lowry, O.H. *et al.* 1951), and is less sensitive to detergent contamination

than Bradford's method and the original Lowry method, but is also less sensitive to protein and therefore requires the use of undiluted protein extract for the assay. Briefly, 20 µl reagent S was mixed with each 1 ml of reagent A required (25 µl of mixed reagent per sample well). Mixed reagent (25 µl) was mixed with 5 µl cell lysate and 200 µl of reagent B was added. Samples were incubated at room temperature for 15 min before reading absorbance at 750 nm.

2.5.3 PROTEIN ELECTROPHORESIS AND ELECTROBLOTTING

Protein electrophoresis and electroblotting was performed using the NuPAGE® X-Cell II® electrophoresis and electroblotting system. These, and all consumables required for the procedure including gels, buffers and membranes were manufactured by Invitrogen.

Prior to gel electrophoresis, protein extracts were incubated for 10 min at 70°C in the presence of 1X LDS sample buffer and 50 mM DTT to promote denaturation of proteins and reduction of disulphide bonds. The final concentration of protein in the denatured extract was controlled to ensure an equal mass of protein was loaded in all lanes (determined by the sample with the lowest protein concentration).

Sub cellular protein fractions were loaded in a mass ratio that reflected their contribution to the total cellular protein. This ratio was given by: 1 ÷ (sub cellular fraction protein mass yield ÷ total protein mass yield). This method enabled sub cellular fractions to be loaded in 'cell equivalents'. Denatured protein samples (0.5-10 µg protein per lane, depending on the experiment) were loaded onto a 4-12% Bis-Tris HCl polyacrylamide gel and electrophoresis was performed at 200 V for 50 min in the X-Cell II® Mini-Cell in the presence of MOPS-SDS running buffer unless otherwise stated. Electrophoresed proteins were then electroblotted from the electrophoresis gel onto nitrocellulose membranes using the X-Cell II® Blot Module. Briefly, gels were extracted from their cassettes and placed into a stack consisting of 2 spacer sponges, the gel and membrane (with membrane closest to the positive electrode) sandwiched between blotting paper and 3 further spacer sponges. The module was then placed in the X-Cell II® Mini-Cell and filled with transfer buffer containing 1X NuPAGE® Transfer buffer and 10% methanol. Proteins were then electroblotted at 30 V for 1 h. Following electroblotting, membranes were washed twice with 10 ml of dH_2O for 5 min at room temperature. Electroblotted membranes were incubated with Ponceau S solution (section 2.1.2) for 30 sec to visualise transferred protein and check for equal protein loading. When required this also enabled membrane cutting between lanes. Following two further washes with dH_2O as above, membranes were incubated with 10 ml TBS-T containing 5% membrane blocking agent (provided as part of

the ECL Advance® Western Blotting Detection Kit, GE Healthcare, Amersham, UK, section 2.5.4) for 1 h at room temperature. Blocked membranes were rinsed thrice with 10 ml TBS-T, followed by one 15 min wash and three subsequent 5 min washes all with 10 ml TBS-T.

2.5.4 IMMUNOBLOTTING

Blocked membranes were incubated for 16 h at 4°C in the presence of diluted primary antibody(ies) in TBS-T containing 5% blocking agent and diluted ($1x10^4$ fold) Phosphatase Inhibitor Cocktail (Santa Cruz). Optimum dilution of previously untested primary antibody was determined empirically. Details of particular antibodies used will be given in the appropriate section of Results. For estimation of molecular weight of proteins, outer lanes of gels were loaded with 10 µl of 1X LDS buffer containing a 20 fold dilution of MagicMark XP® Protein Standard (Invitrogen). To check for equal loading, membranes were incubated overnight at 4°C with one of the following antibodies: 20 ng/ml anti-GAPDH (Santa Cruz), 10 ng/ml anti-β-actin (Abcam, Cambridge, UK) or 10 ng/ml anti-α tubulin (Calbiochem, Nottingham, UK). Following primary stage antibody binding, membranes were rinsed thrice, washed once for 15 min and thrice for 5 min as above. Washed membranes were then incubated with diluted ($5x10^4$ fold) HRP-conjugated anti-mouse or anti-rabbit secondary antibody (GE Healthcare) in TBS-T containing 2% membrane blocking agent for 1 h at room temperature. Finally, membranes were rinsed thrice, washed once for 15 min and thrice for 5 min as above.

Electroblotted proteins labelled with primary and secondary antibodies were visualised using ECL Advance® Western Blotting Detection Kit (GE Healthcare). Immunolabelled membranes were drained of excess wash buffer and incubated under low light for 5 min at room temperature with reconstituted ECL Advance®, a substrate of HRP which becomes chemiluminescent once cleaved. Following incubation, excess ECL Advance® solution was decanted and excess solution was removed from edge using blotting paper. Membranes were placed between two sheets of clean acetate and a LAS-3000 digital imaging device (Fujifilm UK) was used to detect ECL Advance® chemiluminescence. Digital images were processed and analysed using AIDA Image Analyzer v4.19 (Fujifilm UK).

2.6 FLOW CYTOMETRIC ANALYSIS

Cells to be analysed by flow cytometry were first recovered from growth medium by centrifugation at 180 g for 5 min and then washed by resuspension in 1 ml staining buffer (section 2.1.2) per $1x10^6$ cells unless otherwise stated. Following centrifugation as above, washed cells were resuspended in 25 µl staining buffer (unless otherwise stated) and incubated with primary stage antibodies or reagents according to the experimental protocols described in the appropriate section of Results. Subsequent staining stages (secondary, tertiary, etc) were separated by a wash step involving resuspension in 200µl staining buffer followed by centrifugation and resuspension in 25 µl of staining buffer unless otherwise stated. In the case of conjugated antibodies, background fluorescence was established by isotype- and manufacturer-matched irrelevant control antibodies conjugated to the same fluorochromes. In the case of flow cytometric measurement of reporter gene expression, the autofluorescence of mock-infected cultures defined the threshold for GFP or DsRed positivity, with the threshold for positive staining was set to 95% of background fluorescence. Before acquisition, samples to be analysed were resuspended in a maximum of 50 µl FACSflow unless otherwise stated. Data were acquired using a FACSCalibur flow cytometer (BD Biosciences) and a minimum of 10,000 events were collected (unless otherwise stated) and analysed using FCS Express v3 (De Novo Software, Los Angeles, CA). Debris was excluded from analysis using forward and side scatter characteristics.

In some experiments, allophycocyanin(APC)-conjugated microbeads (BD Biosciences) were used to control for cell recovery as follows. A consistent number of microbeads was introduced into each sample by adding 50 µl microbead suspension per well. Control microbead samples (50 µl microbead suspension alone in triplicate) were also prepared. After sample acquisition, microbeads were gated in the basis of APC fluorescence and forward and side scatter characteristics and counted using FCS Express. Microbead data was used to calculate a correction factor for each sample; Correction factor = (Mean number of beads in microbead controls ÷ number of beads in sample).

2.7 STATISTICAL ANALYSES

Significance of difference was determined using one-way ANOVA with Tukey's Honestly Significant Differences Test, Mann-Whitney Test or Student's T-test using Minitab v13.0 (Minitab Ltd., Coventry, UK).

3 Examination of ROS production by human $CD34^+$ haematopoietic cells

Activating Ras mutations are detected in 15-25% of AML cases (Bowen, D.T. *et al.* 2005) and are strongly associated with increased ROS production in human cell lines and cancer models (Liu, R. *et al.* 2001; Seru, R. *et al.* 2004; Lee, A.C. *et al.* 1999), and in animal models of leukaemia (Rassool, F.V. *et al.* 2007; Sallmyr, A. *et al.* 2008) (section 1.4.4). However, it is not currently known whether these mutations lead to increased ROS production in human primary haematopoietic cells.

It is generally accepted that most genetic lesions leading to leukaemia are sustained by early haematopoietic progenitor cells including, but not limited to, $CD34^+$ cells (Blair, A. and Pamphilon, D.H. 2003). Therefore using a model system based on normal human $CD34^+$ haematopoietic progenitor cells, this chapter examined the impact of Ras mutant expression (H-Ras^{G12V} or N-Ras^{G12D}) on the capacity of $CD34^+$ cells to produce ROS. Recently, ROS have been implicated in cell signalling in a variety of normal tissues including haematopoietic cells (section 1.4.3.2). The fact that many cancers overproduce ROS suggests that the signalling functions of ROS may be dysregulated in cancer cells. However, the high reactivity and short life-span of most ROS presents challenges for the detection and quantitation of ROS in physiological systems. This study used several assays to detect superoxide and H_2O_2. To detect superoxide, Diogenes and EPR spectroscopy using the spin trap probe DEMPO were used, whilst H_2O_2 was detected using Amplex Red (section 1.4.5). The use of several techniques in parallel served to overcome some of the limitations of the techniques by providing corroborating evidence. Production of ROS was assayed at several timepoints during cell culture, from day 3 (immediately following isolation) up to day 14. During this period, primary haematopoietic cells (which are predominantly $CD34^+$ progenitor cells at day 3) undergo morphological and phenotypic changes which accompany myeloid lineage commitment and maturation. By day 7 of culture, $CD34^+$ cells are scarce, and mature neutrophils, and macrophages are visible. These cells are professional ROS producing cells which must be considered when evaluating the results.

3.1 AIMS

To investigate the effects of activated Ras expression on ROS production by primary human $CD34^+$ haematopoietic cells, this Chapter aims to:

- Optimise and validate assays for the detection of ROS. This will provide important assay conditions for the detection of superoxide and H_2O_2 in human $CD34^+$ haematopoeitic progenitor cells.

- Determine whether activated Ras can induce ROS production in human $CD34^+$ haematopoietic progenitor cells and to identify the specific ROS produced.

- Determine the source of ROS production in these cells. This will be achieved using organelle specific ROS probes in combination with appropriate ROS inhibitors.

3.2 MATERIALS AND METHODS

3.2.1 DETECTION OF SUPEROXIDE USING DIOGENES

In order to detect superoxide radicals, the chemiluminescent probe Diogenes (National Diagnostics, Atlanta, GA) was used. The following sections give an overview of the mechanism by which Diogenes detects superoxide. This is followed by a description of the validation of Diogenes as a sensitive probe for superoxide; optimisation of Diogenes assay conditions and the use of optimised conditions for measurement of superoxide production by transduced human $CD34^+$ haematopoietic progenitor cells. Diogenes reagent was reconstituted in dH_2O according to the manufacturer's instructions, and aliquots were flash frozen and stored in liquid N_2.

3.2.1.1 Principles of superoxide detection by Diogenes

The Diogenes probes consists of two components; luminol, which reacts with superoxide to form an electronically excited product, which subsequently returns to a stable unexcited state; releasing a photon. The second component is a proprietary enhancer which is stimulated by photons emitted by luminol to emit several additional photons.

Thus the enhancer amplifies luminol chemiluminescence, offering an increased sensitivity over luminol alone. Several reaction steps are necessary for luminol to generate photons in the presence of superoxide. These reactions are shown in Figure 3.1.

3.2.1.2 Determination of sensitivity and specificity of Diogenes to superoxide radicals and H_2O_2

To confirm the specificity of Diogenes for superoxide, Diogenes was exposed to superoxide radicals generated using a cell-free system. Since superoxide radicals can dismutate to form H_2O_2, the sensitivity of Diogenes to H_2O_2 was also determined.

Superoxide radicals were generated as a by product of the oxidation of hypoxanthine (HX) by xanthine oxidase (Roubaud, V. *et al.* 1997). HX was dissolved in 0.1 M NaOH to create a 40 mM stock HX solution. HX working solutions were created by diluting HX stock in Diogenes buffer (section 2.1.2) to 1.3 fold greater than the final HX concentration (0 to 1.8 mM HX) to allow for addition of Diogenes. Working solutions (150 µl) were added to a white FluoroNunc Maxisorp 96 well plate (Thermo Fisher Scientific) followed by 50 µl of reconstituted Diogenes reagent. To initiate superoxide production, 50 mU of xanthine oxidase dissolved in 5 µl Diogenes buffer was added to each well, and time-resolved chemiluminescence was measured using a Dynex MLX Luminometer (Dynex Technologies Ltd., Worthing, UK). All reaction volumes contained 0.1 mM DTPA as a chelating agent to suppress unwanted metal ion-catalysed side-reactions such as the Fenton reaction (section 1.4.1.1).

To test whether Diogenes was reactive with H_2O_2, stock H_2O_2 (8.8 M) was diluted in Diogenes buffer to 1.3 fold greater than the final H_2O_2 concentration, to account for Diogenes addition. Diluted H_2O_2 (150 µl) was added to a 96-well plate followed by addition of 50 µl reconstituted Diogenes and measurement of time-resolved chemiluminescence as above.

3.2.1.3 Ability of Diogenes to detect superoxide generated by PLB-985 cells stimulated with TPA

PLB-985 cells are a promyelocytic cell line and are a subclone of HL60 cells (section 2.2.3.5). PLB-985 cells produce superoxide when treated with 12-O-Tetradecanoylphorbol-13-acetate (TPA).

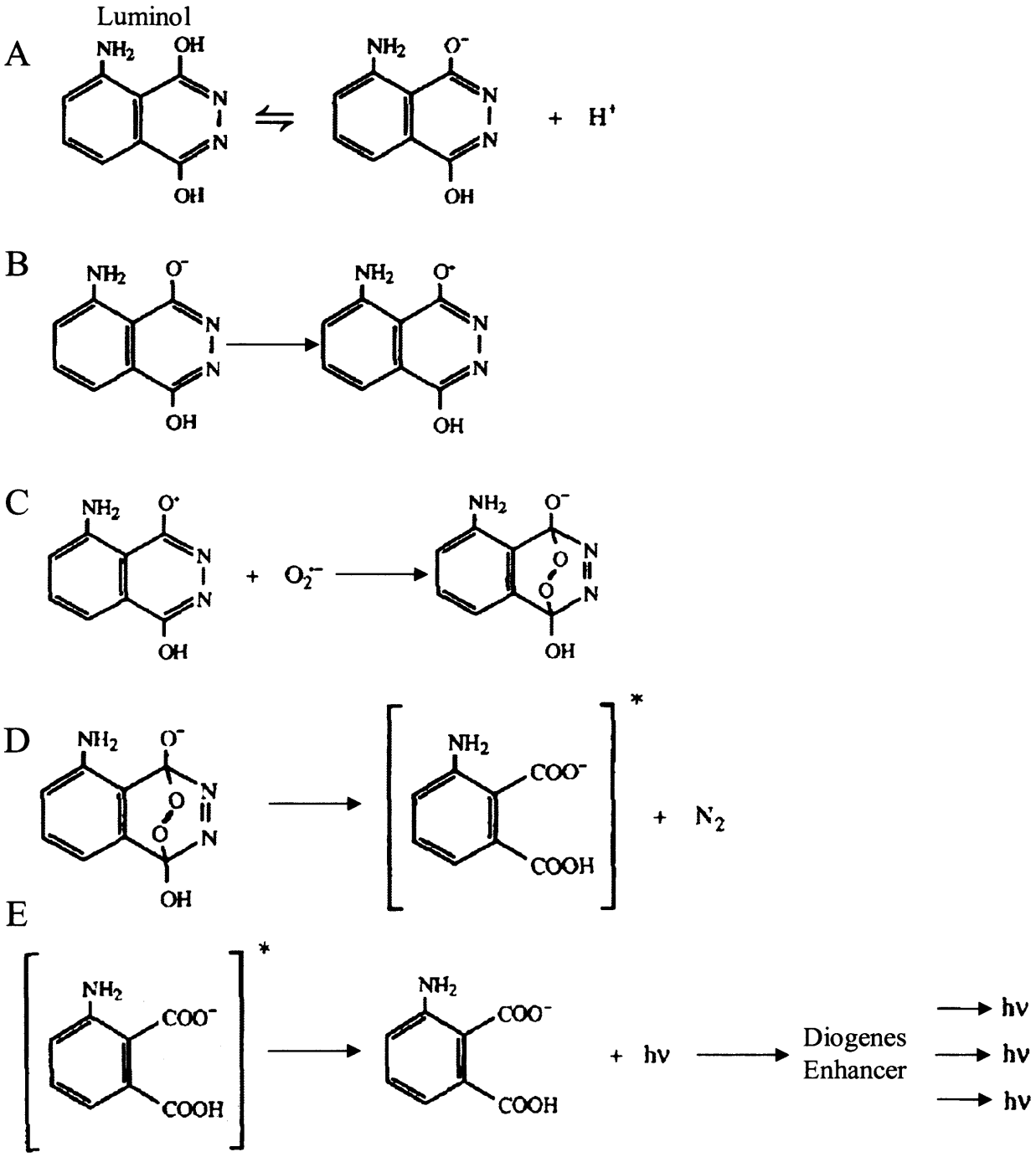

Figure 3.1 Generation of photons by Diogenes in the presence of superoxide

Luminol is an acylhydrazide which undergo simple ionisation to form the luminol anion as shown in **(A)**. The luminol anion may then be oxidised to form a luminol radical **(B)**, and this luminol radical can then react with superoxide to form an unstable endoperoxide **(C)**. The endoperoxide rapidly decomposes to form nitrogen gas and an excited aminopthallate **(D)**, which returns to the ground state releasing a photon (hν) **(E)**. The emitted photon then stimulates the Diogenes enhancer to release several more photons **(E)**, providing a means of amplification of the luminol chemiluminescent signal. Adapted from Faulkner, 1993 (Faulkner, K. and Fridovich, I. 1993).

TPA is a phorbol ester which activates PKC isoforms and results in downstream activation of Phox, a member of the NOX family of oxidases (Lambeth, J.D. 2004). As a negative control, a subline of PLB-985 cells deficient for NOX2 expression (PLB-985 $NOX2^{-/-}$ cells) were used. Without NOX2, these cells cannot produce superoxide via Phox (Zhen, L. *et al.* 1993).

To confirm whether Diogenes was able to detect superoxide production by PLB-985 cells stimulated with TPA, both PLB-985 and PLB-985 $NOX2^{-/-}$ cells ($1.5x10^5$ per well) were washed twice by centrifugation (as above) in 10 ml PBS and resuspended in Diogenes buffer at $1x10^6$ cells/ml. Cell suspension (150 µl; $1.5x10^5$ cells) was added to a FluoroNunc Maxisorp 96 well plate in triplicate and reconstituted Diogenes reagent (50 µl) was added to the cell suspension followed by either 1 µl of 200 µM TPA dissolved in DMSO or 1 µl DMSO alone. Time-resolved chemiluminescence was measured as above.

3.2.1.4 Optimisation of detection of superoxide production by transduced $CD34^+$ haematopoietic progenitor cells

The optimum conditions for detection of superoxide by Diogenes were determined by varying the concentration of Diogenes reagent and the number of cells used in the assay.

To determine optimum cell numbers for the Diogenes assay, transduced $CD34^+$ cells expressing H-Ras^{G12V} or controls (day 8) were recovered from growth medium by centrifugation at 180 g for 5 min. Cells were washed twice in 10 ml PBS by centrifugation as above, and the washed cell pellet was resuspended in Diogenes buffer at $0.1\text{-}3x10^6$ cells/ml. Cell suspension (150 µl; $0.15\text{-}4.5x10^5$ cells) was added in triplicate to white FluoroNunc Maxisorp 96 well plates followed by 50 µl reconstituted Diogenes reagent.

The effect of changing Diogenes concentration was also examined. Transduced $CD34^+$ cells were resuspended in Diogenes buffer at $0.75x10^6$ cells/ml, and 100 µl of cell suspension ($7.5x10^4$ cells) was added in triplicate to a white FluoroNunc Maxisorp 96 well plate followed by either 50µl reconstituted Diogenes reagent and 50 µl Diogenes buffer or 100 µl reconstituted Diogenes reagent alone; to create a final reaction volume of 200 µl. Time-resolved chemiluminescence was then measured as above.

3.2.1.5 Measurement of superoxide production by transduced CD34$^+$ haematopoietic progenitor cells using optimised conditions

Transduced CD34$^+$ cells expressing H-Ras^{G12V}, N-Ras^{G12D} or control (day 3 to 14) were washed twice in 10 ml PBS by centrifugation at 180 g for 5 min and resuspended in Diogenes buffer at 1x10^6 cells/ml. Cell suspension (150 µl) was assayed in triplicate in white FluoroNunc Maxisorp 96 well plates. Reconstituted Diogenes (50 µl) was immediately added and chemiluminescence was recorded as above. Some experiments were performed in the presence of one of the following reagents: 5 µg/ml SOD; 1 µM TPA; 50 µM diphenyleneiodonium (DPI) or 1 mM apocynin (NOX family oxidase inhibitors); 5 µM rotenone (an inhibitor of the mitochondrial electron transport chain); 100 µg/ml purified catalase (40,000-60,000 U[a]/mg protein), all purchased from Sigma-Aldrich.

3.2.1.6 Measurement of superoxide produced by stimulated primary peripheral blood monocytes

In order to compare the level of constitutive superoxide production of transduced CD34$^+$ cells to that of the phagocytic oxidative burst, normal human peripheral blood monocytes were isolated from healthy donors as follows. Freshly isolated (less than 8 h) venous peripheral blood was diluted 2 fold with sterile PBS and 35 ml diluted blood was layered onto 15 ml Ficoll-Paque®, after which total mononuclear cells were isolated from the diluted blood by density centrifugation as described in section 2.3.1.

CD14$^+$ peripheral blood monocytes were isolated from total mononuclear cells by depletion of cells expressing non-monocytic markers using the miniMACS® Monocyte isolation kit according to the manufacturer's instructions. Briefly, mononuclear cells were resuspended in MACS buffer (section 2.1.2) at 3x10^8 cells/ml. The cells were then incubated for 15 min at 4°C with 10 µl biotinylated antibody cocktail (containing biotinylated antibodies raised against CD3, CD7, CD16, CD19, CD56, CD123 and glycophorin A) per 10^8 cells in the presence of an FcR blocking agent. Following incubation, an additional 30 µl of MACS buffer was added per 10^8 cells followed by incubation for 15 min at 4°C with 20 µl of anti-biotin microbeads per 10^8 cells.

Labelled cells were washed with 5 ml MACS buffer and recovered by centrifugation at 180 g for 5 min. Washed cells were passed through an MS$^+$ separation column and unlabelled cells were collected in the column effluent. To maximise CD14$^+$

[a] One unit (U) will decompose 1.0 µmole of H_2O_2 per min at pH 7.0 at 25 °C, while the H_2O_2 concentration falls from 10.3 to 9.2 mM, measured by the rate of decrease of A_{240}.

cell enrichment, column effluent was passed through a second MS^+ column and the effluent obtained was centrifuged at 180 g for 5 min. The supernatant was removed and the cell pellet was resuspended in RPMI 1640 containing 10% FCS, 100 IU/ml penicillin and 100µg/ml streptomycin and incubated at 37°C in humidified 5% CO_2 atmosphere. A small sample of isolated effluent cells (~$1x10^4$) was stained with anti-human CD14 antibody conjugated to FITC (Dako Cytomation, Ely, UK), and analysed by flow cytometry (section 2.6) to check for CD14 positivity. Isolated peripheral blood monocytes were assayed using optimised Diogenes conditions as described in section 3.2.1.5. Immediately before measuring time-resolved chemiluminescence, monocytes were stimulated with 250 µg/ml opsonised zymosan. Opsonised zymosan was prepared as previously described (Tonks, A. *et al.* 2005a).

3.2.1.7 Calculation of total superoxide production measured using Diogenes

Diogenes chemiluminescence traces were plotted as a curve with the light emission rate (measured in relative light units (RLU) per min) on the y axis and time (min) on the x axis (some examples of the curves obtained are shown in Figure 3.7). Using the curves generated during each assay, the total light emission for each assay was determined by finding the area under the curve using the trapezium rule, equivalent to the total light emission (given in RLU). This RLU value was used as a measure of total superoxide production during the assay.

3.2.2 DETECTION OF SUPEROXIDE ANION PRODUCTION BY HUMAN $CD34^+$ PROGENITOR CELLS USING EPR

To confirm the production of superoxide detected by Diogenes chemiluminescence, EPR spectroscopy was performed. EPR spectroscopy is a technique which can detect the presence of unpaired electrons using spin-trap probes (section 1.4.5.3). This is of relevance to ROS detection because several important ROS are radicals (section 1.4.1).

The spin-trap probe 5-(diethoxyphosphoryl)-5-methyl-1-pyrroline-N-oxide (DEPMPO) (Axxora, Nottingham, UK) was used to capture and detect radical species generated by transduced cells. Transduced $CD34^+$ cells were washed by centrifugation at 180 g for 5 min in 10 ml PBS and resuspended at $1x10^7$ cells/ml in Diogenes buffer. Cell suspension (150 µl) was placed in a quartz cuvette in the presence of 60 mM DEPMPO prior to detection of EPR spectra. EPR spectra were detected in ten scans of 60 sec at 37°C

using a Varian 104 EPR spectrometer (Varian Inc., Palo Alto, CA) using X-band microwave radiation (9.5GHz). Typical recording conditions were field centre: 3378 Gauss (G), gain: $2x10^5$, modulation amplitude: 2.0, time constant: 0.25, microwave power: 10 mW, field range: 160 G. A similar xanthine oxidase system to that used in Diogenes experiments was used as a positive control for superoxide detection. Background was established using DEPMPO probe alone. EPR spectral data was recorded and analysed using 'in-house' software developed at the Wales Heart Research Institute (WHRI), Cardiff University, UK. This study gratefully acknowledges the expert assistance of Dr P. E. James (WHRI, Cardiff University, UK) in operation of the Varian 104 EPR spectrophotometer.

3.2.3 DETECTION OF MITOCHONDRIAL ROS PRODUCTION USING MITOSOX

Superoxide can be produced via the NOX family of oxidases (Lambeth, J.D. 2004) or via the mitochondrial electron transport chain (Murphy, M.P. 2009). In order to determine whether mutant Ras increased superoxide production in $CD34^+$ cells via the ETC, mitochondria-specific superoxide was measured using MitoSOX (Invitrogen). Transduced $CD34^+$ cells (day 5 to 7; $2.5x10^4$ per test) were washed twice by centrifugation at 180 g for 5 min in 10 ml warm PBS and resuspended in 25 µl PBS followed by incubation with 5 µM MitoSOX for 15 min at 37°C. Cells were washed by centrifugation at 180 g for 5 min with 1 ml FACSflow (BD Biosciences) and were resuspended in 50 µl FACS flow prior to flow cytometric analysis (section 2.6). For some experiments, cells were incubated for 15 min at 37°C prior to MitoSOX treatment with either 50 µM rotenone (Sigma-Aldrich) as a positive control or 5 µM Iron (III) 5, 10, 15, 20-tetrakis-4-carboxyphenyl porphyrin (FeTCPP), (Frontier Scientific Inc., Logan, UT) as a negative control. Rotenone is a mitochondrial poison which inhibits mitochondrial ETC complex I (Grivennikova, V.G. and Vinogradov, A.D. 2006), and can lead to increased superoxide production (Indo, H.P. *et al.* 2007). FeTCPP is a membrane-permeable SOD mimetic (Wu, A.S. *et al.* 2003).

3.2.4 DETECTION OF H_2O_2 USING AMPLEX RED

3.2.4.1 Principle of H_2O_2 detection by Amplex Red

The Amplex Red probe is a substituted phenoxazine molecule which is not fluorescent. The probe can be oxidised by H_2O_2 in the presence of horseradish peroxidase

(HRP) to form a red-fluorescent product, resurofin, with an excitation maximum of 571 nm and an emission maximum of 585 nm (Figure 3.2).

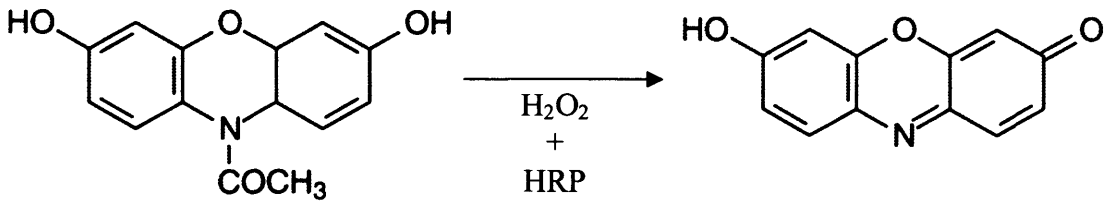

10-acetyl-3,7-dihydroxyphenoxazine (Amplex Red)

Resurofin

Figure 3.2 Oxidation of Amplex Red by H_2O_2 in the presence of HRP to form resurofin

3.2.4.2 Detection of H_2O_2 production by human $CD34^+$ progenitor cells using Amplex Red

Superoxide can dismutate to H_2O_2 spontaneously or via a reaction catalysed by SOD (Bannister, J.V. *et al.* 1987). In order to detect H_2O_2, the H_2O_2-sensitive fluorescent probe Amplex Red (Invitrogen), was prepared according to the manufacturer's instructions. Briefly, Amplex Red working solution was prepared, containing 100 µM Amplex Red reagent, 0.2 U[a]/ml horseradish peroxidase (HRP) dissolved in Krebs-Ringer phosphate-glucose buffer (KRPG buffer; section 2.1.2). Transduced $CD34^+$cells (day 4 to 5; $2x10^5$ per test) were resuspended at $1x10^6$ cells/ml in KRPG buffer for 4 h at 37°C. Subsequently the cell suspension was centrifuged at 180 g for 5 min and the conditioned medium was harvested by aspiration. Conditioned medium (50 µl) was added in triplicate to a 96-well fluorescent assay plate (Thermo Fisher Scientific) and the reaction was initiated by adding 50 µl of Amplex Red working solution prepared above. Amplex Red fluorescence development was recorded for 15 min at 37°C using a FluoStar® Optima instrument (BMG Labtech, Aylesbury, UK) using excitation wavelength of 540 nm and a 590 nm emission filter. A H_2O_2 standard curve was included in each experiment to determine H_2O_2 concentration in conditioned medium. To prepare the H_2O_2 standard curve, H_2O_2 (0-20 µM) was diluted in 50 µl KRPG buffer and added to a 96-well fluorescent assay plate followed by 50 µl Amplex Red working solution. After dilution

[a] One unit (U) will form 1 mg purpurogallin from pyrogallol in 20 sec at pH 6.0 at 20 °C.

with 50 µl Amplex Red working solution, the final concentration of H_2O_2 standards were 0-10 µM.

3.2.5 MEASUREMENT OF SUPEROXIDE PRODUCTION IN PRIMARY MURINE SCA-1$^+$ HAEMATOPOIETIC CELLS EXPRESSING N-RAS^{G12D}

In order to determine the contribution of NOX2 to ROS production promoted by activated Ras, N-Ras^{G12D} was expressed in bone marrow-derived Sca-1$^+$ cells obtained from either wild-type or NOX2 deficient mice (generated previously (Pollock, J.D. *et al.* 1995)). Wild-type or NOX2$^{-/-}$ C57BL/6 male littermates (16 weeks old); killed by cervical dislocation were kindly donated by Professor A. Shah, King's College Hospital, London. Deceased mice were immersed in 70% ethanol and both femurs and tibiae were excised aseptically. Muscle and ligament tissue was removed from the bones, and the ends of the bones were cut off using a sterile scalpel. The bone-channels were flushed thrice with RPMI using a 26 G needle into a 30 mm petri dish containing 10 ml RPMI. Bone-marrow derived cells were collected by centrifugation at 180 g for 10 min and Sca-1$^+$ cells were positively selected using a Sca-1$^+$ cell isolation kit (Miltenyi Biotec) according to the manufacturer's instructions. Total bone marrow cells were resuspended in MACS buffer (section 2.1.2) at 6.5x10^8 cells/ml. The cells were then incubated for 15 min at 4°C with 50 µl anti-Sca-1 antibody conjugated to PE (clone D7) per 10^8 cells in the presence of an FcR blocking agent and were subsequently washed with 5 ml MACS buffer by centrifugation at 180 g for 5 min. Washed bone marrow cells were then incubated at 4°C with magnetic anti-PE microbeads followed by washing as above. Magnetically-labelled Sca-1$^+$ cells were isolated by passing the labelled cells through an MS$^+$ separation column. Sca-1$^+$ cells were then eluted from the column in the absence of a magnetic field by rinsing the column with 1 ml MACS buffer. Freshly isolated CD34$^+$ cells were cultured in supplemented IMDM (as described in section 2.3.2) containing 50 ng/ml muIL-3, muSCF, huFLT3L and 25 ng/ml huIL-6, huG-CSF and muGM-CSF.

Isolated Sca-1$^+$ cells were then transduced with N-Ras^{G12D} or control using the PINCO vector as described in section 2.4.7. Following transduction (day 3), isolated Sca-1$^+$ cells were recovered from growth medium by centrifugation at 180g for 5 min and cultured as described in section 2.2.3.2. A small sample of isolated Sca-1$^+$ cells (~1x10^4) was stained with anti-Sca-1 antibody conjugated to PE, and analysed by flow cytometry as described in section 2.6 to check for purity. Superoxide production by transduced Sca-1$^+$ cells was assayed on day 6 of culture using Diogenes, as described in section 3.2.1.5.

3.3 RESULTS

3.3.1 ECTOPIC EXPRESSION OF MUTANT H-RAS^{G12V} AND N-RAS^{G12D} IN NORMAL HUMAN CD34$^+$ HAEMATOPOIETIC PROGENITOR CELLS

This study used a primary human CD34$^+$ haematopoietic cell model to investigate the effect of mutant Ras expression on ROS production. Human CD34$^+$ haematopoietic cells were positively selected from cord-blood mononuclear cells and ectopic expression of H-Ras^{G12V} or N-Ras^{G12D} in these cells was achieved by retroviral transduction using the PINCO expression vector (which encodes GFP as a reporter gene). Control cells expressed GFP alone. Transduced human CD34$^+$ cells were analysed for GFP expression by flow cytometry 24 h after retroviral transduction (section 2.4.7). Figure 3.3A shows that 70±7% of controls expressed GFP whereas H-Ras^{G12V} and N-Ras^{G12D} had a transduction frequency of 57±6% and 58±7% respectively. To ensure that the transduced cell populations were still enriched for CD34 expression, flow cytometric analysis was performed immediately after retroviral transduction. These experiments demonstrated that control and Ras-transduced cells were predominantly CD34$^+$ (Figure 3.3B and C; see also Appendix 2).

Expression of GFP is an indirect measure of transgene expression; therefore Western blotting was performed to confirm the expression of H-Ras^{G12V} or N-Ras^{G12D}. CD34$^+$ H-Ras^{G12V} cells expressed ~5 fold increase in total Ras protein compared with controls and expression of Ras^{G12V} mutant protein was detected in these cells. As expected, mutant Ras protein was not expressed in CD34$^+$ control cells (Figure 3.3D). CD34$^+$ N-Ras^{G12D} cells showed similar results (data not shown).

3.3.2 DIOGENES CAN DETECT SUPEROXIDE GENERATED BY HUMAN CD34$^+$ HAEMATOPOIETIC PROGENITOR CELLS

3.3.2.1 Diogenes is a sensitive and specific probe for superoxide

To detect superoxide production in transduced CD34$^+$ cells, the chemiluminescent probe Diogenes was used. Diogenes reagent consists of luminol and a proprietary activator which amplifies luminol chemiluminescence providing greater sensitivity to low levels of superoxide.

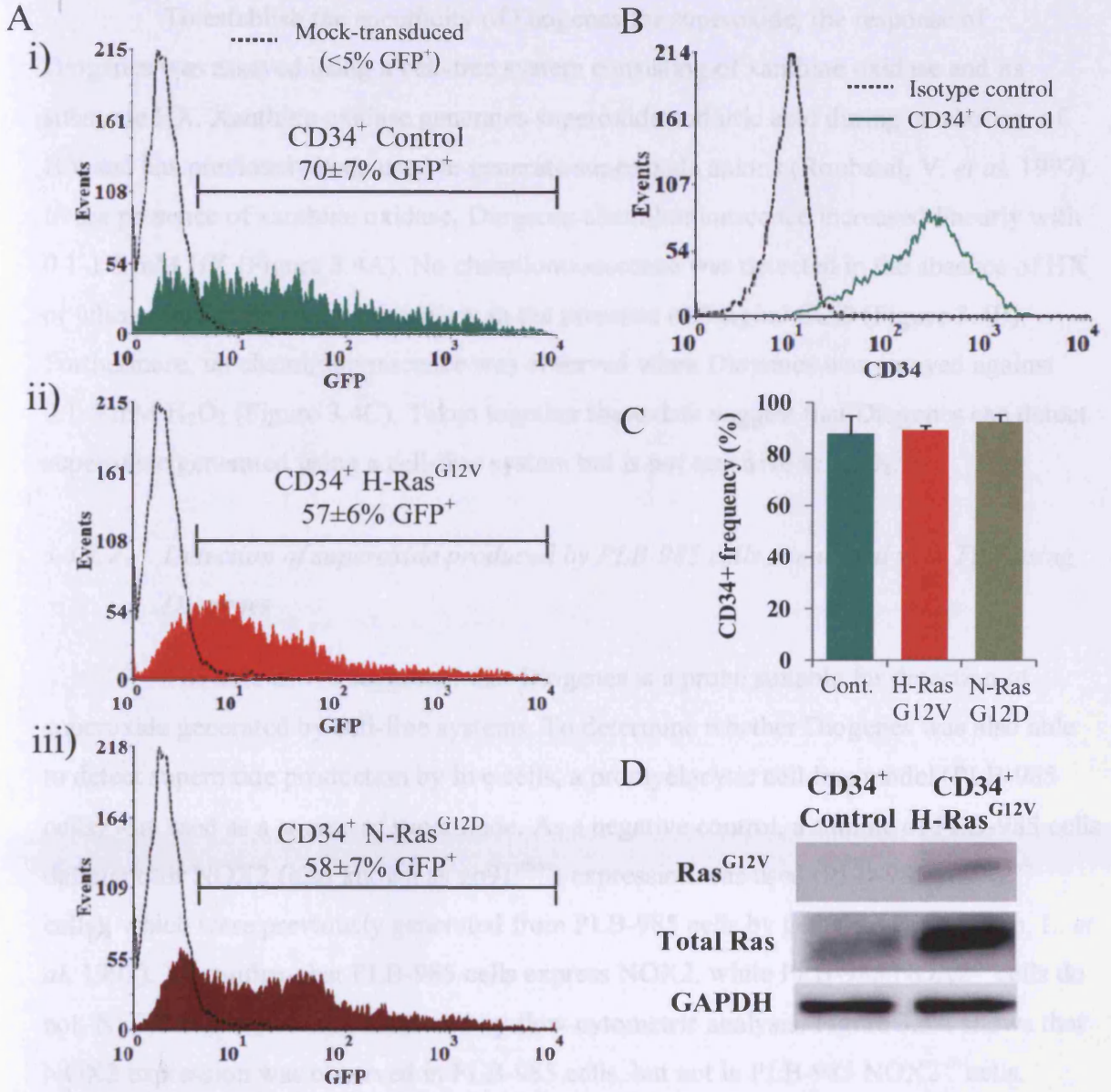

Figure 3.3 Expression of mutant Ras in normal human CD34$^+$ haematopoietic progenitor cells

(A) Transduced human CD34$^+$ haematopoietic progenitor cells were analysed for GFP positivity (filled histograms) on day 3 post transduction. GFP$^+$ threshold was defined by autofluorescence (open histograms) of mock-transduced cells, and typical percentages of viable GFP$^+$ cells are shown for **i)** CD34$^+$ control cells, **ii)** CD34$^+$ H-Ras^{G12V} cells and **iii)** CD34$^+$ N-Ras^{G12D} cells. Data indicates mean GFP$^+$ frequency ± 1 S.D. (n=6). **(B)** Transduced CD34$^+$ cells were labelled with 5 µg/ml anti-CD34 antibody conjugated to PE or isotype matched control antibody (PE conjugate) (both from BD Biosciences) for 30 min at 4°C, and analysed by flow cytometry as described in section 2.6. Figure shows typical histogram, depicting CD34 antigen expression by CD34$^+$ control cells on day 3 post-isolation. **(C)** Mean CD34$^+$ cell frequencies for transduced cultures on day 3. Bar chart represents mean plus 1 S.D. (n ≥2). **(D)** Whole-cell protein extracts of 3x10^5 CD34$^+$ control and CD34$^+$ H-Ras^{G12V} cells (day 4) were prepared as described in section 2.5.1.1, and Western blot analysis was performed as described in section 2.4.7, using 170 ng/ml anti-pan Ras antibody (Cell Signaling, Danvers, MA) or 100 ng/ml anti-pan Ras^{V12} antibody (clone DWP; Calbiochem). 20 ng/ml GAPDH (Santa Cruz) was used as a loading control.

To establish the specificity of Diogenes for superoxide, the response of Diogenes was assayed using a cell-free system consisting of xanthine oxidase and its substrate HX. Xanthine oxidase generates superoxide and uric acid during catabolism of HX and has previously been used to generate superoxide anions (Roubaud, V. *et al.* 1997). In the presence of xanthine oxidase, Diogenes chemiluminescence increased linearly with 0.1-1.5 mM HX (Figure 3.4A). No chemiluminescence was detected in the absence of HX or when experiments were carried out in the presence of 5 μg/ml SOD (Figure 3.4B). Furthermore, no chemiluminescence was observed when Diogenes was assayed against 0.1-5 mM H_2O_2 (Figure 3.4C). Taken together these data suggest that Diogenes can detect superoxide generated using a cell-free system but is not sensitive to H_2O_2.

3.3.2.2 Detection of superoxide produced by PLB-985 cells stimulated with TPA using Diogenes

The data above suggested that Diogenes is a probe suitable for detection of superoxide generated by cell-free systems. To determine whether Diogenes was also able to detect superoxide production by live cells, a promyelocytic cell line model (PLB-985 cells) was used as a source of superoxide. As a negative control, a subline of PLB-985 cells deficient for NOX2 (also known as $gp91^{phox}$) expression was used (PLB-985 $NOX2^{-/-}$ cells), which were previously generated from PLB-985 cells by gene-targeting (Zhen, L. *et al.* 1993). To confirm that PLB-985 cells express NOX2, while PLB-985 $NOX2^{-/-}$ cells do not, NOX2 expression was measured by flow cytometric analysis. Figure 3.5A shows that NOX2 expression was observed in PLB-985 cells, but not in PLB-985 $NOX2^{-/-}$ cells.

To determine whether Diogenes was able to detect superoxide production *in vitro*, PLB-985 cells and PLB-985 $NOX2^{-/-}$ cells were incubated with Diogenes in the presence or absence of TPA (a phorbol ester which is a potent activator PKC and NOX family oxidases, including Phox containing the catalytic subunit NOX2 (Sumimoto, H. 2008)). Unstimulated PLB-985 cells did not produce detectable superoxide, however, when stimulated with TPA, a ~30 fold increase in Diogenes chemiluminescence was observed. As expected PLB-985 $NOX2^{-/-}$ cells gave no detectable Diogenes chemiluminescence under these conditions (Figure 3.5B). These data show that Diogenes is able to detect NOX2-derived superoxide from live cells, and suggest that in PLB-985 cells, NOX2 is the major contributor to TPA induced superoxide production.

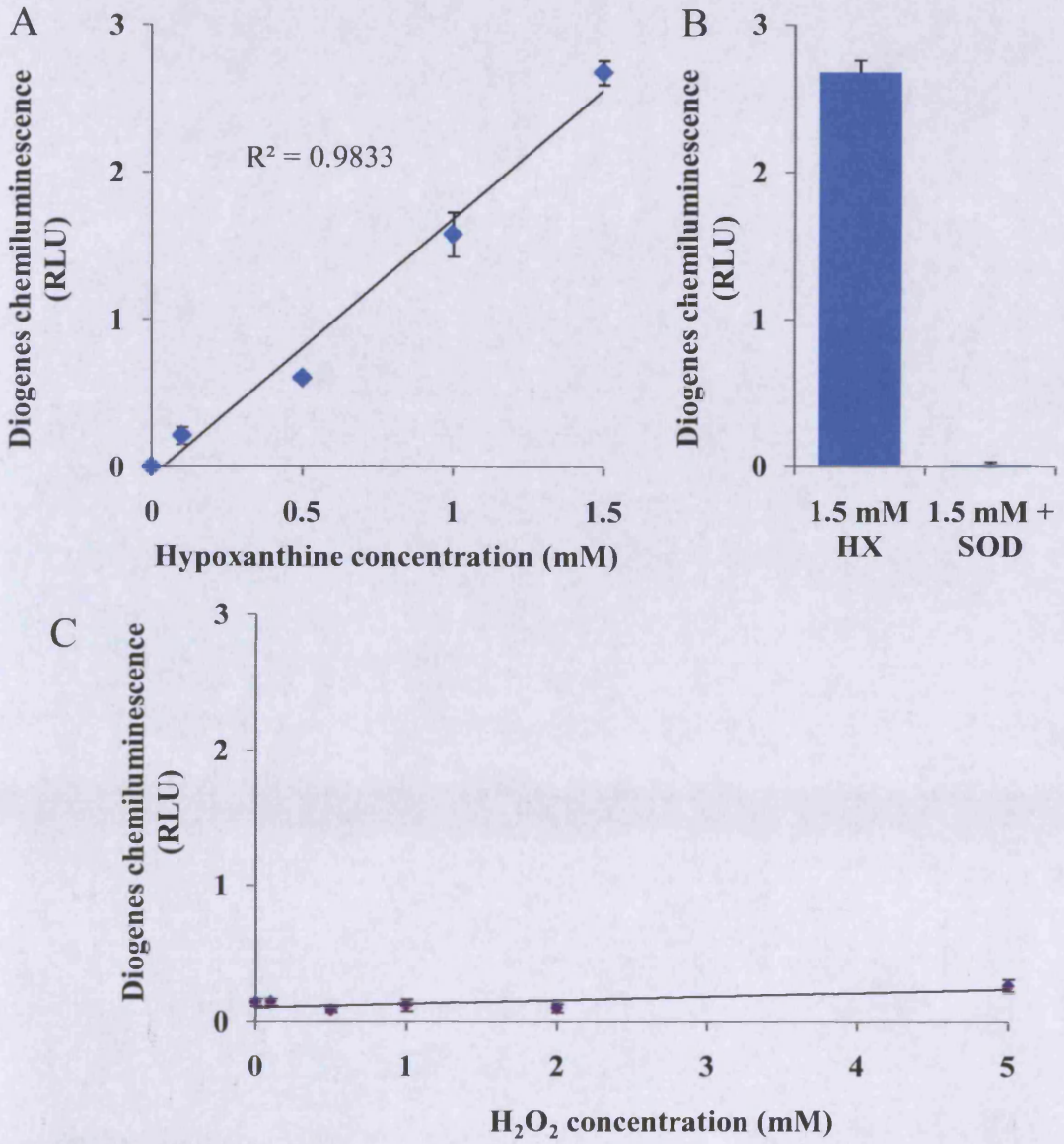

Figure 3.4 Diogenes chemiluminescence in the presence of xanthine oxidase and hypoxanthine or H_2O_2

(A) Diogenes was incubated with 50 mU xanthine oxidase in the presence of 0-1.5 mM HX and time-resolved chemiluminescence was recorded over 50 min (n=3). **(B)** Some experiments were carried out in the presence of 5 µg/ml SOD (n=3). **(C)** Diogenes was incubated with 0.1-5 mM H_2O_2 and time-resolved chemiluminescence was recorded over 50 min (n=4). Data depicts mean total RLU detected ± 1 S.D. RLU values represent total superoxide output during the assay calculated as described in section 3.2.1.7. A linear regression line has been fitted to the scatter data. RLU = relative light units

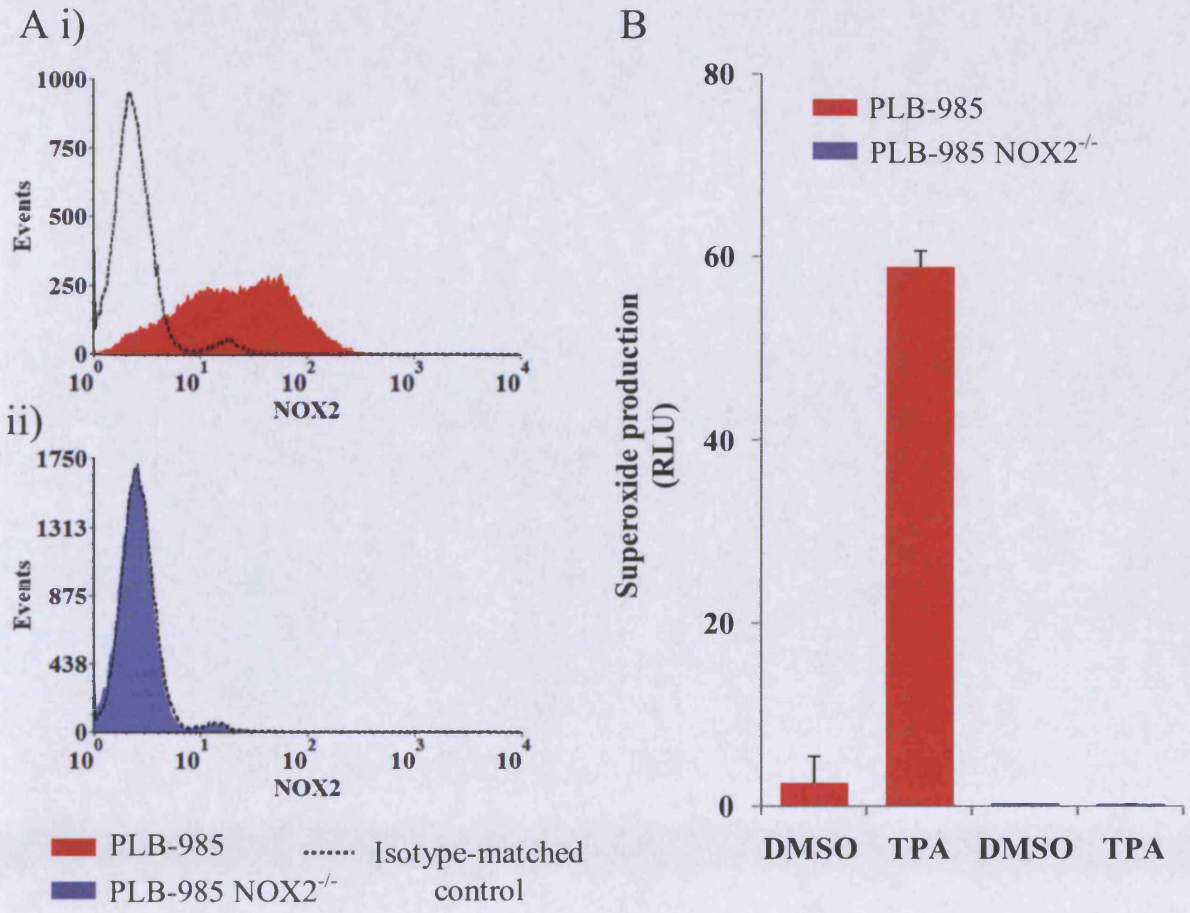

Figure 3.5 Detection of superoxide produced by PLB-985 cells stimulated with TPA

(A) Representative flow cytometric histograms of NOX2 expression by **i)** PLB-985 and **ii)** PLB-985 NOX2$^{-/-}$ cells. NOX 2 expression was analysed by flow cytometry as described in section 2.6, using 5 µg/ml mouse IgG_1 anti-NOX2 unconjugated primary antibody raised against an external epitope of NOX2 (clone 7D5; Caltag Medsystems, Buckinghamshire, UK). To determine background fluorescence, some samples were incubated with 5 µg/ml manufacturer- and isotype-matched unconjugated control antibody. Primary antibody was detected incubation for 15 min at 4°C with 5 µg/ml rat-anti mouse IgG_1-PE secondary antibody (BD Biosciences). **(B)** PLB-985 and PLB-985 NOX2$^{-/-}$ cells were treated with either 1 µM TPA or vehicle control (1% DMSO). Diogenes chemiluminescence was measured over 100 min. Data represents mean plus 1 S.D. RLU values represent total superoxide output during the assay calculated as described in section 3.2.1.7. RLU = relative light units.

3.3.2.3 Optimisation of Diogenes in vitro assay conditions

Prior to this study, it was not known whether human $CD34^+$ haematopoietic cells could produce superoxide, neither was it known whether expression of activated Ras would have an effect on superoxide production. Therefore, optimum conditions for detection of superoxide production by human $CD34^+$ cells using Diogenes were established by variation of the $CD34^+$ cell number used per well and varying the final concentration of Diogenes in the reaction volume.

Diogenes chemiluminescence was observed in a cell-density dependent manner across the entire range tested in both unstimulated $CD34^+$ control cells and $CD34^+$ H-Ras^{G12V} cells (Figure 3.6A). In addition, $CD34^+$ H-Ras^{G12V} cells exhibited a significant 7-fold increase ($P<0.05$) in superoxide production compared with controls during the assay.

These data suggest that Diogenes assays should be performed using the maximum number of cells available. Given that transduced $CD34^+$ cell numbers are often limited, $1.5x10^5$ cells per well was selected as an achievable number of cells for future experiments. In addition, these preliminary data suggest that $CD34^+$ H-Ras^{G12V} cells constitutively produce more superoxide than controls. This observation was investigated further in section 3.3.2.4.

3.3.2.4 Expression of mutant Ras in human $CD34^+$ cells increases superoxide production

Using the optimised conditions for Diogenes assays established in section 3.3.2.3, superoxide production in transduced human $CD34^+$ haematopoietic progenitor cells was examined immediately after transduction and on subsequent days in culture. In early cultures (days 3 to 5), a low level of constitutive superoxide production was observed in control cells, which was strongly augmented by activated Ras (Figure 3.7A). As shown in Figure 3.7B, superoxide induction was typically most efficient with H-Ras^{G12V}, which showed a significant ~4 fold increase compared with controls, while N-Ras^{G12D} showed a similar trend (~2 fold increase in superoxide compared with controls). The presence of SOD quenched Diogenes chemiluminescence, whilst treatment with catalase (which decomposes H_2O_2 but not superoxide) did not, confirming the specificity of the probe and confirming superoxide as the major detectable source of ROS in this assay (Figure 3.7C).

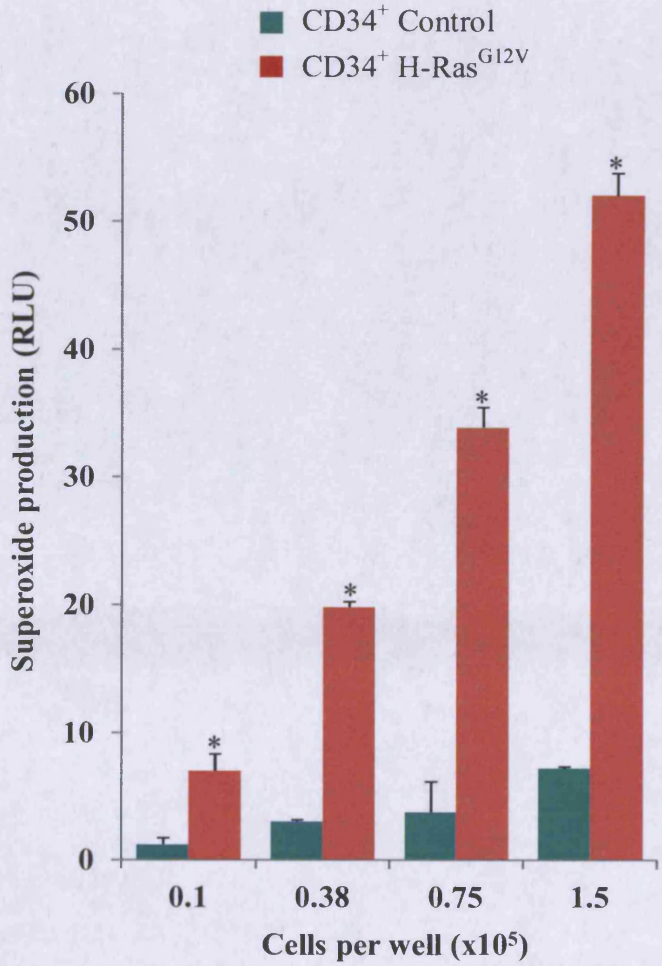

Figure 3.6 Determination of optimal cell number and volume of Diogenes reagent for Diogenes assays

$CD34^+$ control and $CD34^+$ $H\text{-}Ras^{G12V}$ cells ($0.1\text{-}1.5x10^5$) were incubated with 50 µl Diogenes reagent and Diogenes chemiluminescence was measured over 100 min. Data represents mean plus 1 S.D. RLU values represent total superoxide output during the assay calculated as described in section 3.2.1.7. Statistical significance was calculated by Mann-Whitney Test (n=4); $*P<0.05$. RLU = relative light units

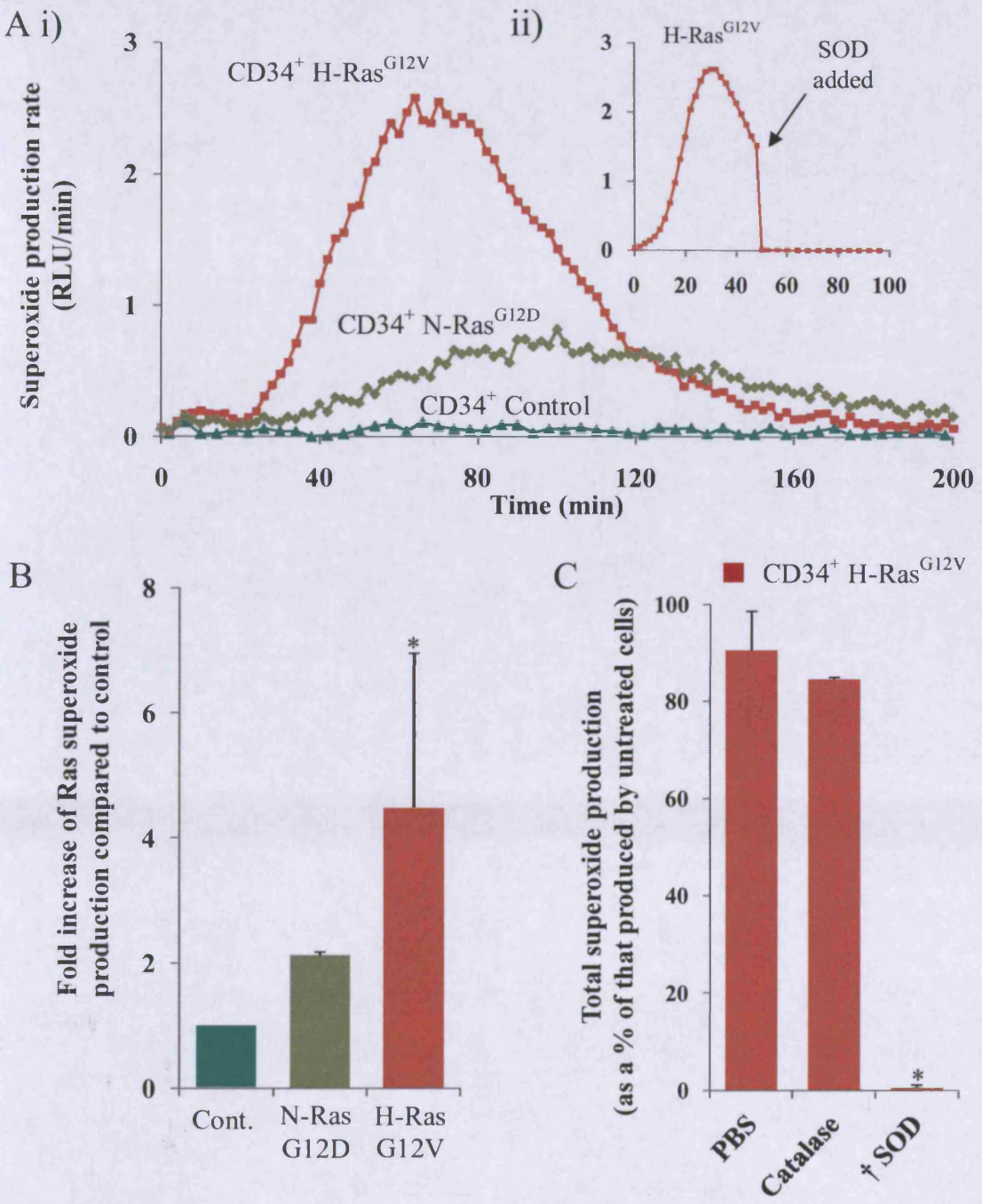

Figure 3.7 Detection of superoxide production by transduced CD34$^+$ cells using Diogenes

(A) i) Representative chemiluminescence traces of superoxide production by CD34$^+$ control, CD34$^+$ H-Ras^{G12V} and CD34$^+$ N-Ras^{G12D} cells measured using Diogenes. **ii)** SOD was added to some replicates at 50 min, indicated by arrow. **(B)** Summary of fold increase of total light emission due to expression of activated Ras over controls during early hematopoietic development. **(C)** Using Diogenes, superoxide production in CD34$^+$ H-Ras^{G12V} cells was measured in the constant presence of 5 µg/ml SOD or 100 µg/ml catalase (n=3). Bar chart represents mean plus 1 S.D. Statistical significance was calculated by Mann-Whitney Test or ANOVA using Tukey's Honestly Significant Differences; *P<0.05; †P<0.001.

To establish whether this increased superoxide production was sustained during subsequent culture, superoxide induction by H-Ras^{G12V} was measured on days 5 to 14 of culture. Superoxide production remained significantly elevated during culture; inducing a maximal ~7-fold increase in superoxide production by day 9. (Figure 3.8).

3.3.2.5 Ras upregulates ROS production by activation of NOX family oxidases

ROS can be generated by several mechanisms, the major sources being oxidase activity (e.g. NOX family) or via the mitochondrial electron transport chain (Finkel, T. 2003). To determine whether NOX enzymes were responsible for the over-production of superoxide, this study focused on the effects of the NOX oxidase inhibitors DPI and apocynin on superoxide production by CD34$^+$ H-Ras^{G12V} cells, since these cells produce the most ROS and were therefore likely to display the strongest phenotype. In the presence of these inhibitors, superoxide production was completely blocked in both CD34$^+$ H-Ras^{G12V} cells and control cells, as determined by Diogenes assay, whereas the mitochondrial poison rotenone had no effect (Figure 3.9A).

To establish whether mutant Ras altered the capacity of CD34$^+$ cells to produce superoxide, CD34$^+$ control and CD34$^+$ H-Ras^{G12V} cells were stimulated with the potent PKC activator, TPA. Both CD34$^+$ control and CD34$^+$ H-Ras^{G12V} cells responded to TPA stimulation with a 58 fold and 33 fold respective increase in superoxide production when compared to unstimulated cells. However, CD34$^+$ H-Ras^{G12V} cells maximal superoxide output was significantly (~1.5 fold) greater than CD34$^+$ control maximal superoxide output ($P<0.01$; Figure 3.9B).

Taken together these data show that normal CD34$^+$ cells constitutively produce superoxide and that mutant Ras induces a significant increase in superoxide production and also increases the maximal superoxide output. These data also suggest NOX family oxidases are the major source of increased superoxide production in CD34$^+$ H-Ras^{G12V} cells, whilst mitochondrial production does not significantly contribute to Diogenes chemiluminescence.

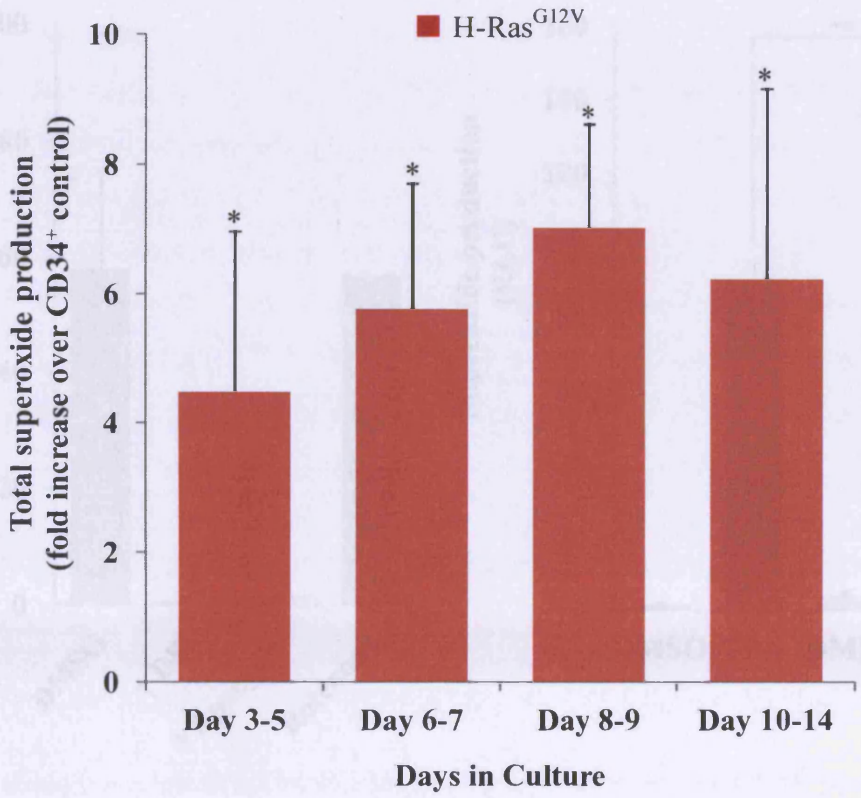

Figure 3.8 Summary of superoxide production by transduced CD34$^+$ cells during culture

Superoxide production by control and H-Ras^{G12V}-transdued cells was measured using Diogenes through early haematopoietic development. Data represent fold increase of total light emission of H-Ras^{G12V}-transduced cells over control cells; where control cell output is represented by dotted line. Data represents mean plus 1 S.D. (n $\geq$3). Statistical significance was calculated using the Mann-Whitney Test, *P<0.05.

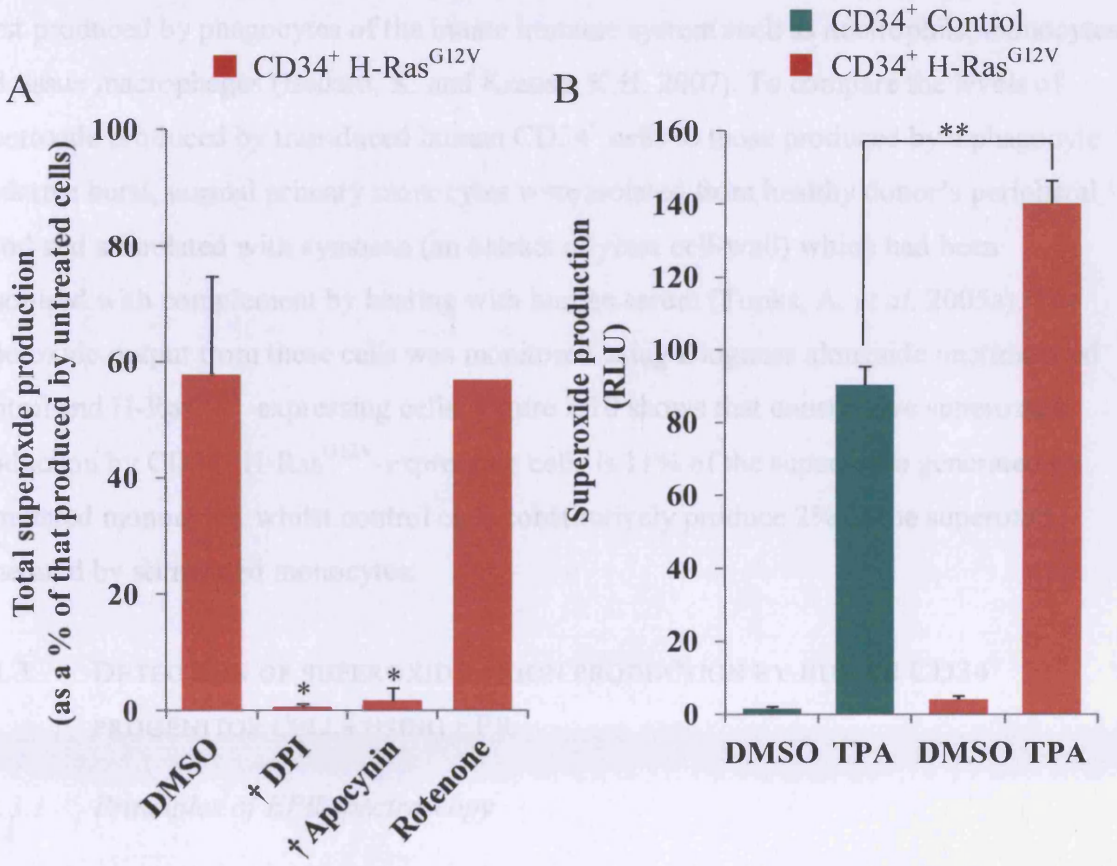

Figure 3.9 Effect of NOX inhibitors, ROS scavengers, and rotenone on superoxide production by transduced CD34$^+$ cells

(A) Using Diogenes, superoxide production in CD34$^+$ H-Ras^{G12V} transduced cells was measured in the presence of 50 µM DPI or 50 µM apocynin (NOX inhibitors) or 5 µM rotenone (inhibitor of mitochondrial electron transport chain) (n=3). **(B)** Using Diogenes, superoxide production in CD34$^+$ control and CD34$^+$ H-Ras^{G12V} cells was measured in the presence of either 1 µM TPA or DMSO control. Data represents mean plus 1 S D. RLU values represent total superoxide output during the assay calculated as described in section 3.2.1.7. Statistical significance was calculated using ANOVA using Tukey's Honestly Significant Differences, *P<0.05, **P<0.01, †P<0.001. RLU = relative light units

3.3.2.6 Comparison of superoxide production by transduced CD34$^+$cells to stimulated primary monocytes

Superoxide production is commonly associated with the phagocytic oxidative burst produced by phagocytes of the innate immune system such as neutrophils, monocytes and tissue macrophages (Bedard, K. and Krause, K.H. 2007). To compare the levels of superoxide produced by transduced human CD34$^+$ cells to those produced by a phagocyte oxidative burst, normal primary monocytes were isolated from healthy donor's peripheral blood and stimulated with zymosan (an extract of yeast cell-wall) which had been opsonised with complement by heating with human serum (Tonks, A. *et al.* 2005a). The superoxide output from these cells was monitored using Diogenes alongside unstimulated control and H-Ras^{G12V}-expressing cells. Figure 3.10 shows that constitutive superoxide production by CD34$^+$ H-Ras^{G12V}-expressing cells is 11% of the superoxide generated by stimulated monocytes, whilst control cells constitutively produce 2% of the superoxide generated by stimulated monocytes.

3.3.3 DETECTION OF SUPEROXIDE ANION PRODUCTION BY HUMAN CD34$^+$ PROGENITOR CELLS USING EPR

3.3.3.1 Principles of EPR spectroscopy

Superoxide production by Ras mutants was confirmed using EPR spin trapping with DEPMPO. DEPMPO is a beta-phosphorylated nitrone which stabilises short-lived radicals such as superoxide by reacting with them forming a relatively long-lived radical molecule known as a spin adduct. Each spin adduct has a unique EPR absorption spectrum which enables free radical identification (Bacic, G. *et al.* 2008). For a more detailed explanation, see section 1.4.5.3.

3.3.3.2 EPR spectroscopy confirms the presence of superoxide radicals and also indicates the presence of hydroxyl radicals

EPR spectroscopy was used to detect DEMPO spin adducts formed in the presence of CD34$^+$ control and CD34$^+$ H-Ras^{G12V} cells. While no spectra were obtained from CD34$^+$ control cells, an EPR spectrum was detected from DEPMPO-treated CD34$^+$ H-Ras^{G12V} cells.

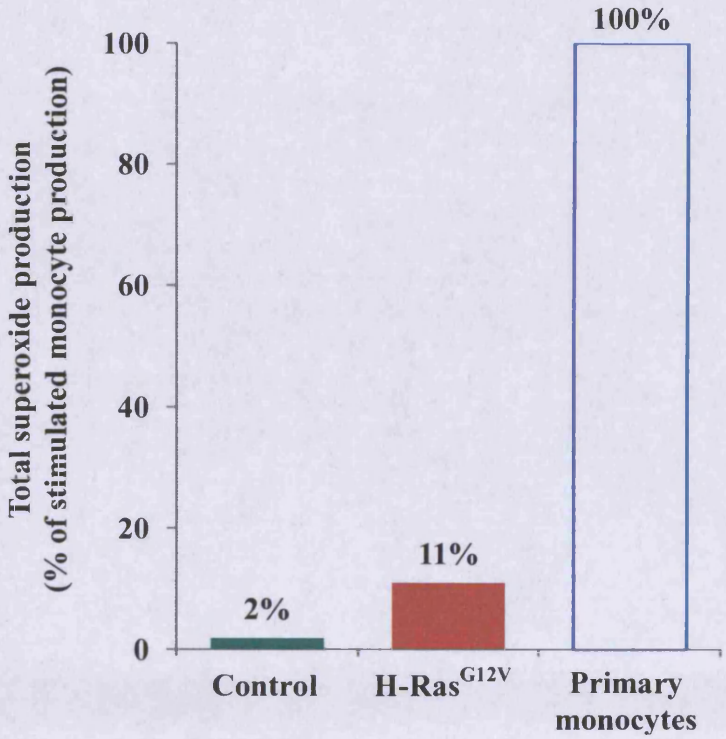

Figure 3.10 Comparison of superoxide production of transduced CD34^{+} cells with the oxidative burst of activated peripheral blood monocytes

Normal human monocytes were isolated from peripheral blood and stimulated with 250 µg/ml opsonised zymosan as previously described (Tonks, A. *et al.* 2005a). Superoxide production was measured using Diogenes and compared with typical constitutive superoxide output from control and H-Ras^{G12V} cultures (day 7).

This spectrum appeared to be a superimposition of two separate EPR spectra. The first EPR spectrum exhibited hyperfine splitting with hyperfine coupling constants typical of the EPR spectrum of the DEPMPO-OOH adduct (a_N=13.1 Gauss (G), $a_{H\beta}$=11.3 G) formed by trapping superoxide. The second spectrum was more intense than the first, and was typical of the DEPMPO-OH adduct (hyperfine coupling constants a_N=14.0 G, $a_{H\beta}$=13.0 G), which is formed by trapping hydroxyl radicals or by slow conversion from the DEPMPO-OOH adduct (Figure 3.11A).

As a positive superoxide control, DEPMPO was incubated with xanthine oxidase and HX under the same conditions as those used in the cell-free assays above. A very similar EPR spectrum to that obtained from cell assays was observed, indicating both the presence of superoxide radicals and hydroxyl radicals (Figure 3.11B).

These data indicate that superoxide radicals are produced by $CD34^+$ H-Ras^{G12V} cells and that hydroxyl radicals are also present. No EPR spectra were obtained from $CD34^+$ control cells, suggesting the levels of superoxide (and possibly hydroxyl radicals) from these cells falls below the sensitivity of this assay.

3.3.4 EXAMINATION OF MITOCHONDRIAL ROS PRODUCTION

3.3.4.1 Optimisation of MitoSOX assay

Experiments using Diogenes to detect superoxide produced by $CD34^+$ control and $CD34^+$ H-Ras^{G12V} cells in the presence of NOX inhibitors suggested that NOX family oxidases are the main source of superoxide in this study. However, mitochondria can also produce superoxide (Murphy, M.P. 2009) and have been previously implicated in ROS production induced by expression of mutant Ras (Kim, J.H. *et al.* 2005).

To assess the effects of mutant Ras on mitochondrial superoxide production, a flow cytometric assay using the red-fluorescent mitochondrial superoxide-sensitive probe MitoSOX was used. Flow cytometry was chosen over fluorescence microscopy because the former lends itself to simpler quantitation of fluorescence intensity and enables simultaneous analysis of additional parameters such as cell-surface marker expression and cell viability. To determine the optimum MitoSOX concentration for future assays, $CD34^+$ control cells were labelled with 1-5 μM MitoSOX reagent and analysed by flow cytometry. Figure 3.12A shows that 5 μM MitoSOX gave the most intense fluorescence, therefore 5 μM MitoSOX was used in subsequent experiments.

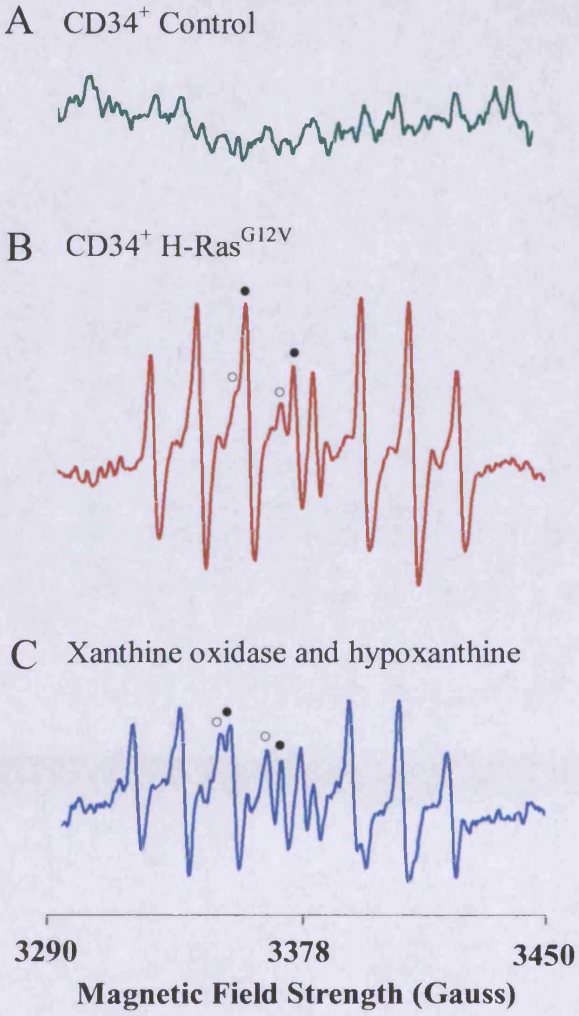

Figure 3.11 Detection of superoxide and hydroxyl radicals using EPR spectroscopy

$CD34^+$ control, $CD34^+$ H-Ras^{G12V} cells and xanthine oxidase in the presence of HX were incubated with the spin-trap probe DEPMPO. Data shows representative EPR signals detected from **(A)** $CD34^+$ control, **(B)** $CD34^+$ H-Ras^{G12V} cells and **(C)** xanthine oxidase and HX. Scans shown are representative of 5 independent experiments, x and y axes in all traces are shown on the same scale. ○ denotes DEPMPO-OOH adduct peaks, ● denotes DEPMPO-OH adduct peaks.

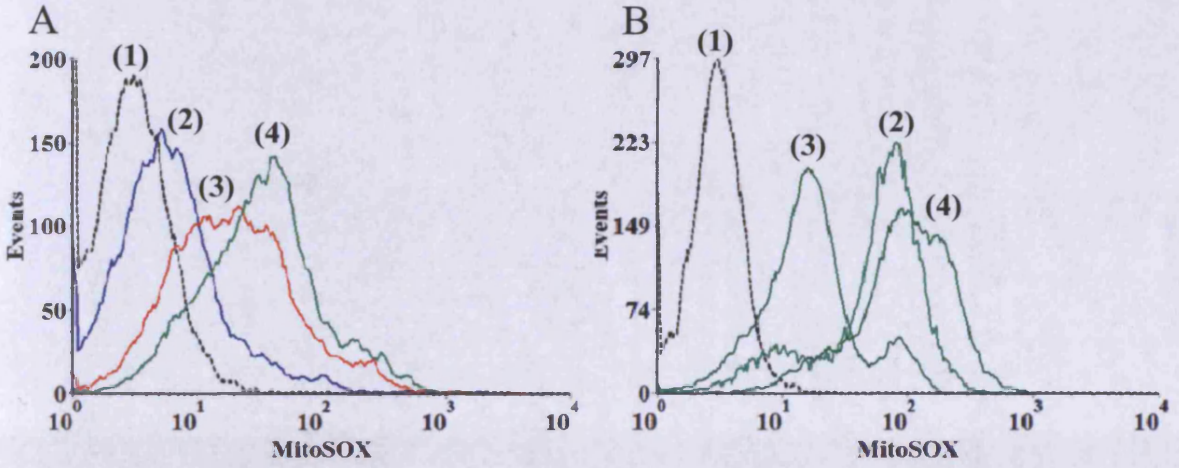

Figure 3.12 Optimisation of MitoSOX assay conditions using $CD34^+$ control cells

Flow cytometric histograms representing MitoSOX fluorescence in $CD34^+$ control cells (day 7). MitoSOX fluorescence was analysed by flow cytometry as described in section 2.6. **(A)** $CD34^+$ control cells were incubated with (1) vehicle control or (2) 1 μM, (3) 2.5 μM or (4) 5 μM MitoSOX reagent. **(B)** $CD34^+$ control cells were labelled with either (1) vehicle control or (2) 5 μM MitoSOX reagent alone; or pre-incubated with either (3) 5 μM FeTCPP (a SOD mimetic) or (4) 50 μM rotenone (a mitochondrial poison) prior to labelling with 5 μM MitoSOX.

In order to determine whether MitoSOX detected changes in superoxide levels in the mitochondria, $CD34^+$ control cells were labelled with MitoSOX under the optimised conditions determined above in the presence of either FeTCPP, a superoxide scavenging molecule (Wu, A.S. *et al.* 2003) which would be expected to decrease MitoSOX fluorescence, or rotenone, an inhibitor of the mitochondrial electron transport chain which can cause an increase in mitochondrial superoxide (Pelicano, H. *et al.* 2003). As expected, peak channel MitoSOX fluorescence was reduced substantially (~ 4 fold) by treatment with FeTCPP, while rotenone treatment caused a ~ 2 fold increase in peak channel MitoSOX fluorescence (Figure 3.12B).

Taken together these data suggest that MitoSOX can be assayed easily by flow cytometry and also that MitoSOX is sensitive to changes in mitochondrial superoxide levels.

3.3.4.2 Mitochondria do not appear to contribute to superoxide overproduction in $CD34^+$ H-Ras^{G12V} cells

Using the optimised MitoSOX labelling protocol devised above, we compared the level of MitoSOX fluorescence in $CD34^+$ control and $CD34^+$ H-Ras^{G12V} cells. No significant differences in mitochondrial ROS were observed in $CD34^+$ H-Ras^{G12V} cells compared to controls (Figure 3.13A). As expected the negative and positive controls (FeTCPP and rotenone) decreased and increased mitochondrial superoxide detection respectively. However, FeTCPP and rotenone induced a similar effect in control and $CD34^+$ H-Ras^{G12V} cultures, causing a consistent decrease or increase in MitoSOX fluorescence respectively (Figure 3.13B). These data suggested that the source of excess superoxide production detected by Diogenes and EPR spectroscopy did not arise from the mitochondria.

3.3.5 DETECTION OF H_2O_2 PRODUCTION BY TRANSDUCED HUMAN $CD34^+$ HAEMATOPOIETIC PROGENITOR CELLS USING AMPLEX RED

3.3.5.1 Mutant Ras promotes H_2O_2 production in transduced $CD34^+$ cells

The data presented thus far strongly indicates that transduced $CD34^+$ cells constitutively produce superoxide, with $CD34^+$ H-Ras^{G12V} cells and $CD34^+$ N-Ras^{G12D} cells producing 5 fold more and 3 fold more superoxide than controls respectively.

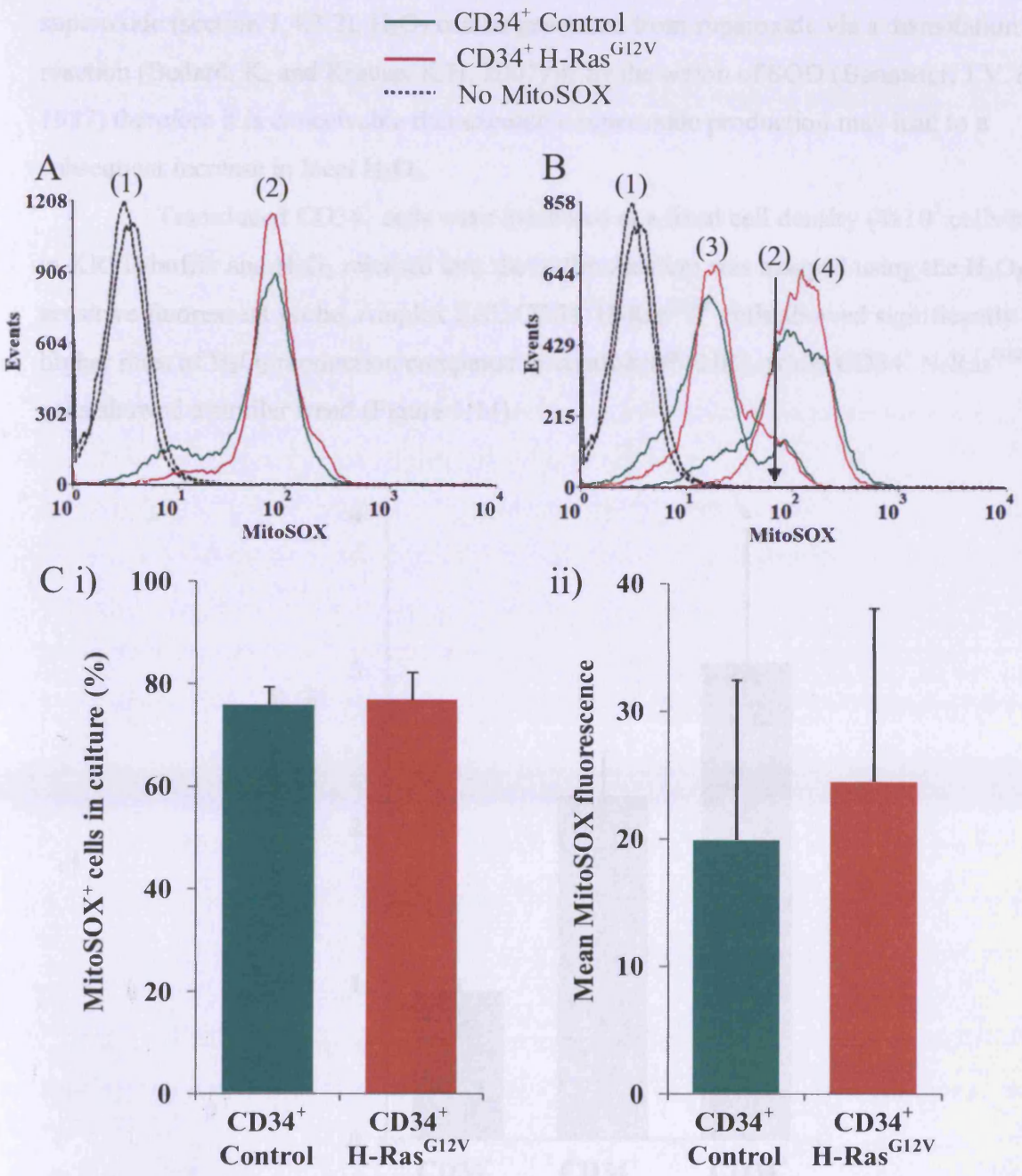

Figure 3.13 Examination of mitochondrial superoxide production in transduced CD34$^+$ cells using MitoSOX

Flow cytometric histograms representing MitoSOX fluorescence in CD34$^+$ control and CD34$^+$ H-Ras^{G12V} cells (day 5). MitoSOX fluorescence was analysed by flow cytometry as described in section 2.6. **(A)** Transduced CD34$^+$ cells were incubated with (1) vehicle control or (2) 5 μM MitoSOX. **(B)** Transduced CD34$^+$ cells were incubated with (1) vehicle control or (2) 5 μM MitoSOX alone (position of peak channel fluorescence of MitoSOX alone is marked with an arrow for comparison). Some samples were pre-incubated with (3) 5 μM FeTCPP or (4) 50 μM rotenone prior to labelling with 5 μM MitoSOX. **(C) i)** Percentage of cells exhibiting positive MitoSOX staining. A PBS control was used to define positive threshold (n=3). **ii)** Mean MitoSOX fluorescence in MitoSOX$^+$ population (n=3). Data represents mean plus 1 S D. Statistical significance was calculated using the Mann-Whitney test.

However, it is H_2O_2 that has been implicated as a second messenger rather than superoxide (section 1.4.3.2). H_2O_2 can be generated from superoxide via a dismutation reaction (Bedard, K. and Krause, K.H. 2007) or by the action of SOD (Bannister, J.V. *et al.* 1987) therefore it is conceivable that excessive superoxide production may lead to a subsequent increase in local H_2O_2.

Transduced $CD34^+$ cells were incubated at a fixed cell density ($4x10^5$ cells/ml) in KRPG buffer and H_2O_2 released into the buffer medium was assayed using the H_2O_2-sensitive fluorescent probe, Amplex Red. $CD34^+$ H-Ras^{G12V} cells showed significantly higher rates of H_2O_2 production compared to controls ($P<0.05$), while $CD34^+$ N-Ras^{G12D} cells showed a similar trend (Figure 3.14).

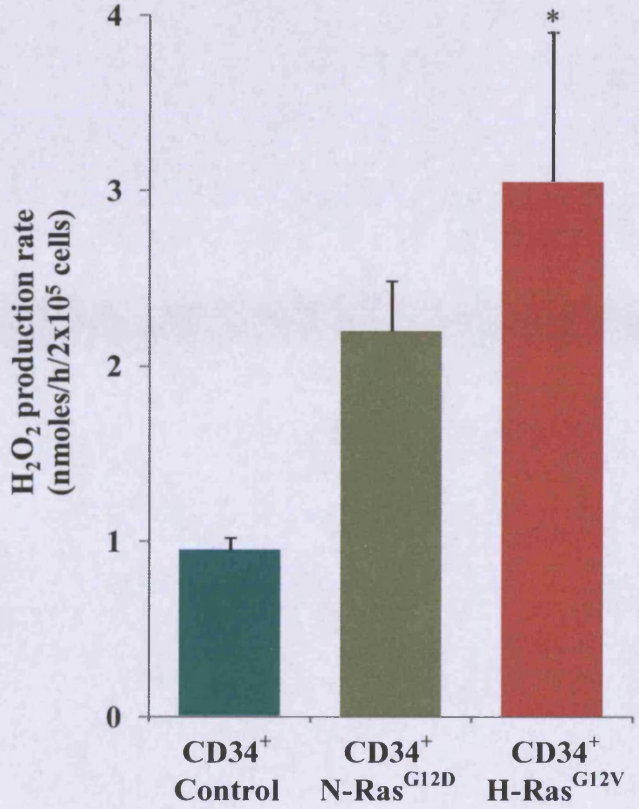

Figure 3.14 Measurement of H_2O_2 production by transduced $CD34^+$ cells using Amplex Red

Transduced $CD34^+$ cells ($2x10^5$) were incubated in KRPG buffer for 4 h and H_2O_2 concentration in the conditioned buffer was measured using Amplex Red (n=3). Amplex Red fluorescence was converted to H_2O_2 concentration using a H_2O_2 standard curve. Data represents mean plus 1 S.D. Statistical significance was calculated using the Student's T Test, $*P<0.05$.

3.3.6 ACTIVATED NOX2 IS THE MAJOR SOURCE OF ROS PRODUCTION IN PRIMITIVE HUMAN AND MURINE HAEMATOPOIETIC CELLS

3.3.6.1 H-Ras^{G12V} promotes expression of NOX2 and membrane translocation of NOX2-regulatory subunits

Taken together, the data presented above (sections 3.3.2.4, 3.3.2.5 and 3.3.4.2) suggest that NOX oxidases are the major contributor to superoxide and H_2O_2 production in mutant Ras transduced CD34$^+$ cells, while the mitochondria do not significantly contribute.

The most likely member of the NOX oxidase family responsible for ROS production in haematopoietic cells is the trans-membrane multi-component enzyme complex, Phox. This enzyme consists of a membrane-bound catalytic complex NOX2 and cytosolic regulatory and organiser components (p47^{phox}, p40^{phox}, p67^{phox} and Rac) which assemble to form a complete complex at the membrane upon activation.(Bedard, K. and Krause, K.H. 2007) To determine whether Phox could be the source of excess ROS production in these cells, the expression and localisation of Phox components was investigated. Flow cytometric analysis showed expression of the Phox catalytic subunit (NOX2) in both CD34$^+$ control and CD34$^+$ H-Ras^{G12V} cells, however, the proportion of cells expressing NOX2 was ~2-fold greater in CD34$^+$ H-Ras^{G12V} cells compared to controls (Figure 3.15A) (P>0.05). In addition, Figure 3.15B shows that H-Ras^{G12V} also promoted the membrane translocation/expression of the Phox activators p67^{phox} and p40^{phox}. Subtle membrane translocation of Rac was also detected together with very faint evidence of p47^{phox} membrane translocation.

Despite our inability to detect large amounts of p47^{phox} membrane translocation, the majority of evidence suggests that H-Ras^{G12V} promotes ROS production by increasing Phox expression and activity in human CD34$^+$ cells.

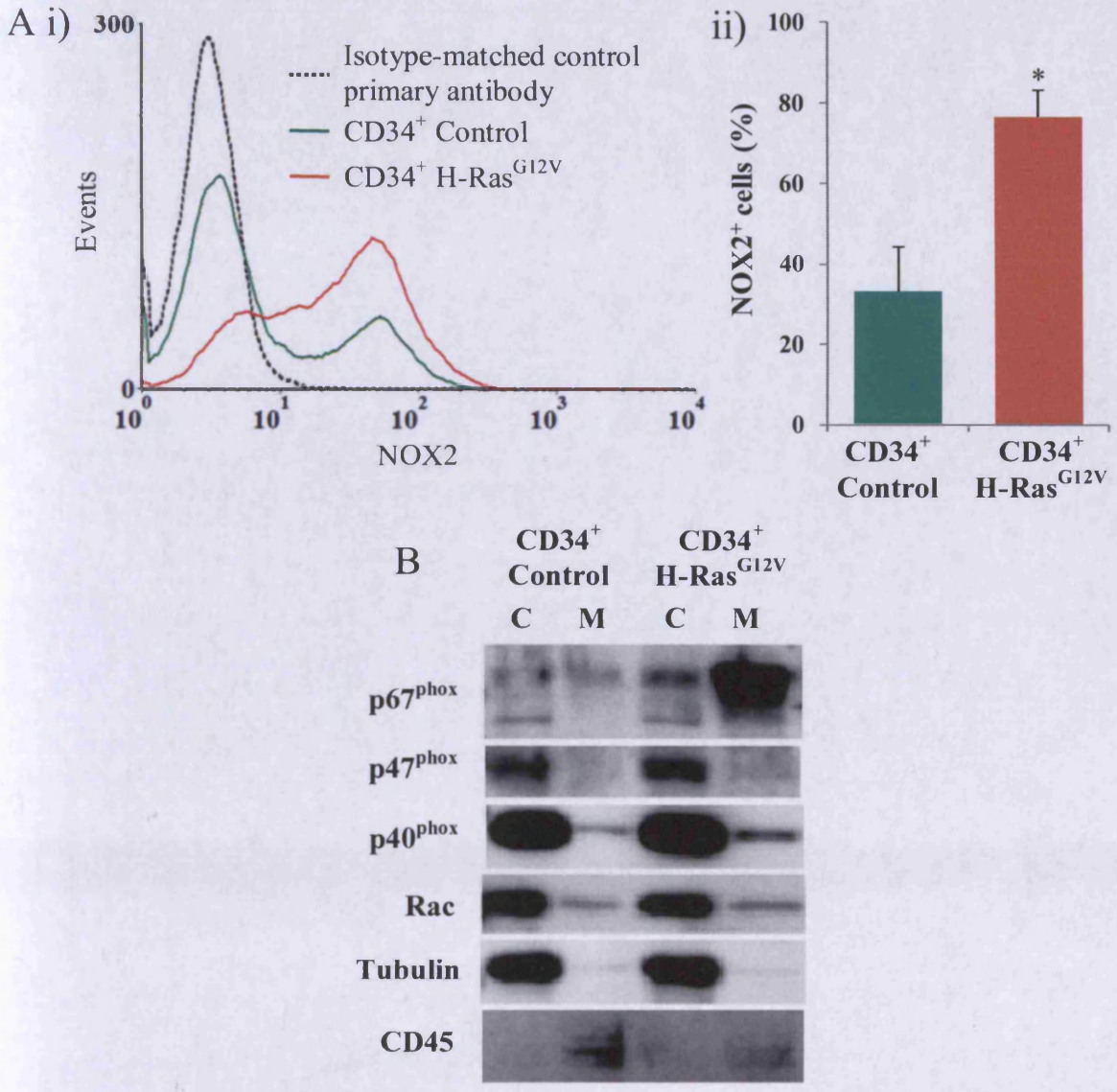

Figure 3.15 The Phox NADPH oxidase is dysregulated in CD34$^+$ H-Ras^{G12V} cells

(A) Transduced CD34$^+$ cells (day 5; 2.5x10^4 per test) were labelled with 5 µg/ml mouse IgG_1 anti-NOX2 antibody (clone 7D5; Caltag Medsystems) or an appropriate isotype-matched control antibody, followed by incubation with 5 µg/ml rat anti-mouse IgG_1 antibody conjugated to PE (BD Biosciences) as described in legend to Figure 3.5; and analysed by flow cytometry as described in section 2.6. **i)** Typical histogram showing anti-NOX2-PE fluorescence. **ii)** Data represents percentage of fluorescent cells after incubation with anti-NOX2-PE. Isotype control antibody was used to define positive threshold (n=5). **(B)** Cytosol/membrane fractionated protein extracts were prepared from 3x10^5 CD34$^+$ control and CD34$^+$ H-Ras^{G12V} cells (day 3) as described in section 2.5.1.2, and analysed by Western blot (section 2.4.7), using 50 ng/ml anti-p67^{phox} (clone H-300), 400 ng/ml anti-p47^{phox} (A-7) or 80 ng/ml anti-p40^{phox} (D-8) (all from Santa Cruz) or 80 ng/ml anti-pan Rac (Cell Signaling). 10 ng/ml anti-α-tubulin (DMA1; Calbiochem) was used as a loading control and cytosolic marker. 250 ng/ml anti-CD45 (clone 69, BD Biosciences) was used a membrane marker. Data represent mean plus 1 S D. Statistical significance was calculated using the Mann-Whitney Test, *P<0.05. C = cytosolic fraction, M = membrane fraction.

3.3.6.2 N-Ras^{G12D} augments ROS production in wild-type murine Sca-1$^+$ haematopoietic cells, but not in those deficient for Nox2

The data presented in section 3.3.6.1, suggested that increased NOX2 activity is responsible for ROS production in haematopoietic cells expressing activated Ras. In order to independently assess the contribution of Nox2 to Ras-induced ROS production, N-Ras^{G12D} was expressed in either wild-type murine Sca-1$^+$ haematopoietic progenitor cells or analogous cells from mice deficient for Nox2 (generated previously using gene-targeting (Pollock, J.D. *et al.* 1995)); isolated cells were >65% Sca-1$^+$ (Figure 3.16A). Retroviral transduction of these cells was relatively inefficient in comparison to human CD34$^+$ transductions with a mean gene transduction efficiency of 50% GFP$^+$ in control cultures and 20% GFP$^+$ in N-Ras^{G12D} cultures (Figure 3.16B).

Following retroviral transduction, superoxide production was assayed using Diogenes. As shown in Figure 3.16C, expression of N-Ras^{G12D} in wild type Sca-1$^+$ cells caused a 1.5 fold increase in constitutive superoxide production when compared with controls. However, no superoxide production was detected in Sca-1$^+$ cells deficient for Nox2, regardless of N-Ras^{G12D} expression. ROS induction in murine Sca-1$^+$ cells expressing N-Ras^{G12D} was less efficient than in human CD34$^+$ cells compared to controls (section 3.3.2.4). This may be due to context-dependent differences, or more likely the low transduction efficiency achieved in Sca-1$^+$ cells compared with CD34$^+$ cells.

These data suggest that NOX2 plays a major dominant role in superoxide generation in normal haematopoietic cells, and furthermore that (at least in murine haematopoietic progenitors) Nox2 is the major source of increased ROS production due to expression of mutant Ras.

3.3.7 H-Ras^{G12V} does not alter the expression of endogenous antioxidants

Aberrant Ras signalling affects transcription of a variety of genes (Chang, F. *et al.* 2003) and could potentially perturb the expression of endogenous antioxidant molecules resulting in an apparent increase in ROS production. In order to examine the expression of common endogenous antioxidants in CD34$^+$ H-Ras^{G12V} cells, Western blot analysis was performed for catalase, Prx1 or Cu/Zn SOD (SOD1) expression.

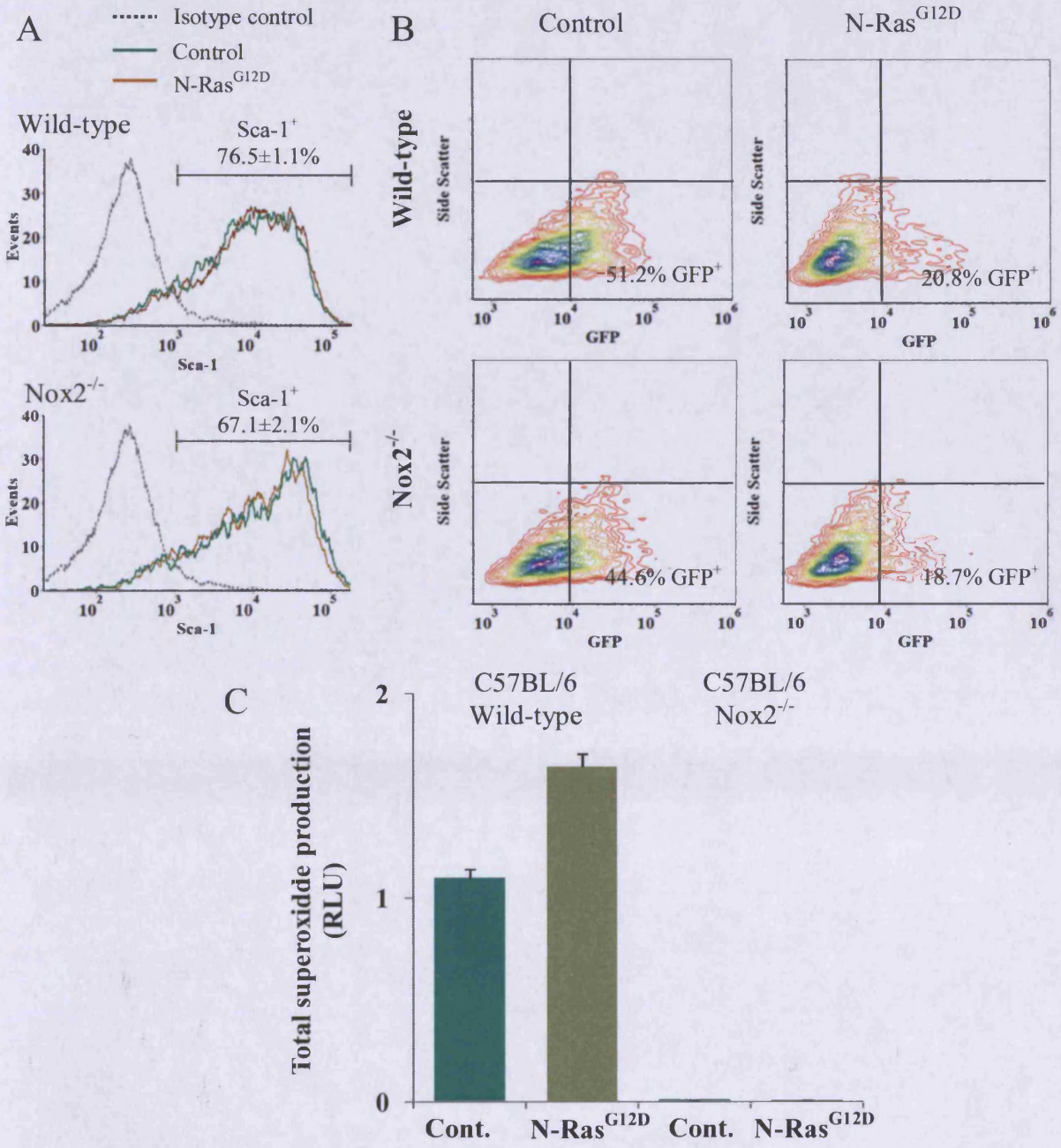

Figure 3.16 Superoxide production by wild type and Nox2-deficient primary murine Sca-1$^+$ haematopoietic cells expressing N-Ras^{G12D}

Sca-1$^+$ cells derived from bone marrow of either wild-type or Nox2-deficient mice were transduced with N-Ras^{G12D} or control. **(A)** Flow cytometric histograms depicting Sca-1 expression in transduced murine bone-marrow derived cells. Transduced cells (day 3; $2.5x10^4$ per test) were labelled by incubating with rat IgG_{2a} anti-Sca-1 antibody conjugated to PE (clone D7; Miltenyi Biotec) or isotype-matched control antibody conjugated to PE (BD Biosciences) for 15 min at 4°C and analysed by flow cytometry as described in section 2.6. **(B)** Bivariate flow cytometric plots depicting GFP fluorescence in transduced Sca-1$^+$ cells (day 3). **(C)** Superoxide production by transduced Sca-1$^+$ cells was assayed on day 6 using Diogenes. Bar chart represents total superoxide production during the assay. Data represents mean ± 1 S.D. RLU values represent total superoxide output during the assay calculated as described in section 3.2.1.7. RLU = relative light units.

There was no difference in the expression levels of these intracellular antioxidants in $CD34^+$ $H\text{-}Ras^{G12V}$ cells compared with controls (Figure 3.17).

These data suggest the observed increase in ROS production in $CD34^+$ cells expressing mutant Ras is unlikely to be due to decreased antioxidant expression. Instead, when considered with the rest of the data presented in this chapter, it is more likely that increased expression and activation of the Phox oxidase complex is responsible.

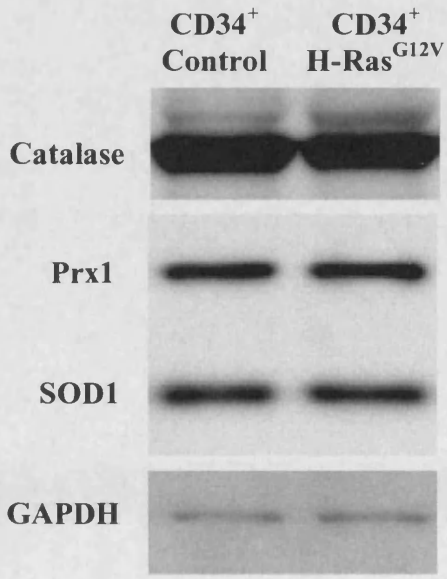

Figure 3.17 Determination of endogenous antioxidant expression in $CD34^+$ control and $CD34^+$ $H\text{-}Ras^{G12V}$ cells

Whole-cell protein extracts of $3x10^5$ transduced human $CD34^+$ cells (day 6) were prepared as described in section 2.5.1.1, and Western blot analysis was performed as described in section 2.4.7, using 5 µg/ml anti-catalase (Abcam), 80 ng/ml anti-Prx1 (Lab Frontier, Korea) or 300 ng/ml anti-SOD1 (Cell Signaling). 20 ng/ml anti-GAPDH (Santa Cruz) was used as a loading control.

3.4 DISCUSSION

Using several validated ROS-sensitive probes, this study detected constitutive production of superoxide and its derivative H_2O_2 in normal human $CD34^+$ haematopoietic progenitor cells. Furthermore this study demonstrated for the first time that ectopic expression of a either $H\text{-}Ras^{G12V}$ or $N\text{-}Ras^{G12D}$ in human $CD34^+$ haematopoietic progenitor cells induces a significant ~4 fold or ~2 fold increase in constitutive superoxide production respectively; with a concomitant ~3 fold or ~2 fold increase in H_2O_2 production rate respectively.

The instability of ROS complicates their detection, therefore this study employed cell-free assays and cell lines to establish the sensitivity and specificity of the probes used. These assays demonstrated that Diogenes was sensitive to enzymatically generated superoxide as well as superoxide generated by stimulated HL60 cells. Amplex Red was shown to be sensitive to very low levels of H_2O_2, verified by addition of catalase, which is an exquisitely specific inhibitor of H_2O_2.

It is important to emphasize that normal $CD34^+$ cells constitutively produced ROS in this study albeit at a comparable low level. This study's findings are consistent with a previous study by Piccoli *et al.*, in which constitutive expression of ROS in normal human $CD34^+$ haematopoietic cells was reported using the intracellular probe DCF for H_2O_2 (Piccoli, C. *et al.* 2007). The exact role of the constitutive ROS production by normal $CD34^+$ cells is unknown. However, ROS are known to play an important role in haematopoietic growth factor signal transduction (Sattler, M. *et al.* 1999; Sundaresan, M. *et al.* 1995) angiogenesis and cell cycle progression (Blanchetot, C. and Boonstra, J. 2008). At the other end of the ROS spectrum, excessive ROS is closely associated with growth arrest (Dolado, I. *et al.* 2007), suggesting that for efficient intracellular function, ROS need to be maintained within a finite range. Indeed, it appears some important transduction pathways require transient inhibition of phosphatases by H_2O_2 to allow efficient signal propagation (Rhee, S.G. 2006). In light of the wide range of roles for ROS in normal cellular function, it may be that constitutive low levels of ROS production in $CD34^+$ cells represents normal homeostasis. However, more research is needed to determine whether this is the case (explored further in Chapter 6).

This is the first study to report Ras-induced ROS production in normal human primary $CD34^+$ haematopoietic cells. Specifically, it appears that Ras augments the low constitutive ROS production seen in normal $CD34^+$ cells. Ras-induced ROS production has been previously demonstrated in a variety of human cell types including embryonic lung

cells (Liu, R. *et al.* 2001), keratinocytes (Yang, J.Q. *et al.* 1999) and neuroblastoma cells (Seru, R. *et al.* 2004) and also in transformed murine cell models (Irani, K. *et al.* 1997; Santillo, M. *et al.* 2001; Dolado, I. *et al.* 2007; Mitsushita, J. *et al.* 2004). In the case of primary human cells, primary human fibroblasts expressing mutant Ras also produced ROS (Wu, C. *et al.* 2004; Lee, A.C. *et al.* 1999). Furthermore, a murine study investigating leukaemic disease in transgenic mice overexpressing human BCL-2 or N-Ras^{G12D} (or both simultaneously) in the myeloid compartment has suggested that Ras-induced ROS contributes to genetic instability, which is a key factor in disease progression. Expression of BCL-2 or N-Ras^{G12D} in myeloid cells under the expression of the myeloid MRP8 promoter caused increased ROS production in both Sca-1^{+} common myeloid progenitor cells and committed Mac1^{+} myeloid progenitors, resulting in single-stranded and double stranded DNA breaks. While N-Ras^{G12D} single transgenic mice exhibited only mild haematological abnormalities, double transgenic mice exhibited greater ROS production than N-Ras^{G12D} alone (attributed to BCL-2 enabling the survival of clones expressing higher levels of N-Ras^{G12D}), and these mice developed haematological disease resembling human AML within 6 months (Rassool, F.V. *et al.* 2007).

EPR spectroscopy was used to confirm the presence of superoxide radicals suggested by Diogenes assays. However, EPR could not detect ROS production by control cells (presumably the low level of superoxide production fell below the sensitivity of the assay) but did detect superoxide production by CD34^{+} H-Ras^{G12V} cells. In addition to superoxide radicals, EPR spectroscopy experiments also detected hydroxyl radicals. While the exact source of hydroxyl radicals in this study are unknown, formation of these radicals can occur downstream of superoxide production. First, superoxide dismutates to form H_2O_2; a reaction which could be catalysed by extracellular SOD3 expression in these cells (Piccoli, C. *et al.* 2007). Hydroxyl radicals can then form from H_2O_2 via Fenton chemistry, a class of radical reactions which can be catalysed by metal ions such as Fe^{3+} or Cu^{2+} in the Haber-Weiss reaction (Simpson, J.A. *et al.* 1988). Alternatively, cellular peroxidases can catalyse the symmetric breakdown of the H_2O_2 molecule resulting in hydroxyl radical formation, though these are not normally expected to be expressed in haematopoietic progenitors. It is important to note that Diogenes (which is based on luminol) is unable to distinguish between superoxide and highly reactive hydroxyl radicals (Wardman, P. 2007); therefore the chemiluminescence detected using this probe is likely to be an indication of both species. The fact that SOD quenched chemiluminescence in Diogenes experiments suggests that production of hydroxyl radicals is indeed downstream of superoxide production in this model, and may progress via a Haber-Weiss mechanism catalysed by

trace transition metal ion impurities in the buffer (Wardman, P. 2007). Hydroxyl radicals are highly reactive and participate in destructive reactions with lipid membranes (which can result in the initiation of lipid peroxidation chain reactions) and oxidative inactivation of proteins (Valko, M. *et al.* 2007). Hydroxyl radicals can further react with endogenous NO to form peroxynitrite, a molecule with similar destructive properties; therefore, downstream production of hydroxyl radicals is likely to be the primary source of toxicity due to superoxide generation production in this model.

Interestingly, the present study consistently observed that H-Ras^{G12V} is more efficient than N-Ras^{G12D} at driving both superoxide and H_2O_2 production in human CD34$^+$ cells. Given that H-Ras^{G12V} and N-Ras^{G12D} were not differentially expressed in our model system, this effect may be attributable to the reported isoform-specific signalling preferences of H-Ras^{G12V} and N-Ras^{G12D} (Omerovic, J. *et al.* 2007). In particular, H-Ras^{G12V} is reported to be a more effective activator of the Rac pathway (important in NOX2 activation) than other Ras isoforms (Shin, I. *et al.* 2005; Oliva, J.L. *et al.* 2004). It is also known that the specific amino acid substitution has an influence on the strength of the phenotype observed, even when comparing mutants of the same Ras isoform mutated at the same residue position, and this could potentially contribute to the difference between the two mutant isoforms used herein. In particular, a valine substitution at position 12 in H-Ras promotes foci formation in NIH 3T3 cells to a greater extent than an aspartate substitution at the same position (Seeburg, P.H. *et al.* 1984).

This study also sought to establish the source of ROS production in this model. ROS can be produced via oxidase activity (e.g. NOX family) or via the mitochondrial electron transport chain (Bedard, K. and Krause, K.H. 2007). This study found no evidence of altered mitochondrial superoxide production as a result of mutant Ras expression. Rather, the results of experiments conducted in the presence of a variety of inhibitors and ROS scavengers suggested that NOX family oxidases were the major source for ROS production detected in our assays supporting the conclusions of (Piccoli, C. *et al.* 2007). It is important to note that the methods used to detect superoxide in the present study are not capable of distinguishing ROS production by differing NOX isoforms. However, experiments showing that NOX2 (the catalytic subunit of Phox) appeared to be both overexpressed and localised with activating subunits in CD34$^+$ cell expressing H-Ras^{G12V}; together with evidence that NOX2 appears to be the exclusive source of ROS (detectable by Diogenes) in murine Sca-1$^+$ cells, suggested that NOX2 is the most probable source of superoxide production.

In haematopoietic cells, NOX2 appears to be indispensible for superoxide production, since both Nox2-deficient primary murine Sca-1^+ cells and NOX2-deficient PLB-985 cells produced no superoxide (detectable by Diogenes) either constitutively or after stimulation with TPA. Furthermore, in those studies where the source of Ras-induced ROS production was investigated, ROS production was primarily ascribed to NOX2 (Seru, R. *et al.* 2004; Yang, J.Q. *et al.* 1999; Santillo, M. *et al.* 2001). Although involvement of NOX1 has been reported (Mitsushita, J. *et al.* 2004), this appears to be in the minority. The significance of NOX1 and NOX2 being the primary sources of Ras-induced ROS (as opposed to other NOX family members) is unclear, however, the predisposition of mutant Ras to activate NOX1 and NOX2 may stem from its ability to activate Rac (Schubbert, S. *et al.* 2007), which contributes to activation of these oxidases, while Rac appears to be dispensable for activation of other NOX family members (Bedard, K. and Krause, K.H. 2007).

Western blot analysis of Phox components revealed that H-Ras^{G12V} induced NOX2 and $p67^{phox}$ expression compared with controls, while the total expression of the other Phox regulatory subunits remained largely unchanged (Figure 3.15). Expression of NOX2, $p47^{phox}$, $p67^{phox}$ and $p40^{phox}$ genes during normal myeloid haematopoietic development is co-ordinated by the myeloid-specifying transcription factor PU.1 (Li, S.L. *et al.* 2002; Li, S.L. *et al.* 1997; Suzuki, S. *et al.* 1998; Gauss, K.A. *et al.* 2002).Given that mutant Ras can accelerate monocyte development (Pearn, L. *et al.* 2007), it is possible that Ras acts via PU.1 to drive monocytic differentiation and simultaneously dysregulates Phox component expression, however, western blot analysis of PU.1 expression in these cells would be required to confirm this. In the present study, a subset of Phox complex genes ($p47^{phox}$, $p40^{phox}$ and Rac) were not upregulated by H-Ras^{G12V} expression. The mechanism of selective upregulation of Phox components was not explored, however, it is known that Phox component regulation is regulated by the expression of several co-operating transcription factors, such as PU.1 and AP-1 (Gauss, K.A. *et al.* 2002; Li, S.L. *et al.* 2001), or PU.1 and IRF1, ICSBP and CBP (Kautz, B. *et al.* 2001), and it may be that suboptimal combination of transcriptions factors such as these may result in inefficient upregulation of some Phox subunits. Alternatively it could be that the Phox complex partially dissociates during protein extract processing, leaving only a remnant of the complex at the membrane. Indeed, it is proposed that phosphorylated $p47^{phox}$ directs and drives $p67^{phox}$ membrane association (section 1.4.2.1), therefore large amounts of membrane-bound $p67^{phox}$ implies that $p47^{phox}$ must also have been present at some point. Techniques such as confocal laser scanning microscopy (CLSM; which allow visualisation of the interior of intact cells) may

serve to clarify whether $p47^{phox}$ is also translocated to the membrane with $p67^{phox}$ in H-Ras^{G12V} cells. Despite the fact that $p47^{phox}$, $p40^{phox}$ and Rac appear to be unchanged in $CD34^+$ H-Ras^{G12V} cells compared with controls, we nevertheless saw increased ROS production, suggesting that the composition of Phox subunits in Ras cells was sufficient to confer an advantage in ROS production.

Finally, cellular ROS production is balanced by the actions of endogenous antioxidants. Previously, it has been shown that an apparent increase in ROS production to due to mutant Ras expression in transformed human and rat fibroblasts could be attributed to a decrease in activity of Prxs, leading to an increase in intracellular ROS (Kopnin, P.B. *et al.* 2007). Also, a study investigating expression of endogenous antioxidants in cells from the bone marrow of AML and MDS patients concluded that there was evidence of increased antioxidant expression in malignant cells compared with controls, suggesting that these cells were subject to oxidative stress (Bowen, D. *et al.* 2003). Lastly, although the expression of FOXO proteins was not examined in detail (see Appendix 3), activated Ras would be expected to suppress FOXO activity (and therefore SOD and catalase expression) via activation of Akt (Tothova, Z. *et al.* 2007). However, in the present study, activated Ras expression did not affect levels of SOD1, catalase or Prx1, suggesting that altered antioxidant expression was unlikely to account for the increased ROS detected; rather, overactivity of NOX2 appeared to be the source of elevated ROS.

In the case of the first study by Kopnin *et al.*, the differences observed here are likely to be due to context-dependent expression and activity of sestrins, but this could potentially be verified by RT-PCR or Western blot analysis. The differing conclusion drawn in the present study compared with that of Bowen *et al.* is most likely to be due to the short experimental time-frames used. $CD34^+$ cells assays were generally conducted within 7 days, whereas malignant cells derived from patients are likely to have been subject to oxidative stress for much longer, and therefore had a longer period within which to upregulate antioxidant defences. Finally, Western blot analysis of FOXO proteins in $CD34^+$ H-Ras^{G12V} cells may reveal why SOD and catalase expression remain unchanged compared with controls. Finally, although GSH levels were not assayed in the present study, deficiencies in GSH homeostasis can also lead to oxidative stress, and it is possible that depletion or disruption of the GSH system could contribute to the increased ROS production by $CD34^+$ cells expressing activated Ras, indeed targeted disruption of GSH production is an emerging concept in cancer therapy (section 1.4.2.3).

In summary, these experiments suggest that activated Ras alone is capable of inducing NOX2 activation in primary $CD34^+$ cells, while mitochondrial ROS production is

not significantly affected. Furthermore, NOX2 activation appears to promote the generation of superoxide and also downstream ROS including H_2O_2 and hydroxyl radicals. However, it is not known whether this excessive production of ROS plays a role in the phenotype of haematopoietic cells expressing activated Ras. This is dealt with in the next chapter.

4 Effect of ROS on the phenotype of $CD34^+$ haematopoietic progenitor cells expressing mutant Ras

One of the best studied roles of Ras proteins is in signal transduction of growth-factor receptor signals, resulting in activation of three main signalling pathways, the PI3K pathway, the MAPK pathway and the Ral pathway (section 1.3.3.2). Normal Ras signalling leads to increased cell survival, cell cycle entry/proliferation cell motility and differentiation (Alvarado, Y. and Giles, F.J. 2007). Constitutive Ras activity can contribute to the increased proliferative drive in cancer cells (section 1.3.5), but can also trigger a cellular senescence program mediated by activation of p53 and/or cell cycle inhibitor molecules such as $p16^{INK4a}$ and $p21^{Cip1}$ which directly opposes this (Malumbres, M. *et al.* 2000; Kwong, J. *et al.* 2009). Furthermore, the strength and duration of Ras signalling may influence which outcome prevails (Deng, Q. *et al.* 2004; Dorrell, C. *et al.* 2004). However, it is not currently known whether expression of activated Ras influences survival of human $CD34^+$ haematopoietic cells and whether any observed effects are mediated via ROS production. In addition, there is no data available regarding the effect of activated Ras and/or ROS production on the proliferation of human $CD34^+$ haematopoietic cells.

Normal $CD34^+$ haematopoietic cells require the presence of several haematopoietic growth factors in order to avoid growth arrest and subsequent apoptosis. This study ectopically expressed H-Ras^{G12V} and N-Ras^{G12D} in normal human haematopoietic $CD34^+$ cells to determine whether activated Ras could rescue $CD34^+$ cells from apoptosis due to growth-factor and serum withdrawal. In addition, $CD34^+$ cells expressing mutant Ras were treated with antioxidants and ROS scavengers to determine whether ROS production influences the phenotype elicited by activated Ras.

This study used annexin V conjugated to Cy5 (which fluoresces in the far red region of the EM spectrum) to detect apoptotic cells by flow cytometry. Flow cytometric analysis offers the additional advantage of accurate counting of cells using APC conjugated to microbeads to control for cell recovery and also allows for detection of additional parameters (e.g. CD34 expression) in the remaining flow cytometer fluorescence channel (FL2).

This study also investigated the effect of Ras on the proliferation of normal human $CD34^+$ haematopoietic cells. When incubated in serum-replete medium without growth factors (note that survival experiments were carried out in medium without serum), normal $CD34^+$ cells show less tendency to undergo apoptosis and instead tend to enter a state of quiescence. This study investigated whether activated Ras can drive $CD34^+$ cells to proliferate under conditions which would normally cause quiescence, and whether antioxidants and ROS scavengers can interfere with proliferation driven by activated Ras. In addition, cell cycle analysis was performed, to determine whether mutant Ras affects the proportion of cells in G_0 or $S+G_2M$ phase of the cell cycle.

4.1 AIMS

In order to understand to role of ROS production in the phenotype of human $CD34^+$ haematopoietic cells expressing activated Ras, this Chapter aims to:

- Determine the effect of activated Ras on growth factor-independent survival of human $CD34^+$ haematopoeitic cells using a model system, in the presence and absence of ROS, using ROS inhibitors.

- Determine whether activated Ras affects the proliferation of these cells in the absence of growth factors, and whether ROS production is repsonsible for any of the effects observed, again using ROS inhibitors and antioxidants.

4.2 METHODS

4.2.1 DETERMINATION OF SURVIVAL OF TRANSDUCED $CD34^+$ HAEMATOPOIETIC CELLS

4.2.1.1 Validation of cell survival assay using annexin V-Cy5 and 7-AAD to detect apoptosis in normal human $CD34^+$ haematopoietic cells

Previous research suggests that expression of activated Ras confers resistance to apoptosis due to growth factor withdrawal, for example in the murine BaF3 cell line (Fukuda, S. and Pelus, L.M. 2004), but it is not currently known whether expression of activated Ras has a similar effect in normal human $CD34^+$ cells. Therefore, a key requirement for this study was the development of a sensitive assay to detect apoptotic cells in response to stress. Phosphatidylserine (PS) is plasma-membrane phospholipid

which is maintained on the inner leaflet of the membrane under normal conditions by the enzymatic action of flippases (van Engeland, M. *et al.* 1998). Under conditions of cellular stress, PS begins to appear on the outer leaflet of the plasma membrane, and this phenomenon is generally considered as a marker of early to intermediate stages of apoptosis (Boersma, H.H. *et al.* 2005). Annexin V (also known as annexin A5) is a member of the annexin protein family with a high avidity for PS (van Engeland, M. *et al.* 1998). Fluorochrome conjugates of annexin V have been developed in order to detect PS expression on the surface of cells by flow cytometry. Late stage apoptosis/necrosis are characterised by loss of homeostasis and subsequent loss of membrane integrity (Wyllie, A.H. 1997). The membrane-impermeable molecule 7-aminoactinomycin D (7-AAD) can enter cells with compromised plasma membranes and intercalates with DNA (Schmid, I. *et al.* 1992) forming fluorescent DNA/7-AAD complexes that are easily detected by flow cytometry.

To detect apoptosis in transduced $CD34^+$ cells, an assay was devised using annexin V conjugated to Cy5 (BioVision, Mountain View, CA, USA) and 7-AAD (Sigma-Aldrich). To confirm that this assay could detect apoptotic cells, normal human $CD34^+$ cells (day 3) were recovered from growth medium by centrifugation at 180 g for 5 min. All traces of growth factors and serum remnants (which would interfere with the survival assay), were removed by washing the cell pellets twice by centrifugation at 180 g for 10 min in 25 ml Hanks Balanced Salt Solution (HBSS; Invitrogen). To induce apoptosis, washed $CD34^+$ cells ($1x10^4$) were incubated in 96U-well microplates (Thermo Fisher Scientific) in duplicate for 24 h in 150 µl IMDM without supplements, serum or growth factors at 37°C in a 5% CO_2 humidified atmosphere. Following incubation, remaining cells were transferred to 96V-well microplates (Thermo Fisher Scientific) and collected by centrifugation at 180 g for 5 min. Cell pellets were washed by centrifugation (180 g for 5 min) in 200 µl staining buffer (section 2.1.2) followed by a further wash by centrifugation in 200 µl annexin V binding buffer (Bender Medsystems, Vienna, Austria) containing 1 µg/ml 7-AAD. Finally, washed cells were resuspended in 25 µl annexin V binding buffer containing 1 µg/ml 7-AAD and 100 fold dilution of annexin V-Cy5 conjugate. Annexin V-Cy5 and 7-AAD enabled discrimination of apoptotic and viable cells. The percentage of recovered cells that were viable (annexin V^{neg} and 7-AAD^{neg}) was determined by flow cytometry (section 2.6).

4.2.1.2 *Detection of apoptosis in transduced human CD34$^+$ haematopoietic cells deprived of growth factors and serum*

To determine whether activated Ras promotes growth factor-independent survival in human CD34$^+$ haematopoietic cells, a modified version of the protocol described in section 4.2.1.1 was used. Briefly, transduced CD34$^+$ cells (day 3) were recovered from growth medium by centrifugation at 180 g for 5 min. Cells (0.1-3x10^5) were washed with HBSS, resuspended in 150 µl IMDM without supplements, serum or growth factors and incubated in a 96-U well or 96-Flat well plate at 37°C in a 5% CO_2 humidified atmosphere as described in section 4.2.1.1. However, the incubation period was increased from 24 h to 48 h to maximise any survival differential between CD34$^+$ control and CD34$^+$ H-Ras^{G12V} cells. Some experiments were carried out in the presence of either 50-500 µg/ml catalase, 0.015-1.5 µM DPI, 0.015-1.5 µM apocynin, 0.075-75 µM NAC or 10-50 µU[a]/ml GOX. Where applicable, the concentration of H_2O_2 generated by GOX treatment was monitored using Amplex Red. After incubation, remaining cells were washed with staining buffer and labelled with 7-AAD and annexin V-Cy5; and the percentage of viable cells was determined by flow cytometry as in section 4.2.1.1.

4.2.1.3 *Measurement of survival of normal human CD34$^+$ haematopoietic cells co-cultured with CD34$^+$ haematopoietic cells expressing H-Ras^{G12V}*

To determine whether increased cell survival observed in CD34$^+$ H-Ras^{G12V} cells was transferable to CD34$^+$ control cells, a co-culture system was used. CD34$^+$ control cells expressing GFP were co-cultured with an increasing proportion of CD34$^+$ H-Ras^{G12V} cells expressing DsRed. These DsRed-expressing cells were generated by subcloning the DsRed gene into the PINCO-H-Ras^{G12V} plasmid in place of the GFP gene. The recombinant PINCO-DsRed-H-Ras^{G12V} plasmid was used to generate retrovirus as described in section 2.4.6 and transduction efficiency was measured by flow cytometry. The use of GFP and DsRed reporter genes enabled independent analysis of both cell populations in mixed culture by flow cytometry.

CD34$^+$ control (expressing GFP) and CD34$^+$ H-Ras^{G12V} cells (expressing DsRed) were recovered from growth medium and washed twice in HBSS as described in section 4.2.1.1. Co-cultures containing a fixed total number of cells (1x10^4) were prepared by resuspending 0.3-1x10^4 CD34$^+$ control cells in a fixed volume (150 µl) of IMDM

[a] One unit (U) will oxidize 1.0 µmole of β-D-glucose to D-gluconolactone and H_2O_2 per min at pH 5.1 at 35 °C, equivalent to an O_2 uptake of 22.4 µl per min.

without supplements, serum or growth factors in the presence of $CD34^+$ H-Ras^{G12V} cells. Co-cultured cells were incubated for 48 h at 37°C in a 5% CO_2 humidified atmosphere. After incubation, remaining cells were washed with staining buffer and labelled with 7-AAD and annexin V-Cy5 and the percentage of GFP^+ viable cells was determined by flow cytometry as in section 4.2.1.1.

4.2.2 EXAMINATION OF PROLIFERATION, CELL CYCLE PROGRESSION AND STATUS OF CELL CYCLE CONTROL PROTEINS IN TRANSDUCED HUMAN $CD34^+$ HAEMATOPOIETIC CELLS

4.2.2.1 Determination of proliferation of transduced $CD34^+$ cells

To determine whether activated Ras promotes proliferation in the absence of growth factors, a protocol similar to that described in section 4.2.1.2 was used, with slight modifications.

$CD34^+$ control, $CD34^+$ N-Ras^{G12D} and $CD34^+$ H-Ras^{G12V} cells (day 3) were recovered from growth medium by centrifugation at 180 g for 5 min. Transduced $CD34^+$ cells ($1x10^4$) were then washed with HBSS and incubated for 48 h at 37°C in a 5% CO_2 humidified atmosphere as described in section 4.2.1.2, with the exception that the cells were resuspended in 150 µl serum-replete, supplemented IMDM without growth factors (as opposed to IMDM without supplements, serum or growth factors used in survival experiments described in section 4.2.1). Some experiments were carried out in the presence of either 10-500 nM DPI, 50-100 µg/ml catalase or 0.05-100 µM NAC. After incubation, remaining cells were washed with staining buffer and labelled with 7-AAD and annexin V-Cy5 as described in section 4.2.1.1, and the absolute number of viable cells was counted by flow cytometry; using APC microbeads to control for recovery (APC microbead correction method is described in section 2.6).

4.2.2.2 Cell cycle analysis of transduced human $CD34^+$ cells

To verify that expression of mutant Ras caused human $CD34^+$ haematopoietic cells to enter the cell cycle, propidium iodide (PI) was used to label intracellular DNA and DNA content was analysed by flow cytometry.

$CD34^+$ control, $CD34^+$ N-Ras^{G12D} or $CD34^+$ H-Ras^{G12V} cells (day 5) were incubated in supplemented IMDM (formulation given in section 2.2.3.1) without growth factors at $4x10^5$ cells/ml for 16 h at 37°C in a 5% CO_2 humidified atmosphere. Growth factors were withheld to minimise cell-cycle entry due to growth factor signalling. After

incubation, $1x10^5$ cells were washed with 15 ml PBS by centrifugation at 180 g for 10 min and the cell pellet was resuspended in 300 µl PBS and incubated on ice for 5 min. Ice-cold ethanol (700 µl) was then added to the cell suspension and the mixture was incubated on ice for 30 min followed by incubation at -20°C for 16 h. After incubation, 10 ml PBS was added to the cell suspension, followed by centrifugation at 300 g for 10 min. The pellet was resuspended in 50 µl PBS containing 40 µg/ml PI and 0.1 mg/ml DNAse-free RNAse (Sigma-Aldrich) and incubated for 30 min at 37°C. PI-labelled cells were analysed by flow cytometry as described in section 2.6. The threshold for inclusion of apoptotic bodies was set at 25% of the fluorescence peak representing cells in G_0. The proportion of cells in G_0 and $S+G_2/M$ was determined using Cylchred v1.0 (T. Hoy, Cardiff University, UK).

4.2.3 Determination of colony-formation capacity and morphology in transduced human $CD34^+$ cells

$CD34^+$ control and $CD34^+$ N-Ras^{G12D} cells (day 4) were recovered from growth medium by centrifugation at 180 g for 5 min, and incubated for 48 h in fresh growth medium at $2x10^5$ cells/ml containing 0.2-1 µM DPI or vehicle control. After incubation, the $CD34^+$ progenitor frequency (method described in legend), cellular morphology and number of colony-forming cells was examined. For morphological assessment, $3.5x10^4$ cells were loaded onto a glass slide (Thermo Fisher Scientific) by centrifugation at 60 g for 5 min using a Cytospin 3 cytocentrifuge (Thermo Fisher Scientific), stained with May-Grünwald-Giemsa using a Pentra DX 120 SPS analyser (Horiba ABX, Northampton, UK) and mounted using DPX mountant (Sigma-Aldrich). Digital photomicrography was performed using a Diaplan microscope with a 40x/0.65 objective lens (Leica, Cambridge, UK) and an Optronics MicroFire digital camera (Optronics, Goleta, CA). Images were acquired using MicroFire v1.1 software (Optronics).

Colony-forming cell frequency was determined using a limiting dilution colony assay. Transduced cells incubated with DPI or vehicle control (as described in this section) were resuspended in fresh growth medium and seeded in 96-well plates in triplicate at a limiting dilution of 1.5 cells/well. After 7 days, colonies with >50 cells were scored.

4.3 RESULTS

4.3.1 THE ROLE OF ROS IN SURVIVAL OF HUMAN CD34$^+$ HAEMATOPOIETIC CELLS

4.3.1.1 Optimisation of survival assay using annexin V-Cy5 and 7-AAD

To assess the role of ROS production in the survival of transduced human CD34$^+$ haematopoietic cells expressing mutant Ras, a suitable method for discrimination of apoptotic and viable cells was required. To this end, a protocol was devised using annexin V-Cy5 binding and internalisation of 7-AAD to exclude apoptotic cells from the analysis.

To verify that these reagents were able to detect apoptosis in transduced CD34$^+$ cells, normal CD34$^+$ were cells labelled with annexin V-Cy5 and 7-AAD both before and after growth factor and serum deprivation for 24 h. As shown in Figure 4.1, normal CD34$^+$ cells were 98% viable (annexin V^{neg} and 7-AAD^{neg}) prior to incubation. After 24 h incubation without growth factors or serum, three clearly defined populations were visible, 79% of remaining cells were viable, 9% were annexin V$^+$ and 7-AAD^{neg} (early apoptotic cells), and 11% were positive for both markers (late apoptotic cells).

These data suggest that annexin V-Cy5 and 7-AAD are able to detect apoptotic CD34$^+$ cells, and are able to discriminate between early and late apoptotic populations in mixed culture. However, following 24 h incubation without serum or growth factors, a large proportion of the culture was still viable. To maximise any survival difference between CD34$^+$ control and CD34$^+$ cells expressing mutant Ras, subsequent experiments extended the 24 h incubation to 48 h.

4.3.1.2 H-Ras^{G12V} promotes growth factor-independent survival of human CD34$^+$ haematopoietic cells

Mutant Ras has been shown to promote growth factor-independent survival in several haematopoietic cell lines; including mutant N-Ras and K-Ras in multiple myeloma cells (Hoang, B. *et al.* 2006), mutant H-Ras in murine BaF3 factor-dependent cells (Fukuda, S. and Pelus, L.M. 2004) and mutant N-Ras in FDC-P1 factor-dependent cells (McGlynn, A.P. *et al.* 2000). However, the effect of activated Ras on growth factor-independent survival of primary human CD34$^+$ cells has not been previously investigated.

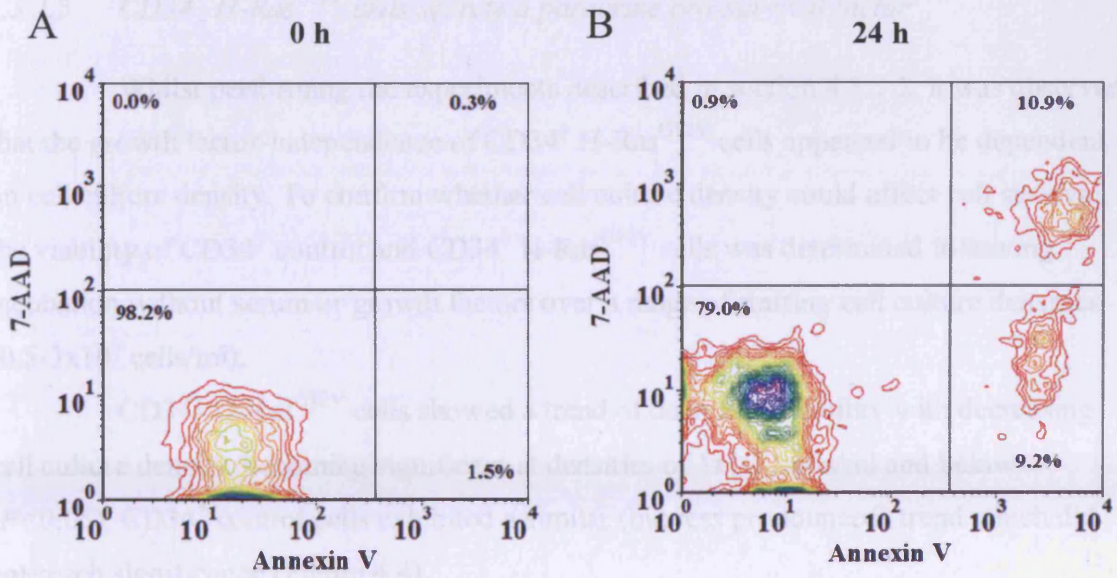

Figure 4.1 Detection of apoptosis of CD34$^+$ control cells deprived of growth factors and serum for 24 h

CD34$^+$ control cells were labelled with annexin V and 7-AAD to detect apoptotic cells prior and after growth factor and serum deprivation. Figure shows bivariate flow cytometric plots showing annexin V and 7-AAD staining **(A)** immediately prior to incubation and **(B)** after 24 h incubation in IMDM without supplements, serum or growth factors. Viable cells are found in the lower left quadrant, early apoptotic cells are in the lower right quadrant and late apoptotic cells are in the upper right quadrant.

To establish whether Ras promotes survival of primary human $CD34^+$ cells, $CD34^+$ control and $CD34^+$ H-Ras^{G12V} cultures were deprived of growth factors and serum for 48 h, and were incubated with annexin V-Cy5 and 7-AAD using the protocol validated in section 4.3.1.1. Representative bivariate flow cytometric plots are shown in Figure 4.2. As shown in Figure 4.3, $CD34^+$ H-Ras^{G12V} cultures showed a significant resistance to apoptosis (59±3.3% viable; $P<0.05$) after 48 h without growth factors when compared to $CD34^+$ control (26±3.9% viable) under the same conditions.

4.3.1.3 $CD34^+$ H-Ras^{G12V} cells secrete a paracrine pro-survival factor

Whilst performing the experiments described in section 4.3.1.2, it was observed that the growth factor-independence of $CD34^+$ H-Ras^{G12V} cells appeared to be dependent on cell culture density. To confirm whether cell culture density could affect cell survival, the viability of $CD34^+$ control and $CD34^+$ H-Ras^{G12V} cells was determined following incubation without serum or growth factors over a range of starting cell culture densities ($0.5\text{-}3x10^5$ cells/ml).

$CD34^+$ H-Ras^{G12V} cells showed a trend of decreased viability with decreasing cell culture density, becoming significant at densities of $1x10^5$ cells/ml and below ($P<0.05$). $CD34^+$ control cells exhibited a similar (but less pronounced) trend which did not reach significance (Figure 4.4).

The data suggest that transduced $CD34^+$ cells secrete a pro-survival factor(s) into the extracellular space which may act in a paracrine manner on neighbouring cells. Furthermore, the increased dependence of $CD34^+$ H-Ras^{G12V} cells on cell density suggests that these cells secrete greater amounts of these same factors; or secrete different, more effective pro-survival factors which contribute to their increased cell survival.

To establish whether these Ras induced putative pro-survival factors could augment survival of neighbouring $CD34^+$ control cells in a paracrine manner, $CD34^+$ control cells (expressing a GFP reporter gene) were co-cultured with increasing proportions of $CD34^+$ H-Ras^{G12V} (expressing a DsRed reporter gene) cells in the absence of serum or growth factors. The use of different reporter genes enabled independent analysis of both cell populations in mixed culture by flow cytometry. Figure 4.5 shows that $CD34^+$ control cells showed a significant increase in viability when cultured with increasing numbers of $CD34^+$ H-Ras^{G12V} cells ($P<0.01$).

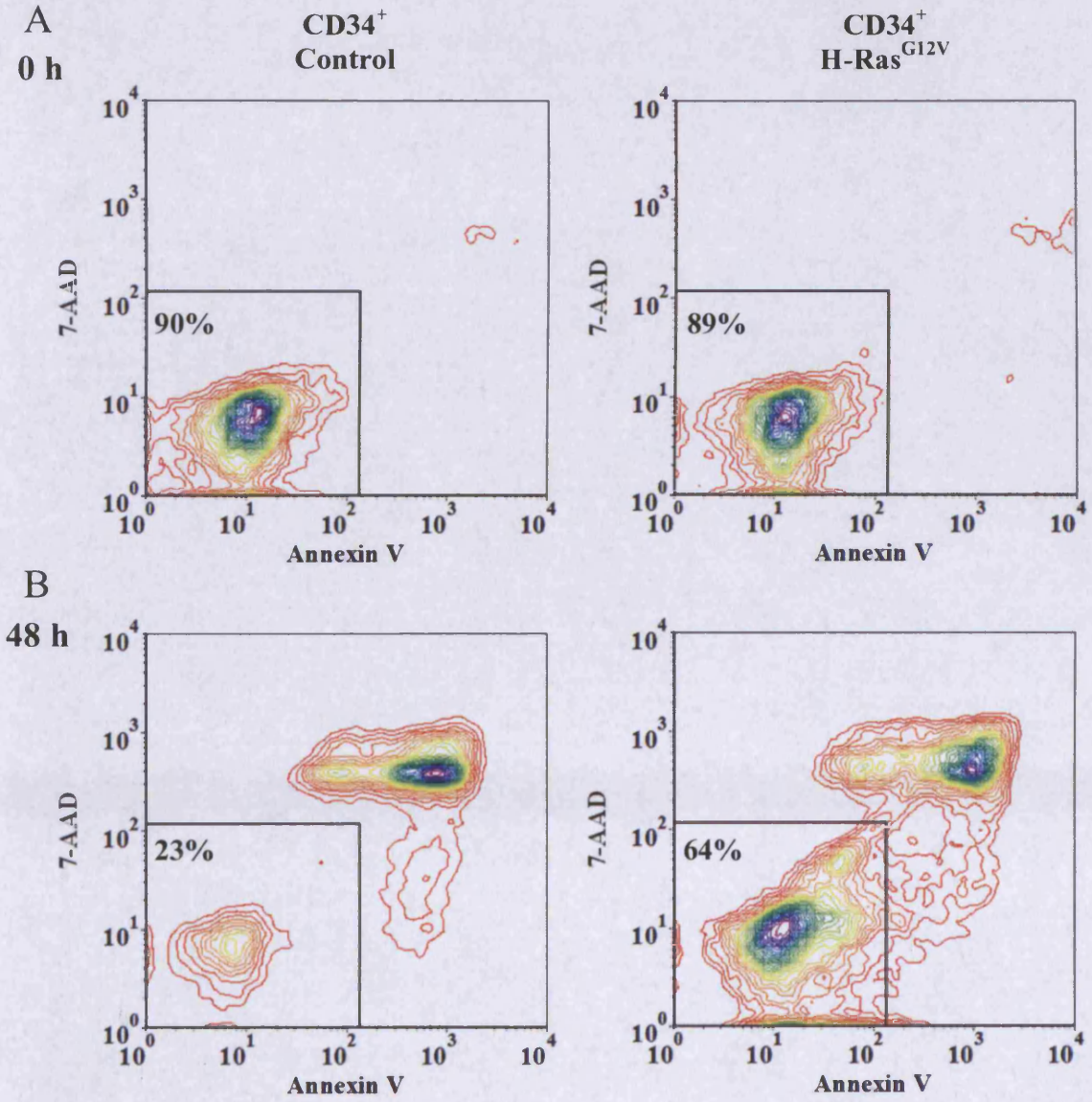

Figure 4.2 Flow cytometric analysis of transduced human CD34$^+$ haematopoietic cells deprived of serum and growth factors for 48 h

Representative bivariate plots show typical annexin V and 7-AAD labelling of CD34$^+$ control and CD34$^+$ H-Ras^{G12V} cells **(A)** prior to growth factor and serum deprivation (0 h) and **(B)** following 48 h incubation in IMDM without supplements, serum or growth factors. Labelled cells were analysed by flow cytometry (section 2.6).

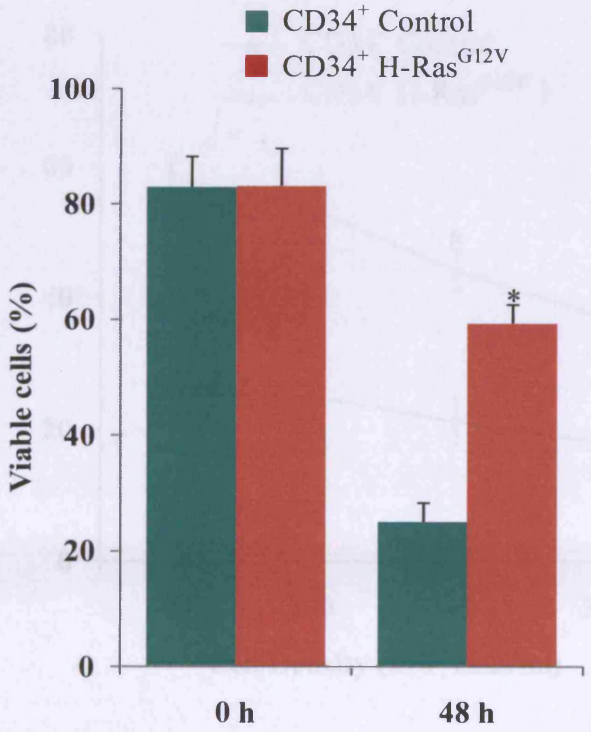

Figure 4.3 Summary of flow cytometric data showing viable transduced CD34$^+$ cells remaining after growth factor and serum deprivation for 48 h

CD34$^+$ control and CD34$^+$ H-Ras^{G12V} cells were deprived of growth factors and serum for 48 h, and labelled with annexin V and 7-AAD. Bar chart represents mean percentage viable cells recovered after 48 h plus 1 S D (n=3). Statistical significance was calculated using the Mann-Whitney Test. *P<0.05.

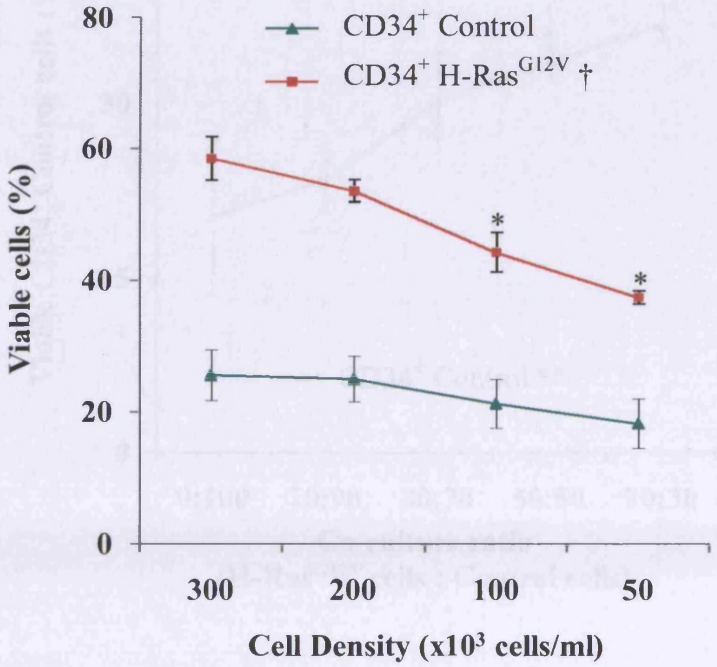

Figure 4.4 The effect of altering cell culture density on survival of transduced CD34$^+$ cells after serum and growth factor deprivation

CD34$^+$ control and CD34$^+$ H-Ras^{G12V} cells were incubated without serum or growth factors for 48 h at 0.5-3x10^5 cells/ml. Data represents mean percentage viable (annexin V^{neg} and 7-AAD^{neg}) cells recovered ± 1 S D (n=3). Statistical significance was calculated using by one-way ANOVA using Tukey's Honestly Significant Differences. †P<0.001, *P<0.05.

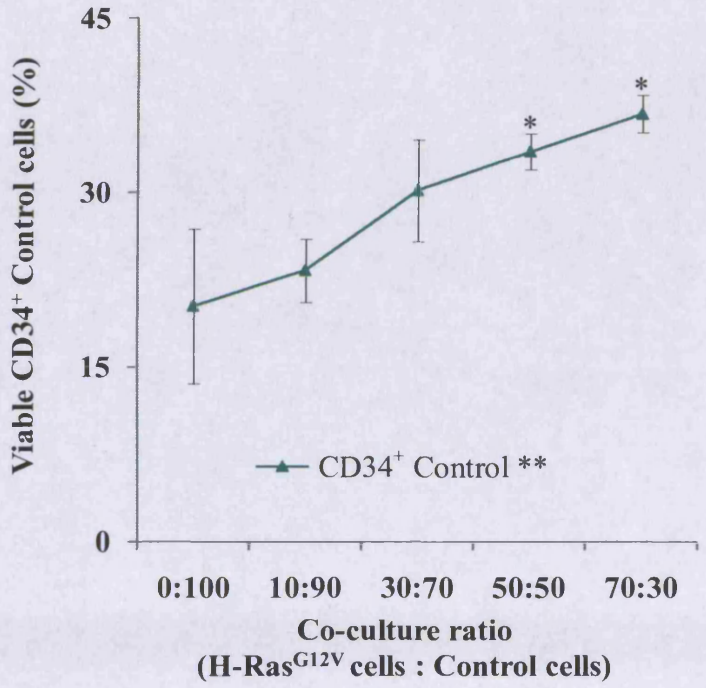

Figure 4.5 Growth factor-independent survival of $CD34^+$ control cells is augmented when co-cultured with $CD34^+$ $H\text{-}Ras^{G12V}$ cells

$CD34^+$ control cells (expressing a GFP reporter gene) were co-cultured without serum or growth factors for 48 h with an increasing proportion of $CD34^+$ $H\text{-}Ras^{G12V}$ cells (expressing a DsRed reporter gene). Data represents mean percentage viable GFP^+ cells recovered from co-culture after 48 h ± 1 S D (n=3). Statistical significance was calculated using by one-way ANOVA using Tukey's Honestly Significant Differences. $^{**}P<0.01$, $^{*}P<0.05$.

Taken together, these data indicate that $CD34^+$ H-Ras^{G12V} cells secrete factors into the extracellular space which can augment growth factor-independent survival in an autocrine manner. Furthermore, these factors appear able to augment growth factor-independent survival of $CD34^+$ control cells in a paracrine manner.

4.3.1.4 Antioxidant treatment improves growth factor-independent survival conferred by H-Ras^{G12V} on human $CD34^+$ haematopoietic cells

The data presented in section 4.3.1.3 indicate that $CD34^+$ H-Ras^{G12V} cells secrete a factor which contributes to their growth factor-independent survival. Exposure to high concentrations of ROS can lead to decreased survival via chemical damage to DNA and lipid membranes (Valko, M. *et al.* 2007), however, it has been demonstrated that NADPH oxidase-derived ROS (specifically H_2O_2) can promote survival of murine retinal cells (Groeger, G. *et al.* 2009). Given that $CD34^+$ H-Ras^{G12V} (and $CD34^+$ N-Ras^{G12D}) cells produce significantly greater amounts of ROS than controls (sections 3.3.2.4 and 3.3.5.1), we investigated whether ROS may be acting as the paracrine factor suggested from section 4.3.1.3. To this end, the survival of $CD34^+$ H-Ras^{G12V} cells was assayed using annexin V and 7-AAD in the presence of several antioxidants and ROS inhibitors.

$CD34^+$ control and $CD34^+$ H-Ras^{G12V} cells were incubated at an optimal cell culture density ($3x10^5$ cells/ml; Figure 4.4) for 48 h without growth factors or serum in the presence of either purified catalase (which destroys H_2O_2), NAC (a precursor of the endogenous antioxidant GSH (Dodd, S. *et al.* 2008)), DPI or apocynin (NOX family oxidase inhibitors). Treatment with DPI and apocynin were well tolerated at low concentrations, with no significant change in viability in $CD34^+$ H-Ras^{G12V} cells or $CD34^+$ control cells. However, the viability of both $CD34^+$ control and $CD34^+$ H-Ras^{G12V} cells was reduced at higher concentrations of DPI, while higher concentrations of apocynin had no significant effects (Figure 4.6A and B). Treatment with catalase or NAC had no significant effects on the survival of $CD34^+$ H-Ras^{G12V} cells or $CD34^+$ control cells, with the exception of a large increase in viability at 75 μM NAC in the control culture. (Figure 4.6C and D).

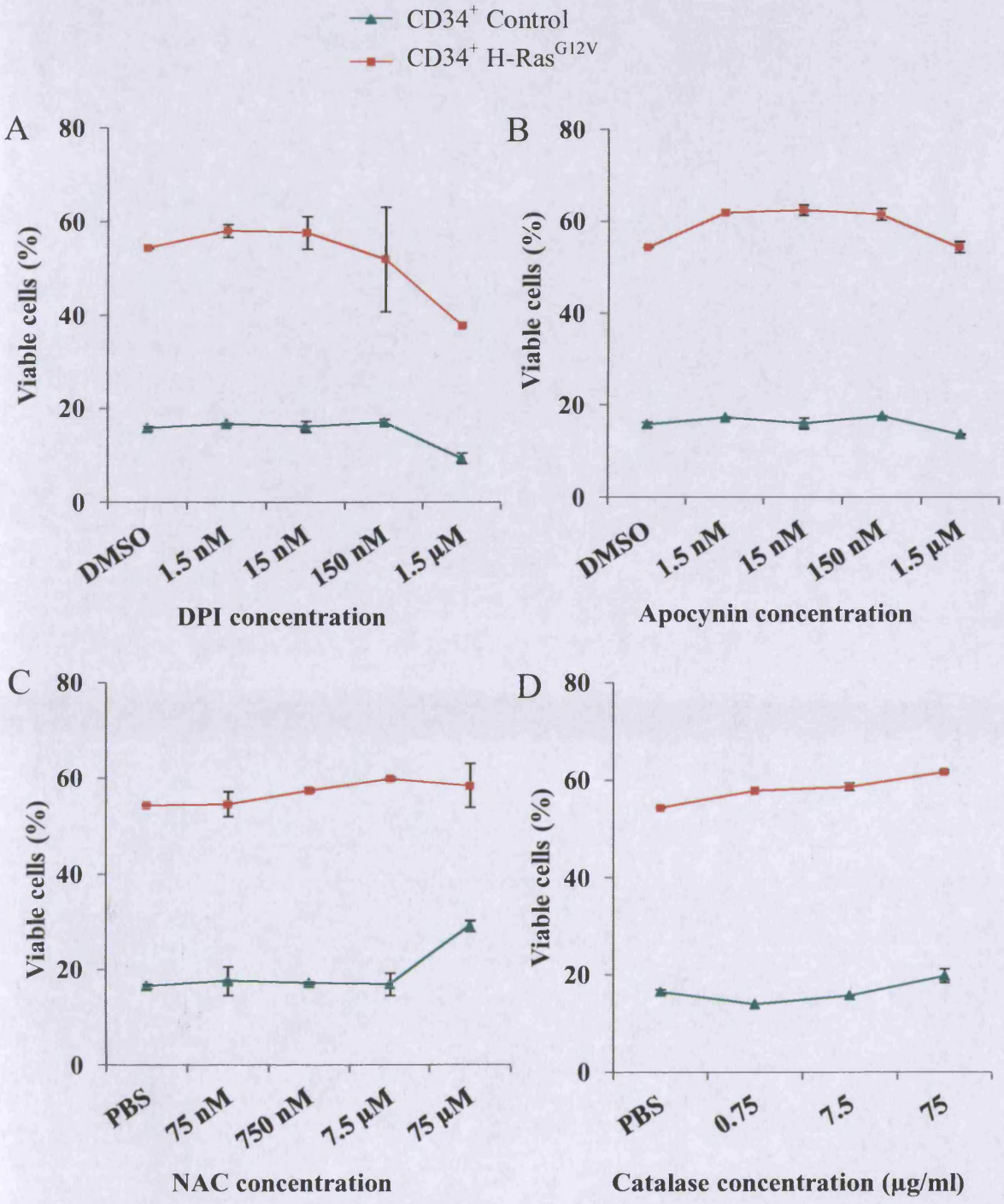

Figure 4.6 The effect of several antioxidants and ROS inhibitors on the survival of transduced CD34$^+$ cells

CD34$^+$ control and CD34$^+$ H-Ras^{G12V} cells were resuspended at an optimal cell culture density ($3x10^5$ cells/ml) deprived of growth factors and serum for 48 h in the presence of **(A)** DPI, **(B)** apocynin, **(C)** NAC or **(D)** catalase. After incubation, remaining cells were labelled with annexin V and 7-AAD and the percentage of viable cells were counted by flow cytometry. Data represents mean ± 1 S D.

These experiments suggested that at optimal culture density (~ $3x10^5$ cells/ml), constitutive ROS production does not significantly influence cell survival, suggesting that ROS were not likely to be the paracrine factor suggested in section 4.3.1.3.

4.3.1.5 H_2O_2 antagonises growth factor-independent survival of human $CD34^+$ haematopoietic cells

Section 4.3.1.4 showed that when $CD34^+$ H-Ras^{G12V} cells were cultured at an optimal cell culture-density ($3x10^5$ cells/ml, determined by data shown in Figure 4.4), antioxidant treatment had no significant effect on cell viability, indicating that ROS do not promote survival in this context. However, it is plausible that ROS may impair cell viability in this system, an effect that may have been masked by performing the experiments at optimal density. Therefore the effect of catalase treatment on $CD34^+$ H-Ras^{G12V} cell viability was investigated again, this time at sub-optimal culture densities (below $1x10^5$ cells/ml, as indicated in Figure 4.4). For comparison, $CD34^+$ control cells were studied under the same conditions.

$CD34^+$ control and $CD34^+$ H-Ras^{G12V} cells were incubated for 48 h without growth factors or serum in the presence of purified catalase at a sub-optimal cell culture density ($0.5x10^5$ cells/ml; Figure 4.4). Figure 4.7A shows that catalase significantly augmented survival of $CD34^+$ H-Ras^{G12V} cells (but not controls) under these conditions ($P<0.05$), suggesting that H_2O_2 production by $CD34^+$ H-Ras^{G12V} cells impaired cell viability in an autocrine manner.

To determine whether H_2O_2 produced by $CD34^+$ H-Ras^{G12V} cells could impair $CD34^+$ control cell viability in a paracrine manner, co-culture experiments were conducted in the presence of purified catalase. These experiments showed that the presence of catalase increased the viability of $CD34^+$ control cells beyond that already observed (Figure 4.7B).

Since H_2O_2 derived from $CD34^+$ H-Ras^{G12V} cells appeared to impair $CD34^+$ control cell viability in a paracrine fashion, this study investigated whether similar concentrations of exogenous H_2O_2 alone could impair viability of normal cells. However, H_2O_2 is unstable in cell culture medium (it is cell permeable and catabolised by intracellular antioxidants), therefore this study used GOX to continuously generate a low level of H_2O_2 throughout the assay. GOX (purified from *A. niger*) generates H_2O_2 by oxidation of β-D-glucose and is a useful long-term source of H_2O_2 generation cell culture. Figure 4.7C i shows that as expected, increased GOX concentration resulted in increased H_2O_2 production. As shown in Figure 4.7C ii, $CD34^+$ control cells exhibited a dose-

dependent decrease in viability in the presence of GOX, but were protected from this effect when 500 μg/ml catalase was also present.

Taken together, these data suggest that ROS (specifically H_2O_2) do not promote growth factor independent survival $CD34^+$ $H\text{-}Ras^{G12V}$ cells, but rather antagonise it in a dose-dependent manner. $CD34^+$ control cells only slightly benefited from antioxidant treatment, which is consistent with their lower ROS production; however, they still exhibited a trend of improved viability at the highest concentrations of NAC and catalase, and showed a dose-dependent decrease in viability in the presence of GOX, further supporting the notion that H_2O_2 hinders survival.

These data also show that H_2O_2 generated by $CD34^+$ $H\text{-}Ras^{G12V}$ cells antagonises the paracrine effects of putative secreted factor(s) on control cells. This study has not pursued investigations into the identity of this paracrine factor(s), however a recent study has shown that human $CD34^+$ cells expressing mutant N-Ras do upregulate mRNA transcripts of several pro-survival factors, including IL-3 and PDGF (Shen, S. *et al.* 2007).

4.3.1.6 $CD34^+$ $H\text{-}Ras^{G12V}$ cells show increased activation of Akt

The data presented in this Chapter thus far shows that $H\text{-}Ras^{G12V}$ promotes growth factor-independent survival of human $CD34^+$ cells. Since Akt activation is closely associated with constitutive Ras signalling in haematopoietic malignancies (Steelman, L.S. *et al.* 2008) this study examined whether altered expression or phosphorylation state of Akt in could explain increased survival observed in $CD34^+$ $H\text{-}Ras^{G12V}$ cells.

Survivin is a member of the inhibitor of apoptosis protein (IAP) family and plays an important role in regulating the survival and cell cycle progression of normal haematopoietic cells (Fukuda, S. and Pelus, L.M. 2004; Fukuda, S. *et al.* 2002), and is over-expressed in a variety of cancers (Sah, N.K. *et al.* 2006). There is also evidence to suggest a link between activation of Akt and subsequent up regulation of Survivin (Fukuda, S. *et al.* 2002). $CD34^+$ control and $CD34^+$ $H\text{-}Ras^{G12V}$ cells were incubated in supplemented serum-replete IMDM without growth factors for 16 h, and Western blot analysis of Survivin and Akt expression was performed.

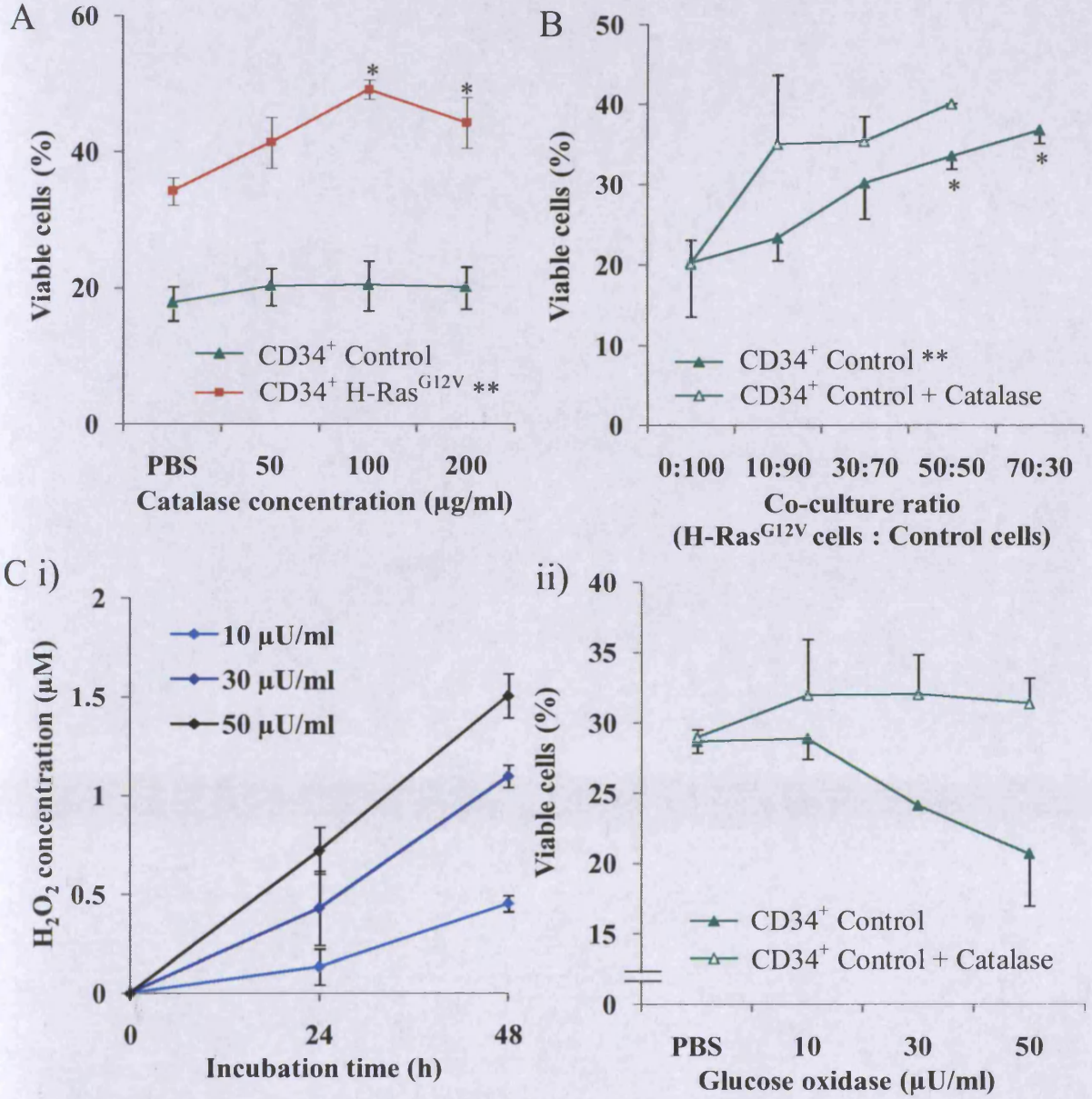

Figure 4.7 The effect of catalase and GOX treatment on the survival of transduced human CD34$^+$ cells

(A) CD34$^+$ control and CD34$^+$ H-Ras^{G12V} cells were resuspended at a sub-optimal cell culture density ($5x10^4$ cells/ml) and were deprived of growth factors and serum for 48 h in the presence of catalase (n=3). **(B)** CD34$^+$ control cells expressing GFP were co-cultured for 48 h with CD34$^+$ H-Ras^{G12V} cells (expressing DsRed) in the absence of growth factors and serum and in the presence of 500 µg/ml catalase (n=3) **(C)** CD34$^+$ control cells were deprived of growth factors and serum for 48 h in the presence of GOX, with or without 500 µg/ml catalase. **i)** H_2O_2 production by GOX during the incubation was measured in cell-free KRPG medium using Amplex Red. 10, 30 and 50 µU/ml GOX generated a final H_2O_2 concentration 0.5, 1.1 and 1.5 µM respectively over 48 h (corresponding to an estimated mean H_2O_2 production rate of 1.5, 3.4 and 5 pmoles/h respectively). **ii)** After 48 h, remaining cells were labelled with annexin V and 7-AAD, and cell viability was analysed by flow cytometry (n=2). Data represents mean ± 1 S D. Statistical significance was calculated using by one-way ANOVA using Tukey's Honestly Significant Differences. *P<0.05, **P<0.01.

This study found no consistent evidence of increased Survivin expression in transduced $CD34^+$ cultures (Figure 4.8A). Similarly there were no detectable differences in expression of total Akt, however, $CD34^+$ H-Ras^{G12V} cells showed phosphorylation of Akt on Serine 473 (suggestive of increased activation of Akt), while $CD34^+$ controls showed little or no detectable phosphorylation on this residue. Finally, $CD34^+$ H-Ras^{G12V} cells which were incubated in the presence of DPI showed no change in Akt phosphorylation compared with vehicle controls, which is consistent with the observation that DPI (and possibly other ROS antagonists) was unable to suppress the survival of these cells (Figure 4.8B).

4.3.2 THE ROLE OF ROS IN PROLIFERATION OF HUMAN $CD34^+$ HAEMATOPOIETIC CELLS

The experiments described in section 4.3.1 used ROS inhibitors and scavengers to demonstrate that ROS up regulation antagonises growth-factor independent survival in $CD34^+$ H-Ras^{G12V} cells. However, it was observed that although antioxidants improved the viability of $CD34^+$ H-Ras^{G12V} cells, they appeared to suppress the total number of viable cells recovered after treatment when compared with $CD34^+$ H-Ras^{G12V} cells treated with vehicle control, suggesting that antioxidants may act to suppress proliferation in this context. These preliminary observations suggested that scavenging of ROS could suppress proliferation; a notion consistent with a study by Sattler *et al.*, which suggested that ROS contribute to haematopoietic growth factor signal transduction (Sattler, M. *et al.* 1999). Therefore, this study investigated whether increased production of ROS played any role in the proliferation of $CD34^+$ H-Ras^{G12V} and $CD34^+$ N-Ras^{G12D} cells.

4.3.2.1 Activated Ras promotes growth factor-independent proliferation of human $CD34^+$ haematopoietic cells

To establish whether activated Ras promotes growth factor-independent proliferation of human $CD34^+$ cells, a modified version of the survival assay protocol (section 4.2.1.3) was used, which was intended to move the emphasis of the assay away from survival towards proliferation.

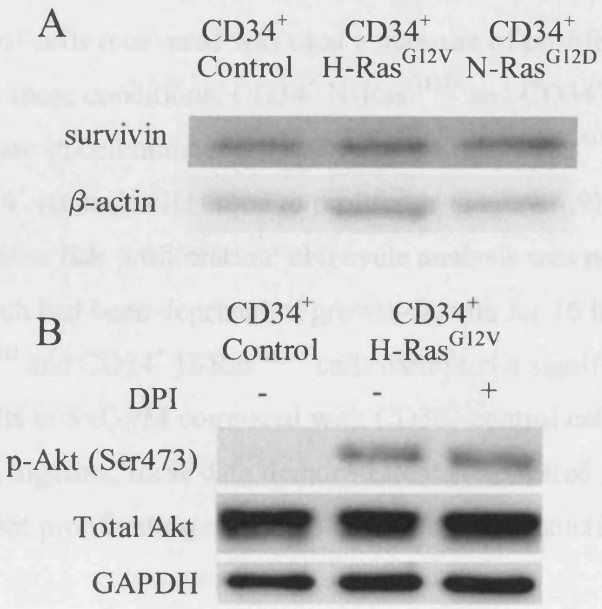

Figure 4.8 Examination of survivin and Akt expression in transduced human CD34$^+$ cells

CD34$^+$ control and CD34$^+$ H-Ras^{G12V} cells were incubated in supplemented IMDM without growth factors at 4x10^5 cells/ml for 16 h at 37°C in a 5% CO_2 humidified atmosphere. Growth-factor withdrawal minimised changes in expression of these proteins induced by growth-factor signalling. Following incubation, 3x10^5 cells were collected by centrifugation and expression of key survival molecules was examined by in whole-cell extracts by Western blot analysis as described in section 2.4.7. **(A)** Protein extracts were probed with anti-survivin antibody (Cell Signaling). 10 ng/ml anti-β-actin (Abcam) was used as a loading control. Representative of 2 independent experiments. **(B)** CD34$^+$ control and CD34$^+$ H-Ras^{G12V} were incubated as in (A), in the presence or absence of 1 μM DPI. Protein extracts were incubated with 10 ng/ml anti-phospho-Akt (Ser473) or 16 ng/ml anti-pan Akt (both from Cell Signaling). 20 ng/ml anti-GAPDH (Santa Cruz) was used as a loading control. Data obtained from one experiment.

$CD34^+$ control, $CD34^+$ N-Ras^{G12D} and $CD34^+$ H-Ras^{G12V} cells ($1x10^4$) were incubated in supplemented, serum-replete IMDM without growth factors for 48 h (as opposed to IMDM without any supplements, serum or growth factors used in survival assays). Under these conditions normal $CD34^+$ cells, showed improved viability, but were unable to proliferate. Following incubation, viable cells were counted by flow cytometry and the number of cells recovered was used a measure of proliferation.

Under these conditions, $CD34^+$ N-Ras^{G12D} and $CD34^+$ H-Ras^{G12V} cells showed a significant increase in cell number (H-Ras^{G12V} 5.2 fold; N-Ras^{G12D} 3.9 fold; $P<0.05$) over 48 h whilst $CD34^+$ control cells failed to proliferate (Figure 4.9). To verify that mutant Ras was promoting *bona fide* proliferation; cell cycle analysis was performed on transduced $CD34^+$ cells which had been deprived of growth-factors for 16 h. As shown in Figure 4.10, $CD34^+$ N-Ras^{G12D} and $CD34^+$ H-Ras^{G12V} cells exhibited a significant 2 fold increase in the proportion of cells in $S+G_2/M$ compared with $CD34^+$ control cells ($P<0.05$).

Taken together, these data demonstrate that activated Ras can promote growth factor-independent proliferation of human $CD34^+$ haematopoietic cells.

4.3.2.2 ROS play a context-dependent role in proliferation of human $CD34^+$ cells

To examine whether the proliferation advantage of $CD34^+$ H-Ras^{G12V} and $CD34^+$ N-Ras^{G12D} cells could be partly due to their increased ROS production (sections 3.3.2.4 and 3.3.5.1), transduced human $CD34^+$ cells were deprived of growth factors for 48 h (as described in section 4.3.2.1) in the presence of either DPI, catalase or NAC. Interestingly, in the presence of these antioxidants, $CD34^+$ H-Ras^{G12V} and $CD34^+$ N-Ras^{G12D} cells exhibited a significant dose-dependent decrease in the number of cells recovered compared with vehicle control ($P<0.05$), while in contrast, $CD34^+$ control cells generally showed an increase in cell numbers under the same conditions (Figure 4.11).

To verify that the decrease in cell numbers observed in $CD34^+$ N-Ras^{G12D} and $CD34^+$ H-Ras^{G12V} cells was not due to reagent toxicity, the viability of cells recovered from ROS scavenger-treated cell cultures was determined using annexin V and 7-AAD. Figure 4.12 shows that the viability of all cultures was either unaffected or improved in the presence of these antioxidants, suggesting that the observed decrease in proliferation was not due to decreased viability. These data suggest that ROS can augment growth factor-independent proliferation of $CD34^+$ cells in the context of mutant Ras. In contrast, ROS appear to have the opposite effect on the proliferation of normal $CD34^+$ cells.

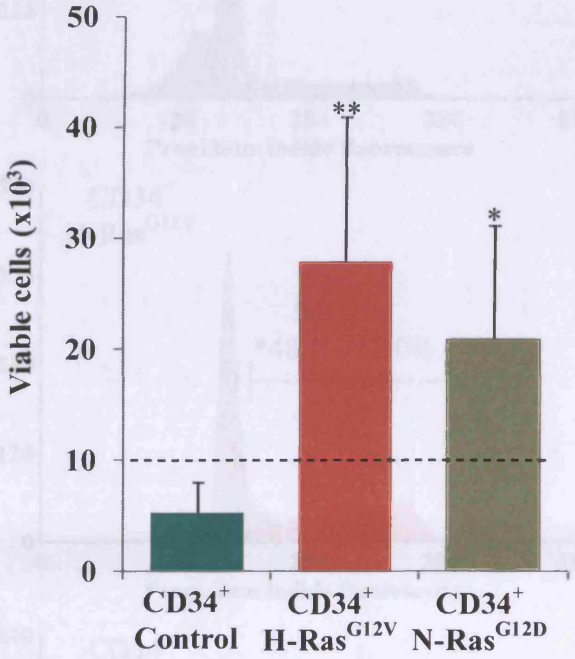

Figure 4.9 Examination of the proliferative capacity of transduced human CD34$^+$ cells in the absence of growth factors

CD34$^+$ control, CD34$^+$ H-Ras^{G12V} and CD34$^+$ N-Ras^{G12D} cells were incubated in serum-replete, supplemented IMDM without growth factors for 48 h, after which viable cells were counted by flow cytometry as described in section 2.6. Dotted line indicates the number of cells at the beginning of the assay. Data represents mean ± 1 S D (n=4). Statistical significance was calculated using the Mann-Whitney Test. *P<0.05, **P<0.01.

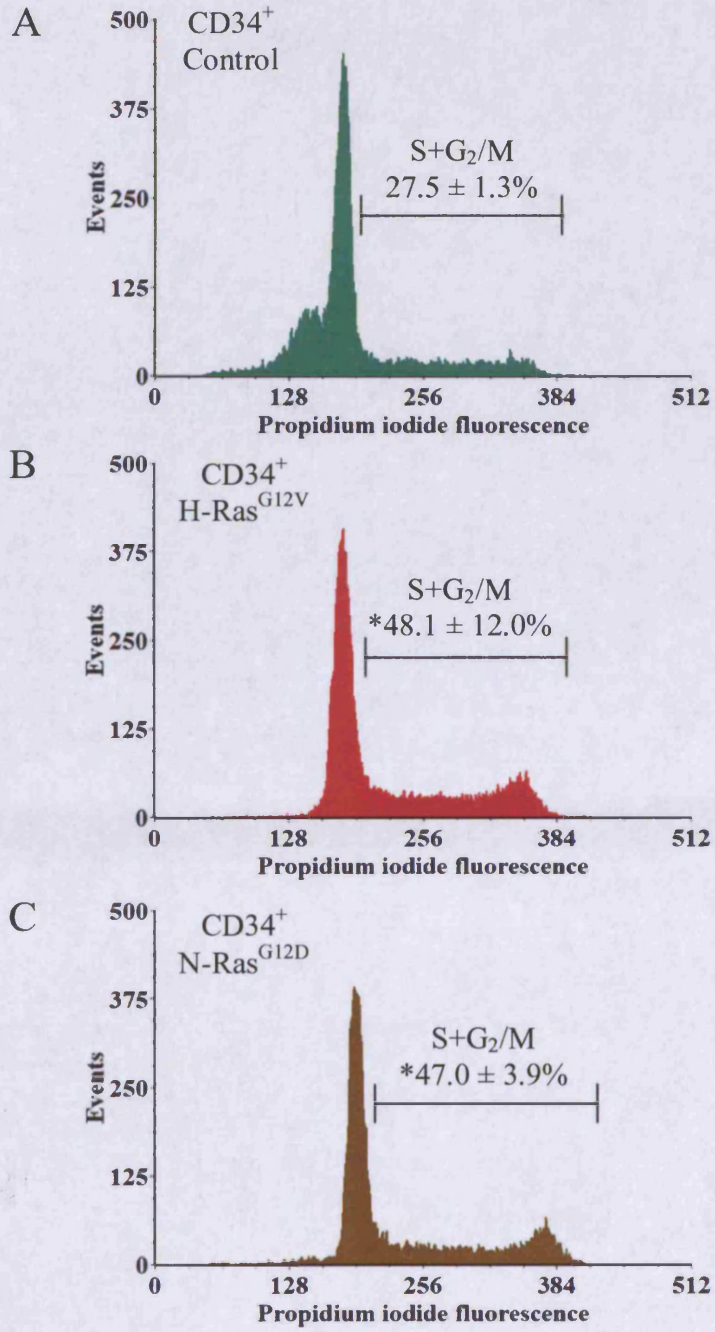

Figure 4.10 Cell cycle analysis of transduced human CD34$^+$ cells

Transduced CD34$^+$ cells were deprived of growth factors for 16 h, after which the cells were fixed and permeablised, and DNA was labelled with 40 µg/ml PI. PI labelled cells were analysed by flow cytometry (section 2.6). Representative flow cytometric histograms obtained from **(A)** CD34$^+$ control, **(B)** CD34$^+$ H-Ras^{G12V} and **(C)** CD34$^+$ N-Ras^{G12D} cells are shown, together with the mean percentage of cells in S+G_2/M ± 1 S D (n=3). Statistical significance was calculated using the Mann-Whitney Test. *P<0.05.

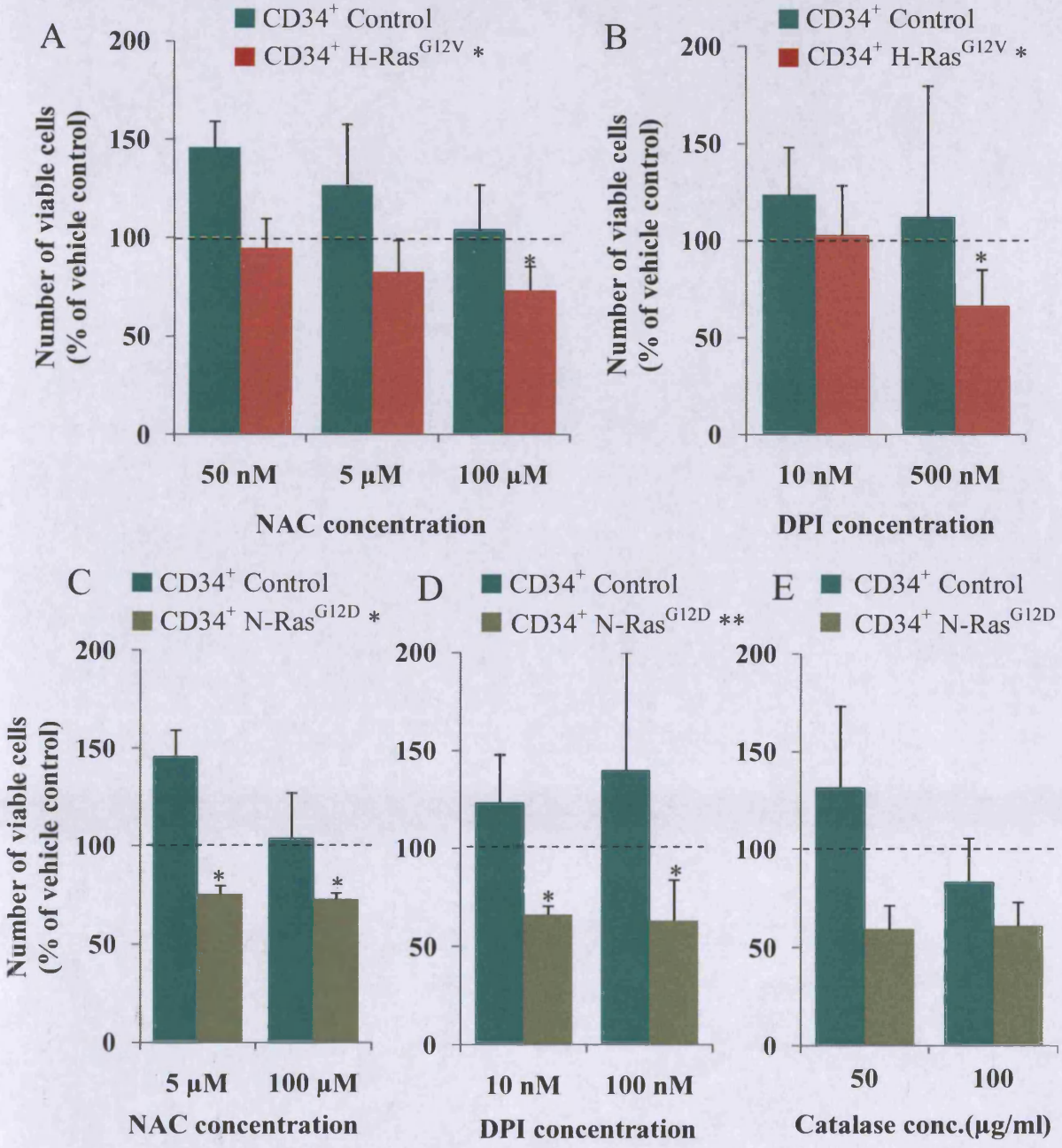

Figure 4.11 The effect of antioxidants and NOX inhibitors on proliferation of transduced human CD34$^+$ cells

CD34$^+$ control, CD34$^+$ H-Ras^{G12V} and CD34$^+$ N-Ras^{G12D} cells were deprived of growth factors for 48 h in the presence of either DPI, NAC or catalase. The number of viable cells recovered from cultures treated with vehicle control was set at 100% (marked with dotted line). CD34$^+$ H-Ras^{G12V} cells and controls were treated with either **(A)** 0.05-100 µM NAC or **(B)** 10-500 nM DPI. CD34$^+$ N-Ras^{G12D} cells and controls were treated with either **(C)** 5-100 µM NAC, **(D)** 10-100 nM DPI or **(E)** 50-100 µg/ml catalase (n=2). Data represents mean plus 1 S D. (n ≥3 unless otherwise stated). Statistical significance was calculated by one-way ANOVA using Tukey's Honestly Significant Differences. *P<0.05; **P<0.01.

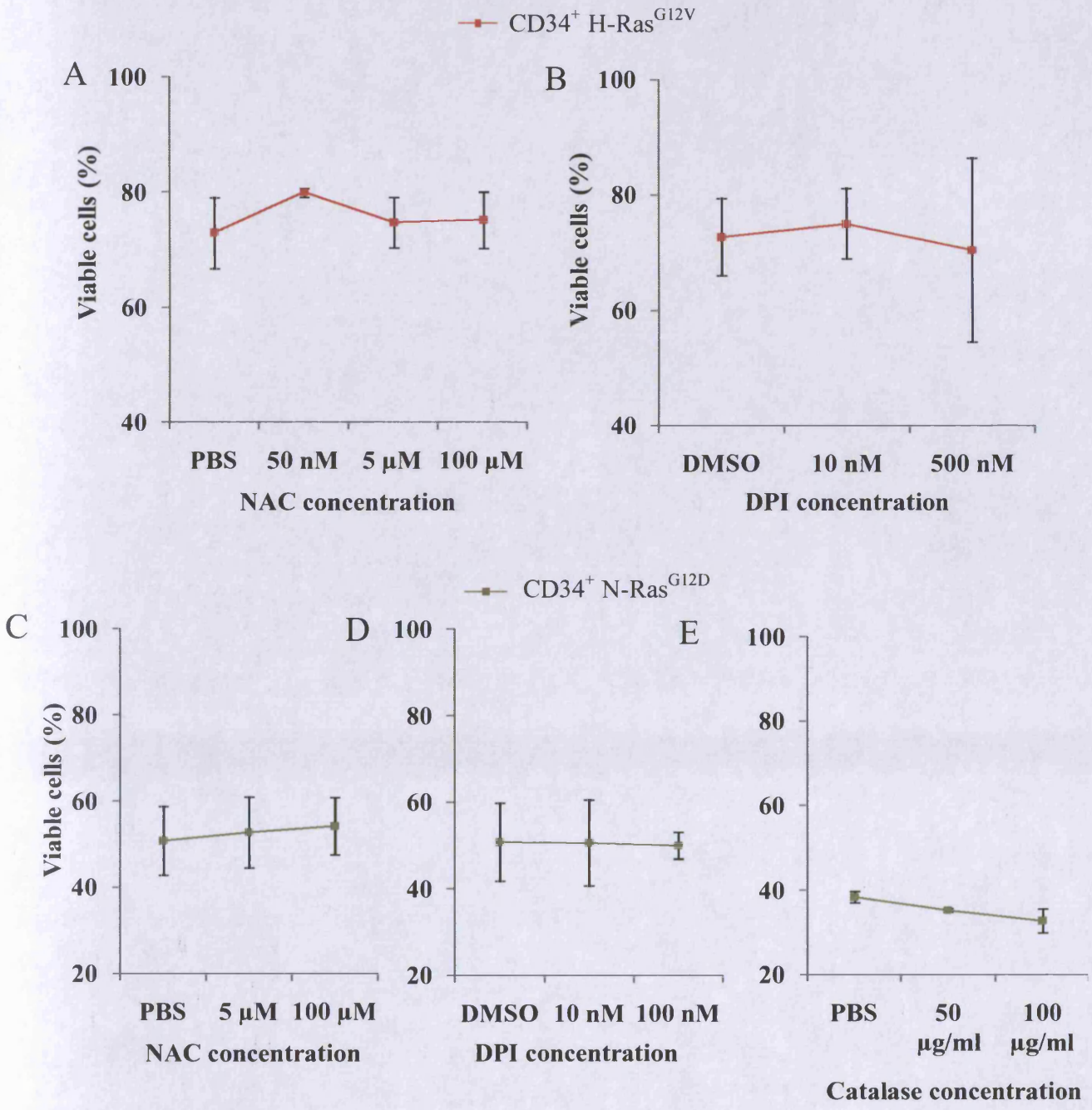

Figure 4.12 The viability of transduced human CD34$^+$ cells treated with antioxidants

To confirm that the suppression of proliferation of CD34$^+$ H-Ras^{G12V} and CD34$^+$ N-Ras^{G12D} cells induced by antioxidants and NOX inhibitors (presented in Figure 4.11) was not due to toxicity, the viability of the recovered cells was examined after treatment at each of the concentrations used. Data represents mean ± 1 S D. Statistical significance was calculated by one-way ANOVA using Tukey's Honestly Significant Differences.

4.3.2.3 *The effect of NOX-inhibition on CD34$^+$ cell frequency, colony-formation capacity and morphology*

Next, this study investigated whether activated Ras influenced the self-renewal capacity of human CD34$^+$ haematopoietic cells, and if so, whether ROS production by these cells was an important factor. Therefore, this study examined the effect of DPI treatment on CD34$^+$ frequency, myeloid lineage colony forming capacity and cellular morphology as a measure of self-renewal capacity (Figure 4.13). CD34$^+$ control and CD34$^+$ N-Ras^{G12D} cells were cultured in serum-replete medium supplemented with cytokines to support myeloid growth (formulation given in section 2.2.3.1) in the presence of DPI or vehicle control for 48 h. Subsequently, the effect of DPI on the number of colony-forming cells (CFC) present was assayed by limiting dilution colony assay, and CD34$^+$ frequency and morphology were examined.

In the absence of DPI, CD34$^+$ control cells and N-Ras^{G12D} cells behaved similarly in all of the assays – both cultures showed similar CD34$^+$ frequency (Figure 4.13A), colony-formation capacity (Figure 4.13B), and morphology (Figure 4.13C). DPI treatment had no significant effect on CD34$^+$ frequency and no noticeable effect on morphology, but did suppress colony formation capacity in a dose-dependent manner. However the effect was similar in both cultures.

These data show Ras does not significantly alter total colony formation capacity or CD34$^+$ progenitor frequency, consistent with previously published data (Pearn, L. *et al.* 2007). In addition, these results suggest that DPI can suppress colony formation capacity, but this effect is independent of Ras expression.

4.3.2.4 *ROS affects the expression of key cell cycle control proteins in human CD34$^+$ haematopoietic cells*

To understand the molecular mechanisms by which ROS augments proliferation, CD34$^+$ control, CD34$^+$ N-Ras^{G12D} and CD34$^+$ H-Ras^{G12V} cells were deprived of growth factors for 16 h as described in section 4.2.2.2 in the presence or absence of DPI, and the expression and phosphorylation state of key cell-cycle regulatory proteins was examined using Western blot analysis.

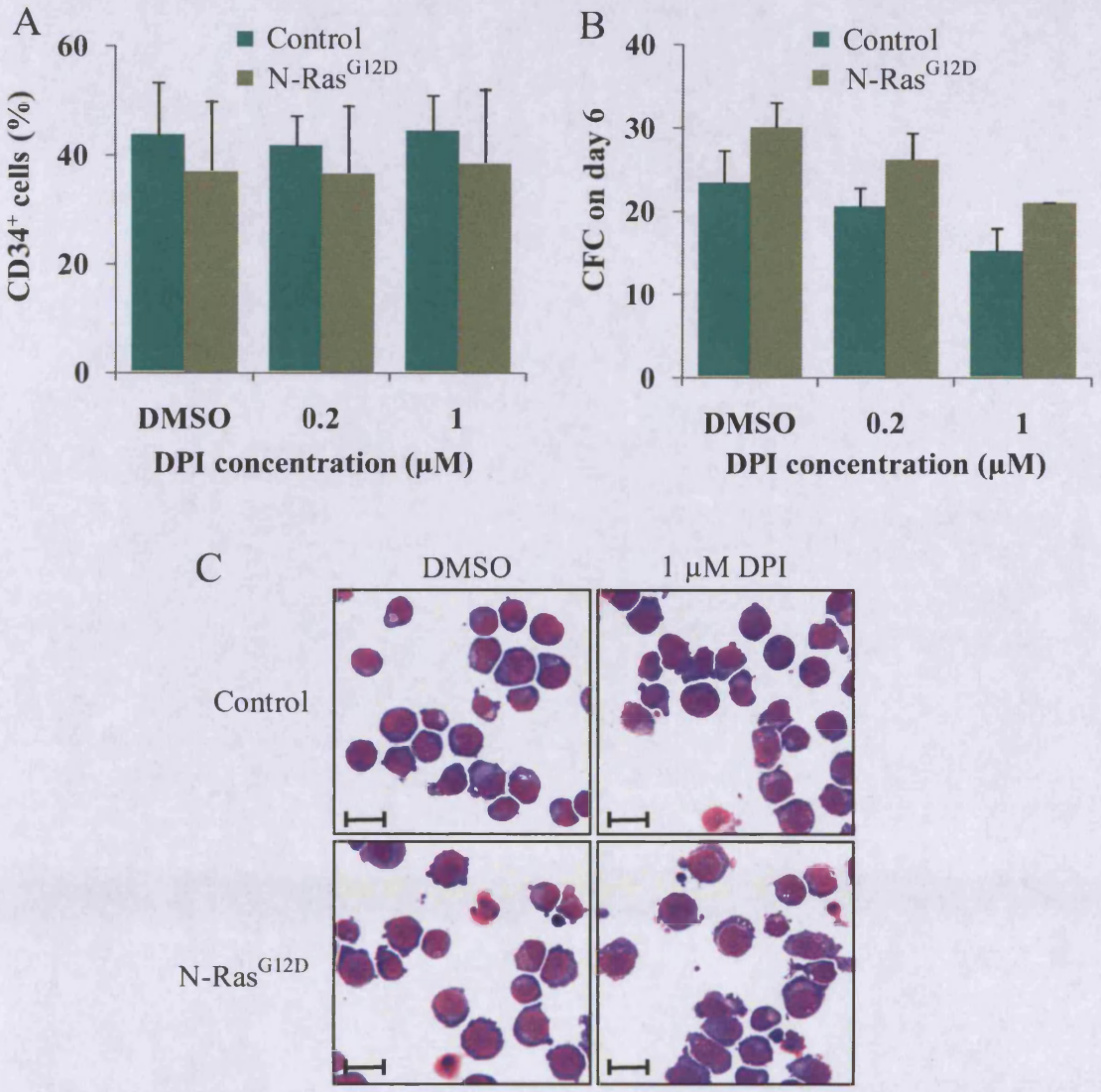

Figure 4.13 Examination of CD34 antigen expression, morphology and colony forming capacity of transduced haematopoietic cells in the presence of DPI

(A) CD34$^+$ N-Ras^{G12D} and controls (day 4) were incubated for 48 h in serum and growth factor-replete medium in the presence of either DPI or vehicle control. After incubation, cells (day 6) were then labelled with 5 μg/ml anti-CD34 antibody conjugated to PE or isotype-matched irrelevant control antibody (both from BD Biosciences) for 30 min at 4°C and analysed by flow cytometry as described in section 2.6. Data represents mean CD34$^+$ cell frequency plus 1 S.D. (n=2). **(B)** The number of colony-forming cells present after incubation as in (A) was examining using a limiting dilution colony assay (methodology described in section 4.2.3). Data represents mean colony forming units scored plus 1 S.D. (n=2). **(C)** Morphological analysis of transduced cells after incubation as in (A). May-Grünwald-Giemsa stain; original magnification is x40 in all panels. Scale bars = 10 μm. CFC = colony-forming cells

Consistent with their pro-proliferative role, N-Ras^{G12D} and H-Ras^{G12V} strongly promoted the expression of D-type cyclins D1 and D3; in each case the influence of H-Ras^{G12V} was greater than N-Ras^{G12D} (a trend also observed in the extent of ROS induction; section 3.4). These oncogenes had no effect on the expression of the cell cycle inhibitor p15^{INK4B}, but did upregulate the cell cycle inhibitor p21^{Cip1}, which seemed contrary to their pro-proliferative effect (Figure 4.14A). Previously, it has been reported that hematopoietic cells express high levels of extra-nuclear p21^{Cip1} (Schepers, H. *et al.* 2003), therefore we examined the sub-cellular location of p21^{Cip1} and found that p21^{Cip1} expression was exclusively cytosolic (Figure 4.14B). Recent reports suggest that cytoplasmic p21^{Cip1} plays an anti-apoptotic role (Zhou, B.P. *et al.* 2001), and this is consistent with the increased survival of CD34^{+} H-Ras^{G12V} cells (described in section 4.3.1.2). The fact that inhibition of ROS production promoted p21^{Cip1} levels indicates that ROS normally act to suppress p21^{Cip1} expression and (in this context) it's associated anti-apoptotic function. This notion is consistent with previously presented data showing that ROS antagonises the survival of CD34^{+} H-Ras^{G12V} cells (section 4.3.1.4).

To assess whether ROS production contributed to the altered expression of cell cycle regulatory proteins, CD34^{+} H-Ras^{G12V} cells were treated with DPI prior to Western blot analysis (Figure 4.14C and D). NOX inhibition resulted in a consistent reduction in cyclin D1 (63% of vehicle control) and cyclin D3 expression (80% of vehicle control), indicating that ROS production cooperated with activated Ras in the induction of these D-type cyclins. Activated Ras also upregulated cyclin dependent kinase 4 (CDK4), a binding partner of D-type cyclins, however, DPI had no effect on the expression of this protein or CDK6 (Figure 4.14C).

Next, we examined the effect of NOX inhibition on the cell cycle inhibitor proteins, p38^{MAPK}, p16^{INK4A}, p15^{INK4B}, p27^{Kip1} and p21^{Cip1} (Figure 4.14D). ROS normally elicit a stress response mediated via phosphorylation of p38^{MAPK}, which leads to the induction of the cell cycle inhibitor, p16^{INK4A} (Dolado, I. *et al.* 2007; Macleod, K.F. 2008). We therefore examined whether this oxidative stress response was operating in CD34^{+} H-Ras^{G12V} cells. H-Ras^{G12V} did promote p38^{MAPK} phosphorylation, but not in the presence of DPI, demonstrating the specificity of ROS in the phosphorylation of p38^{MAPK} (Figure 4.14D). However, this study did not detect expression of p16^{INK4A} in either CD34^{+} control or CD34^{+} H-Ras^{G12V} cells, despite using a primary antibody that was validated using HeLa cell protein extracts (see Appendix 4).

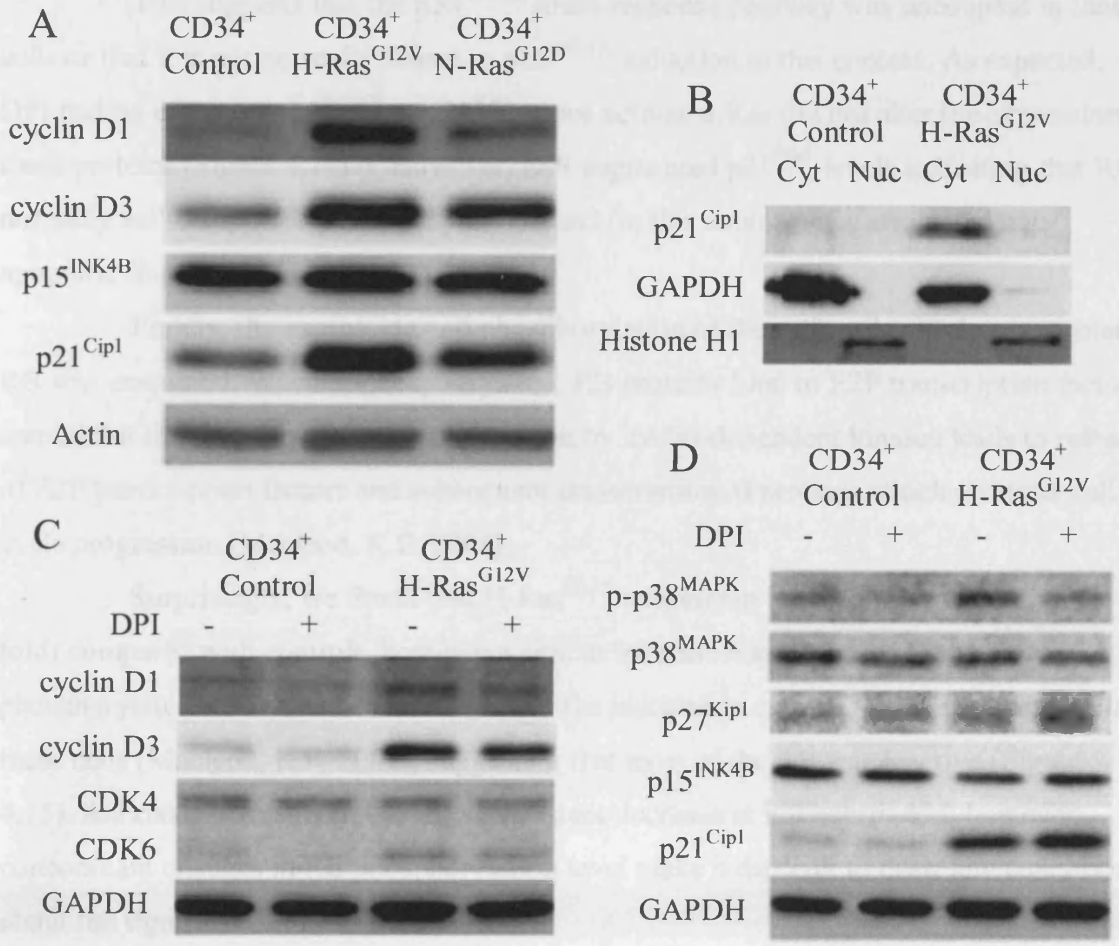

Figure 4.14 Examination of the effect of DPI on the expression and phosphorylation of key cell cycle control proteins

$CD34^+$ control, $CD34^+$ $H\text{-}Ras^{G12V}$ and $CD34^+$ $N\text{-}Ras^{G12D}$ cells were incubated for 16 hours in supplemented IMDM without growth factors, either in the presence or absence of 1μM DPI. Expression and phosphorylation state of key cell cycle regulatory proteins in whole cell or cytosol/nucleus fractionated protein extracts was determined by Western blot analysis as described in section 2.4.7. **(A)** $CD34^+$ control, $CD34^+$ $H\text{-}Ras^{G12V}$ and $CD34^+$ $N\text{-}Ras^{G12D}$ whole cell protein extracts were examined using 143 ng/ml anti-cyclin D1, 280 ng/ml anti-cyclin D3, 7 ng/ml anti-$p15^{INK4B}$ (which sequesters CDK4/6) and 418 ng/ml anti-$p21^{Cip1}$ (which inhibits CDK/Cyclin complexes) demonstrating that $CD34^+$ $N\text{-}Ras^{G12D}$ cells show a similar trend of proteins expression to $CD34^+$ $H\text{-}Ras^{G12V}$ cells. **(B)** $CD34^+$ control and $CD34^+$ $H\text{-}Ras^{G12V}$ cytosol/nuclear fractionated protein extracts were probed with anti-$p21^{Cip1}$ antibody. Extracts were also probed with 20 ng/ml anti-GAPDH (Santa Cruz) and 1 μg/ml anti-Histone H1 (BD Biosciences) and which served as loading controls and as markers of cytosol/nuclear fraction purity. **(C)** Expression of key cell cycle promoter proteins was examined using anti-cyclin D1 and D3 antibodies as in (A), 346 ng/ml anti-CDK6 and 64 ng/ml anti-CDK4. **(D)** Expression and phosphorylation of several cell-cycle inhibitors was examined using 8 ng/ml anti-phospho-$p38^{MAPK}$ (Thr180/182), 2 ng/ml anti-total $p38^{MAPK}$ 213 ng/ml anti-$p27^{Kip1}$ (which has a similar role to $p21^{Cip1}$), $p21^{Cip1}$ and $p15^{INK4B}$ antibodies as in (A). All antibodies were from Cell Signaling unless otherwise stated. 10 ng/ml anti-β-actin (Abcam) and 20 ng/ml anti-GAPDH (Santa Cruz) served as loading controls. Blots are representative of at least 2 independent experiments.

This suggests that the $p38^{MAPK}$ stress-response pathway was uncoupled in these cells or that it is not normally linked to $p16^{INK4A}$ induction in this context. As expected, DPI had no effect on $p15^{INK4B}$ or $p27^{Kip1}$, since activated Ras did not alter the expression of these proteins (Figure 4.14D). However, DPI augmented $p21^{Cip1}$ levels indicating that ROS normally act to suppress $p21^{Cip1}$ expression and (in this context) it's associated anti-apoptotic function (Figure 4.14D).

Finally, the expression and phosphorylation of the cell cycle checkpoint protein, RB was examined. When unphosphorylated, RB proteins bind to E2F transcription factors and inhibit their activity. RB phosphorylation by cyclin-dependent kinases leads to release of E2F transcription factors and subsequent transcription of proteins which promote cell cycle progression (Macleod, K.F. 2008).

Surprisingly, we found that H-Ras^{G12V} expression induced RB expression (3-fold) compared with controls, however a similar increase was observed in the level of phosphorylated RB which is consistent with the increase in cyclin D/CDK4 expression in these cells (Macleod, K.F. 2008), suggesting that most of the RB was inactive (Figure 4.15). Antioxidant treatment caused a consistent decrease in RB expression; however concomitant changes in RB phosphorylation level make it difficult to draw any conclusions about the significance of this observation.

In summary, these data indicate that H-Ras^{G12V} and N-Ras^{G12D} expression promotes expression of the cell cycle promoters cyclin D1 and D3; which provides a possible explanation for their increased proliferative capacity. In addition, these results suggest that ROS production by $CD34^+$ H-Ras^{G12V} cells contributes to activation of CDK4 (via increased expression of both CDK4 binding partners, cyclin D1 and D3); which offers an explanation for the ability of ROS to augment proliferation of these cells. It is likely that a similar mechanism also operates in $CD34^+$ N-Ras^{G12D} cells but was not formally tested herein.

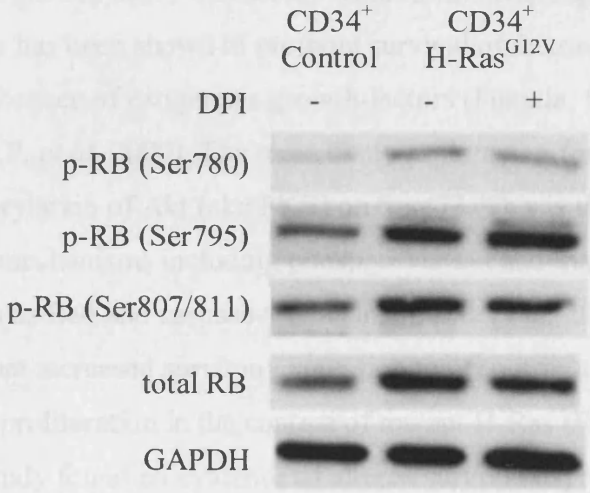

Figure 4.15 Examination of expression and phosphorylation of RB in the presence or absence of DPI

Whole cell protein extracts were prepared from $CD34^+$ control and $CD34^+$ $H\text{-}Ras^{G12V}$ cells (which had been deprived of growth factors as described in Figure 4.14), and the expression and phosphorylation state of the key cell cycle checkpoint regulator Rb was examined. Protein extracts were probed with either 13 ng/ml anti-phospho-Rb (Ser780), 5 ng/ml anti-phospho-Rb (Ser795), 10 ng/ml anti-phospho-Rb (Ser807/811) or 97 ng/ml anti-pan Rb, all purchased from Cell Signaling. 20 ng/ml anti-GAPDH (Santa Cruz) served as a loading control. Blots are representative of 2 independent experiments.

4.4 DISCUSSION

This study investigated the ability of mutant Ras to promote growth factor-independent survival and proliferation in human $CD34^+$ haematopoietic cells, and also investigated the effect of ROS on these phenotypes. This study shows for the first time that mutant Ras alone can promote the survival of primary haematopoietic progenitors under conditions of growth factor and serum withdrawal. This supports previous studies in which activated Ras has been shown to promote survival of factor-dependent haematopoietic cell lines in the absence of exogenous growth-factors (Fukuda, S. and Pelus, L.M. 2004; McGlynn, A.P. *et al.* 2000). The most likely explanation for this increased cell survival was phosphorylation of Akt (aka PKB) on Ser473. This is thought to promote survival via a number of mechanisms including phosphorylation and inactivation of pro-apoptotic proteins such as Bad and caspase-9 (Steelman, L.S. *et al.* 2004). Despite recent evidence suggesting that increased survivin expression may contribute to haematopoietic cell survival and proliferation in the context of mutant H-Ras (Fukuda, S. and Pelus, L.M. 2004), this study found no evidence of altered survivin expression in response to H-Ras^{G12V}. However, Fukuda *et al.* only examined upregulation of survivin in $CD34^+$ cells in response to IL-3 receptor activation, which not only activates Ras but also STAT3 and STAT5 (Steelman, L.S. *et al.* 2004). Since the survival assays herein were performed in the absence of growth factors (and therefore STAT signalling is likely to be minimal) it appears that activated H-Ras alone is insufficient to induce survivin upregulation in $CD34^+$ cells without cooperation with STAT signals. Regardless, in the context of the present study, survivin upregulation is dispensable for the growth factor-independent survival observed in $CD34^+$ H-Ras^{G12V} cells.

This study also showed that survival of $CD34^+$ H-Ras^{G12V} cells was dependent on culture density. Furthermore, $CD34^+$ H-Ras^{G12V} cells could promote the survival of control cells in paracrine fashion. These data strongly suggested the presence of a paracrine pro-survival factor secreted by $CD34^+$ H-Ras^{G12V} cells. Since H_2O_2 has recently been shown to promote cell survival in neuronal cells (Groeger, G. *et al.* 2009), we examined whether ROS may be acting as this putative pro-survival factor. Depletion of ROS using catalase, NAC, DPI or apocynin merely promoted the survival of both $CD34^+$ H-Ras^{G12V} and control cells, demonstrating that ROS production inhibited cell survival in this context. Consistent with the notion that ROS were not supporting survival of these cells, we found that neither DPI nor catalase could suppress Ser473 phosphorylation of Akt. These results were corroborated by experiments showing that GOX-derived H_2O_2 caused a

dose-dependent increase in apoptosis of control cells. As shown in section 3.3.3, production of H_2O_2 can lead to formation of toxic hydroxyl radicals; which offers an explanation for adverse affect of ROS production on survival. Incidentally, it is worth noting that there was a large drop in viability of $CD34^+$ H-Ras^{G12V} cells at high DPI concentrations and to a lesser extent, apocynin (Figure 4.5). This effect was not present with NAC or catalase treatment. Since low concentrations of ROS inhibitors caused a mild augmentation of viability (consistent with data observed with NAC and catalase treatment), the reduced viability observed at high concentrations is likely due to off-target effects DPI and apocynin as opposed to ROS inhibition.

The identity of the paracrine pro-survival factor remains unknown. $CD34^+$ H-Ras^{G12V} cells appear to produce ROS and the pro-survival factor simultaneously and co-culture experiments conducted in presence of catalase demonstrate that ROS antagonises the actions of this factor. Since this putative factor is able to promote survival of control and $CD34^+$ H-Ras^{G12V} cells in a paracrine/autocrine manner (section 4.3.1.3), it must be assumed that both cell types express the appropriate receptor, which may help identification of this factor in future studies. Recently, a gene array analysis of $CD34^+$ N-Ras^{G13C} cells (a Ras mutant with a phenotype similar to N-Ras^{G12D}) has revealed that this Ras mutant strongly promotes the expression of a several cytokine genes, including IL-3 and also both PGDF-A and B and their receptor PDGF-R (Shen, S. *et al.* 2007). Normal $CD34^+$ cells also express the PDGF receptor (Steelman, L.S. *et al.* 2004; Pantazis, P. *et al.* 1990). Though speculative, autocrine signalling through PDGFR could explain the heightened sensitivity of $CD34^+$ H-Ras^{G12V} to culture density, whilst explaining the ability to confer survival on normal cells (which express PDGF receptors). Finally, it should be pointed out that this density-dependent survival could be mediated by more than one factor; or possibly by another mechanism i.e. promotion of survival through cell-to-cell contact (though the low cell culture densities used in co-culture assays suggest that this is less likely). Further insight could be gained by co-culturing transduced $CD34^+$ cells separated by permeable barrier (e.g. a transwell insert) or culturing control cells in the presence of $CD34^+$ H-Ras^{G12V} cell-conditioned medium (which exclude any cell-cell contact mechanism).

In addition to increased cell survival, $CD34^+$ H-Ras^{G12V} and $CD34^+$ N-Ras^{G12D} cells (but not controls) were able to proliferate in serum-replete cultures without the addition of growth factor. Previous studies of the effect of H-Ras^{G12V} on $CD34^+$ cells, including studies at Cardiff, have all made proliferative comparisons in the presence of growth factors (Dorrell, C. *et al.* 2004; Pearn, L. *et al.* 2007) and under these conditions no

proliferative advantage is observed; though N-Ras^{G12D} has previously been shown to promote a growth advantage when CD34$^+$ cells were cultured with the MS5 stromal line (Shen, S.W. *et al.* 2004). Consistent with increased proliferation, H-Ras^{G12V} and N-Ras^{G12D} both induced a strong upregulation of cyclin D1 and D3, which corroborates previous observations (Matsumura, I. *et al.* 2000). H-Ras^{G12V} also upregulated the cyclin D partner kinase, CDK4. CDK6 expression was unaltered. This is in contrast to Lazarov *et al.*, where activated Ras has been reported to suppress expression of CDK4 in primary human epidermal cells (Lazarov, M. *et al.* 2003). Lazarov *et al.* show that suppression of CDK4 in their study is accompanied by characteristics of cellular senescence, namely induction of CDK inhibitor proteins, and growth arrest. In the present study, CD34$^+$ cells expressing mutant Ras appear to avoid Ras-induced senescence (discussed later) and it follows that they may also avoid suppression of CDK4 expression. Forced co-expression of CDK4 and mutant H-Ras results in strong synergy and aggressive melanoma formation (Hacker, E. *et al.* 2006), however, there are no precedents for a similar situation in leukaemias. The cause of differential CDK4 and CDK6 expression in CD34$^+$ H-Ras^{G12V} cells is currently unknown, however recent work suggests that CDK4 and CDK6 are differentially regulated by tyrosine phosphorylation (Bockstaele, L. *et al.* 2009), which is dysregulated in our model (see Chapter 5). An important observation in this study was that ROS production appeared to augment the proliferation advantage of CD34$^+$ H-Ras^{G12V} and CD34$^+$ N-Ras^{G12D} cells, whereas ROS was growth inhibitory for control cells. This suppression of proliferation was not due to changes in cell viability (Figure 4.12). These data also suggest that H-Ras^{G12V} or N-Ras^{G12D} may not only promote ROS production in haematopoietic progenitors, but can simultaneously alter their response to it. Further work is required to understand the mechanism underlying this behaviour.

Increased ROS has previously been associated with increased cell proliferation in several models. For example, mitogenic signalling in Ras-transformed mouse fibroblasts was suppressed with NAC treatment (Irani, K. *et al.* 1997), while overexpression of NOX1 alone (aka Mox1) in mouse fibroblasts resulted in increased ROS production and proliferation (Suh, Y.A. *et al.* 1999). Importantly, NOX inhibitor studies revealed that ROS contributed to both cyclin D1 and D3 expression in this model, providing a molecular explanation for the decreased proliferation observed when CD34$^+$ H-Ras^{G12V} and CD34$^+$ N-Ras^{G12D} cells were treated with antioxidants. Redox regulation of cyclin D1 expression has been previously reported in murine fibroblasts (MEFs). Menon *et al.* demonstrated that treatment of MEFs with the antioxidant NAC caused a decrease in cyclin D1 expression, and suppressed G_1/S progression. The oxidative modification of cysteine residues within

cyclin D1 (presumably affecting cyclin stability) was suggested as a possible mechanism (Menon, S.G. *et al.* 2003). NOX1 derived superoxide has also been reported to delay quiescence in murine lung cells after growth factor withdrawal by promoting cyclin D1 expression. Ranjan *et al.* suggest that ROS mediate this effect by prolonging the activity of AP-1 transcription factors (which regulate cyclin D gene transcription) after factor-withdrawal (Ranjan, P. *et al.* 2006).

There is similar uncertainty about the redox-regulated expression of cyclin D3, about which less is generally known. However one study shows strong upregulation of cyclin D3 in HL60 cells during TPA-induced differentiation, suggesting cyclin D3 may be downstream of PKC signalling (Bartkova, J. *et al.* 1998), which (as discussed in Chapter 5), PKC signalling is highly sensitive to redox regulation. Interestingly, CDK6-cyclin D3 complexes (which presumably exist in $CD34^+$ H-Ras^{G12V} and $CD34^+$ N-Ras^{G12D} cells) are reportedly insensitive to the cyclin-dependent kinase inhibitors $p21^{Cip1}$ and $p27^{Kip1}$ (Lin, J. *et al.* 2001) and this (together with a lack of $p16^{INK4A}$ expression, discussed later) reinforces the pro-proliferative milieu in $CD34^+$ expressing mutant Ras. Further work is needed to fully establish the role of redox-regulated cyclin D expression in the proliferation of these cells. In particular, it not currently known whether ROS regulates cyclin D expression in normal cells. Experiments which examine the ability of exogenous H_2O_2 to induce cyclin D expression in normal cells in the presence of AP-1 and/or PKC inhibitors might prove informative.

Cell cycle progression is also a function of cell cycle inhibitor protein activity. Whilst, $p15^{INK4B}$ and $p27^{Kip1}$ expression was not significantly affected by mutant Ras expression, both mutant Ras isoforms promoted expression of the cell cycle inhibitor $p21^{Cip1}$, which seemed contrary to the proliferative effects of these oncogenes. However, when examined in $CD34^+$ H-Ras^{G12V} cells, $p21^{Cip1}$ appeared to have a purely cytosolic location, making it unlikely that this change was influencing cell cycle progression. Furthermore, constitutive cytoplasmic localisation of $p21^{Cip1}$ (which is likely driven by Akt-dependent phosphorylation of $p21^{Cip1}$ (Zhou, B.P. *et al.* 2001)) is associated with resistance to apoptosis, which is mediated by $p21^{Cip1}$ binding to and suppressing the pro-apoptotic functions of ASK1 (Schepers, H. *et al.* 2003) and procaspase-3 (Suzuki, A. *et al.* 1999). It is worth noting that DPI caused an increase in $p21^{Cip1}$ expression in $CD34^+$ H-Ras^{G12V} cells, suggesting that ROS normally act to suppress $p21^{Cip1}$ (and its anti-apoptotic function) in this context. This may in turn offer further explanation as to why antioxidants promote survival in this study.

Finally, examination of phosphorylation of $p38^{MAPK}$ in $CD34^+$ $H\text{-}Ras^{G12V}$ cells revealed that this was solely a consequence of ROS production by these cells. In other contexts (Dolado, I. *et al.* 2007), $p38^{MAPK}$ activation provokes cell cycle arrest and cellular senescence through induction of $p16^{INK4A}$, but we were unable to demonstrate induction of this cell cycle inhibitor in these cells. Indeed, as alluded to earlier, mutant H-Ras or N-Ras do not induce senescence in primary human $CD34^+$ haematopoietic cells in this study nor in previous studies (Shen, S. *et al.* 2007; Dorrell, C. *et al.* 2004; Pearn, L. *et al.* 2007).

In summary, this chapter presents the first report of growth-factor independent survival of primary $CD34^+$ cells expressing activated Ras alone. These data also highlight the duality of ROS effects on proliferation of these cells, simultaneously promoting proliferation whilst hindering survival. The mechanism whereby ROS augment survival of these is most likely to be via increase cyclin D expression, though how this is accomplished is unknown.

5 The role of ROS in protein phosphorylation in human $CD34^+$ progenitor cells

Chapter 4 demonstrated that endogenous ROS production has significant effects on the proliferation and survival of human $CD34^+$ haematopoietic progenitor cells expressing mutant Ras. Furthermore, the data suggested that ROS promote expression of cyclin D1 and D3, which may explain the ability of ROS to augment proliferation. As discussed in section 1.4.3.2, H_2O_2 has the ability to inactivate phosphatases by reversible oxidation (Rhee, S.G. *et al.* 2000). Since the transcription and stability of cyclin D gene products are governed by phosphorylation events (sections 1.3.3.2 and 1.3.4.3); H_2O_2 may influence cyclin D expression by disturbing the activity of redox-sensitive phosphatases. Phosphatase inactivation results in an increase in phosphorylation of the target proteins, but the consequences of this are likely to be complex. Protein phosphorylation can cause activation, deactivation, increased or decreased stability, and/or sub-cellular targeting. Therefore there is scope for considerable complexity for redox-regulation of signalling in kinase cascades, where ROS-sensitive steps may provide an additional layer of signal regulation (Finkel, T. 2003). The downstream effects of ROS on cell signalling are also likely to be dependent on cell context, the quantity and location of ROS production and the capacity of the cell's intracellular antioxidant pool to cope with ROS generation.

PKC is known to be an important downstream effector of mutant Ras in human haematopoietic cells (together with its important upstream regulator PDK1) (Pearn, L. *et al.* 2007), and may directly promote cyclin D3 expression (Yamamoto, D. *et al.* 2003). Redox regulation of cyclin D3 via PKC and PDK1 could explain redox-sensitive proliferation observed in Chapter 4. Given the importance of PKC and PDK1 signalling in the mutant Ras phenotype, this study investigated whether PKC and PDK1 phosphorylation are sensitive to exogenous and endogenous ROS.

The inhibition of redox-sensitive phosphatases by H_2O_2 is unlikely to be limited to a particular pathway, but instead is likely to affect all pathways where redox-sensitive phosphatases operate. Therefore, studies of 'global' kinase activity (kinomics) are useful for understanding the effects of ROS production on cell signalling as a whole. Kinomic studies are facilitated by the recent development of kinase substrate arrays, which allow the

kinase activity in complex kinase mixture (e.g. whole cell protein extracts) to be assayed. This study used PepChip peptide arrays (described in section 5.2.2) to examine the effects of mutant Ras (and ROS production) on the kinome of human $CD34^+$ haematopoietic cells.

5.1 AIMS

In order to understand whether ROS production driven by activated Ras plays any role in protein phosphorylation in $CD34^+$ haematopoietic cells, this Chapter aims to:

- Examine the effects of exogenous and endogenous ROS on the phosphorylation of the key signalling molecules PKC and PDK1 that mediate dysregulation of haematopoeitic development by activated Ras

- Examine the effects of H-Ras^{G12V} expression on the kinome of $CD34^+$ cells using PepChip peptide arrays, and in particular to look for evidence of changes in the kinome due ROS-mediated phosphatase inhibition

5.2 MATERIALS AND METHODS

5.2.1 INVESTIGATING THE EFFECTS OF ROS ON EXPRESSION AND PHOSPHORYLATION OF PDK1 AND PKC

$CD34^+$ control and $CD34^+$ H-Ras^{G12V} cells were recovered from growth medium by centrifugation at 180 g for 5 min and resuspended at $3x10^5$ cells/ml in HBSS. HBSS with no supplements was used in these experiments to minimise background protein phosphorylation. For experiments investigating the effects of treatment with exogenous H_2O_2, $CD34^+$ control and $CD34^+$ H-Ras^{G12V} cells were treated with 0.1-50 mM H_2O_2 for 0.5-10 min at 37°C in a 5% CO_2 humidified atmosphere. In experiments where the time of exposure to H_2O_2 was studied, the duration of exposure was controlled by addition of 250 pg catalase. For experiments investigating the effects of antioxidant treatment, cells were resuspended in 1 ml HBSS as above in the presence of either catalase, DPI, Tempol (a SOD mimetic) or SOD and incubated for 10 min under same conditions as above.

To determine the effect of cell culture density on PKC and PDK1 phosphorylation, $CD34^+$ control and $CD34^+$ H-Ras^{G12V} cells were resuspended in HBSS as above at $0.1\text{-}0.6x10^6$ cells/ml and incubated at 37°C in a 5% CO_2 humidified atmosphere. Some replicates were incubated in the presence of catalase. After incubation, cells were

collected by centrifugation at 180 g for 5 min. Cell pellets were washed and whole cell protein extracts were prepared for Western blot analysis as described in section 2.4.7.

5.2.2 KINOMIC ANALYSIS USING PEPCHIP PEPTIDE ARRAY TECHNOLOGY

As well as translocations, AML is characterised by frequent abnormalities of protein kinase signalling such as activation of FLT3 and c-KIT which drive protein kinase signalling upstream of Ras (Bowen, D.T. *et al.* 2005; Illmer, T. *et al.* 2005) and PI3 kinase (Doepfner, K.T. *et al.* 2007). Downstream signalling elements are subsequently activated such as Stat5 (Harir, N. *et al.* 2007), MAPK (Milella, M. *et al.* 2001) and Akt (Bardet, V. *et al.* 2006). The high frequency of kinase hyperactivation in AML makes these attractive targets for novel therapeutic approaches. Further, kinases are attractive for drug design since, despite a high degree of conservation in the ATP binding site, highly selective small molecules with favourable pharmaceutical properties can be developed (Zhang, J. *et al.* 2009). Nevertheless, it has been difficult to emulate the success achieved with Imatinib in the treatment of CML when, for instance, targeting FLT3 in AML (Knapper, S. 2007). This may reflect the relative importance of the targeted abnormalities in maintaining survival in these diseases (Knapper, S. *et al.* 2006) or structural factors which reduce their druggability. Parallel to the development of improved kinase inhibitors, efforts have also been made to identify new kinases which could be clinical targets in the treatment of AML. Recently, the development of peptide arrays has enabled the study of global cellular kinase activity. This study employed peptide microarray technology to investigate the kinome of primary human $CD34^+$ haematopoietic cells.

Peptide microarrays consist of an array of peptides mimicking the target motifs of a variety of kinases which are covalently bonded to a glass slide in duplicate (trial chip) or triplicate (full slide) using proprietary surface chemistry. Protein extracts containing cellular kinases are introduced to the array in the presence of γ^{33}P-ATP, allowing phosphorylation of target peptides on the peptide array to be tracked via incorporation of radioactive ^{33}P into the array. Incorporated ^{33}P is detected by exposing the radiolabelled microarray to a phosphor-storage screen, which stores the energy of β-particles emitted during radioactive decay of ^{33}P. When stimulated with photons of the correct wavelength, this stored energy is released from the phosphor-storage screen in the form of photons (critically, these emitted photons have a shorter wavelength than the stimulating photons), which can be measured using conventional photodetectors. The data obtained from peptide arrays can be quantified and analysed using conventional microarray analysis software. The trial PepChip used for this study has 192 different peptides which are substrates for 30

known kinases, however, larger arrays exist with 960 different peptides which are the substrates of a broad range of kinases involved in growth, differentiation and survival (to view peptide details, see Chapter 5 PepChip Data.xls on the accompanying CD).

5.2.2.1 Preparation of protein extracts for kinomic analysis

$CD34^+$ control and $CD34^+$ $H\text{-}Ras^{G12V}$ cells (day 5) were harvested from growth medium by centrifugation at 180g for 5 min. To reduce background kinase activity due to growth factor signalling, all traces of growth factor were removed by washing the cells twice by centrifugation with 25 ml HBSS as described in section 4.2.1.1. Washed cell pellets were resuspended at $4x10^5$ cells/ml in serum-replete, supplemented IMDM without growth factors and incubated for 16 h at 37°C in a 5% CO_2 humidified atmosphere in the presence or absence of 1 μM DPI. After incubation, cells were recovered from the incubation medium by centrifugation at 180 g for 5 min and the cell pellet was washed by centrifugation with 10 ml ice-cold PBS. Washed cells were counted and sedimented again by centrifugation, taking care to remove all supernatant. To encourage cell lysis, cell pellets were flash-frozen in liquid N_2, and allowed to thaw on ice in the presence of 1 μg of DNAse I. Cell pellets were then fully resuspended in 50 μl/$1x10^6$ cells Mammalian Protein Extraction Reagent (MPER; Thermo Fisher Scientific) containing 1 complete mini protease inhibitor tablet (Roche) per 10 ml MPER. Cell suspensions were incubated on ice for 10 min on a rotary shaker (~50 revolutions/min). Detergent-insoluble material was sedimented by centrifugation at 16,000 g for 15 min, and supernatants (protein extracts) were recovered to fresh tubes. Samples of protein extracts were diluted 1 in 40 with dH_2O, and protein concentration in diluted samples was determined using Bradford's assay (section 2.5.2).

5.2.2.2 Radiolabelling of PepChip microarrays and image acquisition

Experiments which involved the use of γ^{33}P-ATP were performed in accordance with standard safety guidelines for handling β-emitters. Geiger-Müller detectors were used frequently throughout all radioactive procedures to monitor radioactive contamination, and disposal of radioactive waste was performed according to university guidelines. Protein extracts (prepared in section 5.2.2.1) were diluted to a protein concentration 1.14 fold greater than the desired final concentration (final concentrations 0.5-1.5 μg/μl) using PepChip dilution buffer (formulation given in section 2.1.2). Diluted extracts (21 μl) were mixed (and consequently diluted 1.14 fold) with 3 μl PepChip activation mix (section

2.1.2) to create the desired final protein concentration. Radioactive extract mixtures were centrifuged at 16,000 g for 15 min to sediment debris, and 18 µl of supernatant was loaded onto a PepChip Trial Array slide (PepScan Presto BV, Lelystad, Netherlands) and covered with a clean 22x40 mm glass coverslip. PepChips were incubated at 37°C for 2 h at saturated humidity, and were then washed once in 30 ml PBS containing 1 % Triton X-100 (PBS-T) to remove the coverslip, followed by washing in 30 ml 2 M NaCl containing 1 % Triton X (NaCl-T). PepChips were washed alternately in 30 ml PBS-T and NaCl-T twice more, followed by 3 rinses in 30 ml purified water and drying with compressed air. Radioactivity on the PepChips was detected by exposure to a phosphor-storage screen (GE Healthcare) for 60 h in a sealed exposure cassette, using a layer of Saran wrap to prevent contamination of the phosphor-screen. Residual and background radiation signals were erased from the phosphor screen prior to use by exposing to a white light source for 16 h. After exposure to the radioactive PepChips, the phosphor-storage screen was scanned using a Typhoon 9400 Variable Mode Imager (GE Healthcare) at a resolution of 50 µm/pixel and digital images were acquired using Typhoon 9400 acquisition software. Images were prepared for quantitation and exported to TIF format using ImageJ (W. Rasband, National Institute of Mental Health, USA).

5.2.2.3 Analysis of PepChip microarray data

Phosphorylation intensity (spot intensity minus background intensity) was quantified using ImageQuant TL (GE Healthcare). Individual background intensity for each spot was determined using ImageQuant's 'spot edge average' algorithm. High intensity spots overshadowing neighbouring spots were removed from the data set. After quantitation, spot intensity data was exported to Microsoft Excel 2007. Bland-Altman analysis was used to determine the positive threshold for spot intensity, and to exclude spot replicates with poor agreement. Briefly, spot intensity data was $\log_{(e)}$-transformed and a Bland-Altman chart was plotted (Bland, J.M. and Altman, D.G. 1986), achieved by plotting the mean $\log_{(e)}$ intensity (x axis) against the difference in $\log_{(e)}$ intensity (y axis) for each pair of replicate spots on the array (Figure 5.5). Interpretation of the graphs is simplified by considering that replicates with good agreement will cluster near the x axis, while replicates with poor agreement will deviate from the x axis. The positive intensity threshold was set as the mean intensity of the lowest (non-zero) pair of replicates on the array. Replicate pairs (spots) where one or both replicates' values fell below this intensity threshold were discarded (in GeneSpring GX, discarded replicates were called as 'absent'; those that remained were called as 'present'). Raw intensity data from replicates which

were not excluded were analysed in GeneSpring GX v10.2 (Agilent Technologies, Stockport, UK). Raw intensity data were $log_{(2)}$-transformed (to de-skew the data) and quantile-normalised (median intensity value set as zero) prior to analysis. Peptide array data generated from each sample group ($CD34^+$ control cells, $CD34^+$ H-Ras^{G12V} cells or $CD34^+$ H-Ras^{G12V} cells treated with DPI) were compared using GeneSpring GX. Unsupervised and supervised hierarchical clustering was performed on non-averaged sample data. Statistical calculations were performed using the averaged data from each group. When comparing the two groups, peptides which showed average phosphorylation intensity difference of >2 fold were selected for further study. Significant differences were calculated in GeneSpring GX using an unpaired T-test.

5.3 RESULTS

5.3.1 THE EFFECT OF H_2O_2 OR ANTIOXIDANTS ON PKC AND PDK1 PHOSPHORYLATION IN HUMAN $CD34^+$ HAEMATOPOIETIC CELLS

PKC and PDK1 are important signalling molecules in the context of human leukaemia (Pearn, L. *et al.* 2007). PDK1 activity is also associated with increased survival via activation of Akt (Introduction section 1.3.3.2 and Results section 4.2.1.3) whilst PKC can is closely associated with Phox activation (section 1.4.2.1) and can also promote cyclin D3 expression (Yamamoto, D. *et al.* 2003). H_2O_2 can oxidise and reversibly inactivate cellular phosphatases, which disturbs the dynamic equilibrium between these phosphatases and their opposing kinases, resulting in a net increase in phosphorylation. To determine whether H_2O_2 could have this effect on phosphorylation of PKC and PDK1 in normal $CD34^+$ cells, $CD34^+$ control cells were treated with H_2O_2 in the absence of growth factors (to reduce background protein phosphorylation), and the effects on PKC and PDK1 phosphorylation was determined by Western blot analysis. PKC phosphorylation on Ser660 was monitored using anti-pan phospho-Ser660 PKC antibody. In the case of PDK1, the anti-PDK1 antibody used herein recognised an unphosphorylated epitope, however, using this antibody it was possible to discriminate several PDK1 protein bands which correspond to differentially phosphorylated forms of the protein (Scheid, M.P. *et al.* 2005) (Figure 5.1A). Incubation of these cells with H_2O_2 for 10 min was sufficient to induce a dose dependent increase in PKC and PDK1 phosphorylation (Figure 5.1A). Interestingly, H_2O_2-treated $CD34^+$ control cells exhibited a PKC and PDK1 phosphorylation profile which appeared similar to untreated $CD34^+$ H-Ras^{G12V} cells. A closer examination of the electrophoretic shift of the 4 main mobility forms of PDK1 visible in $CD34^+$ control cells revealed that the changes due to H_2O_2 treatment were complex, but were consistent with a dose-dependent enrichment of the slowest-migrating PDK1 mobility form consistent with increased phosphorylation.

To establish the time-span over which H_2O_2 promoted PKC and PDK1 phosphorylation, H_2O_2-exposure was terminated at a series of time points (30 s to 8 min) by the addition of catalase. Figure 5.1B shows that promotion of phosphorylation of PKC and PDK1 in $CD34^+$ control cells occurred within 30 s of exposure to H_2O_2, and showed a time-dependent increase up to 8 min. In addition, H_2O_2-treated cells that were allowed to recover from H_2O_2 treatment in the presence of catalase for 45 min showed reduced PKC phosphorylation suggesting that this phosphorylation state was reversible.

The previous results showed that H_2O_2 treatment caused control cells to adopt a similar pattern of PKC and PDK1 phosphorylation to untreated $CD34^+$ H-Ras^{G12V} cells. To establish whether production of endogenous ROS by $CD34^+$ H-Ras^{G12V} cells contributed to their high levels of PKC and PDK1 phosphorylation, $CD34^+$ H-Ras^{G12V} cells were treated for 60 min with either DPI, catalase or Tempol. As shown in Figure 5.2, antioxidant treatment caused a reduction in phosphorylated PKC; and surprisingly appeared to promote the degradation of PDK1 (see Discussion).

Taken together, these results suggest that exogenous high-level H_2O_2 can induce rapid phosphorylation of PKC and PDK1 in a dose and time-dependent manner.

5.3.2 H_2O_2 IS RESPONSIBLE FOR CELL-CULTURE-DENSITY DEPENDENT INCREASES IN PHOSPHORYLATION OF PKC

Given that $CD34^+$ H-Ras^{G12V} cells generate H_2O_2 (section 3.3.5.1), the concentration of H_2O_2 would be expected to be dependent on the density of the cell culture. Hence, it would be predicted that H_2O_2 mediated phosphorylation of PKC and PDK1 signalling molecules will be dependent on the cell density. $CD34^+$ control and $CD34^+$ H-Ras^{G12V} cells were incubated in the absence of growth factors and the effect of varying the cell-culture density on PKC and PDK1 phosphorylation was examined (Figure 5.3).

Cell-density had no overt effect on PKC phosphorylation in $CD34^+$ control cells, while PKC phosphorylation in $CD34^+$ H-Ras^{G12V} cells increased in a cell-density dependent manner. Catalase treatment suppressed the density-dependent phosphorylation of PKC, but was unable to reduce phosphorylation back to control levels. In contrast, PDK1 remained hypophosphorylated in controls (even at high density), whilst PDK1 was consistently hyperphosphorylated in $CD34^+$ H-Ras^{G12V} cells, even in the presence of catalase.

These results extend the conclusions of the previous section suggesting that endogenously generated H_2O_2 can induce phosphorylation of PKC in $CD34^+$ control and $CD34^+$ H-Ras^{G12V} cells, but that the endogenous hyperphosphorylation of PDK1 may arise from alternative mechanisms other than ROS.

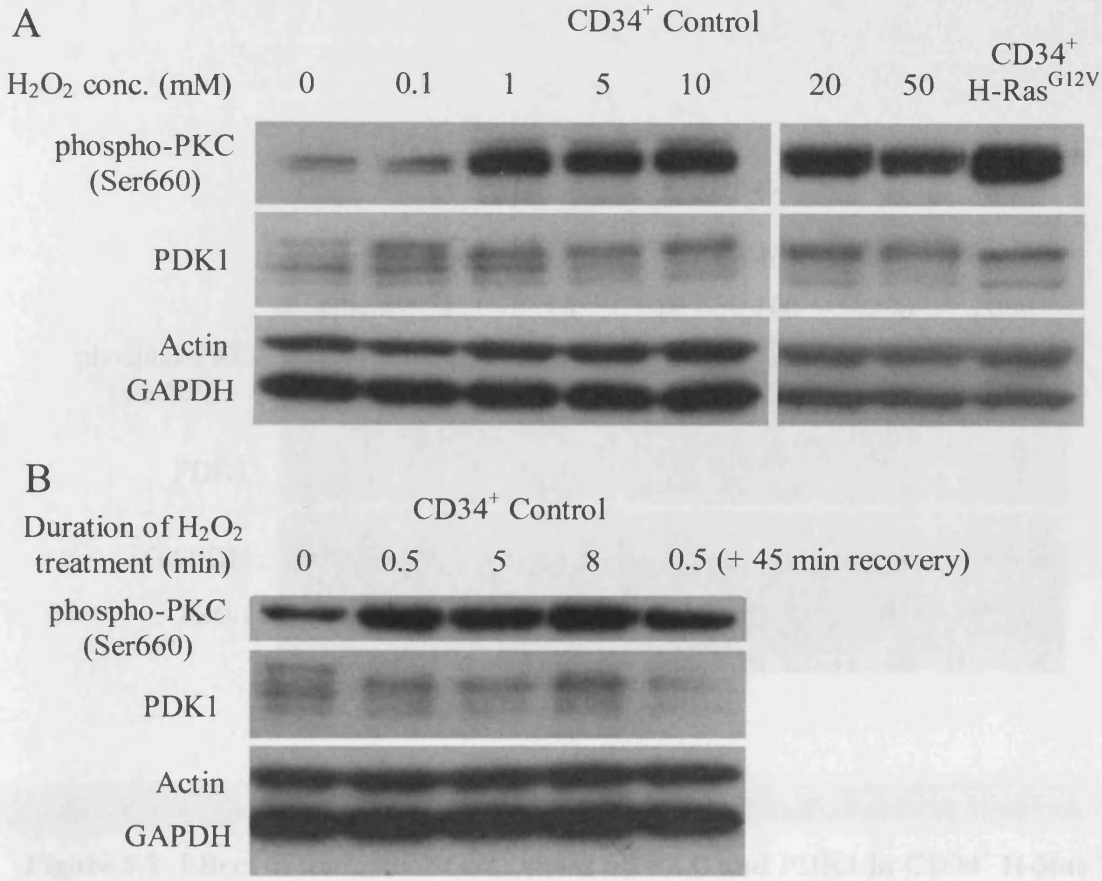

Figure 5.1 Effect of exogenous H_2O_2 on PKC and PDK1 in control cells

(A) $CD34^+$ control cells were incubated in HBSS with 0-50 mM H_2O_2 for 10 minutes at 37°C in a 5% CO_2 atmosphere. Protein extracts from these cells and untreated $CD34^+$ H-Ras^{G12V} cells were prepared and Western blot analysis was performed as described in section 2.4.7. Representative of 3 independent experiments. **(B)** $CD34^+$ control cells were treated with 1 mM H_2O_2 for 0.5-8 minutes at 37°C in a 5% CO_2 atmosphere. Untreated cells were included as a negative control. The reaction was terminated at the stated timepoint by addition of catalase prior to preparation of protein extracts and Western blot analysis. One sample was incubated for 45 min following catalase addition to allow recovery. In both cases, Western blots were probed with 2.9 ng/ml pan-phospho PKC (Ser660) antibody (Cell Signaling) and 125 ng/ml anti-total PDK1 antibody (mouse monoclonal; clone 5; BD Biosciences). 10 ng/ml anti-β-actin and 20 ng/ml anti-GAPDH antibodies were used as loading controls.

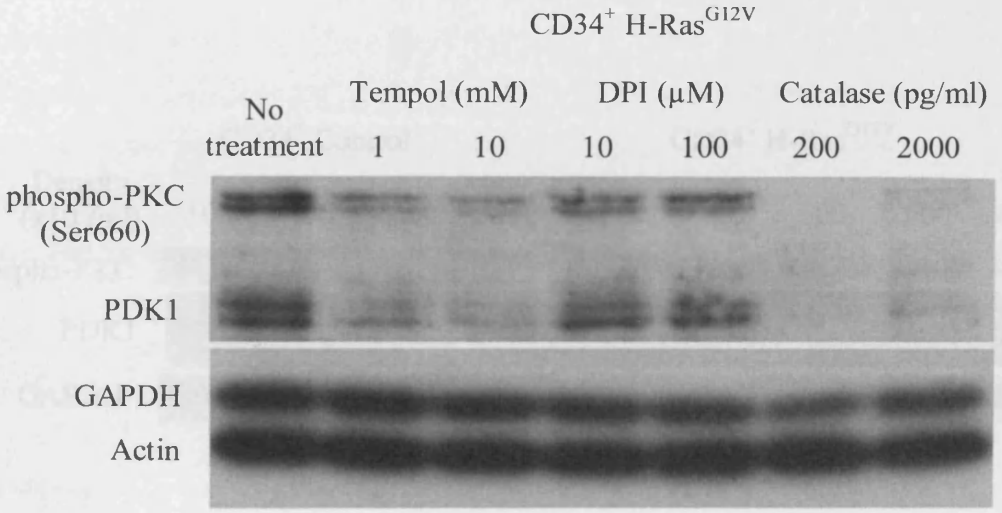

Figure 5.2 Effect of antioxidant treatment on PKC and PDK1 in CD34$^+$ H-Ras^{G12V} cells

CD34$^+$ H-Ras^{G12V} cells (day 7) were treated for 60 minutes at 37°C with 1-10mM Tempol, (a potent SOD mimetic), 10-100μM DPI (a NOX inhibitor) or catalase (which catabolises H_2O_2). Protein extracts from these cells and untreated CD34$^+$ H-Ras^{G12V} cells were prepared and Western blot analysis was performed as described in section 2.4.7, and blots were probed with anti-pan-phospho PKC (Ser660) antibody (Cell Signaling) anti-total PDK1 as described in Figure 5.1.

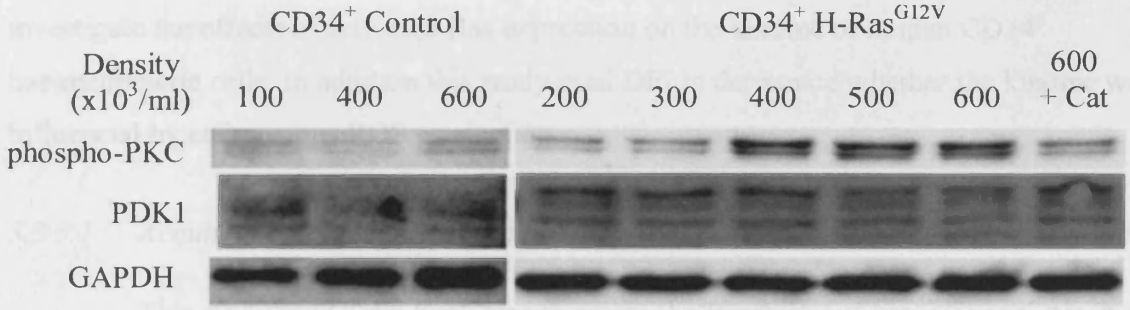

Figure 5.3 Effect of cell culture density on PKC and PDK1 phosphorylation in transduced CD34$^+$ cells

CD34$^+$ control and CD34$^+$ H-Ras^{G12V} cells were incubated at 1-6x10^5 cells/ml in HBSS for 60 min at 37°C in a 5% CO_2 atmosphere. In addition, one sample of CD34$^+$ H-Ras^{G12V} cells was incubated at 6x10^5 cell/ml in the presence of catalase. Protein extracts of these cells were prepared and Western blot analysis was perfromed as described in section 2.4.7. Western blots were probed with anti-pan-phospho-PKC, anti-PDK1 and anti-GAPDH antibodies as in Figure 5.1. Representative of 2 experiments.

5.3.3 KINOMIC ANALYSIS OF TRANSDUCED HUMAN $CD34^+$ HAEMATOPOIETIC CELLS EXPRESSING H-RAS^{G12V}

Endogenous H_2O_2 (e.g. NOX-derived H_2O_2) and exogenous H_2O_2 can promote protein phosphorylation in human haematopoietic $CD34^+$ cells (sections 5.3.1 and 5.3.2), and given that H_2O_2 is a freely diffusible molecule, it has the potential to influence protein phosphorylation throughout the entire cell. PepChip peptide array technology enables examination of the kinome as a whole; therefore this study used this technique to investigate the effects of activated Ras expression on the kinome of human $CD34^+$ haematopoietic cells. In addition this study used DPI to determine whether the kinome was influenced by endogenous ROS production.

5.3.3.1 Acquisition of images from radiolabelled PepChips and Bland-Altman analysis

This study used Trial PepChips to assess the feasibility of kinomic analysis in human $CD34^+$ haematopoietic cells. Figure 5.4A shows the Trial peptide array layout with a positional grid which was used to identify 192 individual peptides on the array. In order to quantify the intensity of each spot and relate this to target peptide expression, an image of the PepChip was acquired using a storage phosphor-screen and scanner system. An example of the peptide array radiograph is shown in Figure 5.4A. After spot intensities had been quantified using ImageQuant TL, data were uploaded into GeneSpring GX v10.2 software for analysis.

Prior to data analysis, array data were $\log_{(2)}$-transformed to reduce artefacts due to areas of low or high intensity. Subsequently, the raw sample dataset was quantile-normalised and displayed as a box plot. This approach confirmed that each sample showed a similar range of signal intensities (equal in size and shape), that there was no evidence of signal saturation and that there were no significant differences between the 9 arrays (Figure 5.4B). Prior to statistical analysis, the raw data were refined using Bland-Altman analysis. Peptides which failed Bland-Altman analysis were called as 'absent' and those that remained were called 'present'. The exclusion stringency was set such that any peptide that was called absent in 5 or more out of the total of 9 samples was excluded from the analysis. Out of 192 peptides on the array, 132 peptides met this criterion. Figure 5.5 shows an example of a Bland-Altman plot generated from $CD34^+$ control cell samples.

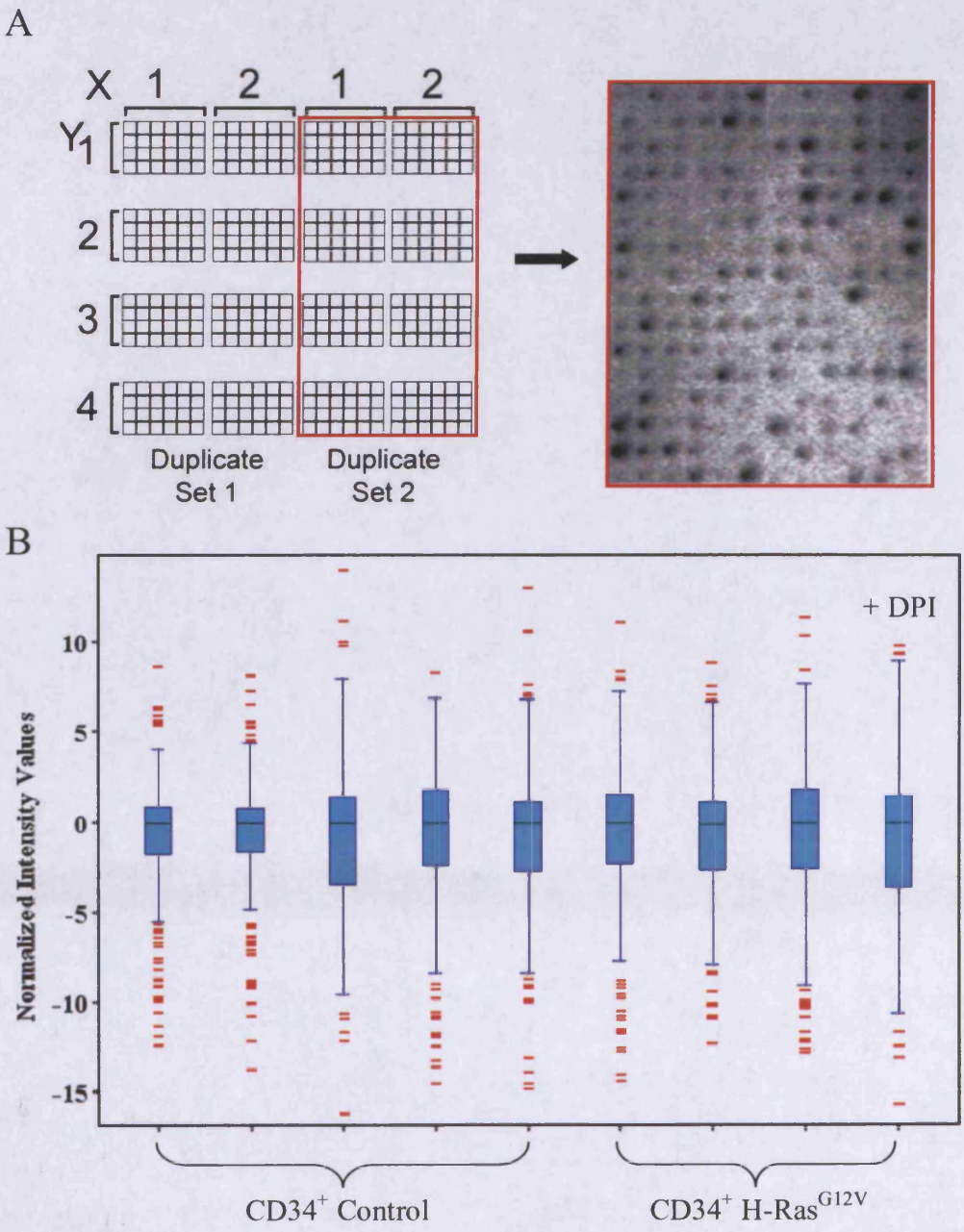

Figure 5.4 Quality control of PepChip peptide array data

(A) Peptide array layout diagram showing positional grid used to identify individual peptides on the array. An example of the radiograph obtained from one peptide array from a typical PepChip is shown. Spot intensity on radiographs was quantified using ImageQuant TL (GE Healthcare), and uploaded into GeneSpring GX for analysis. **(B)** Box-whisker plot representing the whole data set (9 peptide arrays). Samples were $\log_{(2)}$-transformed and quantile normalised prior to generation of box-whisker plot in GeneSpring GX.

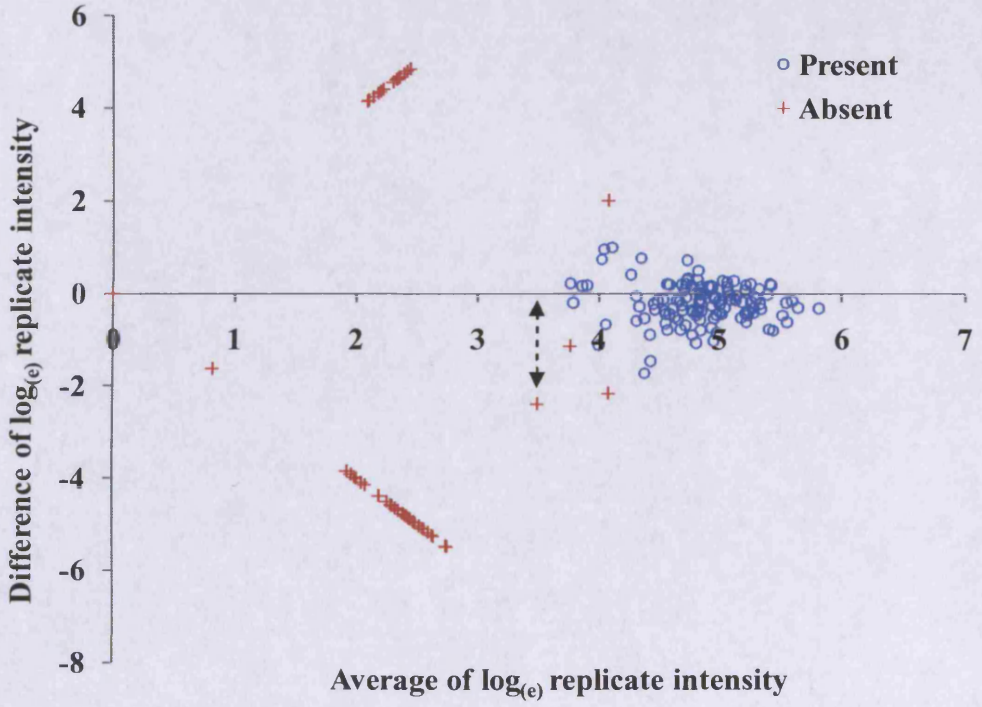

Figure 5.5 Exclusion of replicate spots with poor agreement and determination of positive intensity threshold using Bland-Altman analysis

An example of a typical Bland-Altman plot generated from the sample data is shown. For each sample in the dataset, the intensity data were $\log_{(e)}$-transformed and mean replicate intensity (x axis) was plotted against the difference in replicate intensity (y axis) for each replicate pair. The threshold for positivity was set as the x axis value corresponding to the trailing datapoint in the x axis cluster (the relevant datapoint in this example dataset is marked with an arrow). Replicates where one or both replicates $\log_{(e)}$ intensity values fell below this threshold were excluded and called as 'absent' (red crosses). The remaining datapoints were called as 'present'. These present/absent calls were applied to the raw intensity data, which was then uploaded into GeneSpring GX for further analysis. Peptides which were called absent in 5 or more samples were excluded from the analysis. 132 out of 192 peptides met this criterion.

5.3.3.2 *Comparison of kinomic profiles of CD34$^+$ control and CD34$^+$ H-Ras^{G12V} cells*

In order to detect differences between the kinome of control CD34$^+$ haematopoietic cells and those expressing H-Ras^{G12V}, array signal-intensity data from all 9 PepChips were analysed using GeneSpring GX v10.2. A kinomic profile plot was generated summarising the averaged signal intensities of the 132 peptides remaining after Bland-Altman analysis (Figure 5.6); and this plot highlighted a number of differences in the peptide signal intensities between the two groups. To assess whether H-Ras^{G12V} expression caused any reproducible differences in the kinome of human CD34$^+$ haematopoietic cells, unsupervised hierarchical clustering was performed on the raw dataset. The resulting dendrogram showed that the CD34$^+$ H-Ras^{G12V} kinome profiles (with or without DPI treatment) segregated into a distinct cluster from that of CD34$^+$ control profiles (Figure 5.7). Taken together, these data suggest that when expressed in CD34$^+$ cells, H-Ras^{G12V} is associated with a distinct kinomic profile compared with controls.

In order to determine which of the peptides showed significant changes in phosphorylation when comparing CD34$^+$ H-Ras^{G12V} cells and controls, peptides which showed a 2 fold or greater change in phosphorylation between the two groups were selected for statistical analysis. Data generated from CD34$^+$ H-Ras^{G12V} cells treated with DPI were not included in the statistical analysis, since there was only a single sample for this condition (this data is discussed in section 5.3.3.3). There were 74 peptides which showed a >2-fold change in phosphorylation in the presence of H-Ras^{G12V}, and of these, 7 peptides satisfied the p-value cut-off of 0.05.

This data is summarised as a volcano plot in Figure 5.8A. Of the 7 identified peptides, 3 were increased in phosphorylation in H-Ras^{G12V} cells, while the remaining 4 showed decreased phosphorylation in H-Ras^{G12V} cells (in Figure 5.8B). Five out of 7 of these peptides were substrates for either PKC (2 peptides) or PKA (3 peptides), both members of the AGC protein kinase family, which are regulated by PDK1 (Mora, A. *et al.* 2004). However, there was disagreement as to whether the activity of these proteins was upregulated or downregulated; one of the PKC substrates showed increased phosphorylation, while the other showed decreased phosphorylation. A similar conflict was observed with PKA, one PKA substrate showed increased phosphorylation while the remaining 2 PKA substrates showed decreased phosphorylation (Figure 5.8B).

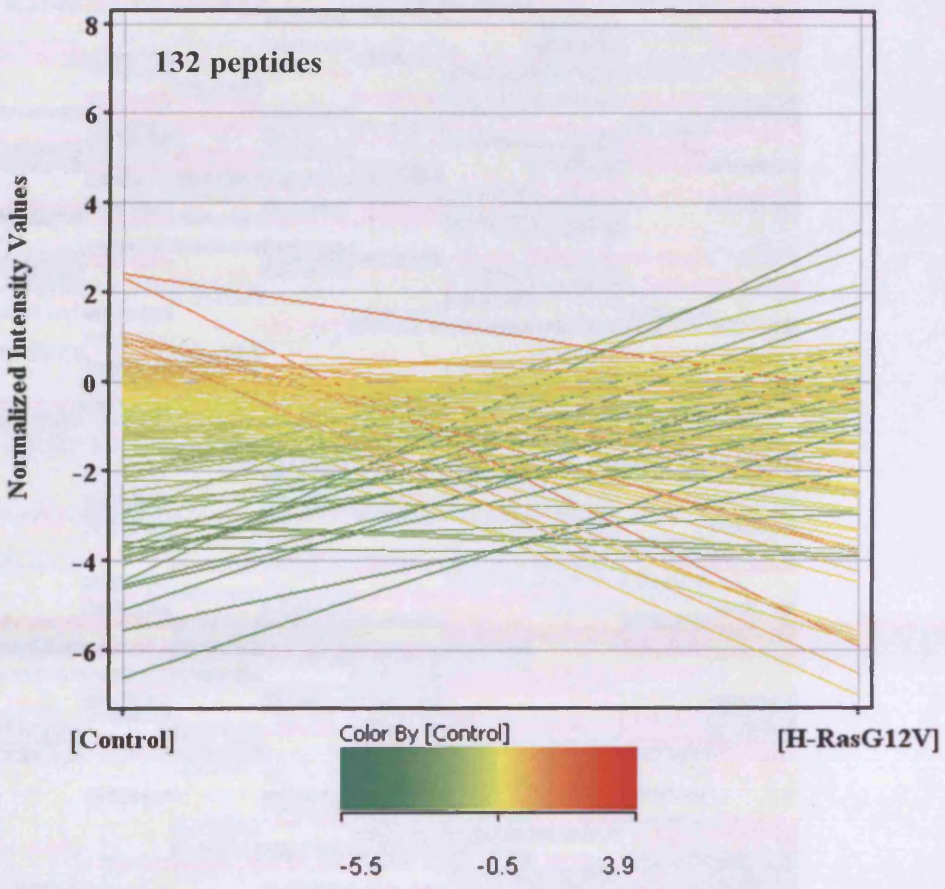

Figure 5.6 Kinome profile plot of averaged peptide phosphorylation intensities

$Log_{(2)}$-transformed, quantile-normalised $CD34^+$ control and $CD34^+$ $H\text{-}Ras^{G12V}$ peptide array data were used to generate a kinome profile plot, by averaging the data within each sample group ($CD34^+$ control or $CD34^+$ $H\text{-}Ras^{G12V}$). Only the peptides which remained after Bland-Altman analysis were plotted (132 out of 192 peptides). Profile colours were determined by normalised intensity of peptide signal in $CD34^+$ control samples.

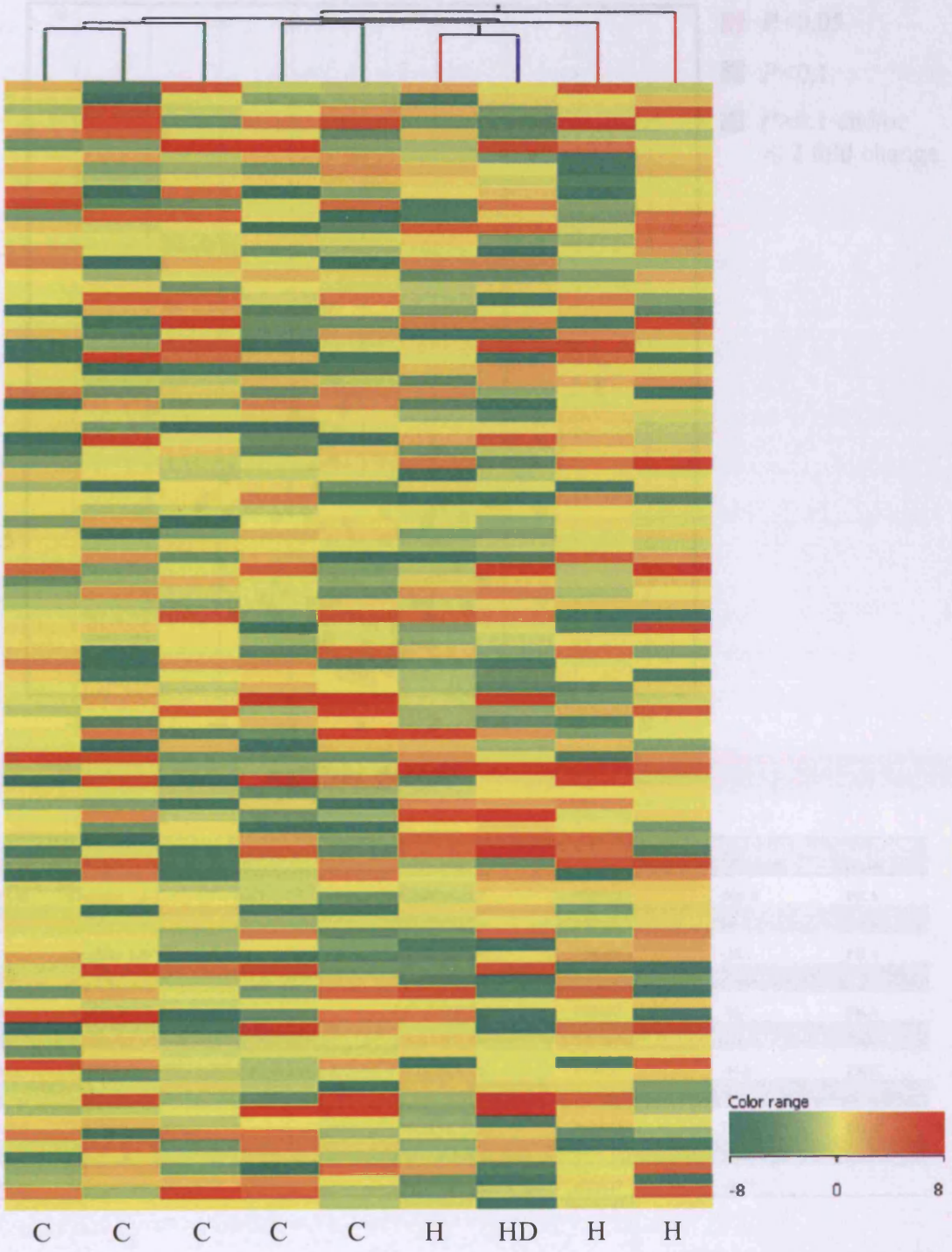

Figure 5.7 Unsupervised hierarchical clustering of non-averaged peptide array data

Unsupervised hierarchical clustering was performed on non-averaged $CD34^+$ control and $CD34^+$ H-Ras^{G12V} sample data (both with and without DPI treatment) in GeneSpring GX using Pearson's Absolute clustering algorithm with Ward's Linkage function. $CD34^+$ control, $CD34^+$ H-Ras^{G12V} and $CD34^+$ H-Ras^{G12V} + DPI are marked with green, red, and blue branches of the dendrogram respectively and are marked at the base of the diagram with C, H and HD respectively.

A

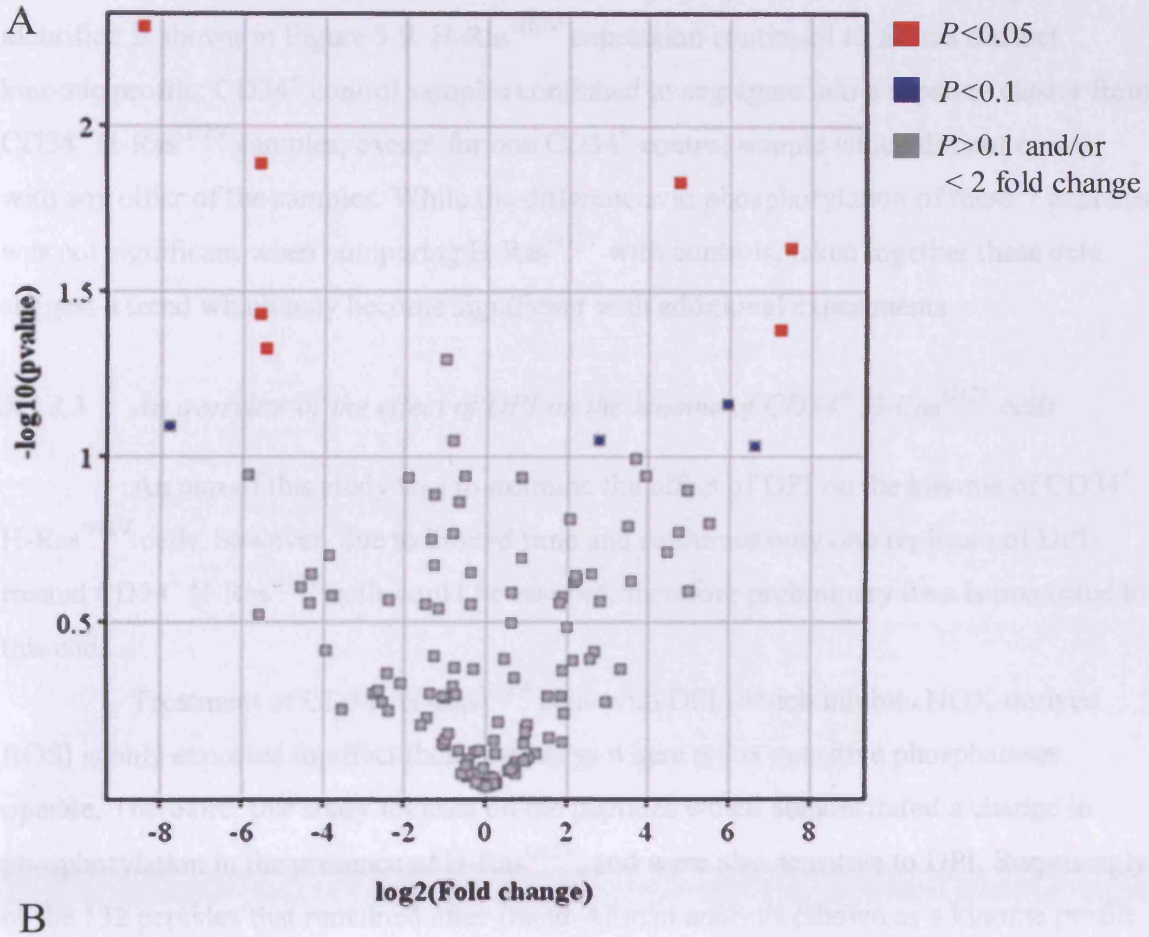

B

P-Value	Substrate ID	Peptide	Swissprot Accession ID	Fold Change	Kinase
0.0050	Fructose 1,6-bisphosphatase-1	KSRPSLPLP	P19112	-306.8	PKA
0.0129	Insulin receptor substrate-1	KSLNYIDLD	P35570	48.2	INSR
0.0146	Fructose 1,6-bisphosphatase	PRRDSTEGF	P09201	-26.5	PKA
0.0233	Histone H4	VKRGISGL	P02304	-176.6	
0.0369	Myelin basic protein	PKRGSGKDG	P02687	48.2	PKA
0.0412	Macrophage-MARCKS	LSGLSFKRN	P28667	-149.5	PKC
0.0467	Choline-phosphate cytidylyltransferase A	LQAISPKQS	P19836	44.5	PKC
0.0691	Histone H1	KASASPRRK	P02256	-61.0	sperm-specific
0.0801	Myelin basic protein	PSQRSKYLA	P02687	230.0	PKA
0.0882	Trophinin	KKASFKAKK		-6.7	PKC
0.0919	Myelin basic protein	PRTPGGRR	P02687	-96.7	

Figure 5.8 Statistical analysis of peptides with a >2 fold change in phosphorylation

(A) Volcano plot of 74 peptides which >2 fold change in phosphorylation in $CD34^+$ H-Ras^{G12V} cells compared with controls. $Log_{(2)}$ fold change is plotted on the x axis against $-log_{(10)}$ P-value (y axis). Peptides with $P<0.05$ are marked in red; peptides with $P<0.1$ are marked in blue; and peptides with $P>0.1$ and/or < 2 fold change are marked in grey. **(B)** Table showing detailed information associated with the 11 most significant peptides. Statistical significance was calculated using an unpaired T-Test. PKA= protein kinase A, PKC = protein kinase C, INSR = insulin receptor, MARCKS = myristoylated alanine-rich C kinase substrate

The results of supervised hierarchical clustering with respect to the 7 peptides identified is shown in Figure 5.9. H-Ras^{G12V} expression continued to form a distinct kinomic profile; CD34$^+$ control samples continued to segregate into a separate cluster from CD34$^+$ H-Ras^{G12V} samples, except for one CD34$^+$ control sample which did not cluster with any other of the samples. While the differences in phosphorylation of these 7 peptides was not significant when comparing H-Ras^{G12V} with controls, taken together these data suggest a trend which may become significant with additional experiments.

5.3.3.3 An overview of the effect of DPI on the kinome of CD34$^+$ H-Ras^{G12V} cells

An aim of this study was to examine the effect of DPI on the kinome of CD34$^+$ H-Ras^{G12V} cells, however, due to limited time and resources only one replicate of DPI-treated CD34$^+$ H-Ras^{G12V} cells could be assayed, therefore preliminary data is presented to this end.

Treatment of CD34$^+$ H-Ras^{G12V} cells with DPI (which inhibits NOX-derived ROS) is only expected to affect those pathways where redox-sensitive phosphatases operate. Therefore, this study focused on the peptides which demonstrated a change in phosphorylation in the presence of H-Ras^{G12V}, and were also sensitive to DPI. Surprisingly, of the 132 peptides that remained after Bland-Altman analysis (shown as a kinome profile plot in Figure 5.10A i), there were none that underwent hyperphosphorylation in the presence of H-Ras^{G12V} that could be suppressed by DPI.

However, a subset of 15 peptides were identified that showed a large decrease in phosphorylation in the presence of H-Ras^{G12V} that was rescued by DPI treatment (Figure 5.10A ii), suggesting that ROS-sensitive phosphatases are responsible for the decreased phosphorylation observed in this peptide subset. Interestingly, a second subset of peptides showed a DPI-insensitive increase in phosphorylation in the presence of H-Ras^{G12V} (Figure 5.10A iii), suggesting that the mechanisms leading to increased phosphorylation of this subset of peptides are not ROS-sensitive. Upon examination of the 7 peptides with the most significantly altered phosphorylation (described in section 5.3.3.2), both DPI-sensitive and DPI-insensitive peptides were represented (Figure 5.10B).

These results do suggest the possibility that the altered activity of some kinase/phosphatase pairs in CD34$^+$ H-Ras^{G12V} cells is due to inhibition of phosphatases by NOX-derived ROS.

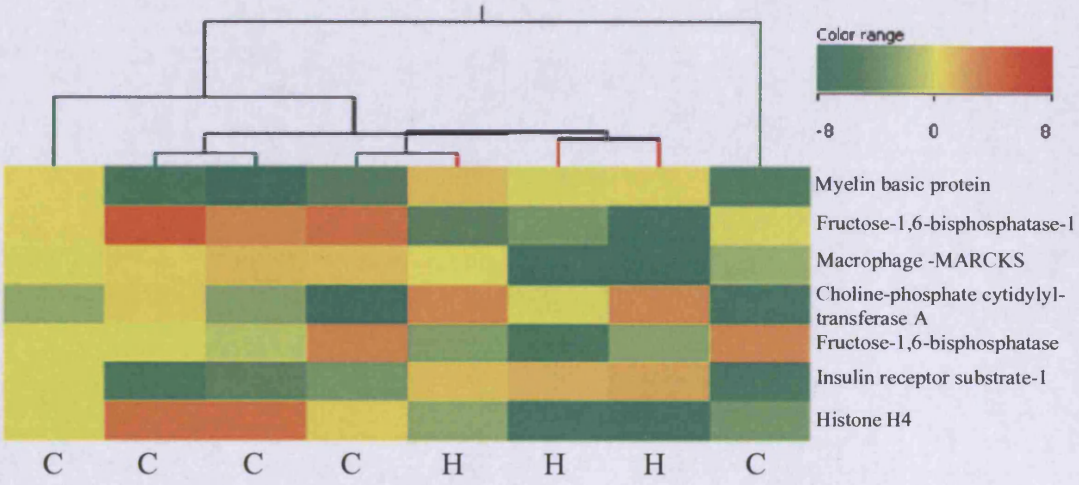

Figure 5.9 Supervised hierarchical clustering of peptide array samples

Supervised hierarchical clustering was performed on non-averaged $CD34^+$ control and $CD34^+$ H-Ras^{G12V} sample data with respect to the 7 most significant peptides identified by unpaired T-test (see Figure 5.8). Data was processed in GeneSpring GX using Pearson's Absolute clustering algorithm with Ward's Linkage function. $CD34^+$ control and $CD34^+$ H-Ras^{G12V} samples are marked with green and red branches of the dendrogram respectively and are marked at the base of the diagram with C and H respectively.

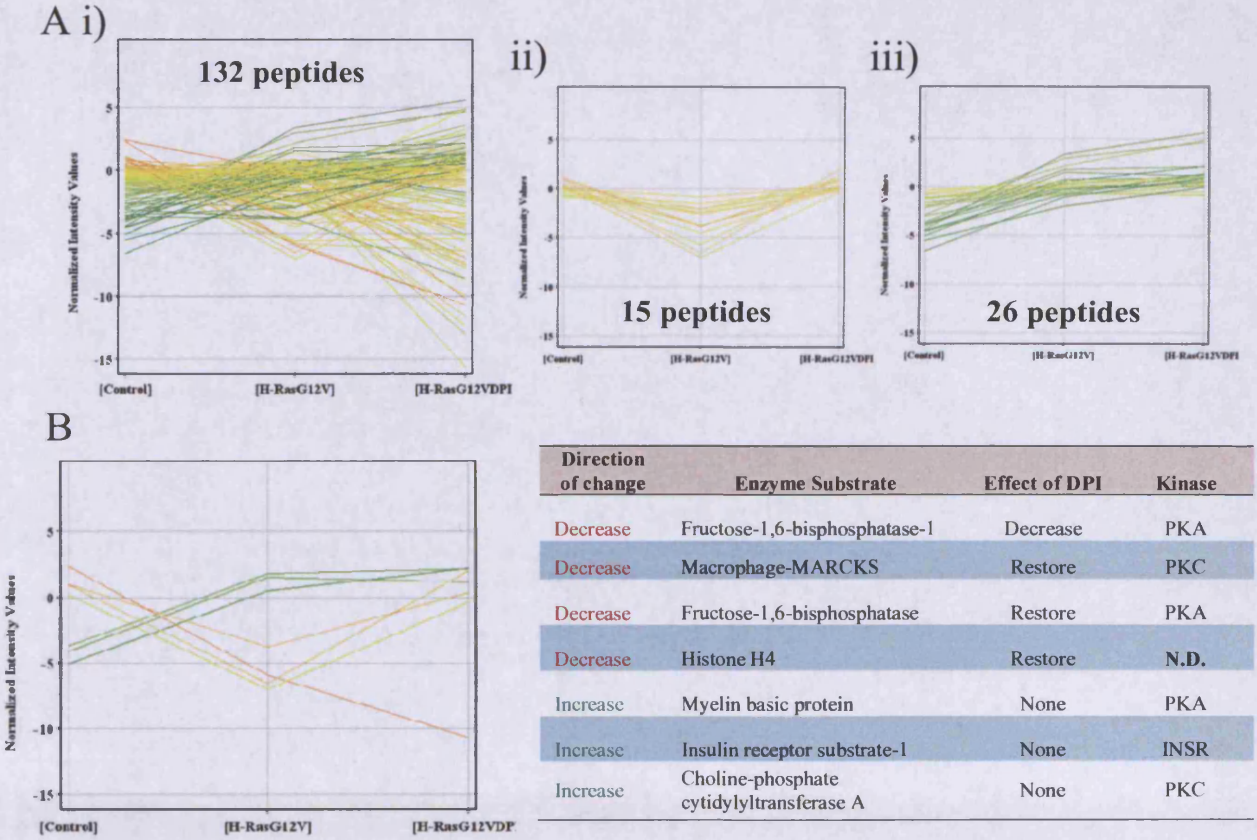

Direction of change	Enzyme Substrate	Effect of DPI	Kinase
Decrease	Fructose-1,6-bisphosphatase-1	Decrease	PKA
Decrease	Macrophage-MARCKS	Restore	PKC
Decrease	Fructose-1,6-bisphosphatase	Restore	PKA
Decrease	Histone H4	Restore	N.D.
Increase	Myelin basic protein	None	PKA
Increase	Insulin receptor substrate-1	None	INSR
Increase	Choline-phosphate cytidylyltransferase A	None	PKC

Figure 5.10 Overview of the effect of NOX-inhibition on peptide phosphorylation in $CD34^+$ H-Ras^{G12V} samples

(A) Kinome profile plots showing samples from $CD34^+$ control, $CD34^+$ H-Ras^{G12V} and $CD34^+$ H-Ras^{G12V} treated with DPI, **i)** Profile of peptides which showed decreased phosphorylation in $CD34^+$ H-Ras^{G12V} samples, and were restored by DPI treatment, **ii)** Profile of peptides which showed increased phosphorylation in $CD34^+$ H-Ras^{G12V} samples, and did not respond to DPI treatment. **(B)** Kinome profile plot showing the effect of DPI treatment on the 7 most significant peptides that were altered in $CD34^+$ H-Ras^{G12V} samples (see Figure 5.8) and table detailing the peptide ID. Direction of change refers to the change in phosphorylation of peptide in $CD34^+$ H-Ras^{G12V} samples with respect to $CD34^+$ control samples. INSR = insulin receptor, MARCKS = myristoylated alanine-rich C kinase substrate, N.D. = not determined

5.4 DISCUSSION

This study aimed to understand whether ROS could influence the phosphorylation of PKC and PDK1, which may offer an explanation for the ability of ROS to promote the expression of D-cyclins. Since ROS production is likely to have a global effect on protein phosphorylation, this study also aimed to examine the effects of ROS on the kinome of $CD34^+$ H-Ras^{G12V} cells using peptide array analysis.

The data generated in this study suggest that H_2O_2 promotes phosphorylation of PKC in $CD34^+$ cells. Phosphorylation of PKC induced by H_2O_2 treatment has been reported previously (Abdala-Valencia, H. and Cook-Mills, J.M. 2006), but this effect has not been previously studied in primary $CD34^+$ cells. In the present study, $CD34^+$ cells treated with H_2O_2 exhibited an increase in phosphorylation of PKC on Ser660 and also showed a marked increase in PDK1 phosphorylation. Since Ser660 on PKC is only autophosphorylated after transphosphorylation by PDK1 (on Ser500 in conventional PKC isoforms (Brognard, J. and Newton, A.C. 2008)); it was possible that increased PKC phosphorylation was to due increased PDK1 activity. Alternatively, the increased phosphorylation of PKC could have been a result of phosphatase inhibition by H_2O_2 (section 1.4.3.2). Since $CD34^+$ H-Ras^{G12V} exhibit high levels of PKC and PDK1 phosphorylation, these cells were incubated with several antioxidants to determine whether oxidative inhibition of phosphatases contributed to these proteins' hyperphosphorylation. Surprisingly, PDK1 expression in $CD34^+$ H-Ras^{G12V} cells appeared to markedly decrease after antioxidant treatment. However, given the short time frame of the experiment, such rapid degradation seems unlikely, rather this may be due a degree of phosphosensitivity of the PDK1-antibody (the binding may be affected by phospho-groups near the antibody epitope), or alternatively may reflect the instability and rapid degradation of PDK1 in the unphosphorylated state (Feldman, R.I. *et al.* 2005; Fujita, N. *et al.* 2002). While it is likely that phosphorylation of PDK1 is influenced by antioxidants; further investigation (perhaps with an alternative antibody) is required to confirm this. In the case of PKC, each antioxidant caused a dose-dependent decrease in Ser660 phosphorylation, suggesting that H_2O_2 strongly contributed toward phosphorylation of PKC by H-Ras^{G12V}; and supporting the notion that PKC is phosphorylated in these cells partly due to phosphatase inhibition by ROS. This study showed that PKC phosphorylation in $CD34^+$ H-Ras^{G12V} cells was highly dependent on cell culture density, and importantly, this effect was mediated by H_2O_2. However, a component of PKC phosphorylation was refractory to antioxidant treatment, which could be explained by the fact that PDK1 remained maximally

hyperphosphorylated, even in the presence of catalase. In summary these data support a scenario in which PKC phosphorylation (and activation) appears to be driven initially by PDK1, and is subsequently amplified by deactivation of PKC phosphatases mediated by H_2O_2 production.

The hyperphosphorylation of PDK1 in normal $CD34^+$ control cells treated with H_2O_2 may be explained by the non-physiological levels of H_2O_2 that these cells were treated with. Four of the five phosphorylation sites on PDK1 are dephosphorylated by the serine/threonine phosphatases PP1 and PP2A (Casamayor, A. *et al.* 1999). Importantly, PP2A and PP1 are inhibited by H_2O_2. Therefore, hyperphosphorylation of PDK1 in response to excessive H_2O_2 in normal $CD34^+$ cells may be due to oxidative inhibition of PP1 and PP2A.

It was also observed that PDK1 phosphorylation was not efficiently suppressed by antioxidants. This is consistent with the notion that activated Ras has an intrinsic ability to promote PDK1 phosphorylation. Indeed, PI3K (which is downstream of activated Ras) has been shown to promote PDK1 phosphorylation via Src in HEK293 cells (Yang, K.J. *et al.* 2008; Park, J. *et al.* 2001). However, an oxidant-insensitive mutant of Src was unable to promote phosphorylation of PDK1 in Ang II-stimulated primary rat glomerular cells (Block, K. *et al.* 2008); suggesting that (at least in rats) ROS generation may also be required for Src-mediated PDK1 phosphorylation. Conversely, excessive ROS levels may lead to hyperactivation of Src and may offer an additional explanation for hyperphosphorylation of PDK1 in the presence of H_2O_2.

Hyperphosphorylation of PDK1 by H_2O_2 can lead to its hyperactivation (Prasad, N. *et al.* 2000), and this implies that H_2O_2 could mimic some of the effects of H-Ras^{G12V} expression. This question could be addressed by examining whether H_2O_2 treatment alone can mimic aspects of the H-Ras^{G12V} phenotype (e.g. monocytic lineage selection) and whether this effect could be blocked by PKC inhibitors.

As discussed above, the hyperphosphorylation of PKC driven by H-Ras^{G12V} is likely to be a composite of direct activation of PKC by Ras via PI3K and PDK1 combined with further phosphorylation due to oxidative inhibition of phosphatases by H_2O_2. As mentioned above, PP1 and PP2A are serine/threonine phosphatases that are sensitive to oxidative inactivation. This is generally undisputed for PP2A (Chen, L. *et al.* 2009; Raghuraman, G. *et al.* 2009; Foley, T.D. *et al.* 2007), however there is disagreement with regard to PP1 (Rao, R.K. and Clayton, L.W. 2002) and (O'Loghlen, A. *et al.* 2003). This may be resolved by the fact that the sensitivity of phosphatases to ROS has been shown to be highly-context dependent, as discussed by den Hertog *et al.* (den Hertog, J. *et al.* 2005).

Importantly, as well as dephosphorylating residues on PDK1, these phosphatases also antagonise the phosphorylation of PKC by PDK1 (Keranen, L.M. *et al.* 1995). Although the activity of PP1 and PP2A was not formally investigated in this study due to time constraints; oxidative inhibition of these phosphatases offers a plausible explanation for our observations, in that inhibition of these phosphatases by H_2O_2 is likely to account for a) hyperphosphorylation of PDK1 in normal $CD34^+$ control cells and b) hyperphosphorylation of PKC in the presence of H-Ras^{G12V}.

Future studies will endeavour to confirm whether oxidative inhibition of PP1 and PP2A is responsible for the increased phosphorylation of PDK1 and PKC observed in $CD34^+$ H-Ras^{G12V} cells. Phosphatase activity in the past has been studied by measuring the removal of radioactive (^{32}P) phosphate groups from target substrate (Matsuzawa, S. *et al.* 1992), however non-radioactive assays are now available in kit form, which measure phosphatase activity by dephosphorylating a non-fluorescent substrate, yielding a fluorescent product. Activity of these phosphatases could also be assayed in the presence of ROS inhibitors to confirm that oxidative inhibition is occurring.

PKC signalling is implicated in cyclin D3 upregulation (Yamamoto, D. *et al.* 2003; Bartkova, J. *et al.* 1998). Therefore, since ROS contributes to PKC phosphorylation, this may explain the contribution of ROS to cyclin D3 expression (described in section 4.3.2.4). It may be of interest to see whether treatment of normal $CD34^+$ cells with H_2O_2 can induce cyclin D3 expression, and if so, whether this can be blocked using PKC inhibitors. In addition, since PKC has been shown to be an important mediator of developmental dysregulation by mutant Ras, it would be interesting to see whether a H_2O_2 scavenger could block this effect. The mechanisms of cyclin D1 upregulation by ROS are still unclear. Cyclin D1 expression is regulated by AP-1 transcription factors, which are directly downstream of Ras signalling via the Raf-MEK-ERK pathway. Phosphorylation events in this cascade are antagonised by the members of the MAPK phosphatase family (MKP-1 and MKP-3), and also PP1 and PP2A. MKP family members (like PP1 and PP2A) are inhibited by H_2O_2, including MKP-3 which specifically targets ERK (Kim, H.S. *et al.* 2003). Therefore it is plausible that H_2O_2 might also promote cyclin D1 expression through amplification of ERK signals. In support of this notion, H_2O_2 can promote ERK signalling in vascular-derived smooth muscle or endothelial cells, (Yamakawa, T. *et al.* 2002; Hsu, Y.H. *et al.* 2004), and in murine 32D haematopoietic cells leading to cell cycle progression (Iiyama, M. *et al.* 2006). Furthermore, NOX-derived H_2O_2 has previously been shown to directly promote cyclin D1 expression and cell cycle progression via increased AP-1 transcription factor activity in murine lung epithelial cells (Ranjan, P. *et al.* 2006).

Constitutive activation of ERK is also detected in AML patients (Lunghi, P. *et al.* 2001), but whether this is associated with increased ROS production by these AML blasts is unknown; such a study does not appear to have been done. Future studies will investigate whether the Raf-MEK-ERK pathway is amplified by H_2O_2 in $CD34^+$ expressing mutant Ras, by analysing the effect of antioxidants on ERK phosphorylation in $CD34^+$ H-Ras^{G12V} (or $CD34^+$ N-Ras^{G12D}) cells by Western blot.

This study examined the kinome of $CD34^+$ cells expressing of H-Ras^{G12V}, to look for evidence of phosphatase inhibition. Of 192 peptides on the array, positive signals were consistently detected for 132 of them. 74 of these peptides exhibited a 2 fold or greater change in phosphorylation in the presence of H-Ras^{G12V} protein extracts compared with controls, 7 of which were statistically significant. However, when multiple testing correction was applied, this significance was lost. This lack of statistical power is most likely due to the low number of replicate samples. In addition, it should be noted that the data generated here was obtained from a protocol that was undergoing optimisation, which may also have influenced reproducibility.

However, hierarchical clustering showed that the kinome profiles of $CD34^+$ control and $CD34^+$ H-Ras^{G12V} cells were sufficiently different from each other to be grouped into separate clusters; confirming expectations that H-Ras^{G12V} expression is associated with a distinct kinomic profile to that of normal $CD34^+$ cells. Interestingly, substrates of AGC kinases (in particular PKC and PKA), were over-represented amongst the 7 peptides which were most significant (5 of these were AGC kinase substrates; compared with a total of 64 (33%) AGC kinase substrates out of 192 on the array). Indeed, when statistical significance was relaxed to $P<0.1$ to detect any trends in peptides which were just short of significant, this trend of over-representation of PKA and PKC substrates continued; 7 out of 11 peptides were substrates for these kinases. This trend supports the data presented here and by others (Pearn, L. *et al.* 2007) that PDK1 (which governs AGC kinase activity) is dysregulated in the presence of H-Ras^{G12V}. However, there was disagreement within the results as to the level of activity of PKC and PKA in H-Ras^{G12V} cells, with some substrates showing an increase in phosphorylation, while other substrates of the same kinase apparently showing down regulation. This could be another example of the need for further data, or it could be due to *in vitro* artefact, since compartmentalised signalling is abolished in the protein extract, which may affect substrate specificity.

Unfortunately, due to time constraints this study was unable to fully address the question of the effect of NOX inhibition on the kinome of H-Ras^{G12V} cells. Although a detailed analysis of the results of DPI treatment is inappropriate given the lack of statistical

power; it is of interest to note, that there appeared to be a subset of peptides that responded to DPI treatment. Interestingly, the phosphorylation of these peptides decreased in the presence of H-Ras^{G12V}, which suggests increased phosphatase activity (the opposite of the expected result). However, this behaviour could be explained by the presence of a ROS-insensitive phosphatase which was itself regulated by a ROS sensitive phosphatase (assuming that phosphorylation of the ROS-insensitive phosphatase is activating). Taken together the results of the kinomics assay are encouraging, but require expansion with a larger dataset. In future studies, the optimised protocol will improve reproducibility which is likely to further improve the statistical significance of the results.

When considered as a whole, the results of this chapter suggest that H-Ras^{G12V} promotes phosphorylation of PDK1 and PKC via direct signalling and also through ROS-mediated inhibition of phosphatases. This mechanism may account for the ability of ROS to augment the expression of cyclin D3 driven by H-Ras^{G12V}. Although N-Ras^{G12D} was not formally examined in this chapter, given that it also promotes ROS production, it is plausible that a similar mechanism may operate in the presence of N-Ras^{G12D}.

In closing, it is useful to consider the implications of the model we propose herein. Firstly, since PKC promotes NOX2 activation by direct phosphorylation of NOX2 regulatory subunits (Bey, E.A. *et al.* 2004; Zhao, X. *et al.* 2005; Bankers-Fulbright, J.L. *et al.* 2001), this suggests that at high culture-density, a feedback loop may operate which boosts NOX2 activation. Furthermore, since H_2O_2 appears able to phosphorylate (and potentially activate) PKC in normal CD34$^+$ cells, PKC activation and NOX2 activation may also occur in neighbouring cells in close proximity to a ROS-generating cell. It is therefore possible that this H_2O_2 feedback loop could possibly be established in a HSC niche containing a cell expressing activated Ras.

Finally, these results suggest that NOX oxidases may be a relevant therapeutic target in AML patients. However, such an approach would have to contend with the increased survival of Ras-mutants that is expected to occur when ROS are scavenged (section 4.3.1.4). In addition, ROS generation by blasts from AML patients is highly variable (unpublished data) and furthermore, it is not known what role ROS generation plays in maintenance of the disease (see Chapter 6 for further discussion of this issue).

6 General Discussion and Further Work

6.1 SUMMARY AND RELEVANCE OF DATA PRESENTED IN THIS STUDY

Activated Ras is closely associated with myeloid neoplasia, with activating mutations in Ras detected in 15-25% of AML cases (Bowen, D.T. *et al.* 2005) and in 4-48% of patients with MDS (Padua, R.A. *et al.* 1998; Paquette, R.L. *et al.* 1993). Activating mutations of the Ras pathway are also frequently detected in other myeloid neoplasias, e.g. JMML; with up to 60% of JMML patients harbouring an activating mutation in Ras or SHP2; or loss-of-function mutations in NF1 (Tefferi, A. and Gilliland, D.G. 2007). Surprisingly, a recent study detected the presence of novel oncogenic mutations of Ras in AML and JMML patients, suggesting that the frequency of Ras mutations in myeloid neoplasia may be underestimated (Tyner, J.W. *et al.* 2009). In addition to their role in myeloid neoplasia, Ras oncogenes are known to drive generation of ROS in both human cell models and animal models of disease (Liu, R. *et al.* 2001; Lee, A.C. *et al.* 1999; Seru, R. *et al.* 2004; Sallmyr, A. *et al.* 2008; Rassool, F.V. *et al.* 2007).

Despite the high frequency of activating Ras mutation found in some human myeloid disorders, it has been difficult to elucidate the exact role that activated Ras plays in the development of human myeloid disease. Several studies have concluded that mutant Ras does not have prognostic significance in human AML (Kiyoi, H. *et al.* 1999; Bowen, D.T. *et al.* 2005; Bacher, U. *et al.* 2006), or, put another way, activated Ras does not significantly influence the 'treatability' of the disease. However, it has been shown in animal models that activated Ras alone can drive leukaemia-like disease (Braun, B.S. *et al.* 2004; Parikh, C. *et al.* 2007), and this can be augmented by overexpression of BCL-2 (Rassool, F.V. *et al.* 2007). Such studies provide support for the 'two hit' hypothesis of myeloid neoplasia in mice (Gilliland, D.G. 2001), though the relatively low number of lesions required may be due to the relative ease of murine cell transformation compared with human cells (Rangarajan, A. *et al.* 2004; Rangarajan, A. and Weinberg, R.A. 2003). Although a central tenet of cancer biology is that several genetic 'hits' are required to subvert major anti-oncogenic systems before tumours can initiate (Hanahan, D. and Weinberg, R.A. 2000); it is proposed that more hits are required to transform human cells than murine cells, due to more robust anti-oncogenic mechanisms in humans. This

increased complexity of genetic alteration in human cancers (compared with murine models) may partly explain why Ras mutations take a more conservative role in human AML, at least when considering prognostic influence – other mutations may assume the role of activated Ras, relaxing the requirement to maintain mutated Ras expression in the malignant clones. Although activated Ras confers increased cell-survival, proliferative drive and mediates developmental dysregulation *in vitro* (Schubbert, S. *et al.* 2007; Pearn, L. *et al.* 2007; Darley, R.L. *et al.* 2002) and is frequently detected in AML, the reason for its lack of influence on prognosis remains unclear.

However, several studies have provided some understanding of the consequences of activated Ras expression in haematopoietic progenitors, which provides insight into the role of Ras in AML pathogenesis. It has been demonstrated that mutant Ras polarises lineage decisions in human haematopoietic progenitors via hyperactivation of conventional PKC isoforms. Specifically, mutant Ras biases CFU-GM lineage decisions towards monocytes, at the expense of granulocytic development (Pearn, L. *et al.* 2007). Activated Ras also disturbs erythroid development, resulting in increased proliferation of EPO-independent erythroid progenitors followed by a block in terminal erythroid development (Darley, R.L. *et al.* 2002). The combination of erythroid progenitor expansion combined with a lack of terminal erythropoiesis driven by activated Ras bears similarity to the most common presenting features of MDS. MDS is a heterogeneous group of clonal (or oligoclonal) haematopoietic disorders, characterised by refractory anaemia in combination with a hypercellular bone marrow and uni- or multi-lineage dysplasia (Vardiman, J.W. *et al.* 2009). MDS is distinct from AML, but is considered to be a pre-leukaemic disorder with a high probability of developing overt AML (Nimer, S.D. 2008). Furthermore, Ras mutations are closely associated with MDS (Gallagher, A. *et al.* 1997); though this is not true for all MDS subtypes since MDS with deletions in 5q show relatively infrequent Ras mutations (Fidler, C. *et al.* 2004). Interestingly, there appears to be a link between myeloid neoplasias (specifically MDS and AML) and oxidative stress (Bowen, D. *et al.* 2003; Farquhar, M.J. and Bowen, D.T. 2003). This link has been further reinforced by murine model studies conducted by Rassool *et al.*, which demonstrated that mutant N-Ras co-operates with BCL-2 overexpression in the myeloid compartment resulting in an MDS-like disorder which quickly progressed to AML-like disease (Rassool, F.V. *et al.* 2007). Importantly, disease progression closely correlated with DNA double strand breaks (DSBs); attributed to increased NOX-derived ROS production in the primitive myeloid progenitors. In their conclusions, these authors propose a model where mutant Ras-derived ROS fosters genomic instability which encourages disease progression. The results of the

present study provide additional evidence of the link between activated Ras and oxidative stress in human haematopoietic cells (section 3.3). Further investigation into a possible correlation between Ras mutations and oxidative stress in MDS patients is therefore encouraged; at the time of writing it appears that such an investigation has not been performed.

There is also evidence of oxidative stress amongst some of the MPNs, including CML, which is positive for the BCR-ABL fusion gene (Ahmad, R. *et al.* 2008). Given that BCR-ABL has been shown to activate Ras (Cortez, D. *et al.* 1996; Sanchez-Garcia, I. and Martin-Zanca, D. 1997), it is plausible that Ras-mediated ROS production is responsible (or contributes) to the oxidative stress in CML. Some reports have concluded that the mitochondria are the sole source of oxidative stress in CML cells (Kim, J.H. *et al.* 2005), while others have suggested that BCR-ABL generates ROS via NOX oxidases; specifically NOX4 (Naughton, R. *et al.* 2009). While it is possible that mitochondria do indeed contribute to ROS generation in CML, it is notable that Kim *et al.* did not address the possibility that NOX oxidases contributed to ROS generated in their model system.

JMML is a form of MPN which has a striking association with mutations of the Ras pathway (Tefferi, A. and Gilliland, D.G. 2007). In addition to activating mutations of Ras itself, activating mutations in SHP2 and loss-of-function mutations in NF1 have been reported in JMML patients. With such a close association with Ras activation, it is expected that JMML cells would produce ROS; however, this also does not appear to have been investigated.

In contrast to MDS and MPNs, there are few reports of previous investigations into the production of ROS by AML blasts. An early study cited superoxide production in leukaemic cells as the probable source of cutaneous tissue damage (Mazzone, A. *et al.* 1986); since then several groups have examined superoxide production in either resting or stimulated leukocytes from myeloid and lymphoid leukaemia patient samples. Unfortunately, there is a lack of consensus in the results of these studies. One study examined M1 and M2 patient samples and detected elevated constitutive and stimulated superoxide production in apparently mixed preparations of AML blasts from these patients compared with control cell samples (Er, T.K. *et al.* 2007). Another study examined stimulated superoxide production in M1-M4 and M5b AML samples and L1-L3 ALL samples, but only found superoxide production in the monocytic leukaemias (M4 and M5b), furthermore, stimulated superoxide production was (at best) similar to levels of superoxide generated by leukocytes from healthy patients (Kato, M. *et al.* 2003). However, Kato *et al.* did not examine constitutive superoxide generation, which is likely to be far

more relevant to leukaemia pathogenesis than stimulated production. To resolve the paucity of data, constitutive ROS production in AML blasts is currently being examined in this Department, and early results suggest that M4 and M5 monocytic AMLs constitutively generate more ROS than M1-M3 AMLs (J. Zabkiewicz, unpublished data). This could be due to the fact that monocytic AMLs are more developmentally equipped to generate ROS than less-differentiated AMLs. Interestingly, activating Ras mutations are also most commonly associated with M4 (Bowen, D.T. *et al.* 2005; Goemans, B.F. *et al.* 2005) and to a lesser extent M5 (Mahgoub, N. *et al.* 1999); though one report disagrees with this trend (Auewarakul, C.U. *et al.* 2006). Given the results of the present study, it is possible that activating Ras mutations in M4 and M5 AMLs are partly responsible for increased constitutive ROS generation in these subtypes; however, examination of Ras mutation status in the patient samples is required to confirm any correlations.

The results of this study raise the question as to whether ROS production may be a relevant therapeutic target in myeloid leukaemia associated with activated Ras. As discussed above, the extent of oxidative stress in AML blasts is currently being determined, therefore the clinical consequences of ROS production (if any) in AML are unknown. If production of ROS was shown to be associated with poorer treatment outcome, this would strengthen the argument for targeting ROS production in AML. Although ROS production is not a prerequisite for tumour formation, ROS production does alter the properties of a tumour cell, conferring upon it both advantages and disadvantages. The results of the present study suggest that ROS blockade may partially suppress the proliferation of blast cells driven by activated Ras, but would have the undesired side-effect of improving survival (sections 4.3.1 and 4.3.2); though whether this is also the case in AML blasts which may have evolved adaptive changes in response to ROS production remains to be established. ROS blockade is associated with decreased proliferation in HER-2/Neu-transformed rat-1 fibroblasts (Preston, T.J. *et al.* 2003) and tumourigenicity in transformed murine keratinocyte (6M90) cells (Finch, J.S. *et al.* 2006), while H_2O_2 can drive proliferation in murine lung epithelial cells (Ranjan, P. *et al.* 2006) and human neuroblastoma cells (Havens, C.G. *et al.* 2006).

ROS could be targeted in AML using two differing strategies; one involves reduction of ROS and oxidative stress using antioxidants, the other involves increasing oxidative stress in the malignant cells beyond a critical point resulting in cell death. There is support for both strategies; however each strategy also has potential disadvantages.

In the case of targeting ROS in cancers using antioxidants, one study reported that antioxidant supplements may not be beneficial when taken as single agents or in

combination with other treatments for a range of disorders including cancers (Bjelakovic, G. *et al.* 2007). However, a more recent study conducted by Block *et al.* concluded that antioxidants were generally beneficial for cancer patients, in some cases significantly reducing the toxic effects of chemotherapy on normal tissues (Block, K.I. *et al.* 2008). In the context of MDS, the antioxidant molecule amifostine can induce transient recoveries in haematopoiesis across all FAB types, and can reduce the requirement for transfusions in some MDS patients. However, it ultimately offered no significant reduction of bone marrow blasts by the end of the treatment (List, A.F. *et al.* 1997). Targeting ROS using antioxidants may indeed be of value in AML treatment; however as yet no studies have been conducted to establish whether this is the case.

The second strategy involves further increasing ROS stress in tumour cells. This strategy proposes that increased ROS stress in tumour cells sensitises them to further ROS insult leading to their demise. Interestingly, this potentiation of stress signals appears to be directly mediated by ROS at the molecular level, for example, ASK1 (an upstream activator of $p38^{MAPK}$) is bound to thioredoxin in an inactive state under normal conditions. Oxidation of thioredoxin by ROS leads to dissociation of ASK1 from thioredoxin and subsequent $p38^{MAPK}$ phosphorylation and activation (Liu, Y. and Min, W. 2002). A similar mechanism operates for JNK bound to glutathione-S-transferase π (Adler, V. *et al.* 1999). In addition, it has been discovered that several mainstay cytotoxic drugs are associated with a large increase in ROS production inside the malignant cell (Benhar, M. *et al.* 2002). For example, in the context of leukaemia, daunorubicin treatment induces ROS upregulation possibly by acting as a direct substrate for NADPH oxidase, resulting in oxidative damage to the mitochondria and subsequent apoptosis (Laurent, G. and Jaffrezou, J.P. 2001). Similarly, the cytotoxic effect of the proteasome inhibitor Bortezomib is dependent on a transient burst of ROS production to induce apoptosis (Yu, C. *et al.* 2004). In addition, the putative NF-κB inhibitor LC-1 (Jenkins, C. *et al.* 2008; Hewamana, S. *et al.* 2008) is currently being trialled in a first-in-man study at Cardiff; and this agent may also depend on ROS induction to exert its effects (Guzman, M.L. *et al.* 2005).

Tumour cells can to adapt to chronic ROS stress. As an example of this, brief exposure to a sub-lethal dose of oxidant can protect Rat L1 cells from toxicity associated with a subsequent more aggressive insult (Choi, J. *et al.* 1997). Similarly, in tumour cells where oxidative stress is prevalent, chronic oxidative stress can initiate upregulation of antioxidant defences, GSH production and catalase/SOD1 expression (Trachootham, D. *et al.* 2009). It is also possible that gradual resistance to oxidative stress occurs due to

selection of clones with augmented antioxidant capacity, resulting in a more ROS-resistant progeny (Bowen, D. *et al.* 2003) or progeny which acquire the ability to bypass the ROS-stress pathways (Dolado, I. *et al.* 2007). Insensitivity to oxidative stress may also contribute to cancer cell drug-resistance by blunting apoptotic mechanisms (Pervaiz, S. and Clement, M.V. 2004; Pervaiz, S. 2006).

Tumour cells which have developed such resistance to ROS stress through increased anti-oxidant defence may be hyperdependent on maintaining adequate antioxidant capacity. Therefore, catastrophic ROS stress may be induced in tumour cells by targeting endogenous antioxidants e.g. GSH or SOD. This would be expected to re-sensitise these cancer cells to oxidative stress. Indeed, such strategies that target antioxidants in cancer cells are proving effective, for example the naturally occurring compound beta-phenylethyl isothiocyanate (PEITC), has been shown to effectively induce cell death in CLL and CML cells resistant to fludarabine and imatinib respectively; by depleting intracellular GSH (Trachootham, D. *et al.* 2008; Zhang, H. *et al.* 2008). This approach engenders selectivity to the treatment, since normal cells produce little ROS and presumably have a large reserve of intracellular antioxidant capacity. In contrast, tumour cells are 'living life on the edge' and probably exist on the limits of their antioxidant capacity. Depletion of intracellular antioxidants is even more effective when combined with pro-oxidant compounds, such as arsenic trioxide (As_2O_3). This strategy is in effect, a 'double-whammy', simultaneously lowering antioxidant defences whilst boosting oxidative stress. For example, a combination of the SOD-inhibitor 2-methoxyestradiol (2-ME) and AsO_3 treatment induced cell-death in CLL cells that were resistant to 2-ME alone (Zhou, Y. *et al.* 2003). However, a significant disadvantage of this general strategy is that it is likely to introduce oxidative stress in normal cells, leading to toxicity.

The treatment strategies discussed above could potentially be applied to mutant Ras-expressing leukaemias that generate increased ROS. Mutant Ras drives production of ROS via NOX oxidases in $CD34^+$ cells, and the results of experiments examining superoxide production induced by TPA revealed that mutant Ras cells are capable of generating 50% more ROS than controls, which is probably due to the increased availability of NOX2 oxidase in the plasma membrane. Interestingly, the synthetic retinoid N-(4-hydroxyphenyl) retinamide (4HPR) is reportedly capable of inducing oxidative stress in part through upregulation of $p67^{phox}$ (Kim, H.J. *et al.* 2005) (which is abundant in $CD34^+$ H-Ras^{G12V} cells) and this may occur via stimulation of PKC activity (Kim, H.J. *et al.* 2006), though the mechanism is not understood. It is important to note however, that upregulation of ROS by cytotoxic drugs usually occurs via the mitochondria (i.e.

intracellular ROS); whereas the model proposed here would result in activation of NOX2, which would result in *extracellular* ROS generation, which may result in a loss of specificity for the target cell, and simultaneously expose neighbouring cells to excessive ROS (since H_2O_2 can diffuse away from the source). Alternatively, suppression of ROS production in AML using antioxidant compounds may suppress malignant cell proliferation, and may also reduce toxicity associated with standard chemotherapy.

6.1.1 CONCLUSION

In conclusion, previous research suggests that Ras mutations are closely associated with AML and myeloid dysplasias. This study demonstrated that normal human primary $CD34^+$ haematopoietic cells transduced with activated Ras ($N\text{-}Ras^{G12D}$ and $H\text{-}Ras^{G12V}$) constitutively generate ROS, attributed to an increase in NOX2-generated superoxide. Furthermore, this study is the first to demonstrate that mutant Ras promotes growth factor-independent survival and proliferation in primary human $CD34^+$ haematopoietic cells. Consistent with their increased cell survival, there was phosphorylation of Akt on Ser473 in $CD34^+$ $H\text{-}Ras^{G12V}$ cells; which was absent in controls. The mechanism underlying growth factor-independent proliferation appeared to be two-fold: evasion of $p38^{MAPK}$-mediated cell-cycle arrest (despite $p38^{MAPK}$ activation); and increased expression and/or stability of cyclin D3 and D1. Whilst endogenous H_2O_2 production hindered survival, it significantly contributed to proliferation driven by mutant Ras. Inhibition experiments indicated that ROS appear to augment cyclin D1 and D3 expression. Finally, this study presented evidence that endogenous H_2O_2 production driven by $H\text{-}Ras^{G12V}$ makes a significant contribution to hyperphosphorylation of PKC in human $CD34^+$ cells (offering an explanation for the ability of ROS to augment expression of cyclin D3).

6.2 FUTURE WORK AND PERSPECTIVES

During this study, there were several lines of investigation which were of interest, but were not possible to pursue due to time constraints. For example, while precipitous amounts of ROS were generated by mutant Ras expressing $CD34^+$ cells, the effects on DNA integrity were not assessed. This may have been a contributing factor to the pro-apoptotic effect of ROS and could be investigated using markers of DNA damage, for examples γ-H2AX or 8-oxo-guanine can be assayed conveniently by flow cytometry.

Also, the results of co-culture experiments strongly suggested the presence of a paracrine pro-survival factor(s) secreted by $CD34^+$ H-Ras^{G12V} cells. Identification of this factor(s) may also provide further insights into mechanisms of growth factor-independent proliferation of these cells. Previous studies showing that activated N-Ras upregulates several growth-factor mRNAs (Shen, S. *et al.* 2007) would provide a good starting point for studies intending to identify these factors. There are soluble factor identification kits sold by several leading reagent manufacturers that would enable detection of factors selected for examination. Alternatively, the possibility that this effect is mediated by cell-cell contact should also be addressed, perhaps by incubating control cells with $CD34^+$ H-Ras^{G12V}-cell conditioned medium. Expansion of the kinomic analysis combined with functional analyses of phosphatase activity will improve the current understanding of the role of phosphatase inhibition in the phenotype of mutant Ras in human $CD34^+$ cells. Identification of the phosphatases thus dysregulated (possibly PP1 and PP2A) may shed more light on the role of ROS production in cell cycle control. Finally, this study noted that inhibition of ROS appeared to augment cyclin D1 and D3 expression; however, the mechanisms behind these observations are unclear and would be interesting to pursue.

Looking to the future, the results of this study provide a rationale for detailed investigation of constitutive ROS production in primary AMLs, as this has not previously been investigated in depth. Preliminary work in this area suggests that AML cells do indeed generate ROS, but more work is required to establish this. Given that ROS appears to play several roles in the Ras phenotype, it may also be of interest to determine whether ROS contributes to the developmental dysregulation caused by activated Ras in $CD34^+$ cells. It may be that ROS could partially or completely mimic the effects of activated Ras and GOX could be used as a source of consistent H_2O_2 production in these experiments. Developmental progress in the presence or absence of ROS can be assayed using flow cytometric analysis of cell-surface markers; these assays have been optimised in Cardiff. Finally, since Nox2-deficient mice are available, the role of ROS in developmental dysregulation by Ras could be determined by expressing activated Ras in Sca-1^+ cells from these mice, and examining whether the developmental dysregulation caused by Ras is ameliorated in the absence of Nox2-derived ROS over-production. Also, since overexpression of activated Ras in murine haematopoietic progenitor cells has previously been shown to cause myeloid disease (Parikh, C. *et al.* 2007), this model system could also be used to investigate the role of ROS in Ras-mediated leukaemogenesis.

References

Abdala-Valencia H., Cook-Mills J.M. 2006. VCAM-1 signals activate endothelial cell protein kinase Calpha via oxidation. *J.Immunol.* 177(9), pp. 6379-6387

Abkowitz J.L., Catlin S.N., Guttorp P. 1996. Evidence that hematopoiesis may be a stochastic process in vivo. *Nat.Med.* 2(2), pp. 190-197

Adachi Y., Shibai Y., Mitsushita J., Shang W.H., Hirose K., Kamata T. 2008. Oncogenic Ras upregulates NADPH oxidase 1 gene expression through MEK-ERK-dependent phosphorylation of GATA-6. *Oncogene* 27(36), pp. 4921-4932

Adler V., Yin Z., Tew K.D., Ronai Z. 1999. Role of redox potential and reactive oxygen species in stress signaling. *Oncogene* 18(45), pp. 6104-6111

Ahmad R., Tripathi A.K., Tripathi P., Singh S., Singh R., Singh R.K. 2008. Malondialdehyde and protein carbonyl as biomarkers for oxidative stress and disease progression in patients with chronic myeloid leukemia. *In Vivo* 22(4), pp. 525-528

Ahmadian M.R., Stege P., Scheffzek K., Wittinghofer A. 1997. Confirmation of the arginine-finger hypothesis for the GAP-stimulated GTP-hydrolysis reaction of Ras. *Nat.Struct.Biol.* 4(9), pp. 686-689

Alberts B. et al. 2002. *Molecular Biology of the Cell.* New York: Garland Science, 4th Ed.

Alexander R.W. 1995. Theodore Cooper Memorial Lecture. Hypertension and the pathogenesis of atherosclerosis. Oxidative stress and the mediation of arterial inflammatory response: a new perspective. *Hypertension* 25(2), pp. 155-161

Alvarado Y., Giles F.J. 2007. Ras as a therapeutic target in hematologic malignancies. *Expert.Opin.Emerg.Drugs* 12(2), pp. 271-284

Andriole G.L., Mule J.J., Hansen C.T., Linehan W.M., Rosenberg S.A. 1985. Evidence that lymphokine-activated killer cells and natural killer cells are distinct based on an analysis of congenitally immunodeficient mice. *J.Immunol.* 135(5), pp. 2911-2913

Antonchuk J., Sauvageau G., Humphries R.K. 2001. HOXB4 overexpression mediates very rapid stem cell regeneration and competitive hematopoietic repopulation. *Exp.Hematol.* 29(9), pp. 1125-1134

Arbiser J.L., Petros J., Klafter R., Govindajaran B., McLaughlin E.R. et al. 2002. Reactive oxygen generated by Nox1 triggers the angiogenic switch. *Proc.Natl.Acad.Sci.U.S.A* 99(2), pp. 715-720

Argiropoulos B., Humphries R.K. 2007. Hox genes in hematopoiesis and leukemogenesis. *Oncogene* 26(47), pp. 6766-6776

Arnold R.S., He J., Remo A., Ritsick D., Yin-Goen Q., Lambeth J.D., Datta M.W., Young A.N., Petros J.A. 2007. Nox1 expression determines cellular reactive oxygen and modulates c-fos-induced growth factor, interleukin-8, and Cav-1. *Am J Pathol.* 171(6), pp. 2021-2032

Artus J., Babinet C., Cohen-Tannoudji M. 2006. The cell cycle of early mammalian embryos: lessons from genetic mouse models. *Cell Cycle* 5(5), pp. 499-502

Auewarakul C.U., Lauhakirti D., Tocharoentanaphol C. 2006. Frequency of RAS gene mutation and its cooperative genetic events in Southeast Asian adult acute myeloid leukemia. *Eur.J.Haematol.* 77(1), pp. 51-56

Babior B.M., Kipnes R.S., Curnutte J.T. 1973. Biological defense mechanisms. The production by leukocytes of superoxide, a potential bactericidal agent. *J Clin.Invest* 52(3), pp. 741-744

Bacher U., Haferlach T., Schoch C., Kern W., Schnittger S. 2006. Implications of NRAS mutations in AML: a study of 2502 patients. *Blood* 107(10), pp. 3847-3853

Bacic G., Spasojevic I., Secerov B., Mojovic M. 2008. Spin-trapping of oxygen free radicals in chemical and biological systems: new traps, radicals and possibilities. *Spectrochim.Acta A Mol.Biomol.Spectrosc.* 69(5), pp. 1354-1366

Bae Y.S., Kang S.W., Seo M.S., Baines I.C., Tekle E., Chock P.B., Rhee S.G. 1997. Epidermal growth factor (EGF)-induced generation of hydrogen peroxide. Role in EGF receptor-mediated tyrosine phosphorylation. *J Biol.Chem.* 272(1), pp. 217-221

Balaban R.S., Nemoto S., Finkel T. 2005. Mitochondria, oxidants, and aging. *Cell* 120(4), pp. 483-495

Baldridge C.W., Gerard R.W. 1932. The extra respiration of phagocytosis. *Am J Physiol* 103(1), pp. 235-236

Baldus C.D., Thiede C., Soucek S., Bloomfield C.D., Thiel E., Ehninger G. 2006. BAALC expression and FLT3 internal tandem duplication mutations in acute myeloid leukemia patients with normal cytogenetics: prognostic implications. *J.Clin.Oncol.* 24(5), pp. 790-797

Ballatori N., Krance S.M., Notenboom S., Shi S., Tieu K., Hammond C.L. 2009. Glutathione dysregulation and the etiology and progression of human diseases. *Biol.Chem.* 390(3), pp. 191-214

Balmain A., Pragnell I.B. 1983. Mouse skin carcinomas induced in vivo by chemical carcinogens have a transforming Harvey-ras oncogene. *Nature* 303(5912), pp. 72-74

Banfi B., Molnar G., Maturana A., Steger K., Hegedus B., Demaurex N., Krause K.H. 2001. A Ca(2+)-activated NADPH oxidase in testis, spleen, and lymph nodes. *J Biol.Chem.* 276(40), pp. 37594-37601

Bangham D.R., Mussett M.V. 1959. The Second International Standard for heparin. *Bull.World Health Organ* 20, pp. 1201-1208

Bankers-Fulbright J.L., Kita H., Gleich G.J., O'Grady S.M. 2001. Regulation of human eosinophil NADPH oxidase activity: a central role for PKCdelta. *J.Cell Physiol* 189(3), pp. 306-315

Bannister J.V., Bannister W.H., Rotilio G. 1987. Aspects of the structure, function, and applications of superoxide dismutase. *CRC Crit Rev.Biochem.* 22(2), pp. 111-180

Barbacid M. 1987. ras genes. *Annu.Rev.Biochem.* 56, pp. 779-827

Bardet V., Tamburini J., Ifrah N., Dreyfus F., Mayeux P., Bouscary D., Lacombe C. 2006. Single cell analysis of phosphoinositide 3-kinase/Akt and ERK activation in acute myeloid leukemia by flow cytometry. *Haematologica* 91(6), pp. 757-764

Bartkova J., Lukas J., Strauss M., Bartek J. 1998. Cyclin D3: requirement for G1/S transition and high abundance in quiescent tissues suggest a dual role in proliferation and differentiation. *Oncogene* 17(8), pp. 1027-1037

Bartram C.R. 1992. Molecular genetic aspects of myelodysplastic syndromes. *Hematol.Oncol.Clin.North Am.* 6(3), pp. 557-570

Bashir T., Dorrello N.V., Amador V., Guardavaccaro D., Pagano M. 2004. Control of the SCF(Skp2-Cks1) ubiquitin ligase by the APC/C(Cdh1) ubiquitin ligase. *Nature* 428(6979), pp. 190-193

Baum C.M., Weissman I.L., Tsukamoto A.S., Buckle A.M., Peault B. 1992. Isolation of a candidate human hematopoietic stem-cell population. *Proc.Natl.Acad.Sci.U.S.A* 89(7), pp. 2804-2808

Becker A.J., McCulloch E.A., Till J.E. 1963. Cytological demonstration of the clonal nature of spleen colonies derived from transplanted mouse marrow cells. *Nature* 197, pp. 452-454

Bedard K., Krause K.H. 2007. The NOX family of ROS-generating NADPH oxidases: Physiology and pathophysiology. *Physiol Rev.* 87(1), pp. 245-313

Behre G., Singh S.M., Liu H., Bortolin L.T., Christopeit M. et al. 2002. Ras signaling enhances the activity of C/EBP alpha to induce granulocytic differentiation by phosphorylation of serine 248. *J.Biol.Chem.* 277(29), pp. 26293-26299

Benedict W.F., Murphree A.L., Banerjee A., Spina C.A., Sparkes M.C., Sparkes R.S. 1983. Patient with 13 chromosome deletion: evidence that the retinoblastoma gene is a recessive cancer gene. *Science* 219(4587), pp. 973-975

Benhar M., Engelberg D., Levitzki A. 2002. ROS, stress-activated kinases and stress signaling in cancer. *EMBO Rep.* 3(5), pp. 420-425

Bennett J.M., Catovsky D., Daniel M.T., Flandrin G., Galton D.A., Gralnick H.R., Sultan C. 1976. Proposals for the classification of the acute leukaemias. French-American-British (FAB) co-operative group. *Br.J.Haematol.* 33(4), pp. 451-458

Berendes H., Bridges R.A., Good R.A. 1957. A fatal granulomatosus of childhood: the clinical study of a new syndrome. *Minn.Med.* 40(5), pp. 309-312

Bey E.A., Xu B., Bhattacharjee A., Oldfield C.M., Zhao X. et al. 2004. Protein kinase C delta is required for p47phox phosphorylation and translocation in activated human monocytes. *J.Immunol.* 173(9), pp. 5730-5738

Bhattacharya S., Chen L., Broach J.R., Powers S. 1995. Ras membrane targeting is essential for glucose signaling but not for viability in yeast. *Proc.Natl.Acad.Sci.U.S.A* 92(7), pp. 2984-2988

Bivona T.G., Philips M.R. 2003. Ras pathway signaling on endomembranes. *Curr.Opin.Cell Biol.* 15(2), pp. 136-142

Bjelakovic G., Nikolova D., Gluud L.L., Simonetti R.G., Gluud C. 2007. Mortality in randomized trials of antioxidant supplements for primary and secondary prevention: systematic review and meta-analysis. *JAMA* 297(8), pp. 842-857

Blair A., Pamphilon D.H. 2003. Leukaemic stem cells. *Transfus.Med.* 13(6), pp. 363-375

Blanchetot C., Boonstra J. 2008. The ROS-NOX connection in cancer and angiogenesis. *Crit Rev.Eukaryot.Gene Expr.* 18(1), pp. 35-45

Bland J.M., Altman D.G. 1986. Statistical methods for assessing agreement between two methods of clinical measurement. *Lancet* 1(8476), pp. 307-310

Block K., Eid A., Griendling K.K., Lee D.Y., Wittrant Y., Gorin Y. 2008. Nox4 NAD(P)H oxidase mediates Src-dependent tyrosine phosphorylation of PDK-1 in response to angiotensin II: role in mesangial cell hypertrophy and fibronectin expression. *J Biol.Chem.* 283(35), pp. 24061-24076

Block K.I., Koch A.C., Mead M.N., Tothy P.K., Newman R.A., Gyllenhaal C. 2008. Impact of antioxidant supplementation on chemotherapeutic toxicity: a systematic review of the evidence from randomized controlled trials. *Int.J Cancer* 123(6), pp. 1227-1239

Bockstaele L., Bisteau X., Paternot S., Roger P.P. 2009. Differential regulation of cyclin-dependent kinase 4 (CDK4) and CDK6, evidence that CDK4 might not be activated by CDK7, and design of a CDK6 activating mutation. *Mol.Cell Biol.* 29(15), pp. 4188-4200

Bodemann B.O., White M.A. 2008. Ral GTPases and cancer: linchpin support of the tumorigenic platform. *Nat.Rev.Cancer* 8(2), pp. 133-140

Boersma H.H., Kietselaer B.L., Stolk L.M., Bennaghmouch A., Hofstra L., Narula J., Heidendal G.A., Reutelingsperger C.P. 2005. Past, present, and future of annexin A5: from protein discovery to clinical applications. *J.Nucl.Med.* 46(12), pp. 2035-2050

Boissel N., Leroy H., Brethon B., Philippe N., de B.S. et al. 2006. Incidence and prognostic impact of c-Kit, FLT3, and Ras gene mutations in core binding factor acute myeloid leukemia (CBF-AML). *Leukemia* 20(6), pp. 965-970

Borlado L.R., Mendez J. 2008. CDC6: from DNA replication to cell cycle checkpoints and oncogenesis. *Carcinogenesis* 29(2), pp. 237-243

Bowen D., Wang L., Frew M., Kerr R., Groves M. 2003. Antioxidant enzyme expression in myelodysplastic and acute myeloid leukemia bone marrow: further evidence of a pathogenetic role for oxidative stress? *Haematologica* 88(9), pp. 1070-1072

Bowen D.T., Frew M.E., Hills R., Gale R.E., Wheatley K. et al. 2005. RAS mutation in acute myeloid leukemia is associated with distinct cytogenetic subgroups but does not influence outcome in patients younger than 60 years. *Blood* 106(6), pp. 2113-2119

Bowen D.T., Frew M.E., Rollinson S., Roddam P.L., Dring A., Smith M.T., Langabeer S.E., Morgan G.J. 2003. CYP1A1*2B (Val) allele is overrepresented in a subgroup of acute myeloid leukemia patients with poor-risk karyotype associated with NRAS mutation, but not associated with FLT3 internal tandem duplication. *Blood* 101(7), pp. 2770-2774

Bradford M.M. 1976. A rapid and sensitive method for the quantitation of microgram quantities of protein utilizing the principle of protein-dye binding. *Anal.Biochem.* 72, pp. 248-254

Brandon M., Baldi P., Wallace D.C. 2006. Mitochondrial mutations in cancer. *Oncogene* 25(34), pp. 4647-4662

Braun B.S., Tuveson D.A., Kong N., Le D.T., Kogan S.C., Rozmus J., Le Beau M.M., Jacks T.E., Shannon K.M. 2004. Somatic activation of oncogenic Kras in hematopoietic cells initiates a rapidly fatal myeloproliferative disorder. *Proc.Natl.Acad.Sci.U.S.A* 101(2), pp. 597-602

Brognard J., Newton A.C. 2008. PHLiPPing the switch on Akt and protein kinase C signaling. *Trends Endocrinol.Metab* 19(6), pp. 223-230

Brouard N., Chapel A., Neildez-Nguyen T.M., Granotier C., Khazaal I., Peault B., Thierry D. 1998. Transplantation of stromal cells transduced with the human IL3 gene to stimulate hematopoiesis in human fetal bone grafts in non-obese, diabetic-severe combined immunodeficiency mice. *Leukemia* 12(7), pp. 1128-1135

Buchschacher G.L., Jr. 2001. Introduction to retroviruses and retroviral vectors. *Somat.Cell Mol.Genet.* 26(1-6), pp. 1-11

Burdon R.H., Gill V., Rice-Evans C. 1989. Cell proliferation and oxidative stress. *Free Radic.Res.Commun.* 7(3-6), pp. 149-159

Burdon R.H., Gill V., Rice-Evans C. 1990. Oxidative stress and tumour cell proliferation. *Free Radic.Res.Commun.* 11(1-3), pp. 65-76

Burdon R.H., Rice-Evans C. 1989. Free radicals and the regulation of mammalian cell proliferation. *Free Radic.Res.Commun.* 6(6), pp. 345-358

Buske C., Feuring-Buske M., Abramovich C., Spiekermann K., Eaves C.J., Coulombel L., Sauvageau G., Hogge D.E., Humphries R.K. 2002. Deregulated expression of HOXB4 enhances the primitive growth activity of human hematopoietic cells. *Blood* 100(3), pp. 862-868

Cairoli R., Beghini A., Grillo G., Nadali G., Elice F. et al. 2006. Prognostic impact of c-KIT mutations in core binding factor leukemias: an Italian retrospective study. *Blood* 107(9), pp. 3463-3468

Calvi L.M., Adams G.B., Weibrecht K.W., Weber J.M., Olson D.P. et al. 2003. Osteoblastic cells regulate the haematopoietic stem cell niche. *Nature* 425(6960), pp. 841-846

Care R.S., Valk P.J., Goodeve A.C., bu-Duhier F.M., Geertsma-Kleinekoort W.M. et al. 2003. Incidence and prognosis of c-KIT and FLT3 mutations in core binding factor (CBF) acute myeloid leukaemias. *Br.J.Haematol.* 121(5), pp. 775-777

Casamayor A., Morrice N.A., Alessi D.R. 1999. Phosphorylation of Ser-241 is essential for the activity of 3-phosphoinositide-dependent protein kinase-1: identification of five sites of phosphorylation in vivo. *Biochem.J.* 342 (Pt 2), pp. 287-292

Chance B., Hollunger G. 1961. The interaction of energy and electron transfer reactions in mitochondria. I. General properties and nature of the products of succinate-linked reduction of pyridine nucleotide. *J.Biol.Chem.* 236, pp. 1534-1543

Chang E.H., Gonda M.A., Ellis R.W., Scolnick E.M., Lowy D.R. 1982. Human genome contains four genes homologous to transforming genes of Harvey and Kirsten murine sarcoma viruses. *Proc.Natl.Acad.Sci.U.S.A* 79(16), pp. 4848-4852

Chang F., Steelman L.S., Lee J.T., Shelton J.G., Navolanic P.M., Blalock W.L., Franklin R.A., McCubrey J.A. 2003. Signal transduction mediated by the Ras/Raf/MEK/ERK pathway from cytokine receptors to transcription factors: potential targeting for therapeutic intervention. *Leukemia* 17(7), pp. 1263-1293

Chen L., Liu L., Yin J., Luo Y., Huang S. 2009. Hydrogen peroxide-induced neuronal apoptosis is associated with inhibition of protein phosphatase 2A and 5, leading to activation of MAPK pathway. *Int.J.Biochem.Cell Biol.* 41(6), pp. 1284-1295

Cheng M., Olivier P., Diehl J.A., Fero M., Roussel M.F., Roberts J.M., Sherr C.J. 1999. The p21(Cip1) and p27(Kip1) CDK 'inhibitors' are essential activators of cyclin D-dependent kinases in murine fibroblasts. *EMBO J* 18(6), pp. 1571-1583

Chiu V.K., Bivona T., Hach A., Sajous J.B., Silletti J., Wiener H., Johnson R.L., Cox A.D., Philips M.R. 2002. Ras signalling on the endoplasmic reticulum and the Golgi. *Nat.Cell Biol.* 4(5), pp. 343-350

Choi J., Liu R.M., Forman H.J. 1997. Adaptation to oxidative stress: quinone-mediated protection of signaling in rat lung epithelial L2 cells. *Biochem.Pharmacol.* 53(7), pp. 987-993

Cobas M., Wilson A., Ernst B., Mancini S.J., Macdonald H.R., Kemler R., Radtke F. 2004. Beta-catenin is dispensable for hematopoiesis and lymphopoiesis. *J Exp.Med.* 199(2), pp. 221-229

Collins S.J., Gallo R.C., Gallagher R.E. 1977. Continuous growth and differentiation of human myeloid leukaemic cells in suspension culture. *Nature* 270(5635), pp. 347-349

Collins S.J., Ruscetti F.W., Gallagher R.E., Gallo R.C. 1978. Terminal differentiation of human promyelocytic leukemia cells induced by dimethyl sulfoxide and other polar compounds. *Proc.Natl.Acad.Sci.U.S.A* 75(5), pp. 2458-2462

Corral D.A., Amling M., Priemel M., Loyer E., Fuchs S., Ducy P., Baron R., Karsenty G. 1998. Dissociation between bone resorption and bone formation in osteopenic transgenic mice. *Proc.Natl.Acad.Sci.U.S.A* 95(23), pp. 13835-13840

Cortez D., Stoica G., Pierce J.H., Pendergast A.M. 1996. The bcr-abl tyrosine kinase inhibits apoptosis by activating a ras- dependent signaling pathway. *Oncogene* 13, pp. 2589-2594

Costantini P., Belzacq A.S., Vieira H.L., Larochette N., de Pablo M.A., Zamzami N., Susin S.A., Brenner C., Kroemer G. 2000. Oxidation of a critical thiol residue of the adenine nucleotide translocator enforces Bcl-2-independent permeability transition pore opening and apoptosis. *Oncogene* 19(2), pp. 307-314

Coulon S., Vandekerckhove J., Dussiot M., Callens C., Suarez F. et al. 2007. Human erythroleukemia: is the two-hit model of mouse leukemogenesis valid in human disease? *Leukemia* 21(10), pp. 2212-2214

D'Autreaux B., Toledano M.B. 2007. ROS as signalling molecules: mechanisms that generate specificity in ROS homeostasis. *Nat Rev.Mol.Cell Biol.* 8(10), pp. 813-824

Dao C., Metcalf D., Bilski-Pasquier G. 1977a. Eosinophil and neutrophil colony-forming cells in culture. *Blood* 50(5), pp. 833-839

Dao C., Metcalf D., Zittoun R., Bilski-Pasquier G. 1977b. Normal human bone marrow cultures in vitro: cellular composition and maturation of the granulocytic colonies. *Br.J.Haematol.* 37(1), pp. 127-136

Dao M.A., Nolta J.A. 1999. Immunodeficient mice as models of human hematopoietic stem cell engraftment. *Curr.Opin.Immunol.* 11(5), pp. 532-537

Darley R.L., Hoy T.G., Baines P., Padua R.A., Burnett A.K. 1997. Mutant N-RAS induces erythroid lineage dysplasia in human $CD34^{+}$ cells. *J.Exp.Med.* 185(7), pp. 1337-1347

Darley R.L., Pearn L., Omidvar N., Sweeney M., Fisher J., Phillips S., Hoy T., Burnett A.K. 2002. Protein kinase C mediates mutant N-Ras-induced developmental abnormalities in normal human erythroid cells. *Blood* 100(12), pp. 4185-4192

Davies H., Bignell G.R., Cox C., Stephens P., Edkins S. et al. 2002. Mutations of the BRAF gene in human cancer. *Nature* 417(6892), pp. 949-954

De Braekeleer M., Morel F., Le Bris M.J., Herry A., Douet-Guilbert N. 2005. The MLL gene and translocations involving chromosomal band 11q23 in acute leukemia. *Anticancer Res.* 25(3B), pp. 1931-1944

de Carvalho D.D., Sadok A., Bourgarel-Rey V., Gattacceca F., Penel C., Lehmann M., Kovacic H. 2008. Nox1 downstream of 12-lipoxygenase controls cell proliferation but not cell spreading of colon cancer cells. *Int.J Cancer* 122(8), pp. 1757-1764

DeCoursey T.E., Ligeti E. 2005. Regulation and termination of NADPH oxidase activity. *Cell Mol.Life Sci.* 62(19-20), pp. 2173-2193

DeFeo D., Gonda M.A., Young H.A., Chang E.H., Lowy D.R., Scolnick E.M., Ellis R.W. 1981. Analysis of two divergent rat genomic clones homologous to the transforming gene of Harvey murine sarcoma virus. *Proc.Natl.Acad.Sci.U.S.A* 78(6), pp. 3328-3332

DeKoter R.P., Singh H. 2000. Regulation of B lymphocyte and macrophage development by graded expression of PU.1. *Science* 288(5470), pp. 1439-1441

den Hertog J., Groen A., van der W.T. 2005. Redox regulation of protein-tyrosine phosphatases. *Arch.Biochem.Biophys.* 434(1), pp. 11-15

den Hertog J., Ostman A., Bohmer F.D. 2008. Protein tyrosine phosphatases: regulatory mechanisms. *FEBS J.* 275(5), pp. 831-847

Deng Q., Liao R., Wu B.L., Sun P. 2004. High intensity ras signaling induces premature senescence by activating p38 pathway in primary human fibroblasts. *J.Biol.Chem.* 279(2), pp. 1050-1059

DePinho R.A. 2000. The age of cancer. *Nature* 408(6809), pp. 248-254

Der C.J., Krontiris T.G., Cooper G.M. 1982. Transforming genes of human bladder and lung carcinoma cell lines are homologous to the ras genes of Harvey and Kirsten sarcoma viruses. *Proc.Natl.Acad.Sci.U.S.A* 79(11), pp. 3637-3640

Dick J.E. 1996. Human stem cell assays in immune-deficient mice. *Curr.Opin.Hematol.* 3(6), pp. 405-409

Dick J.E. 2005. Acute myeloid leukemia stem cells. *Ann.N.Y.Acad.Sci.* 1044, pp. 1-5

Dick J.E., Magli M.C., Huszar D., Phillips R.A., Bernstein A. 1985. Introduction of a selectable gene into primitive stem cells capable of long-term reconstitution of the hemopoietic system of W/Wv mice. *Cell* 42(1), pp. 71-79

Diehn M., Cho R.W., Lobo N.A., Kalisky T., Dorie M.J. et al. 2009. Association of reactive oxygen species levels and radioresistance in cancer stem cells. *Nature* 458(7239), pp. 780-783

Dikalov S., Jiang J., Mason R.P. 2005. Characterization of the high-resolution ESR spectra of superoxide radical adducts of 5-(diethoxyphosphoryl)-5-methyl-1-pyrroline N-oxide (DEPMPO) and 5,5-dimethyl-1-pyrroline N-oxide (DMPO). Analysis of conformational exchange. *Free Radic.Res.* 39(8), pp. 825-836

Dodd S., Dean O., Copolov D.L., Malhi G.S., Berk M. 2008. N-acetylcysteine for antioxidant therapy: pharmacology and clinical utility. *Expert.Opin.Biol.Ther.* 8(12), pp. 1955-1962

Doepfner K.T., Boller D., Arcaro A. 2007. Targeting receptor tyrosine kinase signaling in acute myeloid leukemia. *Crit Rev.Oncol.Hematol.* 63(3), pp. 215-230

Dolado I., Swat A., Ajenjo N., De V.G., Cuadrado A., Nebreda A.R. 2007. p38alpha MAP kinase as a sensor of reactive oxygen species in tumorigenesis. *Cancer Cell* 11(2), pp. 191-205

Dorrell C., Takenaka K., Minden M.D., Hawley R.G., Dick J.E. 2004. Hematopoietic cell fate and the initiation of leukemic properties in primitive primary human cells are influenced by Ras activity and farnesyltransferase inhibition. *Mol.Cell Biol.* 24(16), pp. 6993-7002

Drapkin R., Le R.G., Cho H., Akoulitchev S., Reinberg D. 1996. Human cyclin-dependent kinase-activating kinase exists in three distinct complexes. *Proc.Natl.Acad.Sci.U.S.A* 93(13), pp. 6488-6493

Droge W. 2002. Free radicals in the physiological control of cell function. *Physiol Rev.* 82(1), pp. 47-95

Dudler T., Gelb M.H. 1996. Palmitoylation of Ha-Ras facilitates membrane binding, activation of downstream effectors, and meiotic maturation in Xenopus oocytes. *J.Biol.Chem.* 271(19), pp. 11541-11547

Dusi S., Donini M., Rossi F. 1996. Mechanisms of NADPH oxidase activation: translocation of p40phox, Rac1 and Rac2 from the cytosol to the membranes in human neutrophils lacking p47phox or p67phox. *Biochem.J.* 314 (Pt 2), pp. 409-412

Ellis R.W., DeFeo D., Furth M.E., Scolnick E.M. 1982. Mouse cells contain two distinct ras gene mRNA species that can be translated into a p21 onc protein. *Mol.Cell Biol.* 2(11), pp. 1339-1345

Emmendorffer A., Roesler J., Elsner J., Raeder E., Lohmann-Matthes M.L., Meier B. 1993. Production of oxygen radicals by fibroblasts and neutrophils from a patient with x-linked chronic granulomatous disease. *Eur.J.Haematol.* 51(4), pp. 223-227

Er T.K., Tsai S.M., Wu S.H., Chiang W., Lin H.C., Lin S.F., Wu S.H., Tsai L.Y., Liu T.Z. 2007. Antioxidant status and superoxide anion radical generation in acute myeloid leukemia. *Clin.Biochem.* 40(13-14), pp. 1015-1019

Esteban L.M., Vicario-Abejon C., Fernandez-Salguero P., Fernandez-Medarde A., Swaminathan N. et al. 2001. Targeted genomic disruption of H-ras and N-ras, individually or in combination, reveals the dispensability of both loci for mouse growth and development. *Mol.Cell Biol.* 21(5), pp. 1444-1452

Estey E., Dohner H. 2006. Acute myeloid leukaemia. *Lancet* 368(9550), pp. 1894-1907

Estey E., Thall P., Beran M., Kantarjian H., Pierce S., Keating M. 1997. Effect of diagnosis (refractory anemia with excess blasts, refractory anemia with excess blasts in transformation, or acute myeloid leukemia [AML]) on outcome of AML-type chemotherapy. *Blood* 90(8), pp. 2969-2977

Evans C.A., Pierce A., Winter S.A., Spooncer E., Heyworth C.M., Whetton A.D. 1999. Activation of granulocyte-macrophage colony-stimulating factor and interleukin-3 receptor subunits in a multipotential hematopoietic progenitor cell line leads to differential effects on development. *Blood* 94(5), pp. 1504-1514

Evans T., Rosenthal E.T., Youngblom J., Distel D., Hunt T. 1983. Cyclin: a protein specified by maternal mRNA in sea urchin eggs that is destroyed at each cleavage division. *Cell* 33(2), pp. 389-396

Farquhar M.J., Bowen D.T. 2003. Oxidative stress and the myelodysplastic syndromes. *Int.J.Hematol.* 77(4), pp. 342-350

Faulkner K., Fridovich I. 1993. Luminol and lucigenin as detectors for O2.-. *Free Radic.Biol.Med.* 15(4), pp. 447-451

Feldman R.I., Wu J.M., Polokoff M.A., Kochanny M.J., Dinter H. et al. 2005. Novel small molecule inhibitors of 3-phosphoinositide-dependent kinase-1. *J Biol.Chem.* 280(20), pp. 19867-19874

Fenton H.J.H. 1894. Oxidation of tartaric acid in presence of iron. *J.Chem.Soc.Trans.* 65(65), pp. 899-911

Fidler C., Watkins F., Bowen D.T., Littlewood T.J., Wainscoat J.S., Boultwood J. 2004. NRAS, FLT3 and TP53 mutations in patients with myelodysplastic syndrome and a del(5q). *Haematologica* 89(7), pp. 865-866

Finch J.S., Tome M.E., Kwei K.A., Bowden G.T. 2006. Catalase reverses tumorigenicity in a malignant cell line by an epidermal growth factor receptor pathway. *Free Radic.Biol.Med.* 40(5), pp. 863-875

Finkel T. 2003. Oxidant signals and oxidative stress. *Curr.Opin.Cell Biol.* 15(2), pp. 247-254

Flynn P.J., Miller W.J., Weisdorf D.J., Arthur D.C., Brunning R., Branda R.F. 1983. Retinoic acid treatment of acute promyelocytic leukemia: in vitro and in vivo observations. *Blood* 62(6), pp. 1211-1217

Foley T.D., Petro L.A., Stredny C.M., Coppa T.M. 2007. Oxidative inhibition of protein phosphatase 2A activity: role of catalytic subunit disulfides. *Neurochem.Res.* 32(11), pp. 1957-1964

Frejaville C., Karoui H., Tuccio B., Le M.F., Culcasi M., Pietri S., Lauricella R., Tordo P. 1995. 5-(Diethoxyphosphoryl)-5-methyl-1-pyrroline N-oxide: a new efficient phosphorylated nitrone for the in vitro and in vivo spin trapping of oxygen-centered radicals. *J.Med.Chem.* 38(2), pp. 258-265

Fresno Vara J.A., Casado E., De C.J., Cejas P., Belda-Iniesta C., Gonzalez-Baron M. 2004. PI3K/Akt signalling pathway and cancer. *Cancer Treat.Rev.* 30(2), pp. 193-204

Frisch B.J., Porter R.L., Gigliotti B.J., Olm-Shipman A.J., Weber J.M., O'Keefe R.J., Jordan C.T., Calvi L.M. 2009. In vivo prostaglandin E2 treatment alters the bone marrow microenvironment and preferentially expands short-term hematopoietic stem cells. *Blood*

Frohling S., Schlenk R.F., Breitruck J., Benner A., Kreitmeier S., Tobis K., Dohner H., Dohner K. 2002. Prognostic significance of activating FLT3 mutations in younger adults (16 to 60 years) with acute myeloid leukemia and normal cytogenetics: a study of the AML Study Group Ulm. *Blood* 100(13), pp. 4372-4380

Fruehauf J.P., Meyskens F.L., Jr. 2007. Reactive oxygen species: a breath of life or death? *Clin.Cancer Res.* 13(3), pp. 789-794

Fruehauf J.P., Trapp V. 2008. Reactive oxygen species: an Achilles' heel of melanoma? *Expert.Rev.Anticancer Ther.* 8(11), pp. 1751-1757

Fujita N., Sato S., Ishida A., Tsuruo T. 2002. Involvement of Hsp90 in signaling and stability of 3-phosphoinositide-dependent kinase-1. *J Biol.Chem.* 277(12), pp. 10346-10353

Fukuda S., Foster R.G., Porter S.B., Pelus L.M. 2002. The antiapoptosis protein survivin is associated with cell cycle entry of normal cord blood CD34(+) cells and modulates cell cycle and proliferation of mouse hematopoietic progenitor cells. *Blood* 100(7), pp. 2463-2471

Fukuda S., Pelus L.M. 2004. Activated H-Ras regulates hematopoietic cell survival by modulating Survivin. *Biochem.Biophys.Res.Commun.* 323(2), pp. 636-644

Fukukawa C., Shima H., Tanuma N., Okada T., Kato N., Adachi Y., Kikuchi K. 2005. The oncoprotein I-2PP2A/SET negatively regulates the MEK/ERK pathway and cell proliferation. *Int.J.Oncol.* 26(3), pp. 751-756

Furukawa Y. 2002. Cell cycle control genes and hematopoietic cell differentiation. *Leuk.Lymphoma* 43(2), pp. 225-231

Gallagher A., Darley R., Padua R.A. 1997. RAS and the myelodysplastic syndromes. *Pathol.Biol.(Paris)* 45(7), pp. 561-568

Gallogly M.M., Mieyal J.J. 2007. Mechanisms of reversible protein glutathionylation in redox signaling and oxidative stress. *Curr.Opin.Pharmacol.* 7(4), pp. 381-391

Gardini A., Cesaroni M., Luzi L., Okumura A.J., Biggs J.R. et al. 2008. AML1/ETO oncoprotein is directed to AML1 binding regions and co-localizes with AML1 and HEB on its targets. *PLoS.Genet.* 4(11), pge1000275

Gauss K.A., Bunger P.L., Quinn M.T. 2002. AP-1 is essential for p67(phox) promoter activity. *J.Leukoc.Biol.* 71(1), pp. 163-172

Genova M.L., Bianchi C., Lenaz G. 2003. Structural organization of the mitochondrial respiratory chain. *Ital.J.Biochem.* 52(1), pp. 58-61

Gibbs J.B., Sigal I.S., Poe M., Scolnick E.M. 1984. Intrinsic GTPase activity distinguishes normal and oncogenic ras p21 molecules. *Proc.Natl.Acad.Sci.U.S.A* 81(18), pp. 5704-5708

Gilliland D.G. 2001. Hematologic malignancies. *Curr.Opin.Hematol.* 8(4), pp. 189-191

Goel A., Arnold C.N., Niedzwiecki D., Carethers J.M., Dowell J.M. et al. 2004. Frequent inactivation of PTEN by promoter hypermethylation in microsatellite instability-high sporadic colorectal cancers. *Cancer Res.* 64(9), pp. 3014-3021

Goemans B.F., Zwaan C.M., Miller M., Zimmermann M., Harlow A. et al. 2005. Mutations in KIT and RAS are frequent events in pediatric core-binding factor acute myeloid leukemia. *Leukemia* 19(9), pp. 1536-1542

Gougopoulou D.M., Kiaris H., Ergazaki M., Anagnostopoulos N.I., Grigoraki V., Spandidos D.A. 1996. Mutations and expression of the ras family genes in leukemias. *Stem Cells* 14(6), pp. 725-729

Grandori C., Cowley S.M., James L.P., Eisenman R.N. 2000. The Myc/Max/Mad network and the transcriptional control of cell behavior. *Annu.Rev.Cell Dev.Biol.* 16, pp. 653-699

Grignani F., Kinsella T., Mencarelli A., Valtieri M., Riganelli D. et al. 1998. High-efficiency gene transfer and selection of human hematopoietic progenitor cells with a hybrid EBV/retroviral vector expressing the green fluorescence protein. *Cancer Res.* 58(1), pp. 14-19

Grimwade D., Walker H., Harrison G., Oliver F., Chatters S., Harrison C.J., Wheatley K., Burnett A.K., Goldstone A.H. 2001. The predictive value of hierarchical cytogenetic classification in older adults with acute myeloid leukemia (AML): analysis of 1065 patients entered into the United Kingdom Medical Research Council AML11 trial. *Blood* 98(5), pp. 1312-1320

Grimwade D., Walker H., Oliver F., Wheatley K., Harrison C. et al. 1998. The importance of diagnostic cytogenetics on outcome in AML: analysis of 1,612 patients entered into the MRC AML 10 trial. The Medical Research Council Adult and Children's Leukaemia Working Parties. *Blood* 92(7), pp. 2322-2333

Grivennikova V.G., Vinogradov A.D. 2006. Generation of superoxide by the mitochondrial Complex I. *Biochim.Biophys.Acta* 1757(5-6), pp. 553-561

Groeger G., Mackey A.M., Pettigrew C.A., Bhatt L., Cotter T.G. 2009. Stress induced activation of Nox contributes to cell survival signalling via production of hydrogen peroxide. *J Neurochem.*

Guerrero I., Calzada P., Mayer A., Pellicer A. 1984a. A molecular approach to leukemogenesis: mouse lymphomas contain an activated c-ras oncogene. *Proc.Natl.Acad.Sci.U.S.A* 81(1), pp. 202-205

Guerrero I., Villasante A., Corces V., Pellicer A. 1984b. Activation of a c-K-ras oncogene by somatic mutation in mouse lymphomas induced by gamma radiation. *Science* 225(4667), pp. 1159-1162

Guzman M.L., Rossi R.M., Karnischky L., Li X., Peterson D.R., Howard D.S., Jordan C.T. 2005. The sesquiterpene lactone parthenolide induces apoptosis of human acute myelogenous leukemia stem and progenitor cells
1. *Blood* 105(11), pp. 4163-4169

Haber F., Weiss J. 1932. Über die Katalyse des Hydroperoxydes. *Naturwissenschaften*

Hacker E., Muller H.K., Irwin N., Gabrielli B., Lincoln D. et al. 2006. Spontaneous and UV radiation-induced multiple metastatic melanomas in Cdk4R24C/R24C/TPras mice. *Cancer Res.* 66(6), pp. 2946-2952

Hall A., Marshall C.J., Spurr N.K., Weiss R.A. 1983. Identification of transforming gene in two human sarcoma cell lines as a new member of the ras gene family located on chromosome 1. *Nature* 303(5916), pp. 396-400

Han M., Golden A., Han Y., Sternberg P.W. 1993. C. elegans lin-45 raf gene participates in let-60 ras-stimulated vulval differentiation. *Nature* 363(6425), pp. 133-140

Hanahan D., Weinberg R.A. 2000. The hallmarks of cancer. *Cell* 100(1), pp. 57-70

Hancock J.F., Paterson H., Marshall C.J. 1990. A polybasic domain or palmitoylation is required in addition to the CAAX motif to localize p21ras to the plasma membrane. *Cell* 63(1), pp. 133-139

Harir N., Pecquet C., Kerenyi M., Sonneck K., Kovacic B. et al. 2007. Constitutive activation of Stat5 promotes its cytoplasmic localization and association with PI3-kinase in myeloid leukemias. *Blood* 109(4), pp. 1678-1686

Havens C.G., Ho A., Yoshioka N., Dowdy S.F. 2006. Regulation of late G1/S phase transition and APC Cdh1 by reactive oxygen species. *Mol.Cell Biol.* 26(12), pp. 4701-4711

Hewamana S., Lin T.T., Jenkins C., Burnett A.K., Jordan C.T., Fegan C., Brennan P., Rowntree C., Pepper C. 2008. The novel nuclear factor-kappaB inhibitor LC-1 is equipotent in poor prognostic subsets of chronic lymphocytic leukemia and shows strong synergy with fludarabine. *Clin.Cancer Res.* 14(24), pp. 8102-8111

Heyworth C.M., Alauldin M., Cross M.A., Fairbairn L.J., Dexter T.M., Whetton A.D. 1995. Erythroid development of the FDCP-Mix A4 multipotent cell line is governed by the relative concentrations of erythropoietin and interleukin 3. *Br.J.Haematol.* 91(1), pp. 15-22

Heyworth C.M., Hampson J., Dexter T.M., Walker F., Burgess A.W., Kan O., Cook N., Vallance S.J., Whetton A.D. 1991. Development of multipotential haemopoietic stem cells to neutrophils is associated with increased expression of receptors for granulocyte macrophage colony-stimulating factor: altered biological responses to GM-CSF during development. *Growth Factors* 5(2), pp. 87-98

Heyworth P.G., Curnutte J.T., Nauseef W.M., Volpp B.D., Pearson D.W., Rosen H., Clark R.A. 1991. Neutrophil nicotinamide adenine dinucleotide phosphate oxidase assembly. Translocation of p47-phox and p67-phox requires interaction between p47-phox and cytochrome b558. *J.Clin.Invest* 87(1), pp. 352-356

Hisakawa H., Sugiyama D., Nishijima I., Xu M.J., Wu H. et al. 2001. Human granulocyte-macrophage colony-stimulating factor (hGM-CSF) stimulates primitive and definitive erythropoiesis in mouse embryos expressing hGM-CSF receptors but not erythropoietin receptors. *Blood* 98(13), pp. 3618-3625

Hoang B., Zhu L., Shi Y., Frost P., Yan H. et al. 2006. Oncogenic RAS mutations in myeloma cells selectively induce cox-2 expression, which participates in enhanced adhesion to fibronectin and chemoresistance. *Blood* 107(11), pp. 4484-4490

Hock H., Hamblen M.J., Rooke H.M., Traver D., Bronson R.T., Cameron S., Orkin S.H. 2003. Intrinsic requirement for zinc finger transcription factor Gfi-1 in neutrophil differentiation. *Immunity.* 18(1), pp. 109-120

Hofer F., Fields S., Schneider C., Martin G.S. 1994. Activated Ras interacts with the Ral guanine nucleotide dissociation stimulator. *Proc.Natl.Acad.Sci.U.S.A* 91(23), pp. 11089-11093

Hosokawa K., Arai F., Yoshihara H., Nakamura Y., Gomei Y. et al. 2007. Function of oxidative stress in the regulation of hematopoietic stem cell-niche interaction. *Biochem.Biophys.Res.Commun.* 363(3), pp. 578-583

Hsu Y.H., Chen J.J., Chang N.C., Chen C.H., Liu J.C., Chen T.H., Jeng C.J., Chao H.H., Cheng T.H. 2004. Role of reactive oxygen species-sensitive extracellular signal-regulated kinase pathway in angiotensin II-induced endothelin-1 gene expression in vascular endothelial cells. *J.Vasc.Res.* 41(1), pp. 64-74

Ichikawa M., Asai T., Saito T., Seo S., Yamazaki I. et al. 2004. AML-1 is required for megakaryocytic maturation and lymphocytic differentiation, but not for maintenance of hematopoietic stem cells in adult hematopoiesis. *Nat.Med.* 10(3), pp. 299-304

Iiyama M., Kakihana K., Kurosu T., Miura O. 2006. Reactive oxygen species generated by hematopoietic cytokines play roles in activation of receptor-mediated signaling and in cell cycle progression. *Cell Signal.* 18(2), pp. 174-182

Ikebuchi Y., Masumoto N., Tasaka K., Koike K., Kasahara K., Miyake A., Tanizawa O. 1991. Superoxide anion increases intracellular pH, intracellular free calcium, and arachidonate release in human amnion cells. *J Biol.Chem.* 266(20), pp. 13233-13237

Illmer T., Thiede C., Fredersdorf A., Stadler S., Neubauer A., Ehninger G., Schaich M. 2005. Activation of the RAS Pathway Is Predictive for a Chemosensitive Phenotype of Acute Myelogenous Leukemia Blasts. *Clin.Cancer Res.* 11(9), pp. 3217-3224

Imamura N., Kuramoto A., Ishihara H., Shimizu S. 1993. Detection of high incidence of H-RAS oncogene point mutations in acute myelogenous leukemia. *Am.J.Hematol.* 43(2), pp. 151-153

Indo H.P., Davidson M., Yen H.C., Suenaga S., Tomita K. et al. 2007. Evidence of ROS generation by mitochondria in cells with impaired electron transport chain and mitochondrial DNA damage. *Mitochondrion.* 7(1-2), pp. 106-118

Irani K., Xia Y., Zweier J.L., Sollott S.J., Der C.J., Fearon E.R., Sundaresan M., Finkel T., Goldschmidt-Clermont P.J. 1997. Mitogenic signaling mediated by oxidants in Ras-transformed fibroblasts. *Science* 275(5306), pp. 1649-1652

Ishikawa K., Takenaga K., Akimoto M., Koshikawa N., Yamaguchi A., Imanishi H., Nakada K., Honma Y., Hayashi J. 2008. ROS-generating mitochondrial DNA mutations can regulate tumor cell metastasis. *Science* 320(5876), pp. 661-664

Ito K., Hirao A., Arai F., Matsuoka S., Takubo K. et al. 2004. Regulation of oxidative stress by ATM is required for self-renewal of haematopoietic stem cells. *Nature* 431(7011), pp. 997-1002

Iwasaki-Arai J., Iwasaki H., Miyamoto T., Watanabe S., Akashi K. 2003. Enforced granulocyte/macrophage colony-stimulating factor signals do not support lymphopoiesis, but instruct lymphoid to myelomonocytic lineage conversion. *J.Exp.Med.* 197(10), pp. 1311-1322

Iyer G.Y.N., Islam M.F., Quastel J.H. 1961. Biochemical Aspects of Phagocytosis. *Nature* 192(4802), pp. 535-541

Jackson M.D., Denu J.M. 2001. Molecular reactions of protein phosphatases--insights from structure and chemistry. *Chem.Rev.* 101(8), pp. 2313-2340

Jaffe E.S. et al. 2001. *World Health Organization Classification of Tumours: Pathology and Genetics of Tumours of Haematopoietic and Lymphoid Tissues.* Lyon: IARC Press

Jenkins C., Hewamana S., Gilkes A., Neelakantan S., Crooks P., Mills K., Pepper C., Burnett A. 2008. Nuclear factor-kappaB as a potential therapeutic target for the novel cytotoxic agent LC-1 in acute myeloid leukaemia. *Br.J Haematol.* 143(5), pp. 661-671

Johnson J.E., Goulding R.E., Ding Z., Partovi A., Anthony K.V., Beaulieu N., Tazmini G., Cornell R.B., Kay R.J. 2007. Differential membrane binding and diacylglycerol recognition by C1 domains of RasGRPs. *Biochem.J.* 406(2), pp. 223-236

Jude C.D., Climer L., Xu D., Artinger E., Fisher J.K., Ernst P. 2007. Unique and independent roles for MLL in adult hematopoietic stem cells and progenitors. *Cell Stem Cell* 1(3), pp. 324-337

Kamel-Reid S., Dick J.E. 1988. Engraftment of immune-deficient mice with human hematopoietic stem cells. *Science* 242(4886), pp. 1706-1709

Kamiguti A.S., Serrander L., Lin K., Harris R.J., Cawley J.C., Allsup D.J., Slupsky J.R., Krause K.H., Zuzel M. 2005. Expression and activity of NOX5 in the circulating malignant B cells of hairy cell leukemia. *J.Immunol.* 175(12), pp. 8424-8430

Karnoub A.E., Weinberg R.A. 2008. Ras oncogenes: split personalities. *Nat.Rev.Mol.Cell Biol.* 9(7), pp. 517-531

Kastan M.B., Bartek J. 2004. Cell-cycle checkpoints and cancer. *Nature* 432(7015), pp. 316-323

Kato M., Minakami H., Kuroiwa M., Kobayashi Y., Oshima S., Kozawa K., Morikawa A., Kimura H. 2003. Superoxide radical generation and Mn- and Cu-Zn superoxide dismutases activities in human leukemic cells. *Hematol.Oncol.* 21(1), pp. 11-16

Kaufman T.C. 1978. Cytogenetic Analysis of Chromosome 3 in Drosophila melanogaster: Isolation and Characterization of Four New Alleles of the Proboscipedia (pb) Locus. *Genetics* 90(3), pp. 579-596

Kautz B., Kakar R., David E., Eklund E.A. 2001. SHP1 protein-tyrosine phosphatase inhibits gp91PHOX and p67PHOX expression by inhibiting interaction of PU.1, IRF1, interferon consensus sequence-binding protein, and CREB-binding protein with homologous Cis elements in the CYBB and NCF2 genes. *J.Biol.Chem.* 276(41), pp. 37868-37878

Kawaguchi H., Raisz L.G., Voznesensky O.S., Alander C.B., Hakeda Y., Pilbeam C.C. 1994. Regulation of the two prostaglandin G/H synthases by parathyroid hormone, interleukin-1, cortisol, and prostaglandin E2 in cultured neonatal mouse calvariae. *Endocrinology* 135(3), pp. 1157-1164

Kelley G.G., Reks S.E., Ondrako J.M., Smrcka A.V. 2001. Phospholipase C(epsilon): a novel Ras effector. *EMBO J.* 20(4), pp. 743-754

Kelly L.M., Gilliland D.G. 2002. Genetics of myeloid leukemias. *Annu.Rev.Genomics Hum.Genet.* 3, pp. 179-198

Keranen L.M., Dutil E.M., Newton A.C. 1995. Protein kinase C is regulated in vivo by three functionally distinct phosphorylations. *Curr.Biol.* 5(12), pp. 1394-1403

Khandrika L., Kumar B., Koul S., Maroni P., Koul H.K. 2009. Oxidative stress in prostate cancer. *Cancer Lett.* 282(2), pp. 125-136

Kiel M.J., Morrison S.J. 2008. Uncertainty in the niches that maintain haematopoietic stem cells. *Nat.Rev.Immunol.* 8(4), pp. 290-301

Kiel M.J., Yilmaz O.H., Iwashita T., Yilmaz O.H., Terhorst C., Morrison S.J. 2005. SLAM family receptors distinguish hematopoietic stem and progenitor cells and reveal endothelial niches for stem cells. *Cell* 121(7), pp. 1109-1121

Kill I.R., Hutchison C.J. 1995. S-phase phosphorylation of lamin B2. *FEBS Lett.* 377(1), pp. 26-30

Kim C., Kim J.Y., Kim J.H. 2008. Cytosolic phospholipase A(2), lipoxygenase metabolites, and reactive oxygen species. *BMB.Rep.* 41(8), pp. 555-559

Kim H.J., Chakravarti N., Oridate N., Choe C., Claret F.X., Lotan R. 2006. N-(4-hydroxyphenyl)retinamide-induced apoptosis triggered by reactive oxygen species is mediated by activation of MAPKs in head and neck squamous carcinoma cells. *Oncogene* 25(19), pp. 2785-2794

Kim H.J., Oridate N., Lotan R. 2005. Increased level of the p67phox subunit of NADPH oxidase by 4HPR in head and neck squamous carcinoma cells. *Int.J.Oncol.* 27(3), pp. 787-790

Kim H.S., Song M.C., Kwak I.H., Park T.J., Lim I.K. 2003. Constitutive induction of p-Erk1/2 accompanied by reduced activities of protein phosphatases 1 and 2A and MKP3 due to reactive oxygen species during cellular senescence. *J.Biol.Chem.* 278(39), pp. 37497-37510

Kim J.H., Chu S.C., Gramlich J.L., Pride Y.B., Babendreier E. et al. 2005. Activation of the PI3K/mTOR pathway by BCR-ABL contributes to increased production of reactive oxygen species. *Blood* 105(4), pp. 1717-1723

Kinsella T.M., Nolan G.P. 1996. Episomal vectors rapidly and stably produce high-titer recombinant retrovirus. *Hum.Gene Ther.* 7(12), pp. 1405-1413

Kirkman H.N., Gaetani G.F. 2007. Mammalian catalase: a venerable enzyme with new mysteries. *Trends Biochem.Sci.* 32(1), pp. 44-50

Kiyoi H., Naoe T., Nakano Y., Yokota S., Minami S. et al. 1999. Prognostic implication of FLT3 and N-RAS gene mutations in acute myeloid leukemia. *Blood* 93, pp. 3074-3080

Knapper S. 2007. FLT3 inhibition in acute myeloid leukaemia. *Br.J.Haematol.* 138(6), pp. 687-699

Knapper S., Mills K.I., Gilkes A.F., Austin S.J., Walsh V., Burnett A.K. 2006. The effects of lestaurtinib (CEP701) and PKC412 on primary AML blasts: the induction of cytotoxicity varies with dependence on FLT3 signaling in both FLT3-mutated and wild-type cases. *Blood* 108(10), pp. 3494-3503

Koera K., Nakamura K., Nakao K., Miyoshi J., Toyoshima K., Hatta T., Otani H., Aiba A., Katsuki M. 1997. K-ras is essential for the development of the mouse embryo. *Oncogene* 15(10), pp. 1151-1159

Komatsu H., Obata F. 2003. An optimized method for determination of intracellular glutathione in mouse macrophage cultures by fluorimetric high-performance liquid chromatography. *Biomed.Chromatogr.* 17(5), pp. 345-350

Kopnin P.B., Agapova L.S., Kopnin B.P., Chumakov P.M. 2007. Repression of sestrin family genes contributes to oncogenic Ras-induced reactive oxygen species up-regulation and genetic instability. *Cancer Res.* 67(10), pp. 4671-4678

Kopp H.G., Avecilla S.T., Hooper A.T., Rafii S. 2005. The bone marrow vascular niche: home of HSC differentiation and mobilization. *Physiology.(Bethesda.)* 20, pp. 349-356

Koppenol W.H. 2001. The Haber-Weiss cycle--70 years later. *Redox.Rep.* 6(4), pp. 229-234

Kottaridis P.D., Gale R.E., Frew M.E., Harrison G., Langabeer S.E. et al. 2001. The presence of a FLT3 internal tandem duplication in patients with acute myeloid leukemia (AML) adds important prognostic information to cytogenetic risk group and response to the first cycle of chemotherapy: analysis of 854 patients from the United Kingdom Medical Research Council AML 10 and 12 trials. *Blood* 98(6), pp. 1752-1759

Kozar K., Ciemerych M.A., Rebel V.I., Shigematsu H., Zagozdzon A. et al. 2004. Mouse development and cell proliferation in the absence of D-cyclins. *Cell* 118(4), pp. 477-491

Krengel U., Schlichting I., Scherer A., Schumann R., Frech M., John J., Kabsch W., Pai E.F., Wittinghofer A. 1990. Three-dimensional structures of H-ras p21 mutants: molecular basis for their inability to function as signal switch molecules. *Cell* 62(3), pp. 539-548

Kumar B., Koul S., Khandrika L., Meacham R.B., Koul H.K. 2008. Oxidative stress is inherent in prostate cancer cells and is required for aggressive phenotype. *Cancer Res.* 68(6), pp. 1777-1785

Kwon J., Lee S.R., Yang K.S., Ahn Y., Kim Y.J., Stadtman E.R., Rhee S.G. 2004. Reversible oxidation and inactivation of the tumor suppressor PTEN in cells stimulated with peptide growth factors. *Proc.Natl.Acad.Sci.U.S.A* 101(47), pp. 16419-16424

Kwong J., Hong L., Liao R., Deng Q., Han J., Sun P. 2009. p38{alpha} and p38{gamma} Mediate Oncogenic ras-induced Senescence through Differential Mechanisms. *J.Biol.Chem.* 284(17), pp. 11237-11246

LaBaer J., Garrett M.D., Stevenson L.F., Slingerland J.M., Sandhu C., Chou H.S., Fattaey A., Harlow E. 1997. New functional activities for the p21 family of CDK inhibitors. *Genes Dev.* 11(7), pp. 847-862

Lambeth J.D. 2004. NOX enzymes and the biology of reactive oxygen. *Nat.Rev.Immunol.* 4(3), pp. 181-189

Lander H.M., Ogiste J.S., Teng K.K., Novogrodsky A. 1995. p21ras as a common signaling target of reactive free radicals and cellular redox stress. *J Biol.Chem.* 270(36), pp. 21195-21198

Lanotte M., Martin-Thouvenin V., Najman S., Balerini P., Valensi F., Berger R. 1991. NB4, a maturation inducible cell line with t(15;17) marker isolated from a human acute promyelocytic leukemia (M3). *Blood* 77(5), pp. 1080-1086

Larson R.A., Wang Y., Banerjee M., Wiemels J., Hartford C., Le Beau M.M., Smith M.T. 1999. Prevalence of the inactivating 609C-->T polymorphism in the NAD(P)H:quinone oxidoreductase (NQO1) gene in patients with primary and therapy-related myeloid leukemia. *Blood* 94(2), pp. 803-807

Laurent G., Jaffrezou J.P. 2001. Signaling pathways activated by daunorubicin. *Blood* 98(4), pp. 913-924

Lazarov M., Green C.L., Zhang J.Y., Kubo Y., Dajee M., Khavari P.A. 2003. Escaping G1 restraints on neoplasia--Cdk4 regulation by Ras and NF-kappa B. *Cell Cycle* 2(2), pp. 79-80

Lee A.C., Fenster B.E., Ito H., Takeda K., Bae N.S. et al. 1999. Ras proteins induce senescence by altering the intracellular levels of reactive oxygen species. *J.Biol.Chem.* 274(12), pp. 7936-7940

Lee J.K., Edderkaoui M., Truong P., Ohno I., Jang K.T., Berti A., Pandol S.J., Gukovskaya A.S. 2007. NADPH oxidase promotes pancreatic cancer cell survival via inhibiting JAK2 dephosphorylation by tyrosine phosphatases. *Gastroenterology* 133(5), pp. 1637-1648

Lee S.R., Yang K.S., Kwon J., Lee C., Jeong W., Rhee S.G. 2002. Reversible inactivation of the tumor suppressor PTEN by H2O2. *J Biol.Chem.* 277(23), pp. 20336-20342

Lehmann D.J., Worwood M., Ellis R., Wimhurst V.L., Merryweather-Clarke A.T., Warden D.R., Smith A.D., Robson K.J. 2006. Iron genes, iron load and risk of Alzheimer's disease. *J Med.Genet.* 43(10), pge52

Leslie N.R. 2006. The redox regulation of PI 3-kinase-dependent signaling. *Antioxid.Redox.Signal.* 8(9-10), pp. 1765-1774

Leslie N.R., Bennett D., Lindsay Y.E., Stewart H., Gray A., Downes C.P. 2003. Redox regulation of PI 3-kinase signalling via inactivation of PTEN. *EMBO J.* 22(20), pp. 5501-5510

Levesque A.A., Eastman A. 2007. p53-based cancer therapies: Is defective p53 the Achilles heel of the tumor? *Carcinogenesis* 28(1), pp. 13-20

Lewis C.D., Laemmli U.K. 1982. Higher order metaphase chromosome structure: evidence for metalloprotein interactions. *Cell* 29(1), pp. 171-181

Li S.L., Valente A.J., Qiang M., Schlegel W., Gamez M., Clark R.A. 2002. Multiple PU.1 sites cooperate in the regulation of p40(phox) transcription during granulocytic differentiation of myeloid cells. *Blood* 99(12), pp. 4578-4587

Li S.L., Valente A.J., Wang L., Gamez M.J., Clark R.A. 2001. Transcriptional regulation of the p67phox gene: role of AP-1 in concert with myeloid-specific transcription factors. *J.Biol.Chem.* 276(42), pp. 39368-39378

Li S.L., Valente A.J., Zhao S.J., Clark R.A. 1997. PU.1 is essential for p47(phox) promoter activity in myeloid cells. *J.Biol.Chem.* 272(28), pp. 17802-17809

Lim S.D., Sun C., Lambeth J.D., Marshall F., Amin M., Chung L., Petros J.A., Arnold R.S. 2005. Increased Nox1 and hydrogen peroxide in prostate cancer. *Prostate* 62(2), pp. 200-207

Lin J., Jinno S., Okayama H. 2001. Cdk6-cyclin D3 complex evades inhibition by inhibitor proteins and uniquely controls cell's proliferation competence. *Oncogene* 20(16), pp. 2000-2009

Lindahl T. 1993. Instability and decay of the primary structure of DNA. *Nature* 362(6422), pp. 709-715

List A.F., Brasfield F., Heaton R., Glinsmann-Gibson B., Crook L., Taetle R., Capizzi R. 1997. Stimulation of hematopoiesis by amifostine in patients with myelodysplastic syndrome. *Blood* 90(9), pp. 3364-3369

Liu R., Li B., Qiu M. 2001. Elevated superoxide production by active H-ras enhances human lung WI-38VA-13 cell proliferation, migration and resistance to TNF-alpha. *Oncogene* 20(12), pp. 1486-1496

Liu Y., Min W. 2002. Thioredoxin promotes ASK1 ubiquitination and degradation to inhibit ASK1-mediated apoptosis in a redox activity-independent manner. *Circ.Res.* 90(12), pp. 1259-1266

Lo C.F., Diverio D., Falini B., Biondi A., Nervi C., Pelicci P.G. 1999. Genetic diagnosis and molecular monitoring in the management of acute promyelocytic leukemia. *Blood* 94(1), pp. 12-22

Locatelli F., Nollke P., Zecca M., Korthof E., Lanino E. et al. 2005. Hematopoietic stem cell transplantation (HSCT) in children with juvenile myelomonocytic leukemia (JMML): results of the EWOG-MDS/EBMT trial. *Blood* 105(1), pp. 410-419

Lowry O.H., Rosenbauer F., Farr A.L., Randall R.J. 1951. Protein measurement with the Folin phenol reagent. *J.Biol.Chem.* 193(1), pp. 265-275

Lu J., Chew E.H., Holmgren A. 2007. Targeting thioredoxin reductase is a basis for cancer therapy by arsenic trioxide. *Proc.Natl.Acad.Sci.U.S.A* 104(30), pp. 12288-12293

Lunghi P., Tabilio A., Pinelli S., Valmadre G., Ridolo E. et al. 2001. Expression and activation of SHC/MAP kinase pathway in primary acute myeloid leukemia blasts. *Hematol.J.* 2(2), pp. 70-80

Macleod K.F. 2008. The role of the RB tumour suppressor pathway in oxidative stress responses in the haematopoietic system. *Nat.Rev.Cancer* 8(10), pp. 769-781

Mahgoub N., Taylor B.R., Gratiot M., Kohl N.E., Gibbs J.B., Jacks T., Shannon K.M. 1999. In vitro and in vivo effects of a farnesyltransferase inhibitor on Nf1-deficient hematopoietic cells. *Blood* 94(7), pp. 2469-2476

Malumbres M., Perez D.C., I, Hernandez M.I., Jimenez M., Corral T., Pellicer A. 2000. Cellular response to oncogenic ras involves induction of the Cdk4 and Cdk6 inhibitor p15(INK4b). *Mol.Cell Biol.* 20(8), pp. 2915-2925

Mapp P.I., Grootveld M.C., Blake D.R. 1995. Hypoxia, oxidative stress and rheumatoid arthritis. *Br.Med.Bull.* 51(2), pp. 419-436

Massague J. 2004. G1 cell-cycle control and cancer. *Nature* 432(7015), pp. 298-306

Masters J.R. 2002. HeLa cells 50 years on: the good, the bad and the ugly. *Nat.Rev.Cancer* 2(4), pp. 315-319

Matozaki T., Murata Y., Saito Y., Okazawa H., Ohnishi H. 2009. Protein tyrosine phosphatase SHP-2: a proto-oncogene product that promotes Ras activation. *Cancer Sci.* 100(10), pp. 1786-1793

Matsumura I., Tanaka H., Kawasaki A., Odajima J., Daino H. et al. 2000. Increased D-type cyclin expression together with decreased cdc2 activity confers megakaryocytic differentiation of a human thrombopoietin-dependent hematopoietic cell line. *J.Biol.Chem.* 275(8), pp. 5553-5559

Matsuzawa S., Tamura T., Mizuno Y., Kobayashi S., Okuyama H., Tsukitani Y., Uemura D., Kikuchi K. 1992. Increase in potential activities of protein phosphatases PP1 and PP2A in lymphoid tissues of autoimmune MRL/MpJ-lpr/lpr mice. *J.Biochem.* 111(4), pp. 472-477

Maurice M.M., Nakamura H., van d., V, van Vliet A.I., Staal F.J., Tak P.P., Breedveld F.C., Verweij C.L. 1997. Evidence for the role of an altered redox state in hyporesponsiveness of synovial T cells in rheumatoid arthritis. *J Immunol.* 158(3), pp. 1458-1465

Mazzarello P. 1999. A unifying concept: the history of cell theory. *Nat.Cell Biol.* 1(1), pgE13-E15

Mazzone A., Ricevuti G., Rizzo S.C., Sacchi S. 1986. The probable role of superoxide produced by blast cells in leukaemic cutaneous spreading. *Int.J.Tissue React.* 8(6), pp. 493-496

McConnell B.B., Gregory F.J., Stott F.J., Hara E., Peters G. 1999. Induced expression of p16(INK4a) inhibits both CDK4- and CDK2-associated kinase activity by reassortment of cyclin-CDK-inhibitor complexes. *Mol.Cell Biol.* 19(3), pp. 1981-1989

McGlynn A.P., Padua R.A., Burnett A.K., Darley R.L. 2000. Alternative effects of RAS and RAF oncogenes on the proliferation and apoptosis of factor-dependent FDC-P1 cells. *Leuk.Res.* 24(1), pp. 47-54

McGrath J.P., Capon D.J., Goeddel D.V., Levinson A.D. 1984. Comparative biochemical properties of normal and activated human ras p21 protein. *Nature* 310(5979), pp. 644-649

McMahon K.A., Hiew S.Y., Hadjur S., Veiga-Fernandes H., Menzel U., Price A.J., Kioussis D., Williams O., Brady H.J. 2007. Mll has a critical role in fetal and adult hematopoietic stem cell self-renewal. *Cell Stem Cell* 1(3), pp. 338-345

Menon S.G., Sarsour E.H., Spitz D.R., Higashikubo R., Sturm M., Zhang H., Goswami P.C. 2003. Redox regulation of the G1 to S phase transition in the mouse embryo fibroblast cell cycle. *Cancer Res* 63(9), pp. 2109-2117

Metcalf D., Burgess A.W. 1982. Clonal analysis of progenitor cell commitment of granulocyte or macrophage production. *J.Cell Physiol* 111(3), pp. 275-283

Milburn M.V., Tong L., deVos A.M., Brunger A., Yamaizumi Z., Nishimura S., Kim S.H. 1990. Molecular switch for signal transduction: structural differences between active and inactive forms of protooncogenic ras proteins. *Science* 247(4945), pp. 939-945

Milella M., Kornblau S.M., Estrov Z., Carter B.Z., Lapillonne H. et al. 2001. Therapeutic targeting of the MEK/MAPK signal transduction module in acute myeloid leukemia. *J Clin Invest* 108(6), pp. 851-859

Milligan D.W., Grimwade D., Cullis J.O., Bond L., Swirsky D. et al. 2006. Guidelines on the management of acute myeloid leukaemia in adults. *Br.J.Haematol.* 135(4), pp. 450-474

Mitchell C., Payne J., Wade R., Vora A., Kinsey S., Richards S., Eden T. 2009. The impact of risk stratification by early bone-marrow response in childhood lymphoblastic leukaemia: results from the United Kingdom Medical Research Council trial ALL97 and ALL97/99. *Br.J.Haematol.* 146(4), pp. 424-436

Mitsushita J., Lambeth J.D., Kamata T. 2004. The superoxide-generating oxidase Nox1 is functionally required for Ras oncogene transformation. *Cancer Res.* 64(10), pp. 3580-3585

Miyamoto T., Weissman I.L., Akashi K. 2000. AML1/ETO-expressing nonleukemic stem cells in acute myelogenous leukemia with 8;21 chromosomal translocation. *Proc.Natl.Acad.Sci.U.S.A* 97(13), pp. 7521-7526

Mochizuki T., Furuta S., Mitsushita J., Shang W.H., Ito M. et al. 2006. Inhibition of NADPH oxidase 4 activates apoptosis via the AKT/apoptosis signal-regulating kinase 1 pathway in pancreatic cancer PANC-1 cells. *Oncogene* 25(26), pp. 3699-3707

Mojovic M., Vuletic M., Bacic G.G. 2005. Detection of oxygen-centered radicals using EPR spin-trap DEPMPO: the effect of oxygen. *Ann.N.Y.Acad.Sci.* 1048, pp. 471-475

Mora A., Komander D., van Aalten D.M., Alessi D.R. 2004. PDK1, the master regulator of AGC kinase signal transduction. *Semin.Cell Dev.Biol.* 15(2), pp. 161-170

Moreno J.C., Bikker H., Kempers M.J., van Trotsenburg A.S., Baas F., de Vijlder J.J., Vulsma T., Ris-Stalpers C. 2002. Inactivating mutations in the gene for thyroid oxidase 2 (THOX2) and congenital hypothyroidism. *N.Engl.J Med.* 347(2), pp. 95-102

Mukhopadhyay P., Rajesh M., Hasko G., Hawkins B.J., Madesh M., Pacher P. 2007. Simultaneous detection of apoptosis and mitochondrial superoxide production in live cells by flow cytometry and confocal microscopy. *Nat.Protoc.* 2(9), pp. 2295-2301

Murphy M.P. 2009. How mitochondria produce reactive oxygen species. *Biochem.J.* 417(1), pp. 1-13

Murray M.J., Cunningham J.M., Parada L.F., Dautry F., Lebowitz P., Weinberg R.A. 1983. The HL-60 transforming sequence: a ras oncogene coexisting with altered myc genes in hematopoietic tumors. *Cell* 33(3), pp. 749-757

Murrell G.A., Francis M.J., Bromley L. 1990. Modulation of fibroblast proliferation by oxygen free radicals. *Biochem.J* 265(3), pp. 659-665

Nakano Y., Kiyoi H., Miyawaki S., Asou N., Ohno R., Saito H., Naoe T. 1999. Molecular evolution of acute myeloid leukaemia in relapse: unstable N-ras and FLT3 genes compared with p53 gene. *Brit.J.Haematol.* 104, pp. 659-664

Naughton R., Quiney C., Turner S.D., Cotter T.G. 2009. Bcr-Abl-mediated redox regulation of the PI3K/AKT pathway. *Leukemia*

Nauseef W.M. 2001. Contributions of myeloperoxidase to proinflammatory events: more than an antimicrobial system. *Int.J Hematol.* 74(2), pp. 125-133

Neildez-Nguyen T.M., Chapel A., Arock M., Vetillard J., Thierry D. 1998. Gamma-irradiation does not impair ATRA-induced maturation of myeloid leukaemic cells: implication for combined radiation and differentiation therapy. *Br.J.Haematol.* 103(1), pp. 79-86

Neubauer A., Dodge R.K., George S.L., Davey F.R., Silver R.T. et al. 1994. Prognostic importance of mutations in the ras proto-oncogenes in de novo acute myeloid leukemia. *Blood* 83(6), pp. 1603-1611

Neviani P., Santhanam R., Trotta R., Notari M., Blaser B.W. et al. 2005. The tumor suppressor PP2A is functionally inactivated in blast crisis CML through the inhibitory activity of the BCR/ABL-regulated SET protein. *Cancer Cell* 8(5), pp. 355-368

Nicke B., Bastien J., Khanna S.J., Warne P.H., Cowling V. et al. 2005. Involvement of MINK, a Ste20 family kinase, in Ras oncogene-induced growth arrest in human ovarian surface epithelial cells. *Mol.Cell* 20(5), pp. 673-685

Nimer S.D. 2008. Myelodysplastic syndromes. *Blood* 111(10), pp. 4841-4851

Nishikawa M., Hyoudou K., Kobayashi Y., Umeyama Y., Takakura Y., Hashida M. 2005. Inhibition of metastatic tumor growth by targeted delivery of antioxidant enzymes. *J.Control Release* 109(1-3), pp. 101-107

Nunoi H., Rotrosen D., Gallin J.I., Malech H.L. 1988. Two forms of autosomal chronic granulomatous disease lack distinct neutrophil cytosol factors. *Science* 242(4883), pp. 1298-1301

O'Loghlen A., Perez-Morgado M.I., Salinas M., Martin M.E. 2003. Reversible inhibition of the protein phosphatase 1 by hydrogen peroxide. Potential regulation of eIF2 alpha phosphorylation in differentiated PC12 cells. *Arch.Biochem.Biophys.* 417(2), pp. 194-202

Oken M.M., Creech R.H., Tormey D.C., Horton J., Davis T.E., McFadden E.T., Carbone P.P. 1982. Toxicity and response criteria of the Eastern Cooperative Oncology Group. *Am.J.Clin.Oncol.* 5(6), pp. 649-655

Oliva J.L., Zarich N., Martinez N., Jorge R., Carrillo A. et al. 2004. The P34G mutation reduces the transforming activity of K-Ras and N-Ras in NIH 3T3 cells but not of H-Ras. *J.Biol.Chem.*

Omerovic J., Laude A.J., Prior I.A. 2007. Ras proteins: paradigms for compartmentalised and isoform-specific signalling. *Cell Mol.Life Sci.* 64(19-20), pp. 2575-2589

Omidvar N., Kogan S., Beurlet S., le P.C., Janin A. et al. 2007. BCL-2 and mutant NRAS interact physically and functionally in a mouse model of progressive myelodysplasia. *Cancer Res.* 67(24), pp. 11657-11667

Omidvar N., Pearn L., Burnett A.K., Darley R.L. 2006. Ral is both necessary and sufficient for the inhibition of myeloid differentiation mediated by Ras. *Mol.Cell Biol.* 26(10), pp. 3966-3975

Onken B., Wiener H., Philips M.R., Chang E.C. 2006. Compartmentalized signaling of Ras in fission yeast. *Proc.Natl.Acad.Sci.U.S.A* 103(24), pp. 9045-9050

Ortega S., Malumbres M., Barbacid M. 2002. Cyclin D-dependent kinases, INK4 inhibitors and cancer. *Biochim.Biophys.Acta* 1602(1), pp. 73-87

Osaki M., Oshimura M., Ito H. 2004. PI3K-Akt pathway: its functions and alterations in human cancer. *Apoptosis.* 9(6), pp. 667-676

Padua R.A., Guinn B.A., Alsabah A., Smith M., Taylor C. et al. 1998. RAS, FMS and p53 mutations and poor clinical outcome in myelodysplasias: a 10-year follow-up. *Leukemia* 12, pp. 887-892

Pantazis P., Goustin A.S., Nixon J. 1990. Platelet-derived growth factor and its receptor in blood cell differentiation and neoplasia. *Eur.J.Haematol.* 45(3), pp. 127-138

Paquette R.L., Landaw E.M., Pierre R.V., Kahan J., Lubbert M., Lazcano O., Isaac G., McCormick F., Koeffler H.P. 1993. N-ras mutations are associated with poor prognosis and increased risk of leukemia in myelodysplastic syndrome. *Blood* 82(2), pp. 590-599

Parada L.F., Tabin C.J., Shih C., Weinberg R.A. 1982. Human EJ bladder carcinoma oncogene is homologue of Harvey sarcoma virus ras gene. *Nature* 297(5866), pp. 474-478

Pardee A.B. 1974. A restriction point for control of normal animal cell proliferation. *Proc.Natl.Acad.Sci.U.S.A* 71(4), pp. 1286-1290

Parikh C., Subrahmanyam R., Ren R. 2007. Oncogenic NRAS, KRAS, and HRAS exhibit different leukemogenic potentials in mice. *Cancer Res* 67(15), pp. 7139-7146

Park J., Hill M.M., Hess D., Brazil D.P., Hofsteenge J., Hemmings B.A. 2001. Identification of tyrosine phosphorylation sites on 3-phosphoinositide-dependent protein kinase-1 and their role in regulating kinase activity. *J Biol.Chem.* 276(40), pp. 37459-37471

Parry D., Mahony D., Wills K., Lees E. 1999. Cyclin D-CDK subunit arrangement is dependent on the availability of competing INK4 and p21 class inhibitors. *Mol.Cell Biol.* 19(3), pp. 1775-1783

Pasinelli P., Houseweart M.K., Brown R.H., Jr., Cleveland D.W. 2000. Caspase-1 and -3 are sequentially activated in motor neuron death in Cu,Zn superoxide dismutase-mediated familial amyotrophic lateral sclerosis. *Proc.Natl.Acad.Sci.U.S.A* 97(25), pp. 13901-13906

Pear W.S., Nolan G.P., Scott M.L., Baltimore D. 1993. Production of high-titer helper-free retroviruses by transient transfection. *Proc.Natl.Acad.Sci.USA.* 90, pp. 8392-8396

Pearn L. Subcloning of mutant Ras and control cDNAs and DsRed reporter gene into PINCO retroviral vector plasmid. 2008.

Pearn L., Fisher J., Burnett A.K., Darley R.L. 2007. The role of PKC and PDK1 in monocyte lineage specification by Ras. *Blood* 109(10), pp. 4461-4469

Pelicano H., Carney D., Huang P. 2004. ROS stress in cancer cells and therapeutic implications. *Drug Resist.Updat.* 7(2), pp. 97-110

Pelicano H., Feng L., Zhou Y., Carew J.S., Hileman E.O., Plunkett W., Keating M.J., Huang P. 2003. Inhibition of mitochondrial respiration: a novel strategy to enhance drug-induced apoptosis in human leukemia cells by a reactive oxygen species-mediated mechanism. *J.Biol.Chem.* 278(39), pp. 37832-37839

Pervaiz S. 2006. Pro-oxidant milieu blunts scissors: insight into tumor progression, drug resistance, and novel druggable targets. *Curr.Pharm.Des* 12(34), pp. 4469-4477

Pervaiz S., Clement M.V. 2004. Tumor intracellular redox status and drug resistance--serendipity or a causal relationship? *Curr.Pharm.Des* 10(16), pp. 1969-1977

Peschon J.J., Morrissey P.J., Grabstein K.H., Ramsdell F.J., Maraskovsky E. et al. 1994. Early lymphocyte expansion is severely impaired in interleukin 7 receptor-deficient mice. *J.Exp.Med.* 180(5), pp. 1955-1960

Piccoli C., D'Aprile A., Ripoli M., Scrima R., Lecce L., Boffoli D., Tabilio A., Capitanio N. 2007. Bone-marrow derived hematopoietic stem/progenitor cells express multiple isoforms of NADPH oxidase and produce constitutively reactive oxygen species. *Biochem.Biophys.Res.Commun.* 353(4), pp. 965-972

Pimentel D.R., Adachi T., Ido Y., Heibeck T., Jiang B., Lee Y., Melendez J.A., Cohen R.A., Colucci W.S. 2006. Strain-stimulated hypertrophy in cardiac myocytes is mediated by reactive oxygen species-dependent Ras S-glutathiolation. *J Mol.Cell Cardiol.* 41(4), pp. 613-622

Pinheiro R.F., Moreira E.S., Silva M.R., Greggio B., Alberto F.L., Chauffaille M.L. 2007. FLT3 mutation and AML/ETO in a case of Myelodysplastic syndrome in transformation corroborates the two hit model of leukemogenesis. *Leuk.Res.* 31(7), pp. 1015-1018

Pollock J.D., Williams D.A., Gifford M.A., Li L.L., Du X., Fisherman J., Orkin S.H., Doerschuk C.M., Dinauer M.C. 1995. Mouse model of X-linked chronic granulomatous disease, an inherited defect in phagocyte superoxide production. *Nat.Genet.* 9(2), pp. 202-209

Prasad N., Topping R.S., Zhou D., Decker S.J. 2000. Oxidative stress and vanadate induce tyrosine phosphorylation of phosphoinositide-dependent kinase 1 (PDK1). *Biochemistry* 39(23), pp. 6929-6935

Preston T.J., Muller W.J., Singh G. 2001. Scavenging of extracellular H2O2 by catalase inhibits the proliferation of HER-2/Neu-transformed rat-1 fibroblasts through the induction of a stress response. *J.Biol.Chem.* 276(12), pp. 9558-9564

Preston T.J., Woodgett J.R., Singh G. 2003. JNK1 activity lowers the cellular production of H2O2 and modulates the growth arrest response to scavenging of H2O2 by catalase. *Exp.Cell Res.* 285(1), pp. 146-158

Quie P.G., White J.G., Holmes B., Good R.A. 1967. In vitro bactericidal capacity of human polymorphonuclear leukocytes: diminished activity in chronic granulomatous disease of childhood. *J Clin.Invest* 46(4), pp. 668-679

Rabbitts T.H. 1994. Chromosomal translocations in human cancer. *Nature* 372(6502), pp. 143-149

Raghuraman G., Rai V., Peng Y.J., Prabhakar N.R., Kumar G.K. 2009. Pattern specific sustained activation of tyrosine hydroxylase by intermittent hypoxia: Role of reactive oxygen species-dependent down regulation of protein phosphatase 2A and up regulation of protein kinases. *Antioxid.Redox.Signal.*

Rangarajan A., Hong S.J., Gifford A., Weinberg R.A. 2004. Species- and cell type-specific requirements for cellular transformation. *Cancer Cell* 6(2), pp. 171-183

Rangarajan A., Weinberg R.A. 2003. Opinion: Comparative biology of mouse versus human cells: modelling human cancer in mice. *Nat.Rev.Cancer* 3(12), pp. 952-959

Ranjan P., Anathy V., Burch P.M., Weirather K., Lambeth J.D., Heintz N.H. 2006. Redox-dependent expression of cyclin D1 and cell proliferation by Nox1 in mouse lung epithelial cells. *Antioxid.Redox.Signal.* 8(9-10), pp. 1447-1459

Rao R.K., Clayton L.W. 2002. Regulation of protein phosphatase 2A by hydrogen peroxide and glutathionylation. *Biochem.Biophys.Res.Commun.* 293(1), pp. 610-616

Rassool F.V., Gaymes T.J., Omidvar N., Brady N., Beurlet S. et al. 2007. Reactive oxygen species, DNA damage, and error-prone repair: a model for genomic instability with progression in myeloid leukemia? *Cancer Res* 67(18), pp. 8762-8771

Ravandi F., Burnett A.K., Agura E.D., Kantarjian H.M. 2007. Progress in the treatment of acute myeloid leukemia. *Cancer* 110(9), pp. 1900-1910

Reeves E.P., Lu H., Jacobs H.L., Messina C.G., Bolsover S. et al. 2002. Killing activity of neutrophils is mediated through activation of proteases by K+ flux. *Nature* 416(6878), pp. 291-297

Reth M. 2002. Hydrogen peroxide as second messenger in lymphocyte activation. *Nat.Immunol.* 3(12), pp. 1129-1134

Rhee S.G. 2006. H_2O_2, a necessary evil for cell signaling. *Science* 312(5782), pp. 1882-1883

Rhee S.G., Bae Y.S., Lee S.R., Kwon J. 2000. Hydrogen peroxide: a key messenger that modulates protein phosphorylation through cysteine oxidation. *Sci.STKE.* 2000(53), pgE1

Rhee S.G., Kang S.W., Jeong W., Chang T.S., Yang K.S., Woo H.A. 2005. Intracellular messenger function of hydrogen peroxide and its regulation by peroxiredoxins. *Curr.Opin.Cell Biol.* 17(2), pp. 183-189

Robb L. 2007. Cytokine receptors and hematopoietic differentiation. *Oncogene* 26(47), pp. 6715-6723

Robb L., Drinkwater C.C., Metcalf D., Li R., Kontgen F., Nicola N.A., Begley C.G. 1995. Hematopoietic and lung abnormalities in mice with a null mutation of the common beta subunit of the receptors for granulocyte-macrophage colony-stimulating factor and interleukins 3 and 5. *Proc.Natl.Acad.Sci.U.S.A* 92(21), pp. 9565-9569

Rodriguez-Viciana P., Warne P.H., Dhand R., Vanhaesebroeck B., Gout I., Fry M.J., Waterfield M.D., Downward J. 1994. Phosphatidylinositol-3-OH kinase as a direct target of Ras. *Nature* 370(6490), pp. 527-532

Rosenbauer F., Tenen D.G. 2007. Transcription factors in myeloid development: balancing differentiation with transformation. *Nat.Rev.Immunol.* 7(2), pp. 105-117

Rosenbauer F., Wagner K., Kutok J.L., Iwasaki H., Le Beau M.M., Okuno Y., Akashi K., Fiering S., Tenen D.G. 2004. Acute myeloid leukemia induced by graded reduction of a lineage-specific transcription factor, PU.1. *Nat.Genet.* 36(6), pp. 624-630

Roubaud V., Sankarapandi S., Kuppusamy P., Tordo P., Zweier J.L. 1997. Quantitative measurement of superoxide generation using the spin trap 5-(diethoxyphosphoryl)-5-methyl-1-pyrroline-N-oxide. *Anal.Biochem.* 247(2), pp. 404-411

Royer-Pokora B., Kunkel L.M., Monaco A.P., Goff S.C., Newburger P.E., Baehner R.L., Cole F.S., Curnutte J.T., Orkin S.H. 1986. Cloning the gene for an inherited human disorder--chronic granulomatous disease--on the basis of its chromosomal location. *Nature* 322(6074), pp. 32-38

Russo A.A., Jeffrey P.D., Patten A.K., Massague J., Pavletich N.P. 1996. Crystal structure of the p27Kip1 cyclin-dependent-kinase inhibitor bound to the cyclin A-Cdk2 complex. *Nature* 382(6589), pp. 325-331

Rygiel T.P., Mertens A.E., Strumane K., van der K.R., Collard J.G. 2008. The Rac activator Tiam1 prevents keratinocyte apoptosis by controlling ROS-mediated ERK phosphorylation
1. *J Cell Sci.* 121(Pt 8), pp. 1183-1192

Sagripanti J.L., Goering P.L., Lamanna A. 1991. Interaction of copper with DNA and antagonism by other metals. *Toxicol.Appl.Pharmacol.* 110(3), pp. 477-485

Sah N.K., Khan Z., Khan G.J., Bisen P.S. 2006. Structural, functional and therapeutic biology of survivin. *Cancer Lett.* 244(2), pp. 164-171

Sahai E., Marshall C.J. 2002. RHO-GTPases and cancer. *Nat.Rev.Cancer* 2(2), pp. 133-142

Sallmyr A., Fan J., Rassool F.V. 2008. Genomic instability in myeloid malignancies: increased reactive oxygen species (ROS), DNA double strand breaks (DSBs) and error-prone repair. *Cancer Lett.* 270(1), pp. 1-9

Sanchez-Garcia I., Martin-Zanca D. 1997. Regulation of Bcl-2 gene expression by BCR-ABL is mediated by Ras. *J.Mol.Biol.* 267(2), pp. 225-228

Sander C.S., Hamm F., Elsner P., Thiele J.J. 2003. Oxidative stress in malignant melanoma and non-melanoma skin cancer. *Br.J Dermatol.* 148(5), pp. 913-922

Sanger F., Coulson A.R. 1975. A rapid method for determining sequences in DNA by primed synthesis with DNA polymerase. *J.Mol.Biol.* 94(3), pp. 441-448

Santillo M., Mondola P., Seru R., Annella T., Cassano S. et al. 2001. Opposing functions of Ki- and Ha-Ras genes in the regulation of redox signals. *Curr.Biol.* 11(8), pp. 614-619

Santos E., Tronick S.R., Aaronson S.A., Pulciani S., Barbacid M. 1982. T24 human bladder carcinoma oncogene is an activated form of the normal human homologue of. *Nature* 298(5872), pp. 343-347

Sattler M., Verma S., Shrikhande G., Byrne C.H., Pride Y.B., Winkler T., Greenfield E.A., Salgia R., Griffin J.D. 2000. The BCR/ABL tyrosine kinase induces production of reactive oxygen species in hematopoietic cells. *J.Biol.Chem.* 275(32), pp. 24273-24278

Sattler M., Winkler T., Verma S., Byrne C.H., Shrikhande G., Salgia R., Griffin J.D. 1999. Hematopoietic growth factors signal through the formation of reactive oxygen species. *Blood* 93(9), pp. 2928-2935

Scheid M.P., Parsons M., Woodgett J.R. 2005. Phosphoinositide-dependent phosphorylation of PDK1 regulates nuclear translocation. *Mol.Cell Biol.* 25(6), pp. 2347-2363

Schepers H., Geugien M., Eggen B.J., Vellenga E. 2003. Constitutive cytoplasmic localization of p21(Waf1/Cip1) affects the apoptotic process in monocytic leukaemia. *Leukemia* 17(11), pp. 2113-2121

Schlichting I., Almo S.C., Rapp G., Wilson K., Petratos K. et al. 1990. Time-resolved X-ray crystallographic study of the conformational change in Ha-Ras p21 protein on GTP hydrolysis. *Nature* 345(6273), pp. 309-315

Schmid I., Krall W.J., Uittenbogaart C.H., Braun J., Giorgi J.V. 1992. Dead cell discrimination with 7-amino-actinomycin D in combination with dual color immunofluorescence in single laser flow cytometry. *Cytometry* 13(2), pp. 204-208

Schneider F., Bohlander S.K., Schneider S., Papadaki C., Kakadyia P. et al. 2007. AML1-ETO meets JAK2: clinical evidence for the two hit model of leukemogenesis from a myeloproliferative syndrome progressing to acute myeloid leukemia. *Leukemia* 21(10), pp. 2199-2201

Schnittger S., Kohl T.M., Haferlach T., Kern W., Hiddemann W., Spiekermann K., Schoch C. 2006. KIT-D816 mutations in AML1-ETO-positive AML are associated with impaired event-free and overall survival. *Blood* 107(5), pp. 1791-1799

Schnittger S., Schoch C., Kern W., Mecucci C., Tschulik C., Martelli M.F., Haferlach T., Hiddemann W., Falini B. 2005. Nucleophosmin gene mutations are predictors of favorable prognosis in acute myelogenous leukemia with a normal karyotype. *Blood* 106(12), pp. 3733-3739

Schrenzel J., Serrander L., Banfi B., Nusse O., Fouyouzi R., Lew D.P., Demaurex N., Krause K.H. 1998. Electron currents generated by the human phagocyte NADPH oxidase. *Nature* 392(6677), pp. 734-737

Schroeder T., Lange C., Strehl J., Just U. 2000. Generation of functionally mature dendritic cells from the multipotential stem cell line FDCP-mix. *Br.J.Haematol.* 111(3), pp. 890-897

Schubbert S., Shannon K., Bollag G. 2007. Hyperactive Ras in developmental disorders and cancer. *Nat.Rev.Cancer* 7(4), pp. 295-308

Schuettengruber B., Chourrout D., Vervoort M., Leblanc B., Cavalli G. 2007. Genome regulation by polycomb and trithorax proteins. *Cell* 128(4), pp. 735-745

Seeburg P.H., Colby W.W., Capon D.J., Goeddel D.V., Levinson A.D. 1984. Biological properties of human c-Ha-ras1 genes mutated at codon 12. *Nature* 312(5989), pp. 71-75

Segal A.W., Geisow M., Garcia R., Harper A., Miller R. 1981. The respiratory burst of phagocytic cells is associated with a rise in vacuolar pH. *Nature* 290(5805), pp. 406-409

Segal A.W., Jones O.T., Webster D., Allison A.C. 1978. Absence of a newly described cytochrome b from neutrophils of patients with chronic granulomatous disease. *Lancet* 2(8087), pp. 446-449

Semerad C.L., Poursine-Laurent J., Liu F., Link D.C. 1999. A role for G-CSF receptor signaling in the regulation of hematopoietic cell function but not lineage commitment or differentiation. *Immunity.* 11(2), pp. 153-161

Seoane J., Le H.V., Massague J. 2002. Myc suppression of the p21(Cip1) Cdk inhibitor influences the outcome of the p53 response to DNA damage. *Nature* 419(6908), pp. 729-734

Seru R., Mondola P., Damiano S., Svegliati S., Agnese S., Avvedimento E.V., Santillo M. 2004. HaRas activates the NADPH oxidase complex in human neuroblastoma cells via extracellular signal-regulated kinase 1/2 pathway. *J.Neurochem.* 91(3), pp. 613-622

Shaulian E., Karin M. 2002. AP-1 as a regulator of cell life and death. *Nat.Cell Biol.* 4(5), pgE131-E136

Shen S., Passioura T., Symonds G., Dolnikov A. 2007. N-ras oncogene-induced gene expression in human hematopoietic progenitor cells: upregulation of p16INK4a and p21CIP1/WAF1 correlates with myeloid differentiation. *Exp.Hematol.* 35(6), pp. 908-919

Shen S.W., Dolnikov A., Passioura T., Millington M., Wotherspoon S., Rice A., MacKenzie K.L., Symonds G. 2004. Mutant N-ras preferentially drives human $CD34^+$ hematopoietic progenitor cells into myeloid differentiation and proliferation both in vitro and in the NOD/SCID mouse. *Exp.Hematol.* 32(9), pp. 852-860

Shen W.P., Aldrich T.H., Venta-Perez G., Franza B.R., Jr., Furth M.E. 1987. Expression of normal and mutant ras proteins in human acute leukemia. *Oncogene* 1(2), pp. 157-165

Sherr C.J., Roberts J.M. 1999. CDK inhibitors: positive and negative regulators of G1-phase progression. *Genes Dev.* 13(12), pp. 1501-1512

Shibanuma M., Kuroki T., Nose K. 1988. Superoxide as a signal for increase in intracellular pH. *J Cell Physiol* 136(2), pp. 379-383

Shih L.Y., Huang C.F., Wang P.N., Wu J.H., Lin T.L., Dunn P., Kuo M.C. 2004. Acquisition of FLT3 or N-ras mutations is frequently associated with progression of myelodysplastic syndrome to acute myeloid leukemia. *Leukemia* 18(3), pp. 466-475

Shimizu K., Goldfarb M., Perucho M., Wigler M. 1983. Isolation and preliminary characterization of the transforming gene of a human neuroblastoma cell line. *Proc.Natl.Acad.Sci.U.S.A* 80(2), pp. 383-387

Shin I., Kim S., Song H., Kim H.R., Moon A. 2005. H-Ras-specific activation of Rac-MKK3/6-p38 pathway: its critical role in invasion and migration of breast epithelial cells. *J.Biol.Chem.* 280(15), pp. 14675-14683

Shinohara M., Shang W.H., Kubodera M., Harada S., Mitsushita J., Kato M., Miyazaki H., Sumimoto H., Kamata T. 2007. Nox1 redox signaling mediates oncogenic Ras-induced disruption of stress fibers and focal adhesions by down-regulating Rho. *J.Biol.Chem.* 282(24), pp. 17640-17648

Siena S., Schiavo R., Pedrazzoli P., Carlo-Stella C. 2000. Therapeutic relevance of CD34 cell dose in blood cell transplantation for cancer therapy. *J Clin.Oncol.* 18(6), pp. 1360-1377

Simpson J.A., Cheeseman K.H., Smith S.E., Dean R.T. 1988. Free-radical generation by copper ions and hydrogen peroxide. Stimulation by Hepes buffer. *Biochem.J.* 254(2), pp. 519-523

Sjolander A., Yamamoto K., Huber B.E., Lapetina E.G. 1991. Association of p21ras with phosphatidylinositol 3-kinase. *Proc.Natl.Acad.Sci.U.S.A* 88(18), pp. 7908-7912

Slovak M.L., Kopecky K.J., Cassileth P.A., Harrington D.H., Theil K.S. et al. 2000. Karyotypic analysis predicts outcome of preremission and postremission therapy in adult acute myeloid leukemia: a Southwest Oncology Group/Eastern Cooperative Oncology Group Study. *Blood* 96(13), pp. 4075-4083

Smith M.T., Wang Y., Kane E., Rollinson S., Wiemels J.L., Roman E., Roddam P., Cartwright R., Morgan G. 2001. Low NAD(P)H:quinone oxidoreductase 1 activity is associated with increased risk of acute leukemia in adults. *Blood* 97(5), pp. 1422-1426

Spangrude G.J., Heimfeld S., Weissman I.L. 1988. Purification and characterization of mouse hematopoietic stem cells. *Science* 241(4861), pp. 58-62

Speck N.A., Gilliland D.G. 2002. Core-binding factors in haematopoiesis and leukaemia. *Nat.Rev.Cancer* 2(7), pp. 502-513

Spooncer E., Heyworth C.M., Dunn A., Dexter T.M. 1986. Self-renewal and differentiation of interleukin-3-dependent multipotent stem cells are modulated by stromal cells and serum factors. *Differentiation* 31(2), pp. 111-118

Stanley E., Lieschke G.J., Grail D., Metcalf D., Hodgson G. et al. 1994. Granulocyte/macrophage colony-stimulating factor-deficient mice show no major perturbation of hematopoiesis but develop a characteristic pulmonary pathology. *Proc.Natl.Acad.Sci.U.S.A* 91(12), pp. 5592-5596

Steelman L.S., Abrams S.L., Whelan J., Bertrand F.E., Ludwig D.E. et al. 2008. Contributions of the Raf/MEK/ERK, PI3K/PTEN/Akt/mTOR and Jak/STAT pathways to leukemia. *Leukemia* 22(4), pp. 686-707

Steelman L.S., Pohnert S.C., Shelton J.G., Franklin R.A., Bertrand F.E., McCubrey J.A. 2004. JAK/STAT, Raf/MEK/ERK, PI3K/Akt and BCR-ABL in cell cycle progression and leukemogenesis. *Leukemia* 18(2), pp. 189-218

Stirewalt D.L., Kopecky K.J., Meshinchi S., Appelbaum F.R., Slovak M.L., Willman C.L., Radich J.P. 2001. FLT3, RAS, and TP53 mutations in elderly patients with acute myeloid leukemia. *Blood* 97(11), pp. 3589-3595

Suh Y.A., Arnold R.S., Lassegue B., Shi J., Xu X., Sorescu D., Chung A.B., Griendling K.K., Lambeth J.D. 1999. Cell transformation by the superoxide-generating oxidase Mox1. *Nature* 401(6748), pp. 79-82

Sumimoto H. 2008. Structure, regulation and evolution of Nox-family NADPH oxidases that produce reactive oxygen species. *FEBS J.* 275(13), pp. 3249-3277

Sundaresan M., Yu Z.X., Ferrans V.J., Irani K., Finkel T. 1995. Requirement for generation of H2O2 for platelet-derived growth factor signal transduction. *Science* 270(5234), pp. 296-299

Sundstrom C., Nilsson K. 1976. Establishment and characterization of a human histiocytic lymphoma cell line (U-937). *Int.J.Cancer* 17(5), pp. 565-577

Suzuki A., Tsutomi Y., Yamamoto N., Shibutani T., Akahane K. 1999. Mitochondrial regulation of cell death: mitochondria are essential for procaspase 3-p21 complex formation to resist Fas-mediated cell death. *Mol.Cell Biol.* 19(5), pp. 3842-3847

Suzuki S., Kumatori A., Haagen I.A., Fujii Y., Sadat M.A., Jun H.L., Tsuji Y., Roos D., Nakamura M. 1998. PU.1 as an essential activator for the expression of gp91(phox) gene in human peripheral neutrophils, monocytes, and B lymphocytes. *Proc.Natl.Acad.Sci.U.S.A* 95(11), pp. 6085-6090

Sweet R.W., Yokoyama S., Kamata T., Feramisco J.R., Rosenberg M., Gross M. 1984. The product of ras is a GTPase and the T24 oncogenic mutant is deficient in this activity. *Nature* 311(5983), pp. 273-275

Swerdlow S.H. et al. 2008. *WHO Classification of Tumours of Haematopoietic and Lymphoid Tissues*. Lyon: IARC Press, 4th Ed.

Tarpey M.M., Fridovich I. 2001. Methods of detection of vascular reactive species: nitric oxide, superoxide, hydrogen peroxide, and peroxynitrite. *Circ.Res.* 89(3), pp. 224-236

Taussig D.C., Pearce D.J., Simpson C., Rohatiner A.Z., Lister T.A., Kelly G., Luongo J.L., net-Desnoyers G.A., Bonnet D. 2005. Hematopoietic stem cells express multiple myeloid markers: implications for the origin and targeted therapy of acute myeloid leukemia. *Blood* 106(13), pp. 4086-4092

Teahan C., Rowe P., Parker P., Totty N., Segal A.W. 1987. The X-linked chronic granulomatous disease gene codes for the beta-chain of cytochrome b-245. *Nature* 327(6124), pp. 720-721

Tefferi A., Gilliland D.G. 2007. Oncogenes in myeloproliferative disorders. *Cell Cycle* 6(5), pp. 550-566

Testa U. 2004. Apoptotic mechanisms in the control of erythropoiesis. *Leukemia* 18(7), pp. 1176-1199

Tetradis S., Pilbeam C.C., Liu Y., Herschman H.R., Kream B.E. 1997. Parathyroid hormone increases prostaglandin G/H synthase-2 transcription by a cyclic adenosine 3',5'-monophosphate-mediated pathway in murine osteoblastic MC3T3-E1 cells. *Endocrinology* 138(9), pp. 3594-3600

Thorsteinsdottir U., Mamo A., Kroon E., Jerome L., Bijl J., Lawrence H.J., Humphries K., Sauvageau G. 2002. Overexpression of the myeloid leukemia-associated Hoxa9 gene in bone marrow cells induces stem cell expansion. *Blood* 99(1), pp. 121-129

Till J.E., McCulloch E.A. 1961. A direct measurement of the radiation sensitivity of normal mouse bone marrow cells. *Radiat.Res.* 14, pp. 213-222

Tominaga K., Kawahara T., Sano T., Toida K., Kuwano Y., Sasaki H., Kawai T., Teshima-Kondo S., Rokutan K. 2007. Evidence for cancer-associated expression of NADPH oxidase 1 (Nox1)-based oxidase system in the human stomach. *Free Radic.Biol.Med.* 43(12), pp. 1627-1638

Tonks A., Parton J., Tonks A.J., Morris R.H., Finall A., Jones K.P., Jackson S.K. 2005a. Surfactant phospholipid DPPC downregulates monocyte respiratory burst via modulation of PKC. *Am.J.Physiol Lung Cell Mol.Physiol* 288(6), pgL1070-L1080

Tonks A., Tonks A.J., Pearn L., Mohamad Z., Burnett A.K., Darley R.L. 2005b. Optimized retroviral transduction protocol which preserves the primitive subpopulation of human hematopoietic cells. *Biotechnol.Prog.* 21(3), pp. 953-958

Tonks A.J., Tonks A., Morris R.H., Jones K.P., Jackson S.K. 2003. Regulation of platelet-activating factor synthesis in human monocytes by dipalmitoyl phosphatidylcholine. *J.Leukoc.Biol.* 74(1), pp. 95-101

Tonks N.K., Muthuswamy S.K. 2007. A brake becomes an accelerator: PTP1B--a new therapeutic target for breast cancer. *Cancer Cell* 11(3), pp. 214-216

Tothova Z., Kollipara R., Huntly B.J., Lee B.H., Castrillon D.H. et al. 2007. FoxOs are critical mediators of hematopoietic stem cell resistance to physiologic oxidative stress. *Cell* 128(2), pp. 325-339

Townsend D.M., Findlay V.L., Tew K.D. 2005. Glutathione S-transferases as regulators of kinase pathways and anticancer drug targets. *Methods Enzymol.* 401, pp. 287-307

Townsend D.M., Tew K.D. 2003. The role of glutathione-S-transferase in anti-cancer drug resistance. *Oncogene* 22(47), pp. 7369-7375

Trachootham D., Alexandre J., Huang P. 2009. Targeting cancer cells by ROS-mediated mechanisms: a radical therapeutic approach? *Nat.Rev.Drug Discov.* 8(7), pp. 579-591

Trachootham D., Zhang H., Zhang W., Feng L., Du M. et al. 2008. Effective elimination of fludarabine-resistant CLL cells by PEITC through a redox-mediated mechanism. *Blood* 112(5), pp. 1912-1922

Tsao S.M., Yin M.C., Liu W.H. 2007. Oxidant stress and B vitamins status in patients with non-small cell lung cancer. *Nutr.Cancer* 59(1), pp. 8-13

Tu P.H., Gurney M.E., Julien J.P., Lee V.M., Trojanowski J.Q. 1997. Oxidative stress, mutant SOD1, and neurofilament pathology in transgenic mouse models of human motor neuron disease. *Lab Invest* 76(4), pp. 441-456

Tu P.H., Raju P., Robinson K.A., Gurney M.E., Trojanowski J.Q., Lee V.M. 1996. Transgenic mice carrying a human mutant superoxide dismutase transgene develop neuronal cytoskeletal pathology resembling human amyotrophic lateral sclerosis lesions. *Proc.Natl.Acad.Sci.U.S.A* 93(7), pp. 3155-3160

Tyner J.W., Erickson H., Deininger M.W., Willis S.G., Eide C.A. et al. 2009. High-throughput sequencing screen reveals novel, transforming RAS mutations in myeloid leukemia patients. *Blood* 113(8), pp. 1749-1755

Urao N., Inomata H., Razvi M., Kim H.W., Wary K., McKinney R., Fukai T., Ushio-Fukai M. 2008. Role of nox2-based NADPH oxidase in bone marrow and progenitor cell function involved in neovascularization induced by hindlimb ischemia. *Circ.Res.* 103(2), pp. 212-220

Ushio-Fukai M., Alexander R.W., Akers M., Yin Q., Fujio Y., Walsh K., Griendling K.K. 1999. Reactive oxygen species mediate the activation of Akt/protein kinase B by angiotensin II in vascular smooth muscle cells. *J Biol.Chem.* 274(32), pp. 22699-22704

Ushio-Fukai M., Nakamura Y. 2008. Reactive oxygen species and angiogenesis: NADPH oxidase as target for cancer therapy. *Cancer Lett.* 266(1), pp. 37-52

Valk P.J., Bowen D.T., Frew M.E., Goodeve A.C., Lowenberg B., Reilly J.T. 2004. Second hit mutations in the RTK/RAS signaling pathway in acute myeloid leukemia with inv(16). *Haematologica* 89(1), pg106

Valko M., Leibfritz D., Moncol J., Cronin M.T., Mazur M., Telser J. 2007. Free radicals and antioxidants in normal physiological functions and human disease. *Int.J.Biochem.Cell Biol.* 39(1), pp. 44-84

van Engeland M., Nieland L.J., Ramaekers F.C., Schutte B., Reutelingsperger C.P. 1998. Annexin V-affinity assay: a review on an apoptosis detection system based on phosphatidylserine exposure. *Cytometry* 31(1), pp. 1-9

Vaquero E.C., Edderkaoui M., Pandol S.J., Gukovsky I., Gukovskaya A.S. 2004. Reactive oxygen species produced by NAD(P)H oxidase inhibit apoptosis in pancreatic cancer cells. *J.Biol.Chem.* 279(33), pp. 34643-34654

Vardiman J.W., Thiele J., Arber D.A., Brunning R.D., Borowitz M.J. et al. 2009. The 2008 revision of the World Health Organization (WHO) classification of myeloid neoplasms and acute leukemia: rationale and important changes. *Blood* 114(5), pp. 937-951

Vaupel P. 2004. The role of hypoxia-induced factors in tumor progression. *Oncologist.* 9 Suppl 5, pp. 10-17

Vidriales M.B., San-Miguel J.F., Orfao A., Coustan-Smith E., Campana D. 2003. Minimal residual disease monitoring by flow cytometry. *Best.Pract.Res.Clin.Haematol.* 16(4), pp. 599-612

Vita J.A., Frei B., Holbrook M., Gokce N., Leaf C., Keaney J.F., Jr. 1998. L-2-Oxothiazolidine-4-carboxylic acid reverses endothelial dysfunction in patients with coronary artery disease. *J Clin.Invest* 101(6), pp. 1408-1414

Volpp B.D., Nauseef W.M., Clark R.A. 1988. Two cytosolic neutrophil oxidase components absent in autosomal chronic granulomatous disease. *Science* 242(4883), pp. 1295-1297

Wang W., Chen J.X., Liao R., Deng Q., Zhou J.J., Huang S., Sun P. 2002. Sequential activation of the MEK-extracellular signal-regulated kinase and MKK3/6-p38 mitogen-activated protein kinase pathways mediates oncogenic ras-induced premature senescence. *Mol.Cell Biol.* 22(10), pp. 3389-3403

Wanzel M., Herold S., Eilers M. 2003. Transcriptional repression by Myc. *Trends Cell Biol.* 13(3), pp. 146-150

Wardman P. 2007. Fluorescent and luminescent probes for measurement of oxidative and nitrosative species in cells and tissues: progress, pitfalls, and prospects. *Free Radic.Biol.Med.* 43(7), pp. 995-1022

Warne P.H., Viciana P.R., Downward J. 1993. Direct interaction of Ras and the amino-terminal region of Raf-1 in vitro. *Nature* 364(6435), pp. 352-355

Weissman I.L., Shizuru J.A. 2008. The origins of the identification and isolation of hematopoietic stem cells, and their capability to induce donor-specific transplantation tolerance and treat autoimmune diseases. *Blood* 112(9), pp. 3543-3553

Wennerberg K., Rossman K.L., Der C.J. 2005. The Ras superfamily at a glance. *J.Cell Sci.* 118(Pt 5), pp. 843-846

Whyte D.B., Kirschmeier P., Hockenberry T.N., Nunez-Oliva I., James L., Catino J.J., Bishop W.R., Pai J.K. 1997. K- and N-Ras are geranylgeranylated in cells treated with farnesyl protein transferase inhibitors. *J.Biol.Chem.* 272(22), pp. 14459-14464

Wilson A., Trumpp A. 2006. Bone-marrow haematopoietic-stem-cell niches. *Nat.Rev.Immunol.* 6(2), pp. 93-106

Wu A.S., Kiaei M., Aguirre N., Crow J.P., Calingasan N.Y., Browne S.E., Beal M.F. 2003. Iron porphyrin treatment extends survival in a transgenic animal model of amyotrophic lateral sclerosis. *J.Neurochem.* 85(1), pp. 142-150

Wu C., Miloslavskaya I., Demontis S., Maestro R., Galaktionov K. 2004. Regulation of cellular response to oncogenic and oxidative stress by Seladin-1. *Nature* 432(7017), pp. 640-645

Wu H., Liu X., Jaenisch R., Lodish H.F. 1995. Generation of committed erythroid BFU-E and CFU-E progenitors does not require erythropoietin or the erythropoietin receptor. *Cell* 83(1), pp. 59-67

Wu W.S. 2006. The signaling mechanism of ROS in tumor progression. *Cancer Metastasis Rev.* 25(4), pp. 695-705

Wyllie A.H. 1997. Apoptosis: an overview. *Br.Med.Bull.* 53(3), pp. 451-465

Yamakawa T., Tanaka S., Yamakawa Y., Kamei J., Numaguchi K., Motley E.D., Inagami T., Eguchi S. 2002. Lysophosphatidylcholine activates extracellular signal-regulated kinases 1/2 through reactive oxygen species in rat vascular smooth muscle cells. *Arterioscler.Thromb.Vasc.Biol.* 22(5), pp. 752-758

Yamamoto D., Sonoda Y., Hasegawa M., Funakoshi-Tago M., izu-Yokota E., Kasahara T. 2003. FAK overexpression upregulates cyclin D3 and enhances cell proliferation via the PKC and PI3-kinase-Akt pathways. *Cell Signal.* 15(6), pp. 575-583

Yamanaka R., Barlow C., Lekstrom-Himes J., Castilla L.H., Liu P.P., Eckhaus M., Decker T., Wynshaw-Boris A., Xanthopoulos K.G. 1997. Impaired granulopoiesis, myelodysplasia, and early lethality in CCAAT/enhancer binding protein epsilon-deficient mice. *Proc.Natl.Acad.Sci.U.S.A* 94(24), pp. 13187-13192

Yamaura M., Mitsushita J., Furuta S., Kiniwa Y., Ashida A. et al. 2009. NADPH oxidase 4 contributes to transformation phenotype of melanoma cells by regulating G2-M cell cycle progression. *Cancer Res.* 69(6), pp. 2647-2654

Yang J.Q., Li S., Domann F.E., Buettner G.R., Oberley L.W. 1999. Superoxide generation in v-Ha-ras-transduced human keratinocyte HaCaT cells. *Mol.Carcinog.* 26(3), pp. 180-188

Yang K.J., Shin S., Piao L., Shin E., Li Y. et al. 2008. Regulation of 3-phosphoinositide-dependent protein kinase-1 (PDK1) by Src involves tyrosine phosphorylation of PDK1 and Src homology 2 domain binding. *J Biol.Chem.* 283(3), pp. 1480-1491

Yu C., Rahmani M., Dent P., Grant S. 2004. The hierarchical relationship between MAPK signaling and ROS generation in human leukemia cells undergoing apoptosis in response to the proteasome inhibitor Bortezomib. *Exp.Cell Res.* 295(2), pp. 555-566

Zhang H., Trachootham D., Lu W., Carew J., Giles F.J., Keating M.J., Arlinghaus R.B., Huang P. 2008. Effective killing of Gleevec-resistant CML cells with T315I mutation by a natural compound PEITC through redox-mediated mechanism. *Leukemia* 22(6), pp. 1191-1199

Zhang J., Niu C., Ye L., Huang H., He X. et al. 2003. Identification of the haematopoietic stem cell niche and control of the niche size. *Nature* 425(6960), pp. 836-841

Zhang J., Yang P.L., Gray N.S. 2009. Targeting cancer with small molecule kinase inhibitors. *Nat Rev.Cancer* 9(1), pp. 28-39

Zhang P., Iwasaki-Arai J., Iwasaki H., Fenyus M.L., Dayaram T. et al. 2004. Enhancement of hematopoietic stem cell repopulating capacity and self-renewal in the absence of the transcription factor C/EBP alpha. *Immunity.* 21(6), pp. 853-863

Zhang X.B., Beard B.C., Beebe K., Storer B., Humphries R.K., Kiem H.P. 2006. Differential effects of HOXB4 on nonhuman primate short- and long-term repopulating cells. *PLoS.Med.* 3(5), pge173

Zhang X.F., Settleman J., Kyriakis J.M., Takeuchi-Suzuki E., Elledge S.J., Marshall M.S., Bruder J.T., Rapp U.R., Avruch J. 1993. Normal and oncogenic p21ras proteins bind to the amino-terminal regulatory domain of c-Raf-1. *Nature* 364(6435), pp. 308-313

Zhao X., Xu B., Bhattacharjee A., Oldfield C.M., Wientjes F.B., Feldman G.M., Cathcart M.K. 2005. Protein kinase Cdelta regulates p67phox phosphorylation in human monocytes. *J.Leukoc.Biol.* 77(3), pp. 414-420

Zhen L., King A.A., Xiao Y., Chanock S.J., Orkin S.H., Dinauer M.C. 1993. Gene targeting of X chromosome-linked chronic granulomatous disease locus in a human myeloid leukemia cell line and rescue by expression of recombinant gp91phox. *Proc.Natl.Acad.Sci.U.S.A* 90(21), pp. 9832-9836

Zhou B.B., Elledge S.J. 2000. The DNA damage response: putting checkpoints in perspective. *Nature* 408(6811), pp. 433-439

Zhou B.P., Liao Y., Xia W., Spohn B., Lee M.H., Hung M.C. 2001. Cytoplasmic localization of p21Cip1/WAF1 by Akt-induced phosphorylation in HER-2/neu-overexpressing cells. *Nat.Cell Biol.* 3(3), pp. 245-252

Zhou Y., Hileman E.O., Plunkett W., Keating M.J., Huang P. 2003. Free radical stress in chronic lymphocytic leukemia cells and its role in cellular sensitivity to ROS-generating anticancer agents. *Blood* 101(10), pp. 4098-4104

Ziegler-Heitbrock H.W., Thiel E., Futterer A., Herzog V., Wirtz A., Riethmuller G. 1988. Establishment of a human cell line (Mono Mac 6) with characteristics of mature monocytes. *Int.J.Cancer* 41(3), pp. 456-461

Zimmerman M.C., Oberley L.W., Flanagan S.W. 2007. Mutant SOD1-induced neuronal toxicity is mediated by increased mitochondrial superoxide levels. *J.Neurochem.* 102(3), pp. 609-618

Appendices

Appendix 1

A

N-Ras^{G12D} cDNA

```
  1 GTGTCGCTCC TTGGTGGGGG CTGTTCATGG CGGTTCCGGG GTCTCCAACA TTTTTCCCGG
 61 CTGTGGTCCT AAATCTGTCC AAAGCAGAGG CAGTGGAGCT TGAGGTTCTT GCTGGTGTGA
121 AATGACTGAG TACAAACTGG TGGTGGTTGG AGCAGATGGT GTTGGGAAAA GCGCACTGAC
181 AATCCAGCTA ATCCAGAACC ACTTTGTAGA TGAATATGAT CCCACCATAG AGGATTCTTA
241 CAGAAAACAA GTGGTTATAG ATGGTGAAAC CTGTTTGTTG GACATACTGG ATACAGCTGG
301 ACAAGAAGAG TACAGTGCCA TGAGAGACCA ATACATGAGG ACAGGCGAAG GCTTCCTCTG
361 TGTATTTGCC ATCAATAATA GCAAGTCATT TGCGGATATT AACCTCTACA GGGAGCAGAT
421 TAAGCGAGTA AAAGACTCGG ATGATGTACC TATGGTGCTA GTGGGAAACA AGTGTGATTT
481 GCCAACAAGG ACAGTTGATA CAAAACAAGC CCACGAACTG GCCAAGAGTT ACGGGATTCC
541 ATTCATTGAA ACCTCAGCCA AGACCAGACA GGGTGTTGAA GATGCTTTTT ACACACTGGT
601 AAGAGAAATA CGCCAGTACC GAATGAAAAA ACTCAACAGC AGTGATGATG GGACTCAGGG
661 TTGTATGGGA TTGCCATGTG TGGTGATGTA ACAAGATACT TTTAAAGTTT TGTCAGAAAA
721 GAGCCACTTT CAAGCTGCAC TGACACCCTG GTCCTGACTT CCCTGGAGGA GAAGTATTCC
781 TGTTGCTGTC TTCAGTCTCA CAGAGAAGCT CCTGCTACTT CCCCAGCTCT CAGTAGTTTA
```

B

H-Ras^{G12V} cDNA

```
  1 CATGACGGAA TATAAGCTGG TGGTGGTGGG CGCCGTCGGT GTGGGCAAGA GTGCGCTGAC
 61 CATCCAGCTG ATCCAGAACC ATTTTGTGGA CGAATACGAC CCCACTATAG AGGATTCCTA
121 CCGGAAGCAG GTGGTCATTG ATGGGGAGAC GTGCCTGTTG GACATCCTGG ATACCGCCGG
181 CCAGGAGGAG TACAGCGCCA TGCGGGACCA GTACATGCGC ACCGGGGAGG GCTTCCTGTG
241 TGTGTTTGCC ATCAACAACA CCAAGTCTTT TGAGGACATC CACCAGTACA GGGAGCAGAT
301 CAAACGGGTG AAGGACTCGG ATGACGTGCC CATGGTGCTG GTGGGGAACA AGTGTGACCT
361 GGCTGCACGC ACTGTGGAAT CTCGGCAGGC TCAGGACCTC GCCCGAAGCT ACGGCATCCC
421 CTACATCGAG ACCTCGGCCA AGACCCGGCA GGGAGTGGAG GATGCCTTCT ACACGTTGGT
481 GCGTGAGATC CGGCAGCACA AGCTGCGGAA GCTGAACCCT CCTGATGAGA GTGGCCCCGG
541 CTGCATGAGC TGCAAGTGTG TGCTCTCCTG A
```

cDNA encoding mutant Ras proteins which were subcloned into the PINCO retroviral vector

See Chapter 2 (section 2.4.1). cDNAs encoding **(A)** N-Ras^{G12D} and **(B)** H-Ras^{G12V} protein, depicting translated sequences (blue), position of start codon (underlined green), stop codon (underlined red) and codon 12 containing a point mutation (underlined purple). N-Ras^{G12D}, GGT → GAT mutation encodes a non-silent mutation from glycine to aspartate. H-Ras^{G12V}, GGC → GTC encodes a non-silent mutation from glycine to valine.

Appendix 2

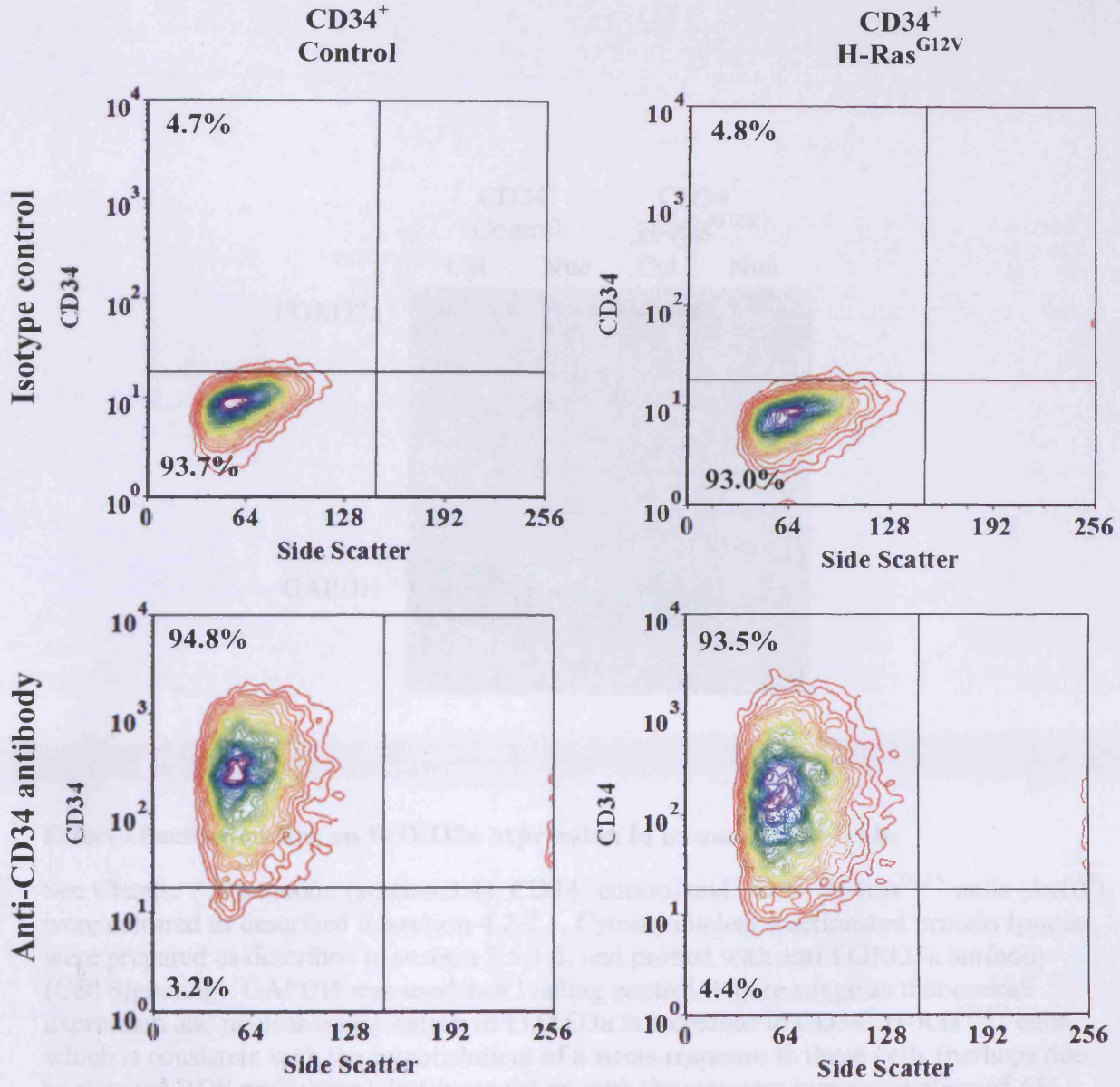

Bivariate flow cytometric plots depicting CD34 antigen expression after isolation and retroviral transduction

See Chapter 3 Results (section 3.3.1). Primary $CD34^+$ cells were isolated from human cord blood and transduced with PINCO as described in chapter 2. To establish the level of CD34 antigen expression in the resulting cultures, $1x10^4$ cells were analysed by flow cytomertry as described in section 2.6, using 5 µg/ml mouse anti-human CD34 antibody conjugated to PE. An isotype and manufacturer-matched antibody conjugated to PE (Isotype control) was used to establish background fluorescence. Figure shows typical CD34 expression observed. See Figure 3.3C for a summary of CD34 expression data obtained during this study.

Appendix 3

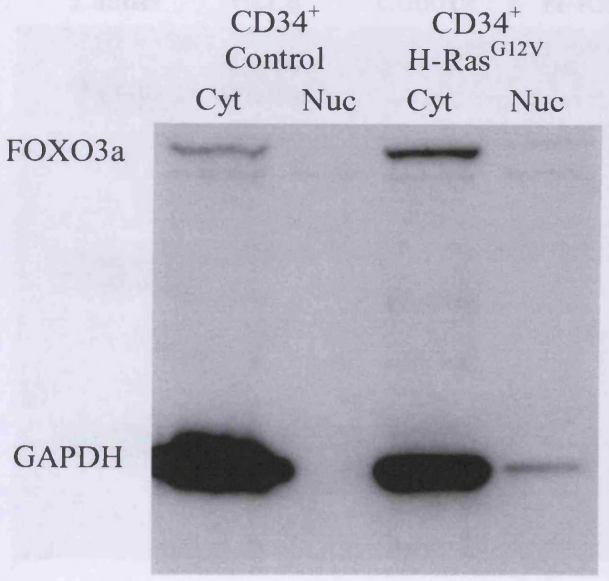

Effect of activated Ras on FOXO3a expression in human CD34$^+$ cells

See Chapter 3 Discussion (section 3.4). CD34$^+$ control and CD34$^+$ H-Ras^{G12V} cells ($3x10^5$) were cultured as described in section 4.2.2.1. Cytosol/nuclear fractionated protein lysates were prepared as described in section 2.5.1.3, and probed with anti-FOXO3a antibody (Cell Signaling). GAPDH was used as a loading control. Figure suggests that overall expression and nuclear translocation of FOXO3a is increased in CD34$^+$ H-Ras^{G12V} cells, which is consistent with the establishment of a stress response in these cells (perhaps due to elevated ROS production), but inconsistent with the apparent hyperactivation of Akt implied by increased phosphorylation of Akt on Ser473 (depicted in Figure 4.8B).

Appendix 4

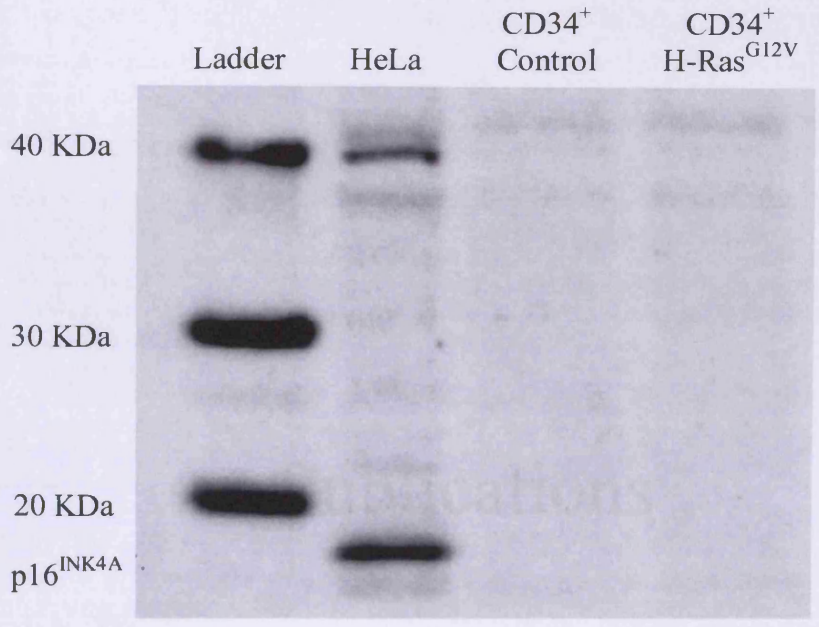

Validation of $p16^{INK4A}$ antibody using Westen blot analysis

See Chapter 4 Results (section 4.3.2.4). $CD34^+$ control and $CD34^+$ $H\text{-}Ras^{G12V}$ cells ($3x10^5$) were cultured as described in section 4.2.2.1 and HeLa cells were cultured as described in section 2.2.3.6. Whole-cell protein extracts were prepared as described in section 2.5.1.1, and were probed with 4 ng/ml anti-$p16^{INK4A}$ antibody (Cell signalling). Figure shows that antibody is capable of detecting $p16^{INK4A}$, but there is little or no expression in primitive $CD34^+$ cells.

Publications

Ras-induced reactive oxygen species promote growth factor–independent proliferation in human CD34$^+$ hematopoietic progenitor cells

Paul S. Hole,[1] Lorna Pearn,[1] Amanda J. Tonks,[2] Philip E. James,[3] Alan K. Burnett,[1] Richard L. Darley,[1] and Alex Tonks[1]

Departments of [1]Haematology, [2]Medical Microbiology, and [3]Cardiology, School of Medicine, Cardiff University, Cardiff, United Kingdom

Excessive production of reactive oxygen species (ROS) is a feature of human malignancy and is often triggered by activation of oncogenes such as activated Ras. ROS act as second messengers and can influence a variety of cellular process including growth factor responses and cell survival. We have examined the contribution of ROS production to the effects of N-Ras^{G12D} and H-Ras^{G12V} on normal human CD34$^+$ progenitor cells. Activated Ras strongly up-regulated the production of both superoxide and hydrogen peroxide through the stimulation of NADPH oxidase (NOX) activity, without affecting the expression of endogenous antioxidants or the production of mitochondrially derived ROS. Activated Ras also promoted both the survival and the growth factor–independent proliferation of CD34$^+$ cells. Using oxidase inhibitors and antioxidants, we found that excessive ROS production by these cells did not contribute to their enhanced survival; rather, ROS promoted their growth factor–independent proliferation. Although Ras-induced ROS production specifically activated the p38^{MAPK} oxidative stress response, this failed to induce expression of the cell-cycle inhibitor, p16^{INK4A}; instead, ROS promoted the expression of D cyclins. These data are the first to show that excessive ROS production in the context of oncogene activation can promote proliferative responses in normal human hematopoietic progenitor cells. (Blood. 2010;115: 1238-1246)

Introduction

Reactive oxygen species (ROS) are a heterogeneous group of inorganic molecules and free radicals, with a wide spectrum of life span and reactivity. In physiologic systems, ROS formation begins with the univalent reduction of diatomic oxygen to produce superoxide radicals. There are 2 main sources of cellular superoxide; the first is the mitochondrial electron transport chain, where incomplete reduction of oxygen to water can result in superoxide formation. The other major source of superoxide is professional oxidases (exemplified by the NADPH oxidase [NOX] protein family),[1] which are expressed and functional throughout hematopoietic development.[2] These proteins form part of a membrane-bound complex that transfers single electrons from cytosolic nicotinamide adenine dinucleotide phosphate via flavin adenine dinucleotide to extracellular oxygen, producing superoxide. Superoxide is a short-lived radical but can dismutate forming hydrogen peroxide (H_2O_2), a relatively long-lived species that lies at the hub of a variety of potential chemical reactions and is the main molecule from which all other physiologic ROS molecules are derived. ROS levels are regulated by a complex network of antioxidant molecules and enzymes that detoxify ROS.[3] For example, superoxide generation is balanced by the actions of superoxide dismutases (SODs), which convert superoxide to H_2O_2. Subsequently, H_2O_2 is destroyed during oxidation reactions involving glutathione or members of the peroxiredoxin family.

Although ROS production can have adverse consequences causing lipid peroxidation and DNA damage, it is also clear that ROS act as cell-signaling molecules. In recent years, it has become clear that H_2O_2 reacts with a variety of proteins sensitive to thiol oxidation.[4] In particular, H_2O_2 can inhibit phosphatases via oxidation of cysteine at the active site and may consolidate growth factor signaling by preventing futile cycles of phosphorylation and dephosphorylation of proteins and phosphoinositides.[5] The fact that H_2O_2 is freely membrane-permeable also has the consequence that its production affects not only the cells generating it but also neighboring cells. This applies particularly to transmembrane-bound NOX oxidases that release ROS into the extracellular environment. Rapid increases in ROS are observed after growth factor stimulation and inhibition of ROS production can lead to abolition of signaling.[5-7] Other reports indicate that ROS may also directly promote G_1-to-S progression, perhaps by direct modification of cell-cycle regulatory proteins.[6,8]

Excessive production of ROS (comprising mainly superoxide and H_2O_2) is a common feature of malignant disease including leukemia.[9,10] Common leukemia-associated abnormalities such as activated Ras,[9,11] activated FMS-like tyrosine kinase 3,[12] and BCR-ABL[13] are associated particularly with overproduction of ROS. One consequence of this is an increase in DNA damage,[14] which may thereby contribute to leukemogenesis; however, its role in cell signaling suggests that overproduction of ROS may have more direct consequences. On the one hand, ROS overproduction may act as a tumor suppressor[15] by promoting a stress response that leads to cell-cycle arrest,[16] senescence, or apoptosis[9]; conversely, it is clear that cancer cells can evolve to evade this stress response,[9] and several models indicate that sustained ROS overproduction is essential to maintain the transformed phenotype.[11,13,17,18] Little is known of the consequences of ROS overproduction in leukemia.

Mutational activation of Ras is observed in 15% to 25% of acute myeloid leukemias.[19] Using a model system based on normal

Submitted June 4, 2009; accepted November 14, 2009. Prepublished online as *Blood* First Edition paper, December 10, 2009; DOI 10.1182/blood-2009-06-222869.

The online version of this article contains a data supplement.

The publication costs of this article were defrayed in part by page charge payment. Therefore, and solely to indicate this fact, this article is hereby marked "advertisement" in accordance with 18 USC section 1734.

human CD34+ hematopoietic progenitor cells, we have therefore examined the impact of this oncogene in terms of its capacity to promote ROS production in these cells and also the contribution that ROS make to the phenotype exhibited by activated Ras–expressing progenitor cells. Here we show that constitutively active Ras strongly promotes superoxide and H_2O_2 production in human CD34+ cells through activation of NOX oxidases. Ras also strongly promoted both survival and growth factor–independent proliferation of CD34+ cells in a culture density–dependent manner. We found that ROS overproduction did not contribute to the prosurvival phenotype, but did contribute to growth factor–independent proliferation by augmenting the expression of cyclins D1 and D3.

Methods

Generation of human CD34+ and murine Sca-1+ hematopoietic progenitor cells expressing activated Ras

Murine bone marrow was extracted from wild-type and Nox2$^{-/-}$C57BL/6 littermates (kindly provided by Professor A. Shah, King's College Hospital) as described elsewhere.[20] Human neonatal cord blood was obtained from healthy full-term pregnancies at the University Hospital Wales. These specimens were obtained with informed consent and with approval from the South East Wales Research Ethics Committee in accordance with the 1964 Declaration of Helsinki. Murine Sca-1+ and human CD34+ hematopoietic progenitor cells were positively selected using the MiniMACS Sca-1+ or CD34+ cell isolation kits, respectively, according to the manufacturer's instructions (Miltenyi Biotec). Ectopic expression of H-Ras^{G12V} or N-Ras^{G12D} and reporter genes (green fluorescent protein [GFP] or DsRed) was achieved using the PINCO retroviral vector. Retroviral transduction was carried out over 2 subsequent days as previously described.[21] Transduced human CD34+ and murine Sca-1+ hematopoietic progenitor cells were cultured in supplemented Iscove modified Dulbecco medium (IMDM), as previously described,[22] containing 20% fetal calf serum, supplemented with either 5 ng/mL human interleukin-3, human granulocyte colony-stimulating factor (CSF), human granulocyte-macrophage CSF, and 20 ng/mL human stem cell factor (for CD34+ cells), or with the same concentrations of murine interleukin-3, murine granulocyte-macrophage CSF, murine stem cell factor, and human granulocyte CSF (for Sca-1+ cells), unless otherwise stated.

Detection of superoxide using the chemiluminescent probe Diogenes

Superoxide measurement was carried out using the chemiluminescent probe Diogenes (National Diagnostics). Transduced human CD34+ cells or murine Sca-1+ cells were washed in phosphate-buffered saline (PBS) and resuspended in standard buffer (KH_2PO_4 4.6mM, Na_2HPO_4 8.0mM, NaCl 13mM, KCl 0.44mM, glucose 5.5mM, bovine serum albumin [low lipopolysaccharide] 0.1%, $MgCl_2$ 0.5mM, $CaCl_2$ 0.45mM dissolved in lipopolysaccharide–low water, pH 7.3) at 1×10^6 cells/mL. Cell suspensions (150 μL) were assayed in triplicate in FluoroNunc Maxisorp 96-well plates (Thermo-Fisher Scientific). Diogenes (50 μL) was added immediately before recording chemiluminescence (Dynex MLX Luminometer; Jencons). Some experiments were carried out in the presence of either 5 μg/mL superoxide dismutase (SOD), 100 μg/mL catalase, 50μM diphenyleneiodonium (DPI), 1mM apocynin, or 5μM rotenone (Sigma). Human peripheral blood monocytes stimulated with opsonised zymosan[23] were used for comparative purposes.

Detection of superoxide using electron paramagnetic resonance spectroscopy

To confirm the presence of the superoxide radical, the spin-trap probe 5-(diethoxyphosphoryl)-5-methyl-1-pyrroline-*N*-oxide (DEPMPO; Axxora) was used. Transduced cells were washed in PBS and resuspended at 1×10^7 cells/mL in standard buffer. DEPMPO (60mM) was added immediately before measurement. Electron paramagnetic resonance (EPR) spectra were detected in 10 scans of 60 seconds at 37°C using a Varian 104 EPR spectrometer (Varian Inc) at X-band (9.5 GHz). Typical recording conditions were field center, 3378 Gauss; gain, 2×10^5; modulation amplitude, 2.0; time constant, 0.25; microwave power, 10 mW; and field range, 160 Gauss. Addition of 5 μg/mL SOD served as a negative control. Background was established using DEPMPO probe alone.

Determination of mitochondrial superoxide production using MitoSOX

Mitochondrial superoxide was measured using MitoSOX (Invitrogen). Transduced CD34+ cells (days 5 to 7) were washed in warm PBS and then incubated with 5μM MitoSOX for 15 minutes at 37°C and washed in FACSFlow (BD Biosciences) before flow cytometric analysis ("Flow cytometric analysis"). For some experiments, cells were incubated for 15 minutes at 37°C before MitoSOX treatment with either 50μM rotenone (Sigma) or 5μM iron (III) 5, 10, 15, 20-tetrakis-4-carboxyphenyl porphyrin (FeTCPP; Frontier Scientific Inc) as a positive or negative control, respectively.

Detection of hydrogen peroxide using Amplex Red

Amplex Red (Invitrogen), a H_2O_2-sensitive fluorescent probe, was prepared according to the manufacturer's instructions. Transduced CD34+ cells (days 4 to 5; 2×10^5) were resuspended at 1×10^6 cells/mL in Krebs-Ringer phosphate buffer containing 5.50mM glucose, pH 7.35, for 4 hours at 37°C. After centrifugation (180*g* for 5 minutes), the conditioned medium (supernatant) was harvested and 50 μL was assayed (in triplicate) in 96-well fluorescent assay plates (Thermo Fisher Scientific) containing 50 μL/well Amplex Red solution. Fluorescence was recorded using a FluoStar Optima instrument (excitation, 540 nm; emission, 590 nm; BMG Labtech). The concentration of H_2O_2 was determined using a standard curve.

Western blotting

Western blotting was performed using the NuPage Bis-Tris (bis(2-hydroxyethyl)iminotris(hydroxymethyl)methane–tris(hydroxymethyl)aminomethane) gel system (Invitrogen) using whole-cell lysates prepared as previously described.[24] In some cases, transduced CD34+ cells (day 5) were incubated at 37°C in supplemented IMDM without growth factors for 16 hours before lysate preparation. For cell fractionation experiments, plasma membrane and cytosol fractions were prepared by 2 freeze-thaw cycles in the presence of homogenization buffer (sucrose 0.25M, *N*-2-hydroxyethylpiperazine-*N*'-2-ethanesulfonic acid–KOH 10mM, magnesium acetate 1mM, ethylenediaminetetraacetic acid 0.5mM, ethyleneglycol-tetraacetic acid 0.5mM, β-mercaptoethanol 10mM, 20 μg/mL DNase, pH 7.2). Homogenate (100 μL) was centrifuged at 16 000*g* for 1 hour at 4°C. Cytosolic proteins (supernatant) were aspirated and the membrane pellet was solubilized in homogenization buffer containing 1% Triton X-100. Nuclear and cytosol fractions were prepared using a cell fractionation kit (PerkinElmer) according to the manufacturer's instructions. Protein concentration was determined using the Bradford method, or by the DC Protein Assay Kit (Bio-Rad) according to the manufacturer's instructions. Subcellular fractions or whole-cell lysates ($2\text{-}5 \times 10^4$ cell equivalents/lane) were loaded onto a 4% to 12% Bis-Tris gel and electroblotting was performed as previously described.[24] Electroblotted membranes were probed overnight at 4°C using antibodies recognizing p67^{phox} (clone H-300), p47^{phox} (A-7), p40^{phox} (D-8; all from Santa Cruz Biotechnology), pan Rac, cyclin D3, cyclin-dependent kinase 4 (CDK4), CDK6, anti-p16^{INK4A}, p15^{INK4B}, p21^{Cip1}, p27^{Kip1}, total p38^{MAPK}, phospho-p38^{MAPK} (Thr180/182), total Akt, phospho-Akt (Ser473), SOD1, anti–phospho-Rb (Ser780), anti–phospho-Rb (Ser795), anti–phospho-Rb (Ser807/811), anti-pan Rb, pan Ras (all from Cell Signaling Technology), catalase (Abcam), pan Ras^{V12} (DWP; Calbiochem), and peroxiredoxin I (Lab Frontier). Anti–glyceraldehyde-3-phosphate dehydrogenase (GAPDH; 6C5; Santa Cruz Biotechnology), anti-β-actin (mAbcam 8226; Abcam) or anti-α-tubulin (DMA1; Calbiochem) was used to confirm equal loading. Purity of plasma membrane and nuclear or cytosolic

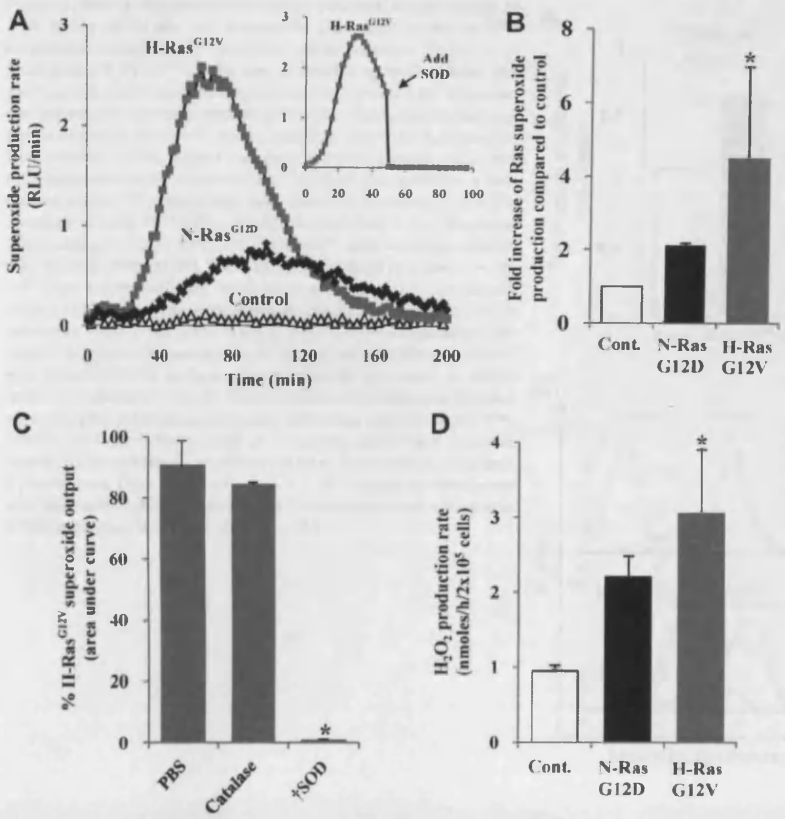

Figure 1. Measurement of ROS production by human hematopoietic progenitor cells expressing N-Ras^{G12D} or H-Ras^{G12V}. (A) Representative chemiluminescence trace of superoxide production measured using Diogenes. In some replicates (inset), superoxide production was quenched by addition of SOD at 50 minutes. (B) Summary of fold increase of total light emission due to expression of activated Ras over controls during early hematopoietic development. (C) Using Diogenes, superoxide production in H-Ras^{G12V}–transduced cells was measured, with either 5 μg/mL SOD or 100 μg/mL catalase present from the start of the assay (n = 3). Bar chart represents total superoxide produced (area under chemiluminescence trace). (D) Using Amplex Red, H_2O_2 production rate was determined over 4 hours. Data represent mean + 1 SD (n ≥ 3). Statistical significance was calculated by ANOVA using Tukey honestly significant differences, Mann-Whitney test, or Student paired *t* test. †$P < .001$; *$P < .05$.

fractions was verified using anti-CD45 (69; BD Biosciences), anti–Histone H1 (AE4; AbD Serotec), and anti-GAPDH. Target proteins were visualized using the ECL Advance Detection Kit (GE Healthcare) according to the manufacturer's instructions. Chemiluminescence was recorded using a LAS-3000 image analyser (Fujifilm UK Ltd), and analyzed using AIDA Image Analyser Version 4.19 (Fujifilm UK Ltd).

Cell survival, proliferation, and cell-cycle analysis assays

After gene transduction (day 3) and 2 washes in Hanks balanced salt solution (Invitrogen), 0.5 to 4 × 10^5 transduced CD34$^+$ cells/mL were cultured in 96-well U-bottom microplates (Thermo Fisher Scientific) at 37°C for 48 hours in either IMDM without supplements, serum, or growth factors (for survival assay), or supplemented IMDM without growth factors (for proliferation assay). In some experiments, cells were incubated with either highly purified catalase (no. C100), DPI, or *N*-acetylcysteine (NAC; Sigma). After incubation, cells were washed in PBS, 1% bovine serum albumin and stained with an annexin V–cyanin 5 conjugate (BioVision) according to the manufacturer's instructions in the presence of 1 μg/mL 7-amino-actinomycin D (7-AAD) to discriminate membrane-permeable cells. Viable cells were counted by flow cytometry as described below using 5 × 10^3 allophycocyanin microbeads (BD Biosciences) to control for cell recovery. For cell-cycle analysis, 0.5 to 1 × 10^5 human CD34$^+$ cells (day 5) were quiesced for 16 hours as in "Western blotting." before fixation and determination of DNA content as previously described.[25] The threshold for inclusion of apoptotic bodies was set at 25% of the fluorescence peak representing cells in G_0. Proportion of cells in G_0 and $S+G_2/M$ was determined using Cylchred Version 1.0 (T. Hoy, Cardiff University). All data were acquired by flow cytometry as described in "Flow cytometric analysis."

Flow cytometric analysis

Transduced CD34$^+$ cells were stained for cytometric analysis with unconjugated mouse anti-NOX2 antibody (7D5; Caltag Medsystems) or anti–CD34$^-$ phycoerythrin (PE) antibody (BD Biosciences). Unconjugated anti-NOX2 antibody was detected using secondary rat anti–mouse immunoglobulin G_1-PE (BD). Background fluorescence was established by isotype-matched controls; autofluorescence of mock-infected cultures defined the threshold for GFP or DsRed positivity. Data were acquired using a BD FACSCalibur and analyzed using FCS Express Version 3 (De Novo Software).

Statistical analysis

Significance of difference was determined using one-way analysis of variance (ANOVA) with Tukey honestly significant differences test, Mann-Whitney test, or Student *t* test using Minitab Version 13.0 (Minitab Ltd).

Results

Expression of N-Ras^{G12D} or H-Ras^{G12V} in human CD34$^+$ hematopoietic progenitor cells promotes ROS production

To establish whether expression of activated Ras promoted ROS production in normal hematopoietic progenitor cells, we transduced human CD34$^+$ hematopoietic cells using the retroviral vector PINCO, encoding N-Ras^{G12D} or H-Ras^{G12V} and a reporter gene (GFP), or reporter gene alone. The resultant cell cultures are referred to hereafter as CD34$^+$ N-Ras^{G12D}, CD34$^+$ H-Ras^{G12V}, or control, respectively, and typically 50% to 80% of the cells were GFP$^+$ after transduction (supplemental Figure 1, available on the *Blood* website; see the Supplemental Materials link at the top of the online article). Superoxide was assayed using the superoxide-sensitive chemiluminescent probe, Diogenes. A low level of constitutive superoxide production was observed in normal cells, and was strongly augmented by activated Ras (Figure 1A). As

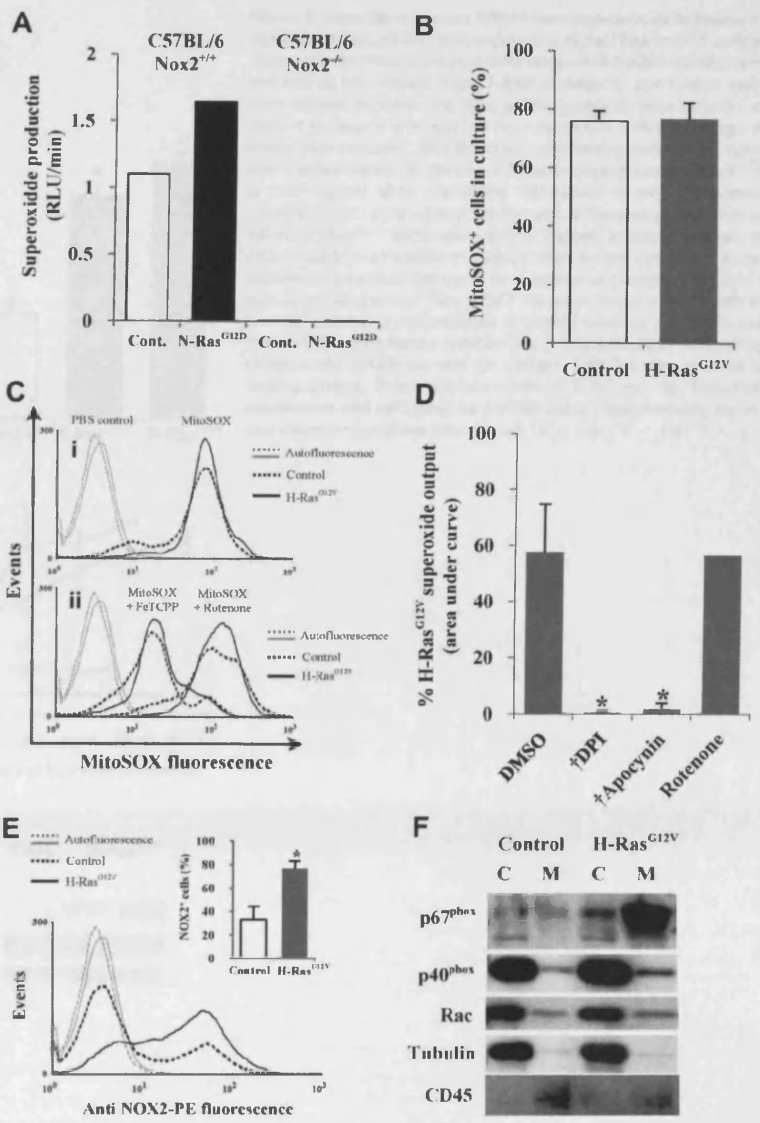

Figure 2. Mutant Ras promotes ROS production via activation of NOX family oxidases. (A) Superoxide production by N-Ras^{G12D}–transduced murine Sca-1$^+$ cells from either wild-type (Nox2$^{+/+}$) or Nox2-deficient (Nox2$^{-/-}$) mice was measured using Diogenes. Bar chart represents total superoxide produced during assay. (B) Mitochondrial superoxide was measured using MitoSOX. Figure depicts percentage of control or H-Ras^{G12V} cells positive for MitoSOX fluorescence after labeling. A PBS control was used to define positive threshold. (C) Representative histograms depict MitoSOX fluorescence in control and H-Ras^{G12V} cells labeled with MitoSOX (i) alone or (ii) in the presence of 5μM FeTCPP or 50μM rotenone. (D) Using Diogenes, superoxide production by CD34$^+$ H-Ras^{G12V} cells was measured in the presence of 50μM DPI, 50μM apocynin, or 5μM rotenone (n = 3). Bar chart represents total superoxide produced. (E) Transduced CD34$^+$ cells were incubated with anti–NOX2-PE and analyzed by flow cytometry. Typical histogram showing anti–NOX2-PE expression; bar chart (inset) indicates percentage of fluorescent cells after incubation with anti–NOX2-PE. Isotype control antibody was used to define positive threshold (n = 5). (F) Cytosol/membrane fractionated lysates were analyzed by Western blot using antibodies recognizing p67^{phox}, p40^{phox}, or Rac. Tubulin acted as a loading control and cytosolic marker. CD45 was used a membrane marker. C indicates cytosol; and M, membrane. Data represent mean + 1 SD. Statistical significance was calculated by ANOVA using Tukey honestly significant differences or Mann-Whitney test. †$P < .001$; *$P < .05$.

shown in Figure 1B, superoxide induction was typically more efficient with H-Ras^{G12V} (~ 4-fold increase compared with controls) than with N-Ras^{G12D} (~ 2-fold increase), though maximal superoxide induction was only a tenth of that generated by activated phagocytes (supplemental Figure 2B). SOD quenched chemiluminescence, whereas treatment with catalase (which decomposes H_2O_2 but not superoxide) did not, demonstrating the specificity of the probe and confirming superoxide as the major source of ROS in this assay (Figure 1C).

Because H_2O_2 rather than superoxide has been implicated as a second messenger, we measured levels of H_2O_2 in medium conditioned by N-Ras^{G12D}– and H-Ras^{G12V}–expressing cells. Hydrogen peroxide (which can be generated from superoxide via a dismutation reaction[26]) was assayed using the H_2O_2-sensitive fluorescent probe, Amplex Red. CD34$^+$ H-Ras^{G12V} cells showed significantly higher rates of H_2O_2 production compared with controls ($P < .05$), whereas CD34$^+$ N-Ras^{G12D} cells showed a similar trend, which did not reach significance (Figure 1D).

Aberrant Ras signaling affects transcription of a variety of genes[27] and could potentially perturb the expression of endogenous antioxidant molecules resulting in an apparent increase in ROS production. However, no differences in the levels of common antioxidants were observed compared with control cultures (supplemental Figure 2D). Taken together, these data demonstrate that activated Ras stimulates significant overproduction of superoxide as well as the more stable and membrane-permeable putative second messenger, H_2O_2, in hematopoietic progenitor cells.

Ras-induced ROS are mediated via NOX family oxidase activity

ROS can be generated by several mechanisms, the major sources being oxidase activity (eg, NOX family oxidases) or the mitochondrial electron transport chain.[28] The NOX family oxidase Phox is a transmembrane multimeric complex consisting of the NOX2 (aka, gp91^{phox}) catalytic subunit and several regulatory subunits. When N-Ras^{G12D} was expressed in Nox2 wild-type Sca-1$^+$ murine hematopoietic cells, a 1.5-fold increase in superoxide production was observed compared with controls, whereas superoxide production was absent in Sca-1$^+$ cells from Nox2$^{-/-}$ mice, suggesting that in murine hematopoietic cells, Nox2 is the major source of ROS in the context of activated Ras (Figure 2A). To establish whether this

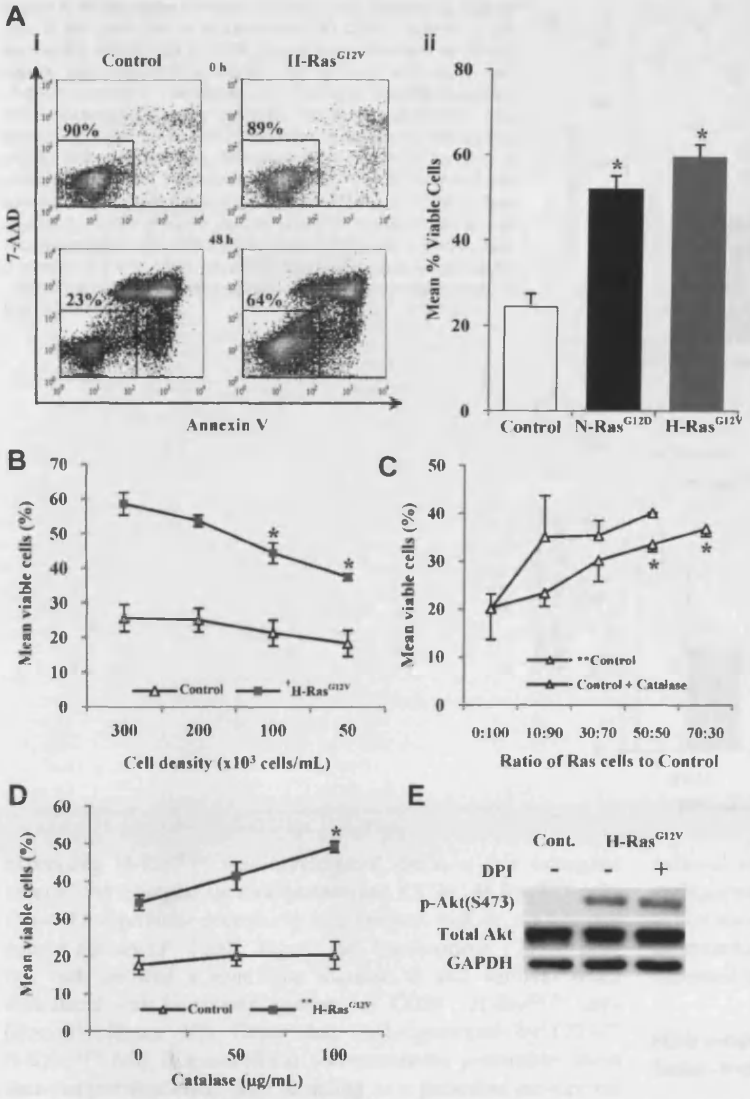

Figure 3. Survival of human CD34$^+$ hematopoietic cells expressing mutant Ras. CD34$^+$ cells expressing mutant Ras or GFP control were incubated in serum-free, growth factor–free medium for 48 hours and stained with annexin V and 7-AAD. Annexin V$^-$ and 7-AAD$^-$ cells were defined as viable. (Ai) Typical flow cytometric plots obtained at start of incubation and after 48-hour incubation with percentage of viable cells indicated. (Aii) Bar chart representing survival averaged over 3 experiments. (B) Viability of CD34$^+$ cells expressing H-Ras^{G12V} or GFP control while decreasing cell-culture density. (C) Normal (control) CD34$^+$ cells were cocultured with an increasing proportion of CD34$^+$ H-Ras^{G12V} cells coexpressing DsRed, enabling analysis of CD34$^+$ control cell viability in mixed culture by flow cytometry. Some experiments were carried out in the presence of catalase. (D) CD34$^+$ cells expressing mutant Ras or GFP were cultured at a cell density of 5×10^4 cells/mL in the presence of purified catalase. (E) Whole-cell lysates were analyzed by Western blot, using antibodies recognizing phospho-Akt (S473) or total Akt protein. GAPDH was used as a loading control. Data represent mean ± 1 SD (n = 3). Statistical significance was calculated by ANOVA using Tukey honestly significant differences or Mann-Whitney test. †$P < .001$; *$P < .05$; **$P < .01$.

was also the case in human cells, we first used the mitochondria-specific superoxide-sensitive probe MitoSOX to determine whether activated Ras promoted ROS production from this source. No significant differences in mitochondrial ROS were observed in CD34$^+$ H-Ras^{G12V} cells (which produced the highest levels of ROS) compared with controls (Figure 2B). The sensitivity of MitoSOX for mitochondrial superoxide was confirmed using the antioxidant FeTCPP or the mitochondrial poison rotenone, which reduce or increase mitochondrial superoxide, respectively (Figure 2C). These data indicated that excess superoxide production detected by Diogenes did not arise from the mitochondria. To determine whether NOX oxidases were the source of increased superoxide production, we used the NOX oxidase inhibitors DPI and apocynin. Superoxide production (measured using Diogenes) was completely blocked by these inhibitors in both CD34$^+$ H-Ras^{G12V} cells and control cells, whereas the mitochondrial poison rotenone had no effect (Figure 2D). These data, together with the data from Nox2$^{-/-}$ mice (Figure 2A), indicate that the major source of increased superoxide production in human CD34$^+$ cells expressing activated Ras is the NOX family oxidase, Phox.

During Phox activation, Phox regulatory subunits translocate from the cytosol to form a complex with NOX2 at the plasma membrane.[26] Therefore, the ability of activated Ras to alter the expression and localization of Phox components was investigated. Flow cytometric analysis showed that activated Ras significantly increased in the expression of NOX2 compared with controls ($P < .05$; Figure 2E). In addition, Figure 2F shows that activated Ras also promoted the membrane translocation/expression of the Phox activators p67^{phox} and p40^{phox}. Taken together, these data support the observations that activated Ras promotes ROS production by increasing Phox activity in human CD34$^+$ cells.

Activated Ras promotes survival in human CD34$^+$ cells but Ras-induced ROS antagonize survival

Constitutively active Ras is associated with increased cell survival.[29] Consistent with this, CD34$^+$ N-Ras^{G12D} and CD34$^+$ H-Ras^{G12V} cells were resistant to apoptosis when incubated in serum-free, growth factor–free medium for 48 hours compared with controls ($P < .05$; Figure 3A). Interestingly, the strength of the survival phenotype correlated with the level of ROS production. Excessive H_2O_2 exposure leads to oxidative stress and cell death, however low levels of H_2O_2 can promote cell survival.[30] Therefore the role of H_2O_2 in the survival of CD34$^+$ cells

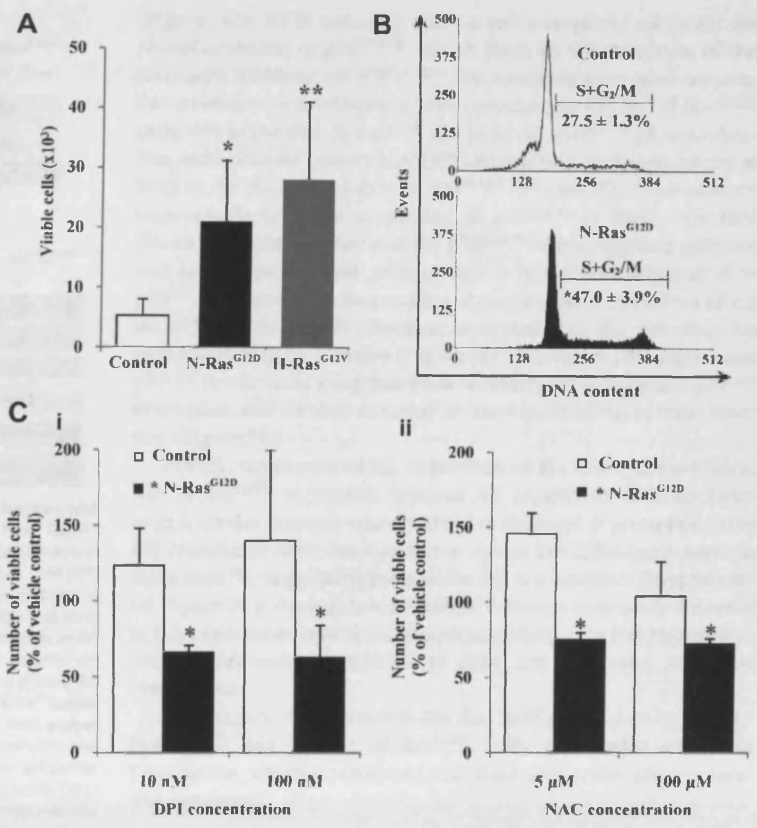

Figure 4. Proliferation of hematopoietic cells expressing mutant Ras in the presence of antioxidants. (A) CD34$^+$ cells (1×10^4) expressing mutant Ras or GFP control were incubated in serum-replete, growth factor–free medium for 48 hours, and viable cells (7-AAD$^-$, annexin V$^-$) were counted by flow cytometry. (B) Representative histograms showing cell-cycle distribution of CD34$^+$ cells expressing N-Ras^{G12D} or GFP control after 16 hours in serum-replete, growth factor–free medium. The percentage of cells in S+G_2/M is indicated. (C) CD34$^+$ cells expressing N-Ras^{G12D} or GFP control were incubated as in panel A in the presence of (i) DPI or (ii) NAC. Data represent number of viable cells remaining as a percentage of that recovered from cells treated with vehicle control, set at 100%. Data are mean ± 1 SD; n ≥ 3. Statistical significance was calculated by ANOVA using Tukey honestly significant differences or Mann-Whitney test. $^{**}P < .01$; $^{*}P < .05$.

expressing H-Ras^{G12V} was investigated (because this oncogene induced the strongest survival phenotype). CD34$^+$ H-Ras^{G12V} cells showed a significant decrease in cell survival with decreasing cell culture density ($P < .001$; Figure 3B). Furthermore, CD34$^+$ control cells showed a significant increase in cell survival when cocultured with increasing numbers of CD34$^+$ H-Ras^{G12V} cells ($P < .01$; Figure 3C). Given that H_2O_2 generated by CD34$^+$ H-Ras^{G12V} cells is extracellular and membrane permeable, these data suggest that H_2O_2 may be acting as a paracrine prosurvival factor. To establish whether H_2O_2 was responsible for this effect, additional coculture experiments were carried out in the presence of catalase. The presence of catalase did not suppress control cell survival, but instead augmented it further, indicating that the prosurvival influence was not mediated by H_2O_2, which in fact antagonized the survival of control cells (Figure 3C). Indeed, catalase treatment also further promoted the survival of CD34$^+$ H-Ras^{G12V} cells themselves, indicating that H_2O_2 production also antagonized the survival of these cells (Figure 3D). A similar trend was seen upon treatment with the antioxidant NAC or the NOX inhibitor DPI (data not shown). As expected, catalase treatment had a modest effect on control cells cultured alone because these cells produced very low levels of H_2O_2 (Figure 3D). Taken together, these data suggest that CD34$^+$ H-Ras^{G12V} cells secrete factors that promote survival, but ROS production appears to antagonize the prosurvival effects of these factors.

In further demonstration of this, we examined the phosphorylation of the prosurvival protein, Akt. H-Ras^{G12V} increased the phosphorylation of Akt, which probably contributed to the increased survival of these cells (Figure 3E). However, incubation with the NOX inhibitor DPI (Figure 3E) or catalase (data not shown) did not reduce the phosphorylation of Akt, supporting our observations that ROS were not contributing to the enhanced survival of CD34$^+$ H-Ras^{G12V} cells. Increased expression of the antiapoptotic protein Survivin has also been reported as an explanation for Ras-induced survival[31]; however, our study found no evidence of increased Survivin expression as a consequence of activated Ras expression (data not shown).

ROS production augments activated RAS-induced growth factor–independent proliferation

We observed that control cells were better able to survive in serum-replete medium but were unable to proliferate without the addition of growth factors, whereas CD34$^+$ cells expressing N-Ras^{G12D} or H-Ras^{G12V} were able to proliferate under these conditions and showed a significant approximately 4-fold increase in cell numbers after 48 hours compared with controls ($P < .05$; Figure 4A). Cell-cycle analysis confirmed that CD34$^+$ N-Ras^{G12D} cells exhibited a significant approximately 2-fold increase in the proportion of cells in cycle (S+G_2/M) compared with controls ($P < .05$; Figure 4B). To determine whether ROS production played a role in the growth factor–independent proliferation, CD34$^+$ N-Ras^{G12D} cells were incubated in serum-replete, growth factor–free medium for 48 hours in the presence of the antioxidants DPI and NAC. Both DPI and NAC suppressed proliferation of these cells, whereas control cells showed increased proliferation (Figure 4C). Similar effects were observed with CD34$^+$ H-Ras^{G12V} cells (supplemental Figure 3). We also examined whether ROS production could influence progenitor frequency. In accordance with previously published work,[32] we found no significant difference in progenitor frequency either in terms of CD34 positivity, morphology, or colony-forming ability. Treatment with DPI had no differential effect in each case, indicating that under these conditions excessive production of ROS (stimulated by Ras) does not

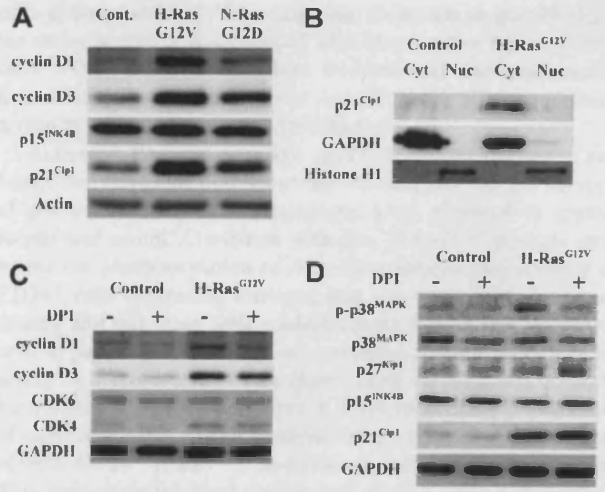

Figure 5. Determination of cell-cycle regulatory protein status by Western blot in CD34+ hematopoietic progenitors transduced with mutant Ras. CD34+ control, CD34+ N-Ras^{G12D}, or CD34+ H-Ras^{G12V} cells were incubated for 16 hours in serum-replete, growth factor–free medium in the presence or absence of 1 μM DPI. Expression and phosphorylation state of key cell-cycle regulatory proteins in whole-cell lysates were determined by Western blot. In all cases, GAPDH was used as a loading control. (A) The endogenous expression of cell-cycle promoters cyclin D3 and cyclin D1 and cell-cycle inhibitors p15^{INK4B} and p21^{Cip1} was determined. (B) Cytosol/nuclear fractionated lysates were probed with antibody recognizing the cell-cycle inhibitor p21^{Cip1}. (C) Whole-cell lysates derived from both CD34+ control and CD34+ H-Ras^{G12V} cells (treated with either DPI or vehicle control) were probed with antibodies recognizing the cell-cycle promoters CDK6, CDK4, cyclin D1, and cyclin D3. (D) Whole-cell lysates as in panel C were probed with antibodies recognizing the following cell-cycle inhibitory proteins; p21^{Cip1} (which inhibits CDK/cyclin complexes); p15^{INK4B} (which sequesters CDK4/6); p27^{Kip1} (which has a similar role to p21^{Cip1}) and p38^{MAPK}, both total and phosphorylated (T180/T182).

significantly influence progenitor frequency (supplemental Figure 4). Taken together, these data suggest that Ras signaling strongly drives factor-independent growth, and indicate that Ras-induced ROS production plays a role in augmenting this proliferative signal.

ROS production modulates key cell-cycle regulatory proteins

Consistent with their proproliferative role, N-Ras^{G12D} and H-Ras^{G12V} strongly promoted the expression of D-type cyclins D1 and D3; in each case the influence of H-Ras^{G12V} was greater than N-Ras^{G12D}. These oncogenes had no effect on the expression of the cell-cycle inhibitor p15^{INK4B}, but did up-regulate the cell-cycle inhibitor p21^{Cip1}, which seemed contrary to their proproliferative effect (Figure 5A). Previously, it has been reported that hematopoietic cells express high levels of extranuclear p21^{Cip1},[33] therefore we examined the subcellular location of p21^{Cip1} and found that p21^{Cip1} expression was exclusively cytosolic (Figure 5B). This suggests that induction of p21^{Cip1} in these cells is concerned with its antiapoptotic cytoplasmic function rather than its nuclear cell-cycle inhibitory role.[34]

To assess whether ROS production contributed to the altered expression of cell-cycle regulatory proteins, CD34+ H-Ras^{G12V} cells were treated with DPI before Western blot analysis (Figure 5C-D). NOX inhibition resulted in a consistent reduction in cyclin D1 and cyclin D3 expression, indicating that ROS production cooperated with activated Ras in the induction of these D-type cyclins. Activated Ras also up-regulated cyclin-dependent kinase 4 (CDK4), a binding partner of D-type cyclins, however, DPI had no effect on the expression of this protein or CDK6 (Figure 5C). Next, we examined the effect of NOX inhibition on the cell-cycle inhibitor proteins p38^{MAPK}, p16^{INK4A}, p15^{INK4B}, p27^{Kip1}, and p21^{Cip1} (Figure 5D). ROS normally elicit a stress response mediated via phosphorylation of p38^{MAPK}, which leads to the induction of the cell-cycle inhibitor, p16^{INK4A}.[9,15] We therefore examined whether this oxidative stress response was operating in CD34+ H-Ras^{G12V} cells. We found that H-Ras^{G12V} did promote p38^{MAPK} phosphorylation, but not in the presence of DPI, demonstrating the specificity of ROS in the phosphorylation of p38^{MAPK} (Figure 5D). However, we were unable to detect expression of p16^{INK4A} in these cells (not shown), indicating either that the p38^{MAPK} stress-response pathway was uncoupled in these cells or that it is not normally linked to p16^{INK4A} induction in this context. As expected, DPI had no effect on p15^{INK4B} or p27^{Kip1}, because activated Ras did not alter the expression of these proteins (Figure 5D). However, DPI augmented p21^{Cip1} levels, indicating that ROS normally act to suppress p21^{Cip1} expression and (in this context) its associated antiapoptotic function (Figure 5D).

Finally, we examined the expression of the cell-cycle inhibitor, RB. H-Ras^{G12V} expression induced RB expression (3-fold), however, a similar increase was observed in the level of phosphorylated RB (consistent with the increase in cyclin D/CDK4 expression in these cells[15]), suggesting most of the RB was inactive (supplemental Figure 3C). Antioxidant treatment caused a consistent decrease in RB expression, however concomitant changes in RB phosphorylation level make it difficult to draw any inference from this observation.

In summary, these data indicate that ROS production by CD34+ N-Ras^{G12D} and CD34+ H-Ras^{G12V} cells contributes to cyclin D induction, which is consistent with these oncogenes' proproliferative influence.

Discussion

In agreement with previous research,[2] we found that normal human CD34+ hematopoietic progenitors constitutively produce low levels of both superoxide and its derivative, H_2O_2. Expression of N-Ras^{G12D} and H-Ras^{G12V} strongly augmented constitutive production of superoxide and H_2O_2 (though the extent of production could also have been influenced by the concomitant overexpression of Ras in these cells). Activated Ras has been shown to promote ROS production in a variety of human cell types including transformed embryonic lung cells,[35] fibroblasts,[36] neuroblastoma cells,[37] as well as in hematopoietic cells in vivo, indicating the potential for ROS to act as a proproliferative stimulus in an N-Ras leukemic context.[12,14] Although untested in this study, activated K-Ras is not usually associated with increased ROS production, possibly due to isoform-specific cellular localization and signaling preferences.[38] Cellular ROS production is balanced by expression of endogenous antioxidants. For example, Ras activity can decrease the activity of peroxiredoxins, leading to an increase in intracellular ROS.[39] In this study, however, Ras expression did not affect levels of the major antioxidant enzymes, peroxiredoxin I catalase, and SOD1, suggesting that altered antioxidant expression was unlikely to account for the increased ROS detected.

ROS can be produced via oxidase activity (eg, NOX family) or via the mitochondrial electron transport chain.[26] In this study, the use of a series of probes and inhibitors demonstrated that the source of excess ROS production was derived from NOX oxidases. This is consistent with other reports of Ras-induced ROS production in a variety of cell types.[14,37,40,41] Specifically, we observed NOX2 overexpression and increased membrane translocation of NOX2 regulatory subunits and N-Ras^{G12D} was unable to induce ROS in

mice deficient in Nox2. Taken together, these data suggest NOX2 is the major source of Ras-induced ROS in primitive hematopoietic cells. NOX1 may also contribute, because it is also expressed in human CD34$^+$ progenitors[2] and contributes to ROS production driven by activated Ras in rat fibroblasts.[17]

Activated Ras can promote survival of hematopoietic cell lines,[31] but this is the first report that Ras can promote the survival of primary hematopoietic progenitors when deprived of growth factors and serum. Consistent with this, H-Ras^{G12V} strongly promoted the phosphorylation of Akt. Observations that survival of CD34$^+$ cells expressing activated Ras was dependent on culture density and that these cells could promote the survival of control cells in paracrine fashion led us to examine whether ROS may be acting as a prosurvival factor (particularly as H_2O_2 has recently been shown to promote cell survival in neuronal cells[30]). Depletion of exogenous H_2O_2 (using catalase) merely promoted the survival of both CD34$^+$ H-Ras^{G12V} and control cells, demonstrating that ROS production inhibited the survival of these cells. Correspondingly, neither catalase nor NOX inhibition suppressed the phosphorylation of Akt in CD34$^+$ H-Ras^{G12V} cells. These data indicate that Ras provokes the secretion of prosurvival factors in CD34$^+$ cells, but that their effects are antagonized by ROS. We have not investigated the nature of these prosurvival factors, however, a gene array analysis of CD34$^+$ N-Ras^{G12D} cells has revealed that Ras strongly promotes the expression of several cytokine genes with this potential.[42]

In addition to promoting survival, we were surprised to observe that CD34$^+$ N-Ras^{G12D} and CD34$^+$ H-Ras^{G12V} cells were able to proliferate in serum-replete cultures without growth factors. Previous studies of the effect of activated Ras on CD34$^+$ cells, including our own, have all made proliferative comparisons in the presence of growth factors,[32,43] and under these conditions no proliferative advantage is observed; though N-Ras^{G12D} has previously been shown to promote a growth advantage when CD34$^+$ cells were cultured with the MS5 stromal line.[44] This increased proliferation is likely driven by the same secreted factors that promoted cell survival. However, unlike the cell survival experiments, we found that ROS production appeared to augment the proliferation of CD34$^+$ N-Ras^{G12D} and CD34$^+$ H-Ras^{G12V} cells, whereas ROS were growth inhibitory for control cells. These data suggest that activated Ras may not only promote ROS production in hematopoietic progenitors, but can simultaneously alter their response to it. Increased ROSs have previously been associated with increased cell proliferation in several models. For example, mitogenic signaling in Ras-transformed mouse fibroblasts was suppressed with NAC treatment,[11] whereas overexpression of NOX1 alone (aka, Mox1) in mouse fibroblasts resulted in increased ROS production and proliferation.[45]

We also examined the changes in cell-cycle control proteins that may have mediated the proliferative changes elicited by activated Ras and ROS in these cells. Activated Ras induced strong up-regulation of cyclins D1 and D3, which has been reported previously,[46] and also up-regulated their partner kinase, CDK4. In this study, ROS were shown to contribute to cyclin D expression, which is consistent with previous observations made in mouse embryo fibroblasts where ROS production was also associated with up-regulation of cyclin D expression and cell-cycle progression.[47] Surprisingly, both isoforms of Ras also promoted expression of p21^{Cip1}; though this appeared to have a purely cytosolic location making it unlikely that increased p21^{Cip1} was influencing cell-cycle progression. Finally, CD34$^+$ H-Ras^{G12V} cells exhibited substantial phosphorylation of p38^{MAPK}, which was solely a consequence of ROS production by these cells. In other contexts,[9] this provokes cell-cycle arrest through induction of p16^{INK4A}, but we were unable to demonstrate induction of this protein in these cells.

In conclusion, these data show that activated Ras strongly promotes the expression of ROS in early human progenitor cells, through a NOX-dependent process. A range of ROS was detected including H_2O_2, which has the capacity to affect a wide range of cell signaling processes. This species is membrane permeable, meaning its production can also influence neighboring cells. Our data therefore suggest that production of ROS may confer a competitive advantage on premalignant/malignant cells by promoting the proliferation of these cells, while at the same time inhibiting the proliferative capacity of normal cells in the surrounding microenvironment.

Acknowledgments

This work was supported by the Medical Research Council and Cardiff University. L.P. is funded by Leukemia Research UK.

Authorship

Contribution: P.S.H. cowrote the paper, designed and executed experiments, and analyzed data; L.P., A.J.T., and P.E.J. provided technical assistance; A.K.B. provided resources and clinical insight; and R.L.D. and A.T. designed experiments, provided project direction, and cowrote the paper.

Conflict-of-interest disclosure: The authors declare no competing financial interests.

Correspondence: Alex Tonks, Department of Haematology, 7th Fl, School of Medicine, Cardiff University, Heath Park, Cardiff, CF14 4XN, United Kingdom; e-mail: tonksa@cf.ac.uk.

References

1. Lambeth JD. Nox enzymes and the biology of reactive oxygen. *Nat Rev Immunol.* 2004;4(3):181-189.
2. Piccoli C, D'Aprile A, Ripoli M, et al. Bone-marrow derived hematopoietic stem/progenitor cells express multiple isoforms of NADPH oxidase and produce constitutively reactive oxygen species. *Biochem Biophys Res Commun.* 2007;353(4):965-972.
3. D'Autréaux B, Toledano MB. ROS as signalling molecules: mechanisms that generate specificity in ROS homeostasis. *Nat Rev Mol Cell Biol.* 2007;8(10):813-824.
4. Veal EA, Day AM, Morgan BA. Hydrogen peroxide sensing and signaling. *Mol Cell.* 2007;26(1):1-14.
5. Rhee SG, Kang SW, Jeong W, et al. Intracellular messenger function of hydrogen peroxide and its regulation by peroxiredoxins. *Curr Opin Cell Biol.* 2005;17(2):183-189.
6. Iiyama M, Kakihana K, Kurosu T, Miura O. Reactive oxygen species generated by hematopoietic cytokines play roles in activation of receptor-mediated signaling and in cell cycle progression. *Cell Signal.* 2006;18(2):174-182.
7. Sattler M, Winkler T, Verma S, et al. Hematopoietic growth factors signal through the formation of reactive oxygen species. *Blood.* 1999;93:2928-2935.
8. Havens CG, Ho A, Yoshioka N, Dowdy SF. Regulation of late G1/S phase transition and APC Cdh1 by reactive oxygen species. *Mol Cell Biol.* 2006;26(12):4701-4711.
9. Dolado I, Swat A, Ajenjo N, et al. p38alpha MAP kinase as a sensor of reactive oxygen species in tumorigenesis. *Cancer Cell.* 2007;11(2):191-205.
10. Pelicano H, Carney D, Huang P. ROS stress in cancer cells and therapeutic implications. *Drug Resist Updat.* 2004;7(2):97-110.
11. Irani K, Xia Y, Zweier JL, et al. Mitogenic signaling mediated by oxidants in Ras-transformed fibroblasts. *Science.* 1997;275(5306):1649-1652.
12. Sallmyr A, Fan J, Rassool FV. Genomic instability

in myeloid malignancies: increased reactive oxygen species (ROS), DNA double strand breaks (DSBs) and error-prone repair. *Cancer Lett.* 2008; 270(1):1-9.

13. Kim JH, Chu SC, Gramlich JL, et al. Activation of the PI3K/mTOR pathway by BCR-ABL contributes to increased production of reactive oxygen species. *Blood.* 2005;105(4):1717-1723.
14. Rassool FV, Gaymes TJ, Omidvar N, et al. Reactive oxygen species, DNA damage, and error-prone repair: a model for genomic instability with progression in myeloid leukemia? *Cancer Res.* 2007;67(18):8762-8771.
15. Macleod KF. The role of the RB tumour suppressor pathway in oxidative stress responses in the haematopoietic system. *Nat Rev Cancer.* 2008; 8(10):769-781.
16. Owusu-Ansah E, Yavari A, Mandal S, Banerjee U. Distinct mitochondrial retrograde signals control the G1-S cell cycle checkpoint. *Nat Genet.* 2008; 40(3):356-361.
17. Mitsushita J, Lambeth JD, Kamata T. The superoxide-generating oxidase Nox1 is functionally required for Ras oncogene transformation. *Cancer Res.* 2004;64(10):3580-3585.
18. Arnold RS, Shi J, Murad E, et al. Hydrogen peroxide mediates the cell growth and transformation caused by the mitogenic oxidase Nox1. *Proc Natl Acad Sci U S A.* 2001;98(10):5550-5555.
19. Bowen DT, Frew ME, Hills R, et al. RAS mutation in acute myeloid leukemia is associated with distinct cytogenetic subgroups but does not influence outcome in patients younger than 60 years. *Blood.* 2005;106(6):2113-2119.
20. Zheng X, Beissert T, Kukoc-Zivojnov N, et al. Gamma-catenin contributes to leukemogenesis induced by AML-associated translocation products by increasing the self-renewal of very primitive progenitor cells. *Blood.* 2004;103(9):3535-3543.
21. Tonks A, Tonks AJ, Pearn L, et al. Optimized retroviral transduction protocol which preserves the primitive subpopulation of human hematopoietic cells. *Biotechnol Prog.* 2005;21(3):953-958.
22. Darley RL, Hoy TG, Baines P, Padua RA, Burnett AK. Mutant N-RAS induces erythroid lineage dysplasia in human CD34$^+$ cells. *J Exp Med.* 1997; 185(7):1337-1347.
23. Tonks A, Parton J, Tonks AJ, et al. Surfactant phospholipid DPPC downregulates monocyte respiratory burst via modulation of PKC. *Am J Physiol Lung Cell Mol Physiol.* 2005;288(6): L1070-L1080.
24. Darley RL, Pearn L, Omidvar N, et al. Protein kinase C mediates mutant N-Ras-induced developmental abnormalities in normal human erythroid cells. *Blood.* 2002;100(12):4185-4192.
25. Tonks A, Pearn L, Tonks AJ, et al. The AML1-ETO fusion gene promotes extensive self-renewal of human primary erythroid cells. *Blood.* 2003;101(2):624-632.
26. Bedard K, Krause KH. The NOX family of ROS-generating NADPH oxidases: Physiology and pathophysiology. *Physiol Rev.* 2007;87(1):245-313.
27. Chang F, Steelman LS, Lee JT, et al. Signal transduction mediated by the Ras/Raf/MEK/ERK pathway from cytokine receptors to transcription factors: potential targeting for therapeutic intervention. *Leukemia.* 2003;17(7):1263-1293.
28. Finkel T. Oxidant signals and oxidative stress. *Curr Opin Cell Biol.* 2003;15(2):247-254.
29. McCubrey JA, Steelman LS, Chappell WH, et al. Roles of the Raf/MEK/ERK pathway in cell growth, malignant transformation and drug resistance. *Biochim Biophys Acta.* 2007;1773(8):1263-1284.
30. Groeger G, Mackey AM, Pettigrew CA, Bhatt L, Cotter TG. Stress induced activation of Nox contributes to cell survival signalling via production of hydrogen peroxide. *J Neurochem.* 2009;109(5): 1544-1554.
31. Fukuda S, Pelus LM. Activated H-Ras regulates hematopoietic cell survival by modulating Survivin. *Biochem Biophys Res Commun.* 2004;323(2):636-644.
32. Pearn L, Fisher J, Burnett AK, Darley RL. The role of PKC and PDK1 in monocyte lineage specification by Ras. *Blood.* 2007;109(10):4461-4469.
33. Schepers H, Geugien M, Eggen BJ, Vellenga E. Constitutive cytoplasmic localization of p21(Waf1/Cip1) affects the apoptotic process in monocytic leukaemia. *Leukemia.* 2003;17(11):2113-2121.
34. Zhou BP, Liao Y, Xia W, et al. Cytoplasmic localization of p21Cip1/WAF1 by Akt-induced phosphorylation in HER-2/neu-overexpressing cells. *Nat Cell Biol.* 2001;3(3):245-252.
35. Liu R, Li B, Qiu M. Elevated superoxide production by active H-ras enhances human lung WI-38VA-13 cell proliferation, migration and resistance to TNF-alpha. *Oncogene.* 2001;20(12): 1486-1496.
36. Lee AC, Fenster BE, Ito H, et al. Ras proteins induce senescence by altering the intracellular levels of reactive oxygen species. *J Biol Chem.* 1999;274(12):7936-7940.
37. Serù R, Mondola P, Damiano S, et al. HaRas activates the NADPH oxidase complex in human neuroblastoma cells via extracellular signal-regulated kinase 1/2 pathway. *J Neurochem.* 2004;91(3):613-622.
38. Schubbert S, Shannon K, Bollag G. Hyperactive Ras in developmental disorders and cancer. *Nat Rev Cancer.* 2007;7(4):295-308.
39. Kopnin PB, Agapova LS, Kopnin BP, Chumakov PM. Repression of sestrin family genes contributes to oncogenic Ras-induced reactive oxygen species up-regulation and genetic instability. *Cancer Res.* 2007;67(10):4671-4678.
40. Santillo M, Mondola P, Seru R, et al. Opposing functions of Ki- and Ha-Ras genes in the regulation of redox signals. *Curr Biol.* 2001;11(8):614-619.
41. Yang JQ, Li S, Domann FE, Buettner GR, Oberley LW. Superoxide generation in v-Ha-ras-transduced human keratinocyte HaCaT cells. *Mol Carcinog.* 1999;26(3):180-188.
42. Shen S, Passioura T, Symonds G, Dolnikov A. N-ras oncogene-induced gene expression in human hematopoietic progenitor cells: upregulation of p16INK4a and p21CIP1/WAF1 correlates with myeloid differentiation. *Exp Hematol.* 2007;35(6): 908-919.
43. Dorrell C, Takenaka K, Minden MD, Hawley RG, Dick JE. Hematopoietic cell fate and the initiation of leukemic properties in primitive primary human cells are influenced by Ras activity and farnesyltransferase inhibition. *Mol Cell Biol.* 2004;24(16): 6993-7002.
44. Shen SW, Dolnikov A, Passioura T, et al. Mutant N-ras preferentially drives human CD34$^+$ hematopoietic progenitor cells into myeloid differentiation and proliferation both in vitro and in the NOD/SCID mouse. *Exp Hematol.* 2004;32(9):852-860.
45. Suh YA, Arnold RS, Lassegue B, et al. Cell transformation by the superoxide-generating oxidase Mox1. *Nature.* 1999;401(6748):79-82.
46. Matsumura I, Tanaka H, Kawasaki A, et al. Increased D-type cyclin expression together with decreased cdc2 activity confers megakaryocytic differentiation of a human thrombopoietin-dependent hematopoietic cell line. *J Biol Chem.* 2000;275(8):5553-5559.
47. Menon SG, Sarsour EH, Spitz DR, et al. Redox regulation of the G1 to S phase transition in the mouse embryo fibroblast cell cycle. *Cancer Res.* 2003;63(9):2109-2117.